



DIPARTIMENTO DI SCIENZE DELLA TERRA
Università degli Studi di Torino

DOCTORAL SCHOOL OF SCIENCE AND INNOVATIVE TECHNOLOGIES
PhD PROGRAM IN EARTH SCIENCES

Characterization, conservation and archaeometric study of geomaterials from Western Alps used in the Cultural Heritage

PhD CANDIDATE: Francesca GAMBINO¹

TUTOR: Prof. Alessandro BORGHI¹

CO-TUTORS: Dott.ssa Anna d'ATRI¹
Dott. Lorenzo APPOLONIA^{2,3}

¹*Dipartimento di Scienze della Terra – Università degli Studi di Torino*

²*Dipartimento soprintendenza per i beni e le attività culturali Regione Autonoma Valle d'Aosta*

³*Laboratori Scientifici (LaboS), Centro Conservazione e Restauro La Venaria Reale*

PhD CYCLE: XXXIII

PhD COORDINATOR: Prof. Anna Maria FERRERO

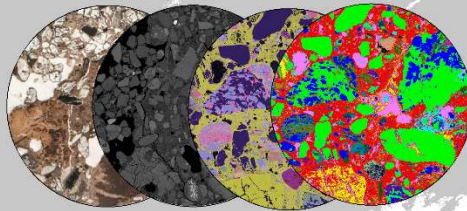
ACCADEMIC YEARS: 2017/2018, 2018/2019, 2019/2020

SCIENTIFIC DISCIPLINARY SECTOR: GEO/07

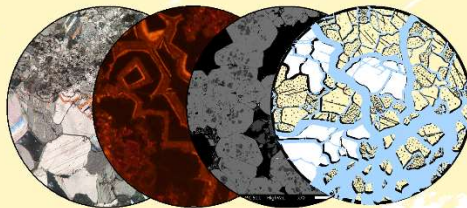
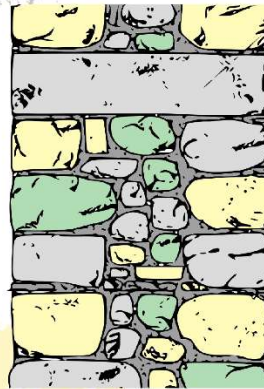


DIPARTIMENTO DI SCIENZE DELLA TERRA
Università degli Studi di Torino

DOCTORAL SCHOOL OF SCIENCE AND INNOVATIVE TECHNOLOGIES
PhD PROGRAM IN EARTH SCIENCES



**Characterization, conservation
and archaeometric study
of geomaterials from
Western Alps used in
the Cultural Heritage**



PhD CANDIDATE: **Francesca Gambino**
TUTOR: Prof. Alessandro Borghi
CO-TUTORS: Dott.ssa Anna d'Atri, Dott. Lorenzo Appolonia

In Italian universities, only 7 out of 84 deans are women.

One of the least discussed, and at the same time most important issues around education in Italy, is the Science, Technology, Engineering and Mathematics Gap phenomenon (hereinafter: STEM Gap), which concerns a significant gender gap in the study of STEM subjects. The most recent data assessing the educational level of female and male students in Italy, indeed, show increasing performance and interest of girls in studying STEM subjects – especially in pre-adolescent and adolescent age – with a sharp decrease as they enter university. Such evident change of trajectory, which seems to be based on individual dispositions, “natural” congenital differences in cognitive capacities between one sex and the other, or even on a presumed inferiority or deficiency of girls and women in relation to their male counterpart, has never been empirically verified.

This thesis is a drop in the ocean. The hope is for it to be part of an increasingly consistent flow of researches and studies of female scholars, to contribute towards achieving equality of opportunities for all.

And now, let us turn to the thanks.

My deepest gratitude goes to my tutor Prof. Alessandro Borghi and co-tutor Anna d'Atri for patiently accompanying me along this path, but above all for teaching me to apply the scientific method, a precious intangible asset that I will be able to take with me wherever I will go.

Another important big thank you is for my co-tutor Lorenzo Appolonia, for sharing his opinions with me and for always believing in me.

A heartfelt thank you to Prof. Lola Pereira and Dr. Fabio Fratini for their punctual corrections and valuable suggestions to further my research.

Thanks also to Elena Pecchioni and Emma Cantisani who, although from afar, I have always held up as an example for the high level of research and scientific competence in the field of archaeometry and diagnostics of Cultural Heritage.

Thanks to Prof. Daniele Castelli, for accompanying and supporting me in the first job of my life as a *conservation scientist*.

Special thanks are also addressed to:

Luca Martire, for his kindness, humanity and teachings.

Luca Barale, colleague and friend, for never getting tired of helping me.

Pietro Mosca, for always valuing my work and helping me to get a 50-person bus through the pedestrian streets of Susa, intact.

Sabrina Bonetto, for her expertise and humanity, which definitely go hand in hand.

Giovanna Dino, for always involving me in her projects.

Roberto Cossio, for making me passionate about the secrets of SEM-EDS and for introducing me to 11-dimensional worlds.

Marco Giardino and Luigi Perotti for sharing their knowledge on the importance of disseminating research results and valuing the "Third Mission" in Academia.

Fabrizio Piana, for his tireless intellectual curiosity.

Carmelo, for the perfect thin sections but, above all, for making me dream of the sea at Christmas.

My mum and dad, for all of love and for teaching me the importance of humility and honesty, in every context of life, and especially, for teaching me what the real priorities in life are.

Nicolò, with whom I have the most important project of all. For always encouraging me, for supporting me in the darkest moments, and for rejoicing with me in the brightest ones. For reminding me, every day, of who I am and who I want to become, in these many lives that have already been lived and that await us.

My uncles Marina and Daniele and my grandmother, for always being ready to celebrate me.

Carla, Arianna and Chiara, for the happy days.

Yaya, for her unconditional affection.

Ele, Eli and Amber, for sharing the joys and sorrows of this PhD.

Vale, who showed me that friendship, even in times of pandemic, knows no distance.

Matte, Luca and Silvia, for the friendship and mutual esteem we have given each other throughout these years.

Michele, Andrea and Christophe, thanks to whom the office has become home (messy and full of food).

Stefano, for taking the time to help me with data analysis and for his human understanding.

Chiara and Tiziana, for always being there for me, even when we stopped being desk neighbors.

Franco, for teaching me to smile instead of complaining.

Dalida and Mario, for always cheering me on.

Teri, Mari and Ste, for having welcomed me, accepted me and above all for having had the patience to listen about my work. Thanks to Manu for his spontaneous gifts in every special occasion.

Fra, Co, Ermione, Miro and Paola, for the empathy they showed me since the first moment.

Marzia, for giving me strength and courage to face my choices.

Index

Preface	1
1. Introduction	5
2. Geo-lithological Map of ornamental stones of Piemonte region	8
2.1. The Geology of Piemonte	11
2.2. Map representation criteria	14
2.3. Map legend	14
2.3.1. Sedimentary rocks	15
2.3.2. Magmatic rocks	17
2.3.3. Metamorphic rocks	18
2.3.4. Fault rocks	24
2.4. Ornamental stone classification	24
2.5. Quarries	25
2.6. Remarks on the geo-lithological map of Piemonte	28
3. Petrographic geodatabase of Piemonte ornamental rocks	29
3.1. The geodatabase	29
3.2. Quarry districts	31
3.2.1. Verbano Cusio Ossola – Sesia Valley district	33
3.2.1.1. The Serizzo	34
3.2.1.2. The Beola	36
3.2.1.3. The acid plutonic rocks	37
3.2.1.4. The basic and ultrabasic plutonic rocks	42
3.2.1.5. The Marble	44
3.2.1.6. The sedimentary rocks	51
3.2.2. Canavese – Biellese district	53
3.2.2.1. The magmatic rocks	53

3.2.2.2.	The Gneiss	58
3.2.2.3.	The Marble	60
3.2.3.	Cottian Alps district	61
3.2.3.1.	The Marble	62
3.2.3.2.	The Gneiss	69
3.2.3.3.	The Prasinite and Ophicalcite	76
3.2.3.4.	The Quartzite	81
3.2.3.5.	The Alabaster	83
3.2.4.	Maritime and Ligurian Alps district	84
3.2.4.1.	The grey and black carbonate “marble”	87
3.2.4.2.	The white marbles	91
3.2.4.3.	The “persichini”	92
3.2.4.4.	The colored marbles	94
3.2.5.	Southern Piemonte hills district	98
3.2.5.1.	Carbonate rocks	99
3.2.5.2.	The sandstone	103
3.2.5.3.	The ophicalcite	105
3.3.	Representative monuments of Piemonte region	107
3.3.1.	Sacra di San Michele	109
3.3.2.	Basilica di Superga	114
3.3.3.	Palazzo Madama	117
3.3.4.	Fenestrelle Fortress	117
3.3.5.	Vicoforte Sanctuary	120
3.3.6.	Oropa Sanctuary	123
4.	The case study of Palazzo Madama façade	125
4.1.	Geological setting of the Chianocco Marble area	127
4.2.	The Palazzo Madama façade	128

4.3. Materials and Methods	132
4.4. The Chianocco Marble	134
4.4.1. Petrography	134
4.4.2. C-O Stable Isotope Analysis	143
4.5. Model evolution	145
4.5.1. Step 1	146
4.5.2. Step 2	146
4.5.3. Step 3 and 4	146
4.5.4. Step 5	147
4.5.5. Step 6	147
4.6. Final considerations on use and conservation of Chianocco Marble	147
5. Petrographic studies of mortars	149
5.1. Historical background	150
5.2. The petrographic approach to the study of mortars	152
5.3. The case study	155
5.3.1. Mortars of the Roman Theatre of Aosta	156
5.3.2. The Roman Theatre of Aosta	157
5.4. Geological setting of Aosta Valley	161
5.5. The original and restoration phases of the Roman Theatre	166
5.5.1. Original phase	166
5.5.2. First restoration phase	167
5.5.3. Second restoration phase	167
5.5.4. Third restoration phase	167
5.5.5. Fourth restoration phase	168
5.6. Materials and Methods	170
5.6.1. The samples	170
5.6.2. Analytical protocol	180

5.6.2.1.	1° step: Characterization by optical microscope	181
5.6.2.2.	2° step: SEM-EDS Quantitative X-ray mapping	182
5.6.2.3.	3° step: Elaboration of the acquired data	186
5.6.2.4.	4° step: Quantitative SEM-EDS spot analyses	192
5.6.2.5.	5° step: interpretation of the acquired data	193
5.7.	Results	195
5.7.1.	Petrography and X-ray maps	195
5.7.1.1.	Original Roman mortars	195
5.7.1.2.	Restoration mortars	204
5.7.2.	Mineral chemistry	221
5.7.2.1.	Principal minerals	222
5.7.2.1.1.	Amphibole	223
5.7.2.1.2.	Chlorite	224
5.7.2.1.3.	Feldspar	226
5.7.2.1.4.	Garnet	229
5.7.2.1.5.	Trioctahedral Mica	230
5.7.2.1.6.	White mica	232
5.7.2.1.7.	Pyroxene	236
5.7.2.1.8.	Epidote	237
5.7.2.2.	Other minerals	239
5.7.3.	Hidraulicity Index (HI)	240
5.8.	Discussion	248
5.8.1.	Production technology	248
5.8.1.1.	Roman mortars	248
5.8.1.2.	Restoration mortars	250
5.8.2.	Supply areas	252
5.8.2.1.	Roman mortars	252

5.8.2.2. Restoration mortars	257
5.8.3. Evaluation of the methodology	259
6. Conclusions	261
6.1. Geo-lithological map of ornamental stones of Piemonte region	261
6.2. Petrographic geodatabase of Alpine ornamental rocks	261
6.3. The case study of Palazzo Madama façade	262
6.4. Petrographic studies of mortars	263
6.5. Future perspectives	264
References	266
Appendix I	288
Appendix II	289
Appendix III	290
Appendix IV	291

1. Preface

This dissertation is submitted for the degree of Doctor of Philosophy at the Università degli Studi di Torino. The manuscript is an original contribution by the author, except where references are made to previous studies. Part of this work has however been presented in already published papers and congress presentations:

Papers:

- Gambino F.*, Borghi A., d'Atri A., Martire L., Cavallo M., Appolonia L., Croveri P. (2019). Minerogeochemical Characterization of Chianocco Marble Employed for Palazzo Madama Façade in Turin (North-West Italy), *Sustainability* 2019, 11(15), 4229; <https://doi.org/10.3390/su11154229>.
- Barale L., Borghi A., d'Atri A., Gambino F.*, Piana F. (2020). Ornamental Stones of Piemonte (NW Italy): an updated geo-lithological map. *Journal of Maps*, 16:2, 867-878, <https://doi.org/10.1080/17445647.2020.1837685>.
- Gambino F., Bellopede R. (2020). La pietra naturale nei Beni Culturali, *Pangea*, Periodico dell'Associazione Georisorse Ambiente GEAM N. 2, 19-25, <https://www.geam.org/pangea2.php>.

Congress presentations:

- Gambino F., Borghi A., Dino G.A., Rossetti P.G., Castelli D., "Balma Syenite (Cervo Valley, northern Italy): a nearly unique material which could be designated as Heritage Stone", I Workshop on Heritage Stones_2-4 October 2018, Salamanca.
- Gambino F., Borghi A., d'Atri A., Martire L., Appolonia L., "Archaeometric study of two of the most important ancient white marbles, for Cultural Heritage exploited in Piemonte region (NW Italy)", EGU General Assembly 7-12/04/2019.
- Borghi A., Gambino F., d'Atri A., Dino G., Favero-Longo S.E., Giardino M., Lombardo V., Martire L., Perotti L., Piana F., "Petrographic geodatabase of Alpine ornamental rocks (Cultural Heritage of Piemonte region, NW Italy) compliant with the "GeoPiemonte Map, web-GIS service", EGU Geophysical General Assembly 7-12/04/2019.

- d'Atri A., Barale L., Borghi A., Dino G., Favero-Longo S.E., Gambino F., Giardino M., Lombardo V., Martire L., Perotti L., Piana F., "The Piemonte Ornamental Stones geodatabase compliant with the "GeoPiemonte Map" web-GIS service", Congresso congiunto SGI-SIMP-SOGEI, Parma, 16-19/09/2019.
- Gambino F., Dino G. A., Borghi A., d'Atri A., Barale L., Favero Longo S. E., Giardino M., Martire L., Perotti L. and Piana F., Geo-referenced database of Ornamental and Building Stones from Piemonte region: from Heritage Stone exploitation to potential economical and social impacts., EGU General Assembly 2020, Online, 4–8 May 2020, EGU2020-17808. doi:10.5194/egusphere-egu2020-17808, 2020.
- Gambino F., Borghi A., d'Atri, Martire L., Croveri P., Russo D., Cardinali M., Appolonia L., Archaeometric characterization of Chianocco Marble employed for Palazzo Madama façade in Turin (North-West Italy), 43rd International Symposium on Archaeometry Lisbon, 18th – 22nd May 2020 (abstract accepted but postponed to 2022 for Covid-19 emergence).
- Gambino F., Borghi A., Cossio R., d'Atri A., Martire L., Appolonia, Glarey A., Vendrell M., Characterization of ancient mortars: an archaeometric protocol of analysis, 43rd International Symposium on Archaeometry Lisbon, 18th – 22nd May 2020 (abstract accepted but postponed to 2022 for Covid-19 emergence).

Abstract:

This PhD Thesis proposes a multidisciplinary approach that allowed to collect different types of data in the field of the study of geomaterials used in the Cultural Heritage. It regards the characterization, conservation and archaeometric study of geomaterials from Western Alps employed in the Cultural and Architecture Heritage. The study of "geomaterials" concerns ornamental stones and ancient mortars in order to investigate these materials and to support the correct diagnosis of their conservation state.

The starting point of the research is the editing of the "*Map of Ornamental Stones of Piemonte Region*" at 1:250,000 scale. It is a simplified lithological map, consisting of 21 lithological classes, showing the distribution of the ornamental stones exploited

in Piemonte and it was obtained by modifying the Geological Map of Piemonte (GeoPiemonteMap, Piana et al., 2017a) and its Data Model. The Map represents a lithological synthesis of a very complex geological setting that comprehends a large number of lithotypes and geological units.

Closely related to the geo-lithological map is the *Geodatabase of the Piemonte ornamental stones* gathering all those geomaterials used in historical buildings of the Piemonte region. It contains the following informations: the quarry district, coordinates, quarry state—active/inactive, tectonic unit, commercial name of ornamental stone, petrographic name, rock type, a short petrographic description and finally the main uses in architecture in Piemonte region and the main references. This is an original work that brings together geological, historical and modern knowledge, archaeometry and architecture.

Additionally, six representative historical religious and civil buildings have been chosen in order to furnish an overview of the employments of some of the most used ornamental stones quarried in Piemonte.

The UNESCO World Heritage *Palazzo Madama* in Torino is one of these important buildings, where a multidisciplinary geological study on the used ornamental stones (the so-called *Chianocco Marble*) is performed. A detailed petro-architectonic relief and minero-petrographic and isotopic analyses were carried out comparing quarry samples coming from the historic sites of exploitation with selected fragments detached from the façade. The petro-architectonic survey allowed to recognize all lithotypes used for the façade and it can be consulted by restorers, architects and engineers who will deal with the future restoration of the façade. The minero-petrographic characterization of the *Chianocco Marble* allowed to define the reasons of its degradation. It shows that some characteristics, detected on the Palazzo Madama façade, such as a vacuolar structure and local reddening, usually absent in ornamental marbles, that are primary features of the rock itself and are

not due to degradation in an urban context. Only gypsum crystals grown in voids and the application of mortars in natural voids, enhancing the physical degradation of the stone, are due to pollution and anthropic interventions respectively. This research underlines the importance of studying the characteristics of stone materials in conservation issues in Cultural Heritage.

Finally, regarding geomaterials used in the Cultural Heritage, this thesis focuses on the study of mortars. This kind of research provides many information about supply areas, variation of raw materials over the time, network/transportation systems, development and production processes. *Original and restoration mortars of the Ancient Roman Theatre of Aosta* (Aosta Valley, Italy) were studied and an original analytical protocol for the characterization of mortars based on automated acquisition and semi-automated processing of quantitative multi-elemental X-ray maps has been designed. A new Software called *GeomatMap* has been developed consisting in a semi-automated image processing procedure based on multivariate statistical analysis of X-Ray spectrum images. Data regarding the production technology of mortars, both Roman and restoration, the supply areas of raw materials and the Hidraulicity Index are investigated.

The study of aggregate of the Roman mortars sites the source of supply of the raw material to the area of Aosta, it is therefore material found in close proximity to the Roman Theatre. The study of binder, a calcic aerial lime, highlights that it is entirely compliant with its function as a bedding material.

The study of aggregate of the restoration mortars sites the source of supply of the raw material to the entire Aosta Valley, an area, although local, larger than that of Roman mortars. Moreover, the hydraulic composition of the binder which places them in the field of cement mortars.

1. Introduction

Ancient buildings, artifacts and findings are mainly made up of natural and artificial materials obtained from geological resources. The development of geosciences applied to Cultural Heritage highlights how the study of the genesis and characteristics of stones materials is primarily a geological matter and has to be solved by a geologic approach. A proper characterization of these materials requires minero-petrographic studies in order to define their composition, provenance and conservation state, being fundamental for the application of good preservation strategies.

This PhD Thesis regards the characterization, conservation and archaeometric study of geomaterials from Western Alps employed in the Cultural and Architecture Heritage. The study of “geomaterials” concerns ornamental stones and ancient mortars; in this regard, the role of Geosciences is crucial to better characterize these materials and to support the correct diagnosis of their conservation state.

In this context, the Thesis is organized in four main chapters developed with the aim to properly face the complex role of Geosciences in the study and comprehension of geomaterials.

Chapter 2 regards the achievement of the **“Map of Ornamental Stones of Piemonte Region” at 1:250,000 scale.** This research was carried out in collaboration with Istituto di Geoscienze e Georisorse of C.N.R. (Torino unit) and in the framework of the project GeoDIVE “From rocks to stones, from landforms to landscapes” co-financed by Compagnia di San Paolo and University of Torino. The compilation of this map aims to gather all the ornamental stone heritage of Piemonte at the regional scale. The map derives from a thorough revision of the available literature (e.g. the official register of quarrying activities of the Piemonte Region, 2019), integrated with unpublished original data showing the location of 117 quarries of ornamental

stones of the region. Besides, a new geo-lithological map (starting from the GeoPiemonte Map of Piana et al., 2017) was produced with the aim to simplify the geological complexity of the region using strictly lithological criteria. This process led to the definition of only 21 synthetic lithological type for the pre-Quaternary rocks of the region used as ornamental stones.

Closely related to the geo-lithological map, the **Chapter 3** shows the **geodatabase of the Piemonte ornamental stones** used in historical buildings of the Piemonte region. The database includes the commercial and scientific name of the rock, the quarry location, the Tectonic units, the petrographic description, their main uses in the historical buildings of Piemonte region and the references.

Moreover, six representative historical religious and civil buildings have been reported on the Map as ancillary graphics, to provide an overview of the final use of some ornamental stones quarried in Piemonte.

One of these buildings, the UNESCO World Heritage Palazzo Madama in Torino, is the topic of **Chapter 4** where a **multidisciplinary geological study** on the adopted ornamental stones (the so-called *Chianocco Marble*) is reported. In the frame of an ongoing project on the conservation state of the monument carried out in collaboration with “Centro Conservazione e Restauro La Venaria Reale” a detailed petro-architectonic relief and minero-petrographic and isotopic analyses were carried out comparing quarry samples coming from the historic sites of exploitation with selected fragments detached from the façade.

Concerning geomaterials used in the Cultural Heritage, **Chapter 5** focuses on the study of mortars. Indeed, the study of geomaterials in cultural heritage cannot be separated from the study of mortars. Moreover, within this thesis work, it represented an important experimental aspect, essential for innovative and pioneering research. This kind of research is not very diffused even though it

provides many information about supply areas, variation of raw materials over the time, network/transportation systems, development and production processes. In particular, the characterization of mortar samples allows to investigate the production technology, to understand which kind of stone has been used to produce the lime, the ratio between binder and aggregate, the origin of the aggregate and its composition (Fratini et al., 2018). This study was focused on the original and restoration **mortars of the Ancient Roman Theatre of Aosta** (Aosta Valley, Italy). The research was carried out in collaboration with the Superintendence Department for Cultural Heritage and Activities of Aosta Valley Region and with Patrimoni 2.0, a *spin-off* of the University of Barcelona (Spain). An original analytical protocol for the characterization of mortars based on automated acquisition and semi-automated processing of quantitative multi-elemental X-ray maps has been developed.

Archaeometry and restoration diagnostics in the Cultural Heritage is a very multifaceted field that can be divided into many different specializations that study different materials using different analysis techniques. Furthermore, being a multi-disciplinary field, it coordinates harmoniously with other fields. In such cases, research is often possible in several case studies that provide the space to investigate certain issues and/or topics. This type of research is therefore intrinsically heterogeneous and ranges from natural rocks to mortars, anthropic in nature, so as to allow the widest possible panorama of study of geomaterials in the geosciences.

2. Geo-lithological Map of ornamental stones of Piemonte region



Figure 2.1: Logo of Geo-lithological map of ornamental stones of Piemonte region

Natural stone has been used as a construction material since ancient times (e.g., since about 4700 BC in Egypt). Initially, these expensive materials were used for temples, tombs, palaces, civic buildings and major infrastructure as well as decoration and sculptures. Selection of stone was guided partly by suitability but was also influenced by personal prestige and social and mystic beliefs. (Pereira and Market, 2016). The use of stone has never suffered a setback during the history up to the present day. Knowing the areas of outcrop and cultivation makes it possible to plan conservation measures that are better suited to the architecture of the monument and the territory (Pereira and Pratt, 2016; Prikryl and Smith, 2007).

Moreover, natural rocks represent a heritage to be valued and preserved. In Piemonte region (NW Italy) over one hundred varieties of rocks have been quarried over the centuries as both building and ornamental stones. Quarrying activity is attested since Roman times (e.g., Borghi et al., 2016) and had a progressive development starting from 16th century under the push of the expanding Savoy Kingdom (Borghi et al., 2014). At present, ornamental

stone quarrying is still an important economic activity in the north-eastern part of the region (Verbano-Cusio-Ossola–Sesia Valley district; Cavallo et al., 2019a and b; Dino and Cavallo, 2014), whereas elsewhere it underwent a progressive decay during the 20th century (with a few exceptions, as the Luserna Stone district in the Cottian Alps; Barisone et al., 1979; Sandrone et al., 2004).

The great variety of ornamental and building stones of Piemonte (e.g., Catella, 1969) is due to the extreme geological diversity of the region, which encompasses rock types pertaining to very different geological contexts (Piana et al., 2017a, b) (see [Paragraph 2.1](#)).

A concise graphic representation on a map of such a complex geology and geodiversity requires the setting up of some classification criteria suitable for the task at hand. The proposed map (*Figure 2.1* and *Figure 2.2* and **Appendix I**; Barale et.al, 2020) is thus a simplified lithological map, consisting of 21 lithological classes, showing the distribution of the ornamental stones exploited in Piemonte.

It was obtained by modifying the Geological Map of Piemonte (GeoPiemonteMap, Piana et al., 2017a) and its Data Model, also available as a WebGIS service

https://webgis.arpa.piemonte.it/Geoviewer2D/index.html?config=other-configs/geologia250k_config.json). A detailed version of the Map at the original scale is reported as PDF file in the **Appendix I**.

The information about the quarry site and the quarried material is reported in the database described in [Chapter 3](#) and entirely reported in **Appendix II**. Six representative historical buildings have been reported on the Map as ancillary graphics, to provide an overview of the final use of some ornamental stones quarried in Piemonte (see [Paragraph 3.3](#)).

2.1 The Geology of Piemonte

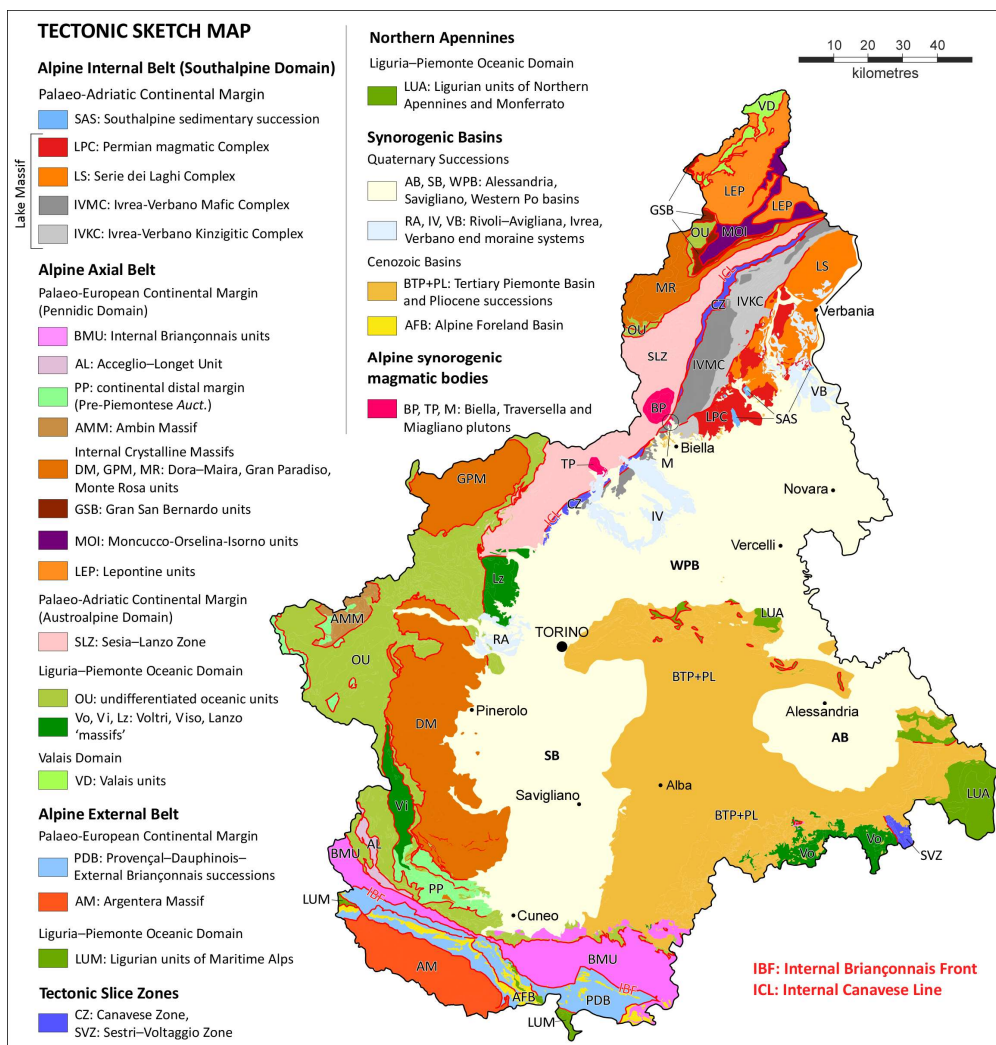


Figure 2.3: Tectonic sketch map of Piemonte Region (Piana et al., 2017).

The geological setting of Piemonte consists of fragments of different lithospheric sections ranging from deep lithospheric mantle rocks to oceanic basalts and relevant sedimentary covers, from plutonic and volcanic continental rocks to the overlying carbonate and siliciclastic sedimentary successions, as well as many kinds of metamorphic rocks originated in different geodynamic contexts and under different pressure and

temperature conditions. A long-lasting sequence of magmatic, metamorphic and sedimentary events can be recognized.

The above-mentioned geological complexity is the result of a continuous geodynamic process, which, since the beginning of Mesozoic, led, in Jurassic times, to the development of two continental passive margins: the “Palaeo-European Margin” and the “Palaeo-Adriatic Margin”, and of two interposed oceanic zones: the Liguria-Piemonte Domain and the Valais Domain (Handy et al., 2010 for a review).

Since Late Cretaceous, the European and the African (Adria) continental plate margins started to converge inducing the subduction of the interposed oceanic lithosphere. This process led, since middle-late Eocene, to the collision and mutual indentation of the two plate margins. In this framework, the Alpine orogenic system originated, involving both continental and oceanic crustal units that were affected, to very different degrees, by metamorphic and tectonic reworking (Dal Piaz, 2010 for a review). An extensive development of magmatic bodies, intrusive into the orogenic belt, occurred in the early Oligocene.

Contemporaneously, since middle Eocene, synorogenic sedimentary basins developed in the external (Alpine Foreland Basin) and internal (Tertiary Piemonte Basin, Pliocene and Quaternary basins) part of the Alpine chain.

These events led to the formation of the present Alpine chain, where units of pre-Alpine continental basements and of the interposed Mesozoic oceanic units, metamorphosed at depth during the Alpine orogenesis, were exposed on the Earth’s surface after having been uplifted and exhumed since middle Eocene. Discontinuous portions of the Mesozoic sedimentary covers of the continental and oceanic units, metamorphosed as well at different degrees, are extensively exposed in Cottian, Maritime and Ligurian Alps and, to a

lesser extent, in the Ossola region and “Lakes district” in the northern part of the Piemonte region. Portions of these sedimentary successions, which did not undergo metamorphic transformations at depth, are now part of the northern Apennines and of the Maritime and Ligurian Alps. Furthermore, wide areas of Piemonte are made up of sediments of the Eocene to Quaternary synorogenic basins that have recorded very clearly the above described geodynamic evolution. In turn, these sediments progressively became part of the overall orogenic system.

The geological and structural subdivisions used in the Geo-lithological map of ornamental stones of Piemonte region are the following (*Figure 2.3*):

- 1) **Alpine Internal Belt** (Southalpine Domain) belonging to the Adriatic plate and only partially involved in the Alpine orogenic process;
- 2) **Alpine External Belt** corresponding to the Helvetic, Dauphinois, Provençal and External Briançonnais domains of the geological literature, which underwent only anchizone to subgreenschist-facies metamorphism;
- 3) **Alpine Axial Belt**, i.e. the Austroalpine-Penninic collisional wedge, corresponding to the continental and oceanic nappes bounded by two main tectonic discontinuities, the Canavese Line on the inner side and the Penninic Frontal thrust on the outer side, respectively (Beltrando et al., 2010). These HP metamorphic units originally belonged to the Piemonte-Liguria oceanic Domain, to portions of the paleo-European margin (Middle Penninic Briançonnais Domain, Lower and Upper Penninic Domains such as Monte Rosa, Gran Paradiso and Dora Maira units) and/or to the paleo-Adriatic margin (Austroalpine Domain).
- 4) **Synorogenic Cenozoic basins**, corresponding to the external Alpine

Foreland Basin and to the internal Tertiary Piemonte Basin, Pliocene and Quaternary basins.

5) Alpine synorogenic magmatic bodies.

2.2 Map representation criteria

The complex legend of the GeoPiemonteMap (Piana et al. 2017a, b), which includes more than two hundred items representing the complex geological setting of the region, has been simplified here, using strictly lithological criteria. In this way, only 21 synthetic lithological units were created for the pre-Quaternary rocks of the region, each grouping rocks characterized by homogeneous lithology, even if belonging to geological units characterized by different paleogeographic origin, geological evolution and age. The Quaternary deposits are present too.

The topographic basemap is composed of a raster DEM base (the only basemap suitable for representation at this scale and available over the entire region; the same used in Piana et al. 2017a), integrated by the following vector levels:

- hydrography and coastlines;
- region and country boundaries;
- toponyms (cities, rivers, lakes, peaks, passes, adjoining regions and countries). The choice of toponyms was pondered in order to include also localities of lesser but important for the regional geology (e.g., localities that are namesakes of geological units or ornamental stones).

2.3 Map legend

The 21 lithological units of substrate rocks have been grouped into Sedimentary Rocks, Magmatic Rocks, Metamorphic Rocks and Fault Rocks.

Quaternary deposits have been subdivided into four units (Recent alluvial deposits; Terraced alluvial deposits; Glacial deposits; Landslide, block stream and rock glacier deposits), which are not further described here since they have no relevance for ornamental stone quarrying. A short description of the rock types included in each lithological unit is given in the following, with essential bibliographic references (for an extended regional bibliography, the reader is referred to Piana et al., 2017b). For each lithological unit, the main ornamental stones are also listed.

2.3.1 Sedimentary rocks

They are subdivided into five units according to their origin (terrigenous, allochemical, and orthochemical) and age (Mesozoic or Cenozoic) (*Figure 2.4*).

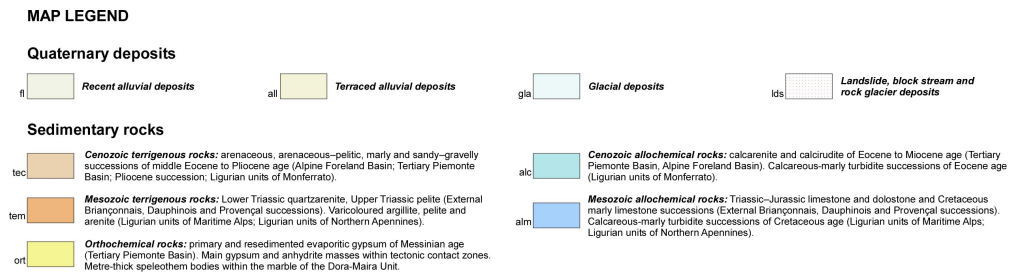


Figure 2.4: Map legend for the quaternary deposits and the sedimentary rocks.

- **Cenozoic terrigenous rocks (tec):** arenaceous, arenaceous–pelitic, marly and sandy–gravelly successions of middle Eocene–Miocene age (Tertiary Piemonte Basin, BTP); upper Eocene-lower Oligocene arenaceous-pelitic successions (Alpine Foreland Basin); pelitic and arenaceous Pliocene successions; conglomerate and chaotic pebbly mudstone successions (Ligurian units of Monferrato). Cemented arenites and greywackes of the BTP succession were exploited as dimensional stones in the past (Vico Stone; Villadeati Stone; Montaldero Stone) and are locally still exploited (Langa Stone).

- **Mesozoic terrigenous rocks** (*tem*): Lower Triassic quartzarenite, Upper Triassic pelite (Provençal, Dauphinois, External Briançonnais successions); varicoloured argillite, pelite and arenite (Ligurian units of Maritime Alps; Ligurian units of Northern Apennines). Mesozoic terrigenous rocks were only rarely exploited for local uses (Monte Fenera Sandstone, an Early Jurassic lithic greywacke from the mainly carbonate succession of the Southalpine Domain).

- **Cenozoic allochemical rocks** (*alc*): calcarenite and calcirudite of Eocene to Miocene age (BTP; Alpine Foreland Basin); calcareous-marly successions of Eocene age (Ligurian units of Monferrato). In the BTP succession, the Gassino Limestone, a biocalcirudite of Eocene age (Campanino and Ricci, 1991), was used as ornamental stone in Torino in the 18th-19th centuries, largely employed in the Basilica di Superga. Miocene biocalcarenite and biocalcirudite of the BTP were exploited in Monferrato (Pietra da Cantoni) and Alto Monferrato sectors (Visone Stone).

- **Mesozoic allochemical rocks** (*alm*): Middle Triassic–Jurassic carbonate and Cretaceous marly limestone successions of the Palaeo-European Continental Margin (Provençal, Dauphinois, External Briançonnais successions), Middle Triassic–Jurassic limestone and dolostone of the Palaeo-Adriatic Continental Margin (Southalpine sedimentary succession), and calcareous-marly successions of Cretaceous age (Ligurian units of Maritime Alps; Ligurian units of Northern Apennines). Historic ornamental stones were exploited from the Triassic–Jurassic succession of the External Briançonnais Domain (Persichino di Garesio, Persichino di Corsaglia, Bardiglio di Garesio, Portoro di Nava, Nero di Ormea, Casotto Breccia), largely used in Torino in the 18th-19th century, and from the Middle Triassic–Lower Jurassic

Southalpine sedimentary succession (Angera Stone, Gozzano Limestone), mostly for local uses.

- **Orthochemical rocks** (*ort*): primary and resedimented Messinian evaporite gypsum (BTP), main gypsum and anhydrite masses within tectonic contact zones, speleothems. Metre-thick bodies of speleothems (calcite alabaster) filling fissures within the dolomite marble of Dora Maira Unit were exploited in the past as Busca Onyx.

2.3.2 Magmatic rocks

They are subdivided into four classes according to their composition (acid or basic) and emplacement mechanisms (plutonic or volcanic) (*Figure 2.5*).

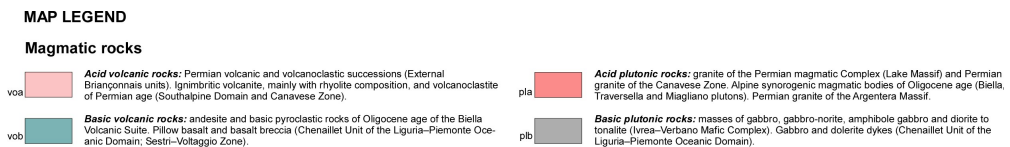


Figure 2.5: Map legend for the magmatic rocks.

- **Acid volcanic rocks** (*voa*): Permian volcanic and volcanoclastic rocks of the palaeo-European continental margin (Provençal, Dauphinois, External Briançonnais successions) and of the Palaeo-Adriatic continental margin (Permian magmatic Complex, Southalpine Domain; Canavese Zone). Several meter-thick dykes of subvolcanic porphyritic rocks intruded in Permian volcanites (Rongio Stone) and granites (Ponte Guelpa Stone) of Biellese area were quarried for local uses.

- **Acid plutonic rocks** (*pla*): Permian granite (Southalpine Domain, Lake Massif, Cavallo et al., 2004b; Canavese Zone; Argentera Massif). Permian granites of the Southalpine Domain were and still are largely quarried in the Lago Maggiore-lower Sesia Valley sector (Montorfano, Baveno, Alzo, Quarona granites). Alpine synorogenic magmatic bodies of Oligocene age

(Biella, Traversella, and Miagliano plutons; Bigioggero et al., 1994; Alagna et al., 2010); these provided important building stones (Vico, Traversella and Brosso Diorite; Balma Syenite), largely used in Torino from 15th to 20th century.

- **Basic volcanic rocks** (*vob*): Oligocene andesite and basic pyroclastic rocks of the Biella Volcanic Suite (Alpine synorogenic magmatic bodies). Rare bodies of pillow basalt and basalt breccia derived from the Liguria–Piemonte Oceanic Domain, which escaped Alpine metamorphism (Chenaillet Unit, Polino, 1984; Figogna Unit of the Sestri–Votaggio Zone; Cortesogno and Haccard, 1984). No ornamental stones from these lithotypes are reported on the map.

- **Basic plutonic rocks** (*plb*): masses of gabbro, gabbro-norite, amphibole gabbro and diorite to tonalite (Ivrea–Verbano Mafic Complex, IVMC, of Southalpine Domain; Rivalenti et al., 1984; Mazzucchelli et al., 2014). Gabbro and dolerite dykes of the Chenaillet Unit (Liguria–Piemonte Oceanic Domain). The Anzola Black Granite, a gabbro-norite of the Ivrea-Verbano Zone, was extensively used for funerary art during 20th century.

2.3.3 Metamorphic rocks

They are subdivided into 11 classes on a merely lithological basis (*Figure 2.6*).

MAP LEGEND

Metamorphic rocks

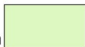
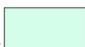









sch		Phyllite, slate and calcareous schist: phyllite and slate with limestone layers of Early Cretaceous age (Sestri–Volltaggio Zone). Calcareous schist of Cretaceous age (Internal Briançonnais units).
cls		Calcschist: calcschist with intercalations of phylladic schist, calc-micaschist and paragneiss of Cretaceous age (Liguria–Piemonte Oceanic Domain and Valais Domain) and of Jurassic–Cretaceous age (Pre-Piemontese Auct.).
mrb		Marble: marble and dolomitic marble of Triassic–Jurassic age in the meta-sedimentary cover units (Pre-Piemontese Auct.; Palaeo-European Continental Margin). Marble lenses of pre-Mesozoic age (Palaeo-European Continental Margin units; Palaeo-Adriatic Continental Margin units: Southalpine and Austroalpine domains). Marble and silicate-bearing marble of Triassic–Early Jurassic age (Liguria–Piemonte Oceanic Domain and Valais Domain).
qtz		Quartzite: quartzite of supposed Permian–Early Triassic age at the base of meta-sedimentary cover units (Pre-Piemontese Auct.; Internal Briançonnais units and Dora–Maira Unit). Rare quartzite of Jurassic age at the base of meta-sedimentary successions of oceanic units (Liguria–Piemonte Oceanic Domain and Valais Domain).
mbs		Metabasite: Mesozoic metabasite (meta-basalt, meta-gabbro, prasinite, amphibolite, eclogite) of oceanic units (Liguria–Piemonte Oceanic Domain and Valais Domain), pre-Mesozoic metabasite of the Palaeo-European and Palaeo-Adriatic Continental Margin units, Paleozoic amphibolite with lesser masses of meta-gabbro and serpentinite (Serie dei Laghi Complex) and migmatitic amphibolite with eclogite and granulite relics (Ivrea–Verbano Kinzigite Complex; Argentera Massif).
umf		Ultramafite and serpentinite: more or less metamorphosed ultramafite (Lanzo and Voltri ‘massifs’), main masses of serpentinite (Liguria–Piemonte Oceanic Domain), meta-peridotite and serpentinite (Lepontine units; Sesia–Lanzo Zone; Canavese Zone), more or less serpentinitized mantle peridotite (Ivrea–Verbano Mafic Complex).
grf		Graphite schist: graphite-rich schist with graphite lenses and graphite-bearing paragneiss (Dora–Maira Unit). Upper Carboniferous graphite-bearing phyllite (Internal Briançonnais units).
msc		Micaschist s.l.: micaschist and metamorphic rocks of the pelitic system of the polycyclic metamorphic basements of the Palaeo-European Continental Margin units and of the Palaeo-Adriatic Continental Margin units (Southalpine and Austroalpine domains).
gne		Orthoderivate rocks s.l.: metamorphic rocks derived from late Paleozoic magmatic rocks of the polycyclic metamorphic basements of the Palaeo-European Continental Margin (Internal Crystalline Massifs; Lepontine Units). Jadeite-bearing meta-granite and orthogneiss of the Sesia–Lanzo Zone. Paleozoic orthoderivates (Serie dei Laghi Complex; Ambin Massif; Internal Briançonnais units). Permian meta-volcanoclastites (Internal Briançonnais units).
mig		Migmatite: migmatitic rocks of various composition and texture (Argentera Massif; Ivrea–Verbano Kinzigite Complex).
gra		Granulite and high-grade schist: felsic granulite and quartz-feldspar-garnet paragneiss (Ivrea–Verbano Kinzigite Complex), sillimanite–garnet-bearing micaschist and paragneiss (Ivrea–Verbano Kinzigite Complex; Sesia–Lanzo Zone).

Figure 2.6: Map legend for metamorphic rocks.

- **Phyllite, slate and calcareous schist (sch):** Early Cretaceous phyllite and slate (Sestri–Volltaggio Zone; Cortesogno and Haccard, 1984). Cretaceous calcareous schist of the Internal Briançonnais Units. No ornamental stones from these lithotypes are reported on the map.

- **Calcschist (cls):** Cretaceous calcschist and calc-micaschist, locally containing bodies of paragneiss, marble, carbonate breccia and ophicarbonates (Liguria–Piemonte Oceanic Domain and Valais Domain; e.g. Elter, 1971; Lagabrielle et al., 1984; Deville et al., 1992; Martin et al., 1994). Alternations of prevailing calcareous schist, quartz-micaschist and phyllite, with carbonate breccia

bodies, of Jurassic-Cretaceous age, belonging to the Palaeo-European Continental Distal Margin (Pre-Piemontese Auct.; Caron, 1971). Calcschist were not reported among the ornamental stones on the Geo-lithological map because no proper quarries of these rocks existed, though in the past they had a widespread local and rural usage (e.g. roof coverings, drywalls), and were also used in numerous architectural elements of historic buildings in the Cottian Alps (e.g., Fenestrelle Fortress, Sacra di San Michele; see below).

- **Marble** (mrb): marble and dolomitic marble of different age are widespread in many units of Piemonte Alps (Borghi et al., 2009). They mainly consist of Triassic-Jurassic marble in the meta-sedimentary units of Alpine Axial Belt (Internal Briançonnais units; Continental Distal Margin; Dora Maira Unit). Marble lenses occur in the crystalline basements of pre-Mesozoic age of the Palaeo-European Continental Margin (Dora Maira Unit) and of the Palaeo-Adriatic Continental Margin (Ivrea Verbano Zone, Southalpine Domain; Sesia-Lanzo Zone, Austroalpine Domain). Marble and silicate-bearing marble of Triassic-Early Jurassic age are present in Liguria-Piemonte Oceanic Domain and Valais Domain.

Several varieties of these marbles were exploited in the past: Mesozoic marbles from the Internal Briançonnais units of the Monregalese area (e.g., Bianco di Gressio, Nero nuvolato di Miroglio, Viola Piemonte, Bigio di Moncervetto, Seravezza di Moncervetto, and Frabosa marble, with the varieties Bianco, Verzino, Giallo, Bigio, Nero) and from the Lepontine units (Crevoladossola Marble); pre-Mesozoic marbles from Sesia-Lanzo Zone (Pont Canavese Marble, Massucco Marble) and from Ivrea-Verbano Zone (Candoglia, Ornavasso, Valle Strona Marble); marbles of the Dora-Maira Unit, both from Mesozoic sedimentary covers (Foresto and Chianocco Marble) and from pre-Mesozoic basement units (Prali, Paesana and Brossasco Marble);

coloured marbles associated with ophi-carbonate bodies of the Liguria Piemonte Oceanic Domain (Rosso Cesana, “Livernea Est” quarry). Moreover, hectometre-sized bodies of marble, originated by hydrothermal processes within the non-metamorphic Mesozoic Provençal-Dauphinois succession (Valdieri Marble, Bertok et al., 2019) were exploited as Bardiglio di Valdieri and Cipollino di Valdieri. The marbles of Piemonte were widely used in the past centuries throughout the region, and especially in Torino. A particular mention is due to the Candoglia Marble, exploited since the 14th century uniquely for the building and restoration of the Duomo di Milano. The Aisone Stone (Carraro et al., 1970), an impure marble charged in detrital quartz and feldspar grains, which derived from hydrothermal transformations of Cenozoic Alpine Foreland Basin sediments, has been included within the ‘stone’ class on the Geo-lithological map because it was only used as rough building material for local uses (polishing being hampered by the high content of siliciclastic grains).

- **Quartzite** (*qtz*): quartzite of supposed Permian–Early Triassic age occurs at the base of meta-sedimentary units of Alpine Axial Belt (Pre-Piemontese Auct.; Internal Briançonnais Units; Acceglio–Longet Unit; Ambin Massif; Dora–Maira Unit). Quartzite of Jurassic age at the base of meta-sedimentary successions of oceanic units (Liguria–Piemonte Oceanic Domain and Valais Domain). The quartzite of the southern Dora Maira Unit was extensively quarried up to a few years ago (Barge Quartzite); quartzite of the same unit was also quarried for local uses in the Susa Valley (Baume Quartzite).

- **Metabasite** (*mbs*): these include the Mesozoic metabasite (meta-basalt, meta-gabbro, prasinite, amphibolite, eclogite) of oceanic units (Liguria–Piemonte Oceanic Domain and Valais Domain). Lenses of pre-Mesozoic metabasite intercalated in continental crust units (Argentiera Massif; basement of Internal

Briançonnais units; Dora Maira, Gran Paradiso and Monte Rosa units; Ambin Massif; Sesia Lanzo Zone) are also included. This class also comprehends the Paleozoic amphibolite with minor masses of meta-gabbro and serpentinite (Serie dei Laghi Complex) and migmatitic amphibolite with eclogite and granulite relics (Ivrea–Verbano Kinzigite Complex; Argentera Massif). Due to their discontinuous occurrence in outcrop and their mineralogical-textural heterogeneity, these rocks are not usually used as ornamental stones, apart from few local cases (e.g., Susa Valley prasinite widely used in the Sacra di San Michele abbey; see below).

- **Ultramafite and serpentinite** (*umf*): ultrabasic rocks, more or less metamorphosed, of the Lanzo and Voltri massifs, main masses of serpentinite (Liguria–Piemonte Oceanic Domain; Valais Domain; Sestri-Voltaggio Zone); meta-peridotite and serpentinite (Lepontine units, Cervandone – Geissfpfad Complex; Sesia–Lanzo Zone, Rocca Canavese Unit; Canavese Zone, Pesmonte Serpentinite); more or less serpentinitized mantle peridotite (Ivrea–Verbano Mafic Complex, Finero, Balmuccia and Baldissero bodies). Several ornamental stones, widely used in the 20th century, were obtained from the ophicarbonates of the Liguria-Piemonte oceanic domain cropping out in the Cottian Alps (Verde Acceglio, Verde Susa, Verde del Frejus, Verde e Rosso Cesana) and in the Ligurian Apennine (Verde Polcevera). The Laugera Stone (used as a soapstone in the past) and the Verde Oira, a dark green serpentinitised peridotite, are also included.

- **Graphite schist** (*grf*): graphite-rich schist with lenses of pure graphite and graphite-bearing paragneiss (Dora–Maira Unit; monometamorphic “Pinerolese Graphitic Complex” Auct, Sandrone et al., 1993). Upper Carboniferous graphite-bearing phyllite of the Internal Briançonnais Units (Malusà et al., 2005). No ornamental stones from these lithotypes are reported on the map.

- **Micaschist s.l.** (*msc*): this class groups all metamorphic rocks of the pelitic system belonging to the pre-Mesozoic metamorphic basements of the Palaeo-European Continental Margin (Dora–Maira, Gran Paradiso, Monte Rosa units; Ambin Massif; Pre-piemontese units Auct.; Gran San Bernardo Unit; Lepontine units; Moncucco–Orselina-Isorno Unit), of the Palaeo-Adriatic Continental Margin (Sesia Lanzo Zone; Serie dei Laghi Complex) and of the Canavese Zone. Although this lithology is one of the most widespread in the western Alps, it has been used only locally (e.g., Forte di Fenestrelle; see below), due to its strong planar anisotropy.

- **Orthoderivate rocks s.l.** (*gne*): metamorphic rocks derived from late Paleozoic magmatic rocks of the polycyclic metamorphic basements of the Palaeo-European continental margin (Dora-Maira, Gran Paradiso, Monte Rosa units; Lepontine units). Jadeite-bearing orthogneiss of the Sesia–Lanzo Zone, Paleozoic orthoderivate (Serie dei Laghi Complex; Ambin Massif; Internal Briançonnais units) and Permian meta-volcanoclastite (Internal Briançonnais units) are also included.

A great number of ornamental stones derive from these lithotypes. These include the orthogneiss of the Dora-Maira Massif (Borghi et al., 2016), such as the Luserna Stone, widely used for roof coverings (e.g., dome of the Mole Antonelliana in Torino) and pavement/road flooring and still largely extracted at present, and other orthogneiss (Malanaggio, Perosa, Cumiana and San Basilio stones; Borgone and Vaie gneisses). Jadeite- and phengite-bearing orthogneiss have been exploited in the Sesia-Lanzo Zone (Verde Jaco, Verde Selene, Verde Oropa, the latter widely used in the Oropa Sanctuary). Several varieties of Beola and Serizzo orthogneiss are widely extracted in the Lepontine Units, such as Beola Bianca, Grigia, Ghiandonata, Favalle; Serizzo Antigorio, Formazza, Sempione, Monte Rosa (Cavallo et al., 2004a)

- **Migmatite** (*mig*): migmatitic rocks of various composition and texture (Argentera Massif; Ivrea–Verbano Kinzigite Complex). No ornamental stones from these lithotypes are reported on the map.

- **Granulite and high-grade schist** (*gra*): felsic granulite and quartz-feldspar-garnet paragneiss (Ivrea–Verbano Kinzigite Complex), sillimanite–garnet-bearing micaschist and paragneiss (Ivrea–Verbano Kinzigite Complex; Sesia–Lanzo Zone). No ornamental stones from these lithotypes are reported on the map.

2.3.4 Fault rocks

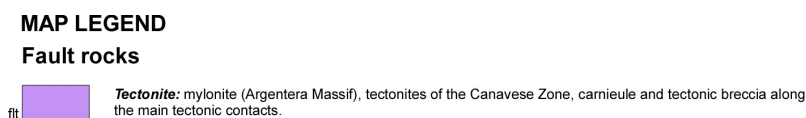


Figure 2.7: Map legend for the fault rocks.

Fault rocks developed along main tectonic contacts have been grouped in one lithological class (**Tectonite**, *ftt*) (Figure 2.7). This class includes carnieule and tectonic breccia, mylonite of the Ferriere-Mollières shear zone (Argentera Massif; Compagnoni et al., 2010), and tectonites of the Canavese Zone (Fobello and Rimella Schist; Sacchi, 1977). Within the latter, two varieties of mylonitic orthogneiss were quarried (White Quartzite, Verde Vogogna).

2.4 Ornamental stone classification

The ornamental stones have been subdivided into six classes, each indicated by a different quarry symbol colour:

- **sedimentary rocks: allochemical and orthochemical** (yellow colour in Map);
- **sedimentary rocks: terrigenous** (brown colour in Map);

- **'granite'** (red colour in Map): following the traditional commercial definition, this term refers to as quartz- and feldspar-bearing, mostly magmatic rocks, which receive polishing for ornamental purposes;
- **'stone'** (grey colour in Map): following the traditional commercial definition, this term refers to as quartz- and feldspar-bearing metamorphic rocks which are used as ornamental stones without polishing;
- **'marble'** (blue colour in Map): this term indicates only 'true' marbles, i.e., metamorphic rocks of carbonate composition. Non-metamorphic carbonate rocks traditionally included in the commercial definition of 'marble', have been here classed among 'sedimentary, allo-/orthochemical rocks';
- **mafic and ultramafic rocks** (green colour in Map): metamorphic and magmatic rocks of mafic and ultramafic composition.

2.5 Quarries

The selection of quarries to be represented on the geo-lithological map derives from the first comprehensive review of stone material made at the regional scale for Piemonte. Quarries and materials of historical, artistic and architectural interest have been selected. Distinction was made between active and inactive quarry, based on the latest release of the official record of quarrying activities of the Piemonte Region (Regione Piemonte, 2019). Over the entire Region, 115 quarries have been mapped (Figure 3.8). For some lithotypes, which occur in a wide area and were subjected to a diffuse exploitation in many localities, only the largest or most significant quarries were mapped. As an example, for the Pietra da Cantoni, which counts tens of small quarries all over the eastern Monferrato hills (Sassone, 2005), only four main quarries were selected. Moreover, for the Luserna Stone, which counts 68 active quarries over the territory of three municipalities (Luserna San

Giovanni; Rorà; Bagnolo Piemonte; Regione Piemonte, 2019), three areas have been indicated, each corresponding to the territory of a municipality and comprehending several active quarries.

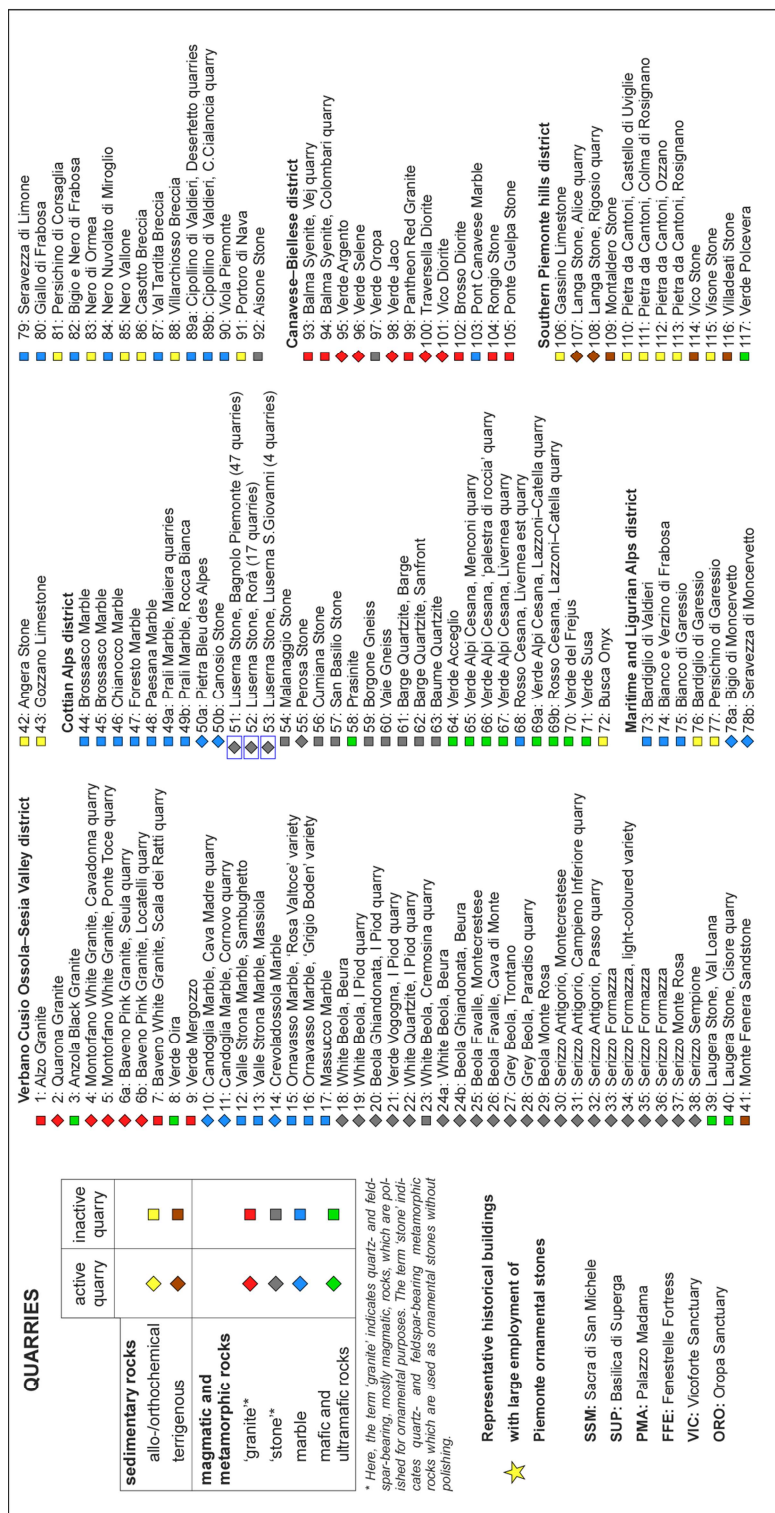


Figure 2.8: List of the selected quarries divided by quarrying district and type of rock.

2.6 Remarks on the geo-lithological map of Piemonte

The 1:250,000 geo-lithological map of ornamental stones of Piemonte, besides scientific aspects, represents a source of information for people operating in the fields of cultural heritage and geo-environmental sciences. The Map represents a lithological synthesis of a complex geological setting that comprehends a large number of lithotypes. Since the Map derives from the interactive GeoPiemonteMap (Piana et al., 2017a, b) available on the Web, it provides an added informative value to the graphic documentation. This work is proceeding to ensure that the geodatabase is available on the web too in order to get to the reader the access to more detailed information on the historical, geological and physical properties of rocks and stones, by querying the GeoPiemonteMap database, which has a structure compliant with that of the presented Map of Ornamental Stones.

Software

The geological map (polygons and lines) was compiled using QuantumGIS, version 2.18 Las Palmas. The final layout of the map, including the tectonic sketch and legend, was assembled using Canvas X GIS 2018 and Adobe Illustrator CS5 Version 15.1.0.

3. Petrographic geodatabase of Piemonte ornamental rocks

3.1 The geodatabase

The geo-lithological map described in [Chapter 2](#) is based on an updated geodatabase, which will be the base for the creation of a WebGIS service.

Each mapped quarry, indicated by a number on the Geo-lithological Map, corresponds to an instance in the geodatabase of **Appendix II**. This contains the basic information about the quarry site (quarry district, coordinates, quarry state—active/inactive), the quarried material (commercial name, petrographic name, rock type, age, short petrographic description) the main uses in architecture in Piemonte region and the main references. In *Table 3.1* an excerpt of the database has been reported.

Commercial name	Coordinates	Location	Quarry state	Petrographic Name	Rock Type	Age	Tectonic Unit (referred to tectonic sketch map)	Tectonic Unit (referred to tectonic sketch map)
<i>Cottian Alps district</i>								
44 Brossasco Marble	44°34'58.91"N 7°21'55.91"E	Rore (CN); Varaita Valley	inactive	Saccaroid marble	Metamorphic	Triassic	Alpine Axial Belt (Penninic Domain)	DM: Dora–Maira Unit
45 Brossasco Marble	44°35'28.88"N 7°22'24.62"E	Rore (CN); Varaita Valley	inactive	Saccaroid marble	Metamorphic	Triassic	Alpine Axial Belt (Penninic Domain)	DM: Dora–Maira Unit
46 Chianocco Marble	45°8'53.96"N 7°10'15.78"E	Chianocco (TO); Susa Valley	inactive	Dolomitic marble	Metamorphic	Triassic	Alpine Axial Belt (Penninic Domain)	DM: Dora–Maira Unit
47 Foresto Marble	45°8'37.56"N 7°7'0.49"E	Foresto (TO); Susa Valley	inactive	Dolomitic marble	Metamorphic	Triassic	Alpine Axial Belt (Penninic Domain)	DM: Dora–Maira Unit
48 Paesana Marble	44°41'6.80"N 7°14'15.24"E	Calcinere Inferiore, Paesana (CN)	inactive	Marble	Metamorphic	Palaeozoic	Alpine Axial Belt (Penninic Domain)	DM: Dora–Maira Unit
49a Prali Marble	44°54'23.79"N 7°4'55.20"E	Cave della Maiera, Prali (TO); Germanasca Valley	inactive	Silicate marble	Metamorphic	Palaeozoic	Alpine Axial Belt (Penninic Domain)	DM: Dora–Maira Unit
49b Prali Marble	44°54'18.00"N 7°5'33.58"E	Rocca Bianca, Prali (TO); Germanasca Valley	inactive	Silicate marble	Metamorphic	Palaeozoic	Alpine Axial Belt (Penninic Domain)	DM: Dora–Maira Unit
50a Bleu des Alpes Stone	44°23'28.4"N 7°18'31.7"E	Saretto, Monterosso Grana (CN)	active	Listed marble	Metamorphic	Early Jurassic	Alpine axial belt (Liguria – Piemonte Oceanic Domain)	OU: undifferentiated oceanic units
50b Canosio Stone	44°27'10.2"N 7°04'19.0"E	Bagnolo Piemonte (CN)	active	Listed marble	Metamorphic	Jurassic	Alpine axial belt (Liguria – Piemonte Oceanic Domain)	OU: undifferentiated oceanic units
51 Luserna Stone	44°44'59.61"N 7°13'50.02"E	Rorà (TO)	active	Orthogneiss, micro- augen gneiss	Metamorphic	Permian	Alpine Axial Belt (Penninic Domain)	DM: Dora–Maira Unit

Petrographic description	Main uses	References
<i>Cottian Alps district</i>		
44 White marble with isotropic structure, xenoblastic texture and coarse grained size. Abundant silicate accessory minerals.	Torino: statues and vases on top of the Juvarrà façade of Palazzo Madama, columns and architrave of S.Filippo Neri Church façade, Corinthian capitals of the aedicule of Superga Church.	Borghì A., Vaggelli G., Marcon C., Fiora L. (2009) The Piedmont white marbles used in antiquity: an archaeometric distinction inferred by a minero-petrographic and C-O stable isotope study. <i>Archaeometry</i> , 51, 913-931.
45 White marble with coarse grain size and isotropic structure, weakly micaceous.	Torino: statues and vases on top of the Juvarrà façade of Palazzo Madama, columns and architrave of S.Filippo Neri Church façade, Corinthian capitals of the aedicule of Superga Church.	Borghì A., Vaggelli G., Marcon C., Fiora L. (2009) The Piedmont white marbles used in antiquity: an archaeometric distinction inferred by a minero-petrographic and C-O stable isotope study. <i>Archaeometry</i> , 51, 913-931.
46 Brecciated marble, white to yellow in color, characterized by vuggy texture and weakly foliation	Torino: plinths of Duomo di Torino façade. Palazzo Madama façade, columns of Piazza S. Carlo arcades. Susa (TO): Arch of Augustus.	Gambino F., Borghì A., d'Attri A., Martire L., Cavallo M., Appolonia L., Croveri P. (2019) Minero-Petrographic Characterization of Chianocco Marble Employed for Palazzo Madama Façade in Turin (Northwest Italy). <i>Sustainability</i> , 11(15), 4229.
47 Micaceous dolomitic marble, with medium-fine grain size and anisotropic structure. White to gray in color.	Torino: Duomo di Torino façade, pillars and plinths of Sindone Chapel, bases of the columns of S. Carlo and S. Cristina churches, internal uses in S.Lorenzo Church. Susa: Arch of Augustus, portal of S. Francesco Church.	Agostoni, A.; Barello, F.; Borghì, A.; Compagnoni, R. (2017) The white marble of the Arch of Augustus (Susa, North-Western Italy): Mineralogical and petrographic analysis for the definition of its origin. <i>Archaeometry</i> , 59, 395-416.
48 White marble with isotropic structure, heteroblastic grain size and granoblastic texture.	Saluzzo: portal of Casa Cavassa.	Borghì A., Cossio R., Fiora L., Pianea E., Sandrone R. (2005) Catodoluminescenza pan e monocromatica di marmi bianchi piemontesi. In: D'Amico C. Ed. <i>Innovazioni tecnologiche per i beni culturali</i> , 351-360, Patron Editore Bologna.
49a Fine-grained calcitic marble. Banded structure characterized by gray to green in color levels made up of femic minerals (amphibole, wilfite mica and other silicates).	Torino: pillars of the railing of Palazzo Reale, statues of Gran Madre di Dio Church, external sculptures of the Basilica Mauriziana.	Borghì A., Vaggelli G., Marcon C., Fiora L. (2009) The Piedmont white marbles used in antiquity: an archaeometric distinction inferred by a minero-petrographic and C-O stable isotope study. <i>Archaeometry</i> , 51, 913-931.
49b Fine-grained calcitic marble. Banded structure characterized by gray to green in color levels made up of femic minerals (amphibole, wilfite mica and other silicates).	Torino: pillars of the railing of Palazzo Reale, statues of Gran Madre di Dio Church, external sculptures of the Basilica Mauriziana.	Borghì A., Vaggelli G., Marcon C., Fiora L. (2009) The Piedmont white marbles used in antiquity: an archaeometric distinction inferred by a minero-petrographic and C-O stable isotope study. <i>Archaeometry</i> , 51, 913-931.
50a Calcitic marble with anisotropic structure, fine grained grain size and granoblastic texture. Gray in color.	Public and private contemporary buildings, rural architecture.	
50b Calcitic marble with anisotropic structure. Gray in color.		
51 Micro-augen orthoneiss, gray to green in color with foliation defined by plerengite. Principal minerals: quartz, albite, K-feldspar and micas.	Torino: slabs covering the dome of the Mole Antonelliana, paving of Piazza Castello and other squares of the city, coverings old prisons Nuove, façade of the Automobile Museum, sidewalk of Vittorio Emanuele I and Umberto I bridges.	Borghì A., Cadoppi P., Dino G.A. (2016) The Doma Maira Unit (Italian Cottian Alps): a reservoir of ornamental stones since roman time. <i>Geoscience Canada</i> , 43, 13-30.

Table 3.1: Example of geodatabase entirely reported in **Appendix II**. Section of Cottian Alps district Information about the quarry site (quarry district, coordinates, quarry state—active/inactive), the quarried material (commercial name, petrographic name, rock type, age, tectonic unit, short petrographic description), the main uses in architecture in Piemonte region and main references are furnished.

3.2 Quarry districts

The quarrying for ornamental stones of Piemonte can be subdivided into five main quarry districts (which include both active and inactive quarries) based on geographical and historical criteria (*Figure 3.1*).

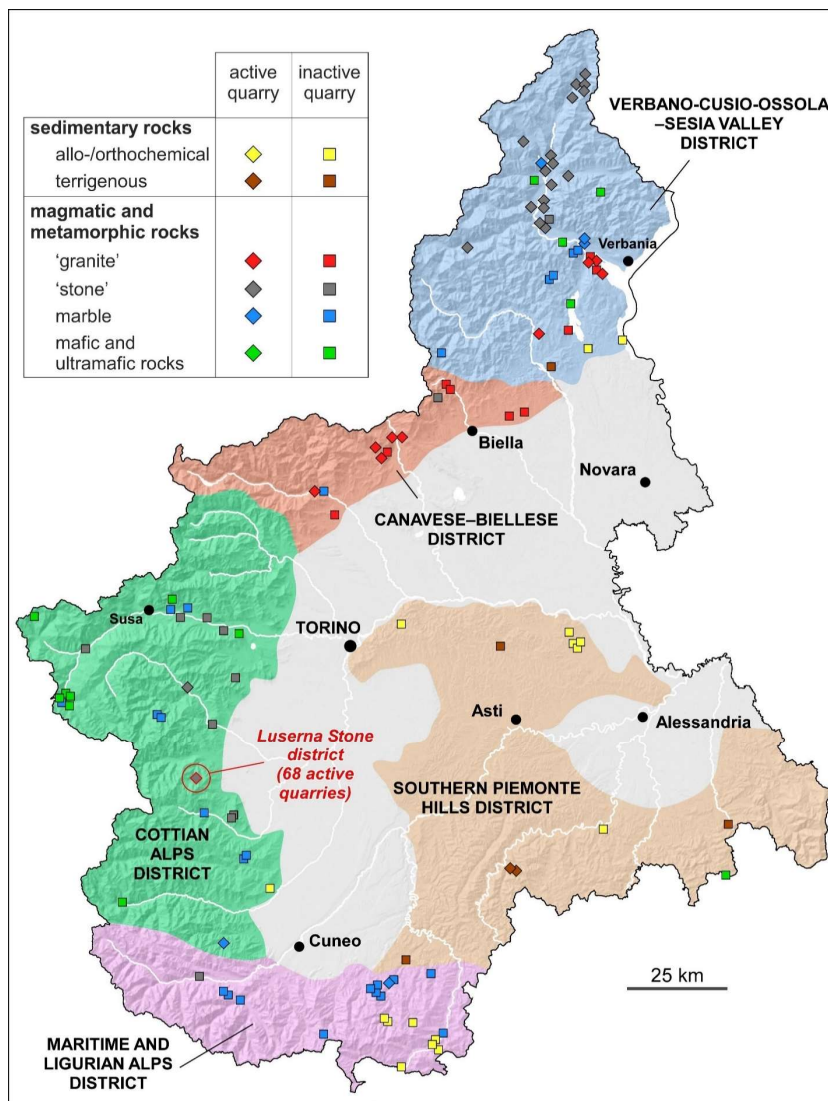


Figure 3.1: Scheme of the quarry districts of Piemonte.

- **Verbano-Cusio-Ossola-Sesia Valley district:** it includes the Lago Maggiore area and the Sesia and Ossola valleys in northeastern Piemonte. The main

quarried lithotypes are represented by orthoderivate metamorphic rocks and granites (Boriani et al., 1988; Dino and Cavallo, 2014).

- **Canavese–Biellese district:** this district encompasses the northwestern Piemonte area between the Sesia and Orco valleys; the main varieties of ornamental stones are represented by magmatic and metamorphic lithotypes.

- **Cottian Alps district:** it corresponds to the Alpine segment comprised between the Stura di Lanzo and Grana valleys, where several varieties of metamorphic rocks (mainly orthoderivate from the Dora Maira Unit) were quarried.

- **Maritime and Ligurian Alps district:** it corresponds to the mountain area of southern Piemonte, where a wide variety of marble and sedimentary carbonate rocks were quarried and includes the historic “Monregalese” district (G.A.L. Mongioie, 2005).

- **Southern Piemonte hills district:** this district corresponds to the hilly sector of central and southeastern Piemonte, where some units of the Cenozoic sedimentary successions of the Tertiary Piemonte Basin and a metamorphic rock of the Liguria-Piemonte oceanic unit were exploited as ornamental stones.

3.2.1 Verbano Cusio Ossola – Sesia Valley district

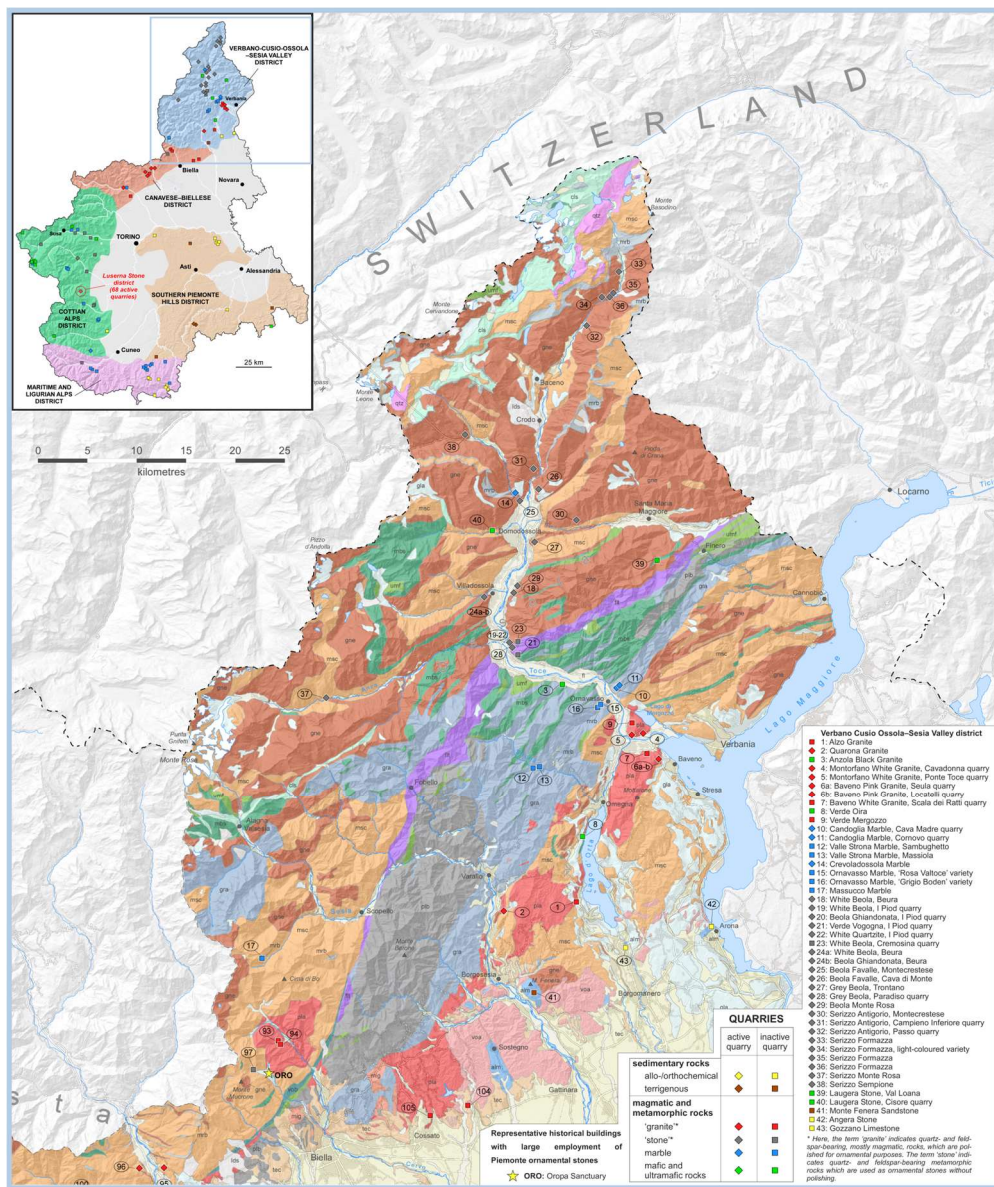


Figure 3.2: Verbano-Cusio-Ossola-Sesia Valley district, detail of Geo-lithological map of ornamental stones of Piemonte region.

Exploitation in the Verbano-Cusio-Ossola province (VCO) takes place among the area of Cusio and Verbano lakes and the northern Ossola Valley, up to the border with Switzerland (*Figure 3.2*). It is one of the most important quarrying

districts of Piemonte since Roman Age representing a natural and economic resource for the local community.

In the Database of ornamental stones of Piemonte region, 43 different lithotypes are reported within this district.

Such diversity is strictly related to its peculiar geological setting. Indeed, it shows one of the most complete and complex structural section of the Alpine chain. The most significant ornamental stones belonging to this area are: Serizzo and Beola orthogneiss, granite, marble, ultramafite and carbonate rocks (Cavallo et al., 2004b).

3.2.1.1 The Serizzo

Serizzo is the most important and widely exploited ornamental stone from the VCO and it shows four varieties: *Serizzo Antigorio*, *Serizzo Formazza*, *Serizzo Sempione* and finally *Serizzo Monte Rosa* (**Figure 3.3**).

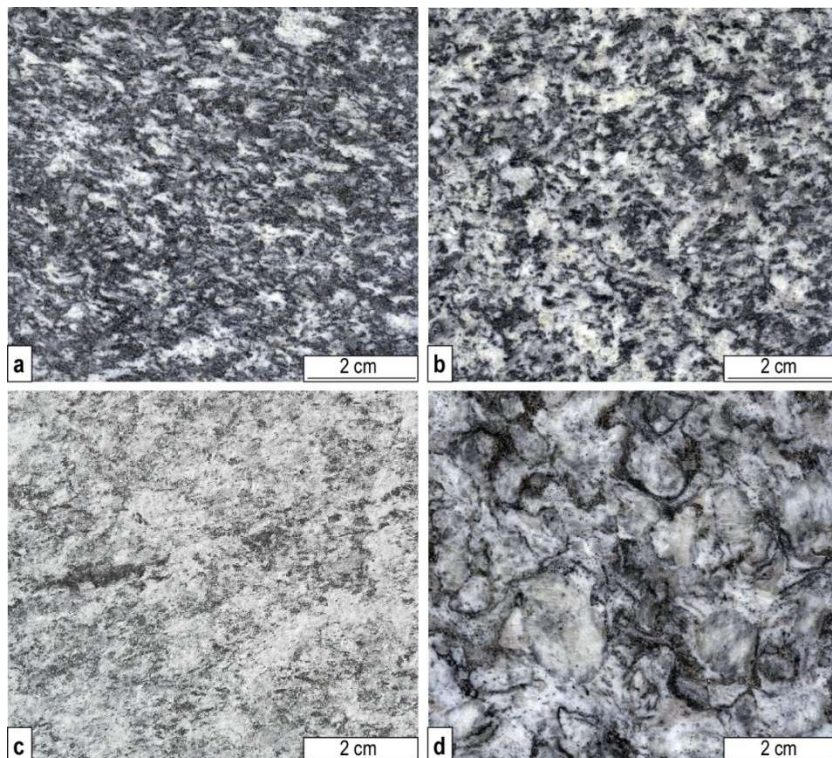


Figure 3.3: Macroscopic pictures of the four varieties of Serizzo. **a.** *Serizzo Antigorio* **b.** *Serizzo Formazza* **c.** *Serizzo Sempione* **d.** *Serizzo Monte Rosa*

They are all augen or micro-augen orthogneiss, from dark to light gray in color, characterized by a foliated texture. They belong to the Antigorio Unit with the only exception of *Serizzo Monte Rosa* which belongs to the Monte Rosa Unit.

Concerning the uses, they are all employed for local and rural architecture. Furthermore, all over the Piemonte and Lombardia regions they are also used as coating of buildings, pavements and street furniture.

Serizzo Antigorio is the most abundant and used Serizzo variety. It consists of a micro-augen gneiss with medium to fine grain texture, dark gray color, showing porphyroclasts of pale K-feldspar and abundant dark levels of biotite which defines the foliation.

Among its principal uses, it is widely employed in Torino, the capital city of Piemonte. It occurs in the columns of the arcades of Via Roma in the blocks between Piazza S. Carlo and Piazza Carlo Felice (*Figure 3.4*), in the basement of the Po and Dora Riparia statues as well as in the basements of the external apses of S. Carlo and S. Cristina churches in Piazza C.L.N.

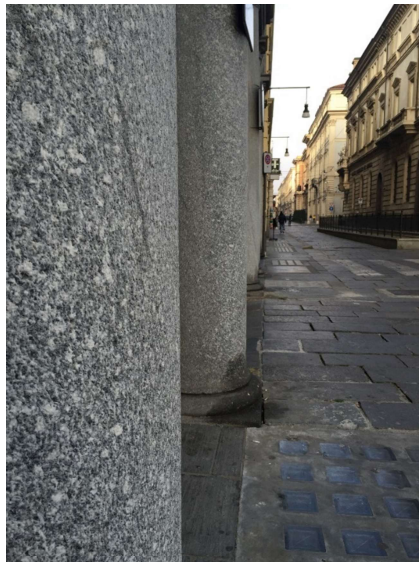


Figure 3.4: Columns of the arcades of Via Roma in the blocks between Piazza S. Carlo and Piazza Carlo Felice in Torino made up of *Serizzo Antigorio* (Italy).

3.2.1.2 The Beola

The second important class of ornamental stones is the *Beola* (also known as *Bevola*) (Figure 3.5). It is a gneissic dimension stone extensively quarried in the lower-medium part of the Ossola Valley, between the villages of Vogogna and Montecrestese-Crevoladossola. Like *Serizzo*, different varieties belong to this class: *Beola Bianca*, *Beola Ghiandonata*, *Beola Favalle*, *Beola Grigia*, *Beola Monte Rosa*, *Verde Vogogna* and *Quarzite Bianca*.

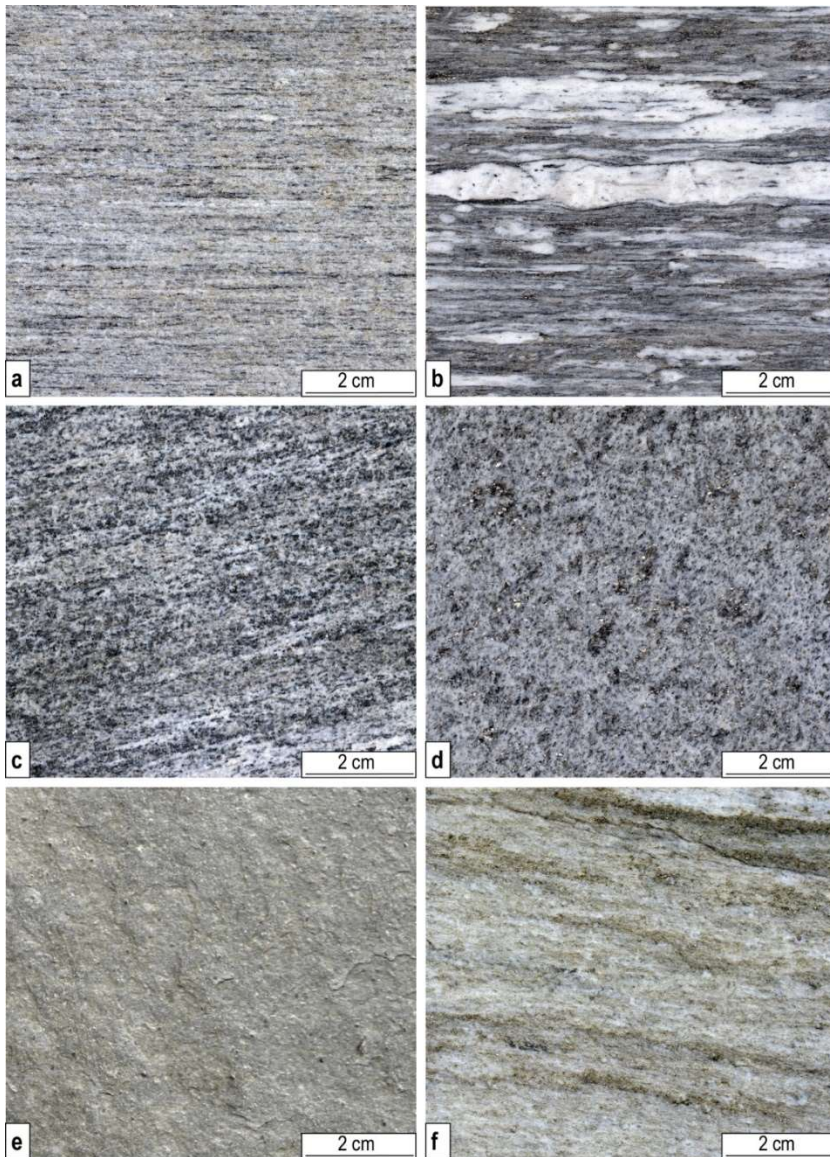


Figure 3.5: Macroscopic pictures of the most representative varieties of Beola. **a.** *Beola Bianca* **b.** *Beola Ghiandonata* **c.** *Beola Favalle* **d.** *Beola Grigia* **e.** *Verde Vogogna* **f.** *Quarzite Bianca*.

Except for *Verde Vogogna* that is a schist, all the other varieties consist of augen granitic orthogneiss characterized by a milonitic foliation ranging from light gray to silver in color.

Interestingly, the same commercial variety belongs to different geological units. In fact, according to their geological and structural setting, these rocks are exploited in four main geological units: *Beola Bianca*, *Beola Ghiandonata*, *Quarzite Bianca* and *Verde Vogogna* belong to the Fobello-Rimella Schists of the Canavese Zone, *Beola Bianca* and *Beola Ghiandonata* refers to the Monte Rosa Unit, *Beola Grigia* refers to the Orselina-Moncucco-Isorno Unit and, finally, *Beola Favalle* and *Beola Grigia* refers to the Monte Leone Unit.

Since the Roman Age, *Beola* slabs were used as roof covering, but transportation problems limited their use to the only areas near the quarries. At the end of the 17th century, the *Beola* was massively utilized for building houses in the Ossola Valley (Dematteis, 1985; Cavallo et al., 2004a).

The principal varieties are reported following: *Beola Bianca* was used for the façade of the building of RAI (Radiotelevisione italiana) in Torino and for the internal pavement of the Sacro Cuore di Gesù Church in Vogogna. *Beola Ghiandonata* was adopted for the façade of the building of RAI, too. *Beola Grigia* was used for the façade of the Santa Maria Assunta Church in Montecretese. *Beola* was also employed for local architecture of the Ossola Valley and, widely, for coating of buildings, pavements and street furniture in Torino.

3.2.1.3 The acid plutonic rocks

Third for commercial importance in the VCO province, after *Serizzo* and *Beola*, granites occur. In the past the quarries were located close to Alzo, nowadays active quarries are sited in the Baveno-Gravellona-Mergozzo area. They

belong to the Permian magmatic complex of “Serie dei Laghi” in the Southalpine basement.

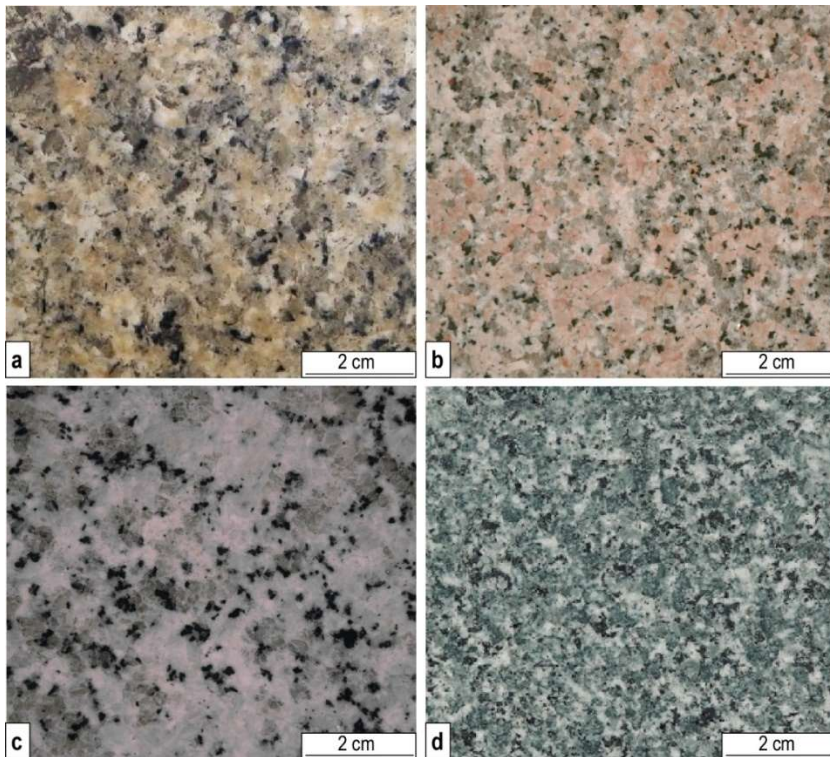


Figure 3.6: Macroscopic pictures of the most representative varieties of Acid Plutonic rocks. **a.** *Alzo Granite* **b.** *Baveno Granite* **c.** *Montorfano Granite* **d.** *Verde Mergozzo*.

Alzo Granite (**Figure 3.6a**), cropping out in Alzo (NO), is a light gray phaneritic granite with granular texture and medium-fine grained texture. The main mineral phases are quartz, white K-feldspar, plagioclase and black biotite. Its quarry, now inactive, was operative from Roman Age up to the 19th century and the exploited granite used as building and ornamental stone. Among the others, it has been used in Torino as paving of San Vincenzo block of Via Roma, the 19th century façade of Palazzo Carignano (Piazza Carlo Alberto) and balustrade of Umberto I bridge (**Figure 3.7**).



Figure 3.7: Umberto I bridge in Torino.

Quarona Granite crops out in Quarona (NO); its petrography is the same of Alzo Granite, and it is still exploited. As ornamental stone it is used for the columns of S. Giacomo Church in Quarona and, during the 20th century, it was widely employed for local architecture.

Baveno Granite (Figure 3.6b) crops out in Baveno (Seula and Locatelli quarries) and it consists of a pink phaneritic granite with medium-fine grained texture. The main mineral phases are quartz, pink K-feldspar (the color is due to hematite micro-dispersions), white plagioclase and black biotite. Because of its color, hardness, texture and durability it was widely used from the 16th to the 20th century and, in Torino, it shows several employments. The most significant ones are: the columns, plinths, capitals, architraves and skirting in Via Roma blocks between Piazza S. Carlo and Piazza Castello, the columns and the plinth of Mole Antonelliana (Figure 3.8), the 19th century façade of Palazzo Carignano in Piazza Carlo Alberto (Figure 3.9), the 19th century columns of the gate of Castello del Valentino, the façade and the columns of

S. Carlo Church in Piazza S. Carlo (*Figure 3.10*), the columns of S. Massimo Church.

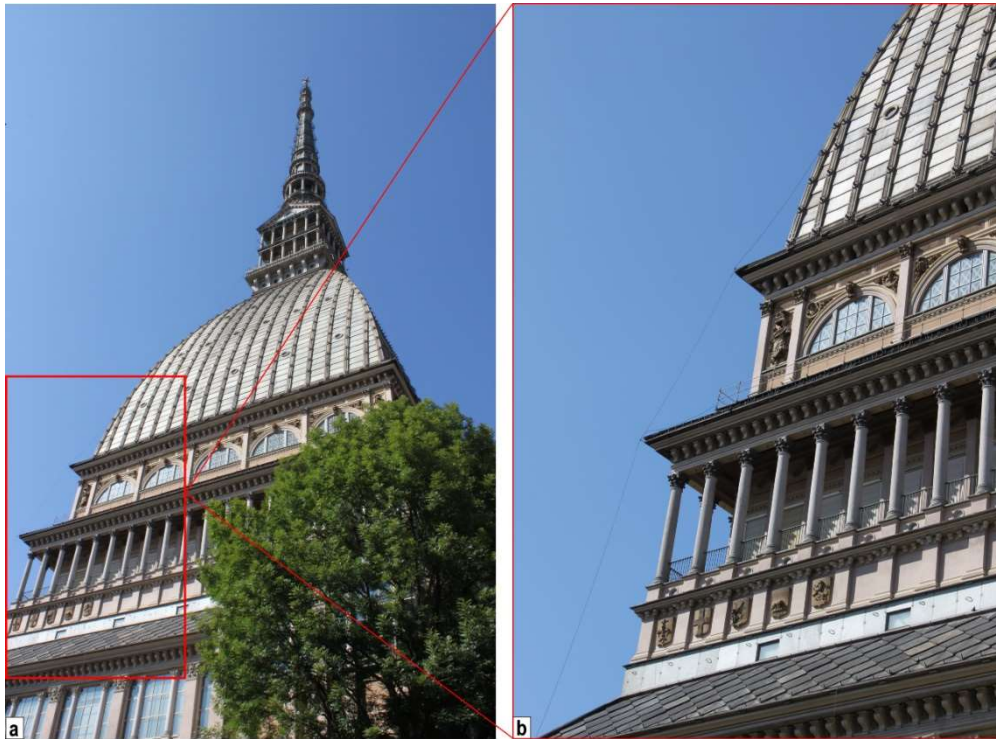


Figure 3.8: a. Mole Antonelliana building; b. Detail of the columns made up of *Baveno Granite*.



Figure 3.9: a. 19th century façade of Palazzo Carignano in Piazza Carlo Alberto in Torino b. Detail of columns made up of *Baveno Granite*.

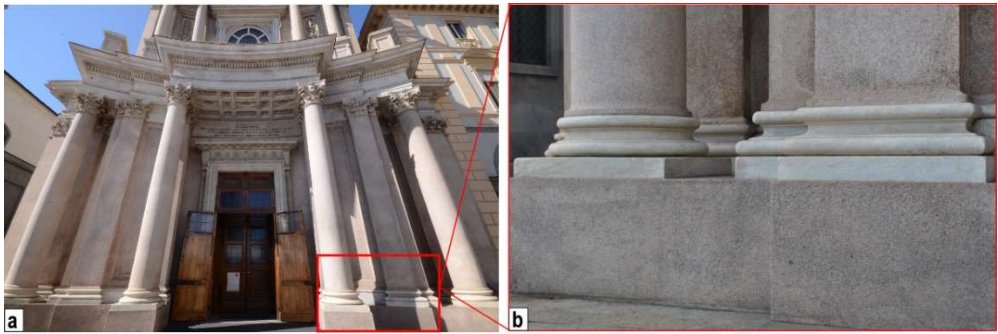


Figure 3.10: *Baveno Granite* used in the façade (a.) and the columns (b.) of S. Carlo Church in Piazza S. Carlo in Torino.

Montorfano Granite crops out in Montorfano (Mergozzo municipality) (*Figure 3.11*) and it is made up of a medium to fine grain phaneritic monzogranite, light gray in color (*Figure 3.6c*). The main minerals are quartz, white feldspars and black biotite. As for the *Baveno Granite*, it was extensively used in architecture and, in Torino, shows several employments: the columns, plinths, capitals, plates and angle pilasters of S. Vincenzo block in Via Roma arcades, the 19th century façade of Palazzo Carignano in Piazza Carlo Alberto, the cornices and archways of upper side façade of Porta Nuova Railway Station, the columns of Via Pietro Micca, Via Viotti and Via Sacchi arcades. Importantly, it has been employed also in Roma (Lazio region) for the façade of the San Paolo Fuori le Mura Church.

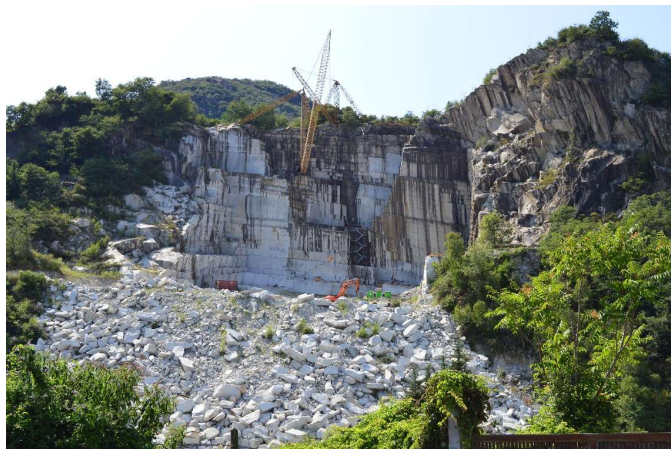


Figure 3.11: *Montorfano Granite* quarry.

Mergozzo Granite (Figure 3.6d) crops out along the northwestern area of Montorfano, near the Toce river, in the Mergozzo municipality. It is a phaneritic granite with medium-fine grain, green in color. It is strongly altered by hydrothermal metasomatism, which led to the partial dissolution of quartz, alteration of K-feldspar into albite and biotite into chlorite. The age of several buildings in Milano (Lombardia region) (e.g. Palazzo Mellerio) attest that the exploitation was surely active since the 18th century and was abandoned at the end of the 20th century. It was mostly used for the slabs for façades and paving (Cavallo et al., 2004b; Dino, 2004).

3.2.1.4 The basic and ultrabasic plutonic rocks

Pietra Laugera is a chlorite-schist with medium-fine grain, it shows a foliation defined by abundance of chlorite. It crops out in Loana and Vigezzo Valleys and belongs to the Complesso degli Gneiss Minuti of the Sesia Lanzo Zone.

Pietra di Laugera, also known as *Pietra Ollare*, was extracted in Bognanco Valley in the Cisore quarry which is the most famous district, active at least since the 17th century. It belongs to Moncucco-Orselina-Isorno Unit and it is a serpentine-schist and a chlorite-schist with medium-fine grain. The foliation is defined by abundant chlorite, talc and serpentine. It was used since the Bronze Age and it shows many applications: the typical “laveggi” (cooking pots), stoves and fireplaces (still in use, due to the excellent temperature resistance), millstones for cereals. It was also employed in many churches and buildings in the Ossola Valley. In Domodossola, for example, many details of the columns, the capitals and the bas-reliefs of the Sacro Monte del Calvario chapels (now UNESCO heritage) and the Collegiale Church are made up of this stone.

Because of its easy workability, in the past the *Pietra Laugera* was manually extracted and processed, as attested by many outcrops and erratic boulders

that show the typical cavities of the cookstone known as “laveggi”. The use of hydraulic lathes was introduced only at the beginning of the 19th century, to produce pipes and pots of any kind of shape (Cavallo et al., 2004b).

Verde Oira crops out in Nonio and it belongs to the Strona-Ceneri Zone of the Serie dei laghi Unit. It is a dark green serpentinised peridotite with medium-fine grain and characterized by irregular clear veining. Its principal minerals are olivine and pyroxene with accessory magnetite. The serpentinization may be very extensive, obliterating the original texture.

This lithotype was used between the 15th and the 20th century and it shows some important employments in Milano: the architrave of the portal of S. Maria delle Grazie Church, the capitals of courtyard of Canonici next to S. Ambrogio Church, the panels of the S. Raffaele Church façade. This rock replaced Saltrio Stone in the Certosa di Pavia façade during the restorations of the beginning of the 20th century. Finally, it was widely adopted in architecture and cemetery decoration up to the first decade of the 20th century (Dino and Cavallo, 2014).

Anzola Black Granite is a phaneritic gabbro-norite with granoblastic texture and medium-fine grain. Its principal minerals are grey calcium-rich plagioclase and femic black minerals. Optical microscopy reveals that the ortho- and clinopyroxene are partially replaced by hornblende (*Figure 3.12*).

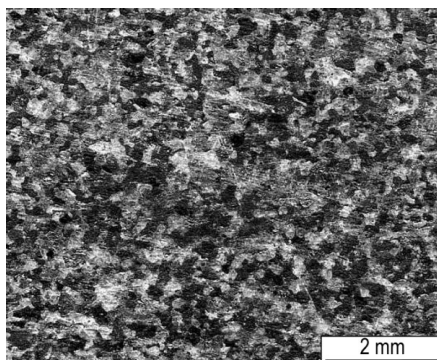


Figure 3.12: *Anzola Black Granite* macroscopic photograph.

This rock belongs to the Mafic Complex of Ivrea Zone and was exploited near Anzola (middle Ossola Valley) (*Figure 3.13*), close to the Toce river, during the 20th century and it was used as paving of the S. Maria Maddalena block in Via Roma, the plinth and staircase of Santissima Annunziata Church in Via Po in Torino and for the funerary art all over the region (e.g. Museo Cadorna in Pallanza). Nowadays, the Anzola quarry produces only crushed stones (Cavallo et al., 2004b).



Figure 3.13: a. and b. *Anzola Black Granite* quarry (middle Ossola Valley, Italy)

3.2.1.5 The Marble

The marbles of VCO are very important ornamental stones; they have been extensively quarried since the Renaissance and used for buildings and monuments in Lombardia and in Piemonte regions, *Ornavasso Marble*, *Candoglia Marble*, *Valle Strona Marble*, belong to the Kinzigitic Unit of the Ivrea Zone, *Crevoladossola Marble* belongs to the Mesozoic cover of the Antigorio Unit and, finally, *Massucco Marble* belongs to the Sesia-Lanzo Zone.

Candoglia Marble is one of the most important marble of the VCO district from the point of view of Cultural Heritage (*Figure 3.14*). It is a calcitic marble (80–

85% of CaCO_3) that shows a characteristic pink to gray color and a coarse-grained texture (>3 mm). Frequent centimeter-thick, dark-greenish silicate layers (mainly represented by diopside and tremolite) characterize the texture of this marble.

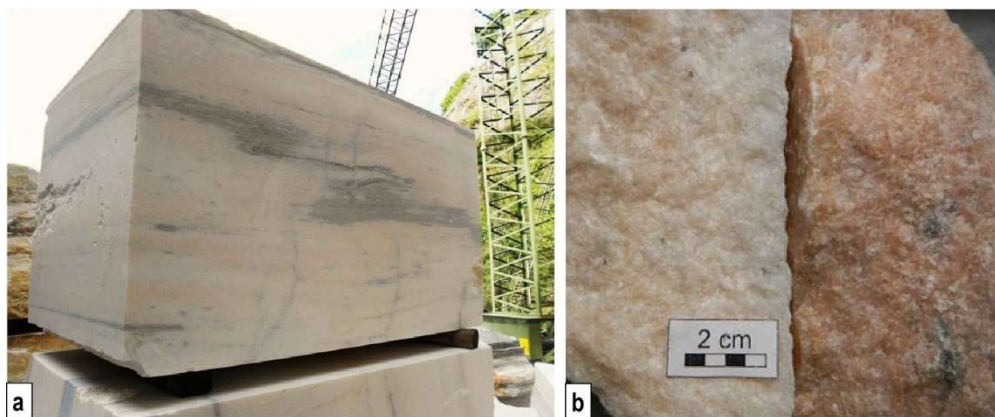


Figure 3.14: a. Block of *Candoglia Marble*. b. Macroscopic aspect of *Candoglia Marble*.

Romans used this rock for altars and columns (e.g. the two columns in the Chiostro Arcivescovile of Novara). In 1387, the Duke Gian Galeazzo Visconti obtained the authorization to the exclusive exploitation of the *Candoglia Marble*. From that time onward, *Candoglia Marble* have been quarried by the “Veneranda Fabbrica del Duomo of Milano” and the exploited material, nearly 1.000 tonn/year, uniquely employed for the maintenance and restoration of the Cathedral (Dino et al.2019) (*Figure 3.15*). Despite this, other uses must be mentioned: the Certosa di Pavia façade, the Colleoni Chapel in Bergamo, the S. Petronio Cathedral in Bologna (Cavallo et al., 2004b).

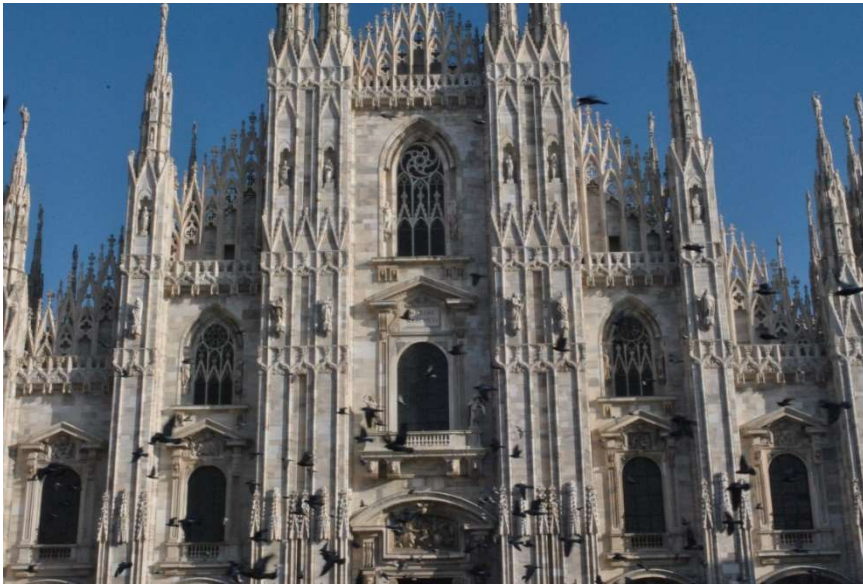


Figure 3.15: Façade of Cathedral of Milan. The *Candoglia Marble* have been quarried by the “Veneranda Fabbrica del Duomo of Milano” and the exploited material is uniquely employed for the maintenance and restoration of the Cathedral.

The Madre and Cornovo quarries (*Figure 3.16*), located close to Candoglia municipality, are the two historical quarries of this marble.

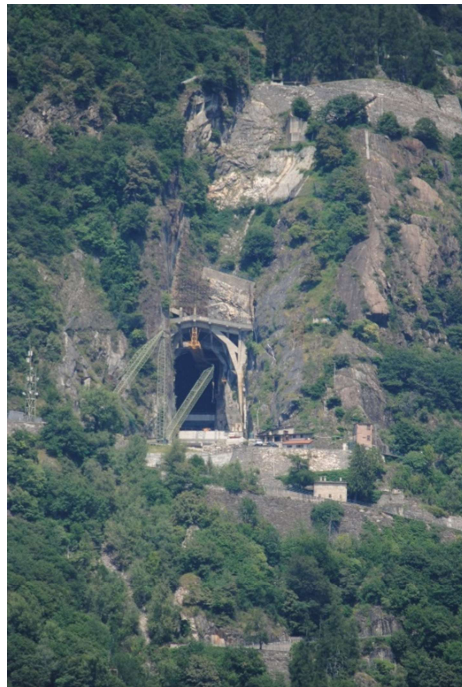


Figure 3.16: Cornovo quarry of *Candoglia Marble*.

Ornavasso Marble pertains to the same marble lenses of *Candoglia Marble* and is locally known as the Candoglia “bastard brother” (Dino et al., 2019). Similarly, to its “brother”, it is less valuable than the Candoglia, due to the coarse-grained texture. It occurs in the *Rosa Valtoce* variety, which is pinkish in color with more abundant dark veins, and in the *Grigio Boden* variety, dark in color.

The first traces of the marble exploitation in the Ornavasso territory date back to the Roman period and the quarrying of this material crosses the history. Nowadays the activity has ceased but the “Antica Cava Moschini” quarry is visitable (*Figure 3.17*). In Torino, it was used for the external coating of the apses of S. Cristina and S. Carlo churches in Piazza C.L.N. (*Figure 3.18*), and in Pallanza for the portal of Madonna di Campagna Church (Cavallo et al., 2004b).

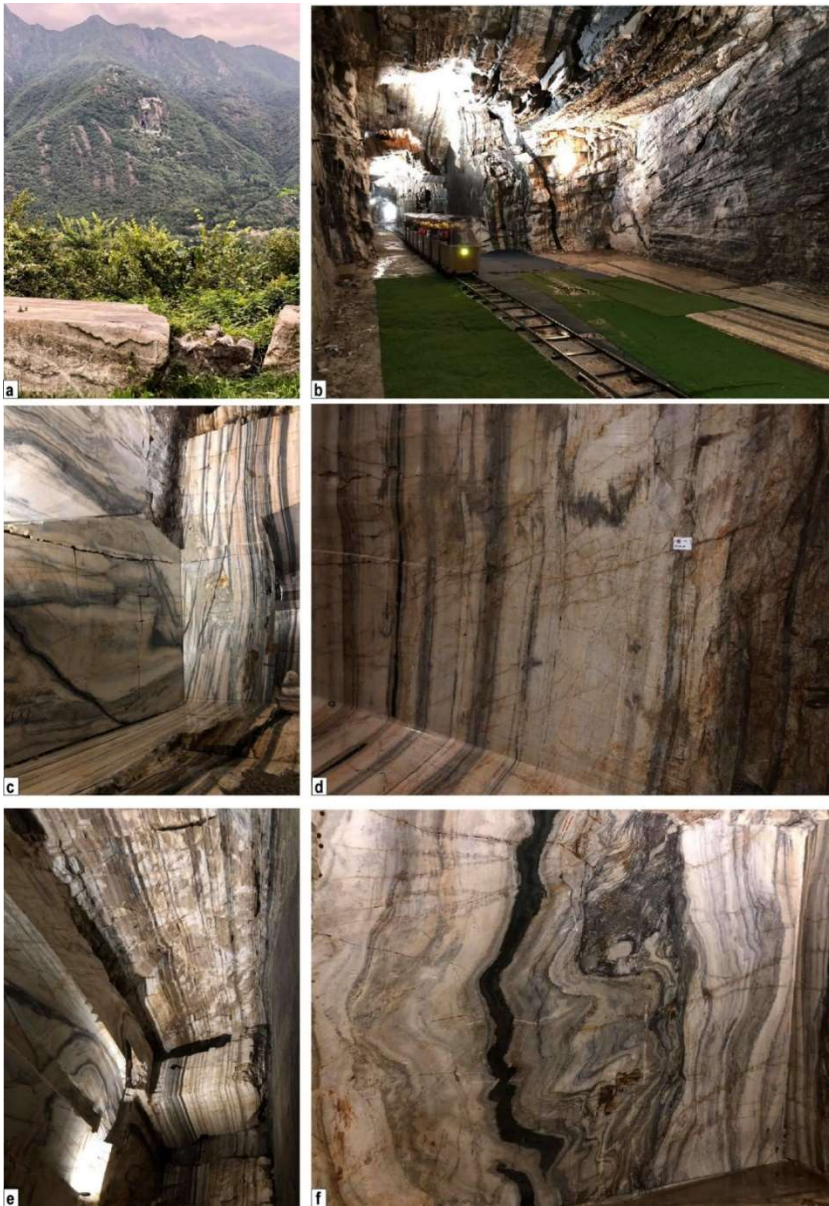


Figure 3.17: **a.** External view of “Antica Cava Moschini” quarry of *Ornavasso Marble*; **b.** Visit of the quarry; **c., d., e., and f.** Interior of the quarry where the marble shows the characteristic pink to gray color and a coarse-grained texture. Frequent centimeter-thick, dark-greenish silicate layers are also observable.



Figure 3.18: External coating of the apses of S. Cristina and S. Carlo churches in Piazza C.L.N. (Torino) made up of *Ornavasso Marble*.

Valle Strona Marble is a calcitic marble with isotropic medium to coarse grained texture. Ivory to light gray in color, this marble shows three varieties: *Bianco Avorio di Vallestrona*, *Grigio di Vallestrona* and *Bianco Rosato*. It was largely exploited since 1881 until 1973 from the Massiola and Sambughetto quarries. This marble was used for the upper coatings of the buildings of Piazza C.L.N. and Via Roma between Piazza C.L.N. and Piazza Carlo Felice and for the coating of the Banca Popolare di Torino in Torino. It was also used in Pallanza for the statues of "Fante" in the Mausoleo di Cadorna. Finally, it occurs in several buildings in Italy such as Palazzo delle Assicurazioni in Venezia, Palazzo di Giustizia in Milano, Ministero delle Corporazioni in Roma, Nuovo Palazzo delle Poste in Napoli but it was also exported in USA (New York) (Cavallo et al., 2004b).

The last valuable marble of VCO is the *Crevoladossola Marble*, that is a silicate-bearing dolomite marble, in contrast to the *Ornavasso* and *Candoglia* calc-rich marbles, with fine grain and white to yellow color due to the abundance of phlogopite, also responsible of the anisotropic texture. It belongs to the

Teggiolo Unit (Lepontine Units) of the Penninic Domain. The location of the quarry (Lorgino di Crevoladossola) is the same of the historic Pavia quarry of the «Fabbrica del Duomo di Pavia», active at the beginning of the 16th century. Nowadays, there is only one active quarry which produces the commercialized varieties: *Palissandro Bluette*, *Palissandro Blu Nuvolato*, *Palissandro Classico* and *Palissandro Oniciato* (**Figure 3.19**).

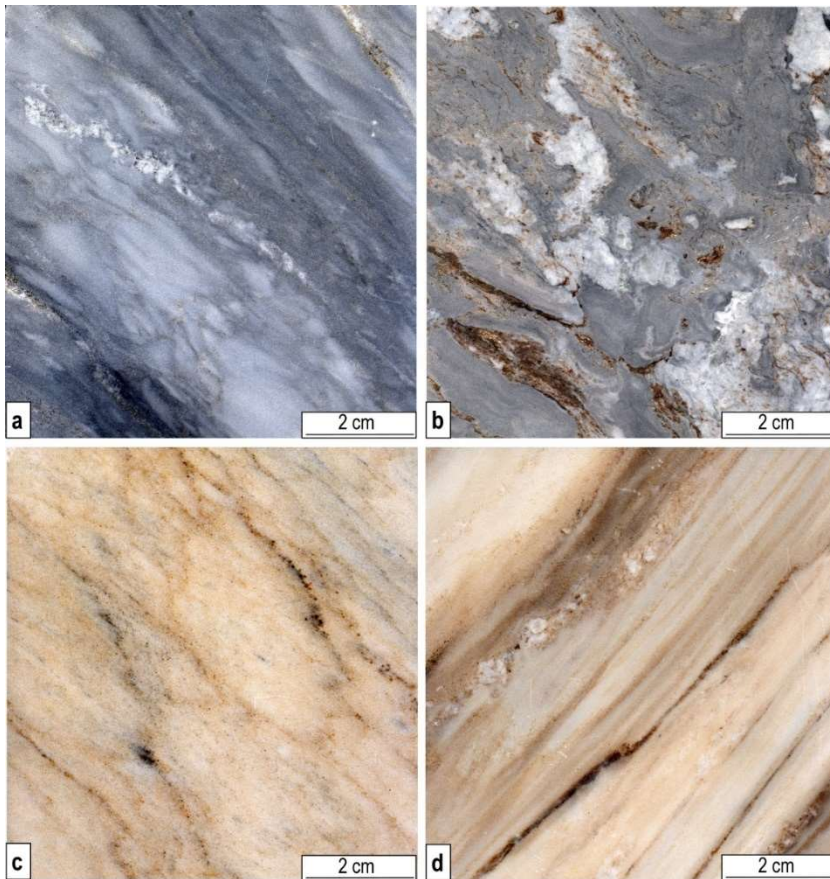


Figure 3.19: Macroscopic pictures of the four commercialized varieties of Palissandro. **a.** *Palissandro Bluette* **b.** *Palissandro Blu Nuvolato* **c.** *Palissandro Classico* **d.** *Palissandro Oniciato*.

Since the 13th and 14th centuries this marble was used for the local architecture of Domodossola, Baceno and Montecrestese. It shows some important employments in Lombardia such as the eight monolithic marble

columns (10 m in height) of the Arco della Pace of Milano and the Duomo of Pavia (Cavallo et al., 2004b).

Finally, *Marmo di Massucco* is a calcite white marble with anisotropic texture and accessory white mica. It was used for the local architecture of Sesia Valley (e.g. Church of Rassa; Fiora, 2009).

3.2.1.6 The sedimentary rocks

The sedimentary rocks of the VCO district have minor importance compared to the previously described *Serizzo*, *Beola* and *Granites*. They are *Dolomia di Arona*, *Monte Fenera Sandstone* and *Gozzano Limestone* and belong to the sedimentary successions of the Southalpine domain.

Dolomia di Arona is a pinkish, yellowish to whitish very fine-grained dolostone characterized by high and homogeneous porosity.

This lithotype was quarried on the western shore of the Maggiore Lake near Arona municipality and it was used for the local architecture.

A similar dimension stone was quarried near Angera municipality on the eastern shore of the Maggiore Lake (VA) (*Pietra di Angera*) since Roman times and mainly used in Lombardia region up to the middle of the 20th century. In the 17th century the exploitation was abandoned, because it damaged the stability of the Rocca dei Borromeo in Angera (Cavallo et al. 2004b).

Monte Fenera Sandstone is a medium to fine-grained lithic greywacke, grey in color, with clasts made up of dolostone fragments, quartz and rare glauconite. It was quarried during the first half of the 19th century at Cava Bianchi (Monte Fenera) and it belongs to the Early Jurassic Arenarie di San Quirico Formation. This sandstone was used for civil and religious buildings of many villages in the Sesia Valley and in Torino for the Isabella Bridge rose windows (now replaced) (Fantoni et al., 2005).

Gozzano Limestone is a calcareous breccia made up of pinkish micritic clasts and fractures filled up by calcite spar. It belongs to the Arenarie di San Quirico, Early Jurassic in age (Montanari, 1969). It was used for local architecture and for the balustrade of the church of Gozzano (Montanari, 1969).

3.2.2 Canavese - Biellese district

The Canavese-Biellese district (*Figure 3.20*) is located in the NW Piemonte between the lower Sesia Valley and Orco Valley. The most relevant ornamental stone varieties belong to different geological units and are represented by magmatic and metamorphic lithotypes.

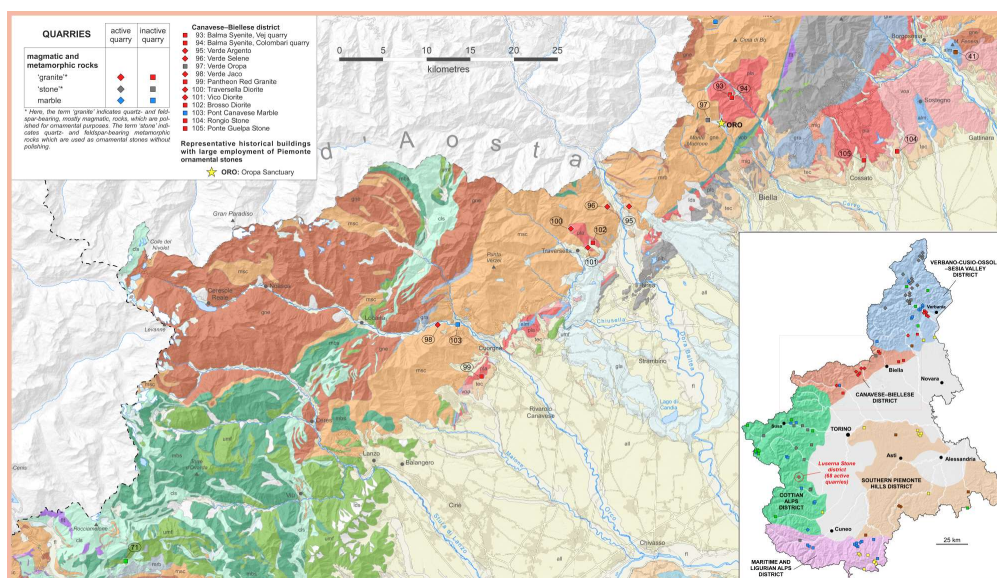


Figure 3.20: Canavese-Biellese district, detail of Geo-lithological map of ornamental stones of Piemonte region.

3.2.2.1 The magmatic rocks

The magmatic rocks mainly belong to the Biella and Traversella plutons. They pertain to the Alpine synorogenic magmatic bodies of Oligocene age intruded in the eclogitic micaschists complex of the Sesia-Lanzo Zone. From an extractive point of view, the following commercial varieties can be distinguished: *Balma Syenite*, *Pantheon Red Granite*, *Traversella Diorite*, *Vico Diorite* and *Brosso Diorite*. *Rongio Stone* and *Ponte Guelpa Stone* belong to magmatic rocks geologically attributed to the Permian magmatic Complex of the Alpine Internal Belt.

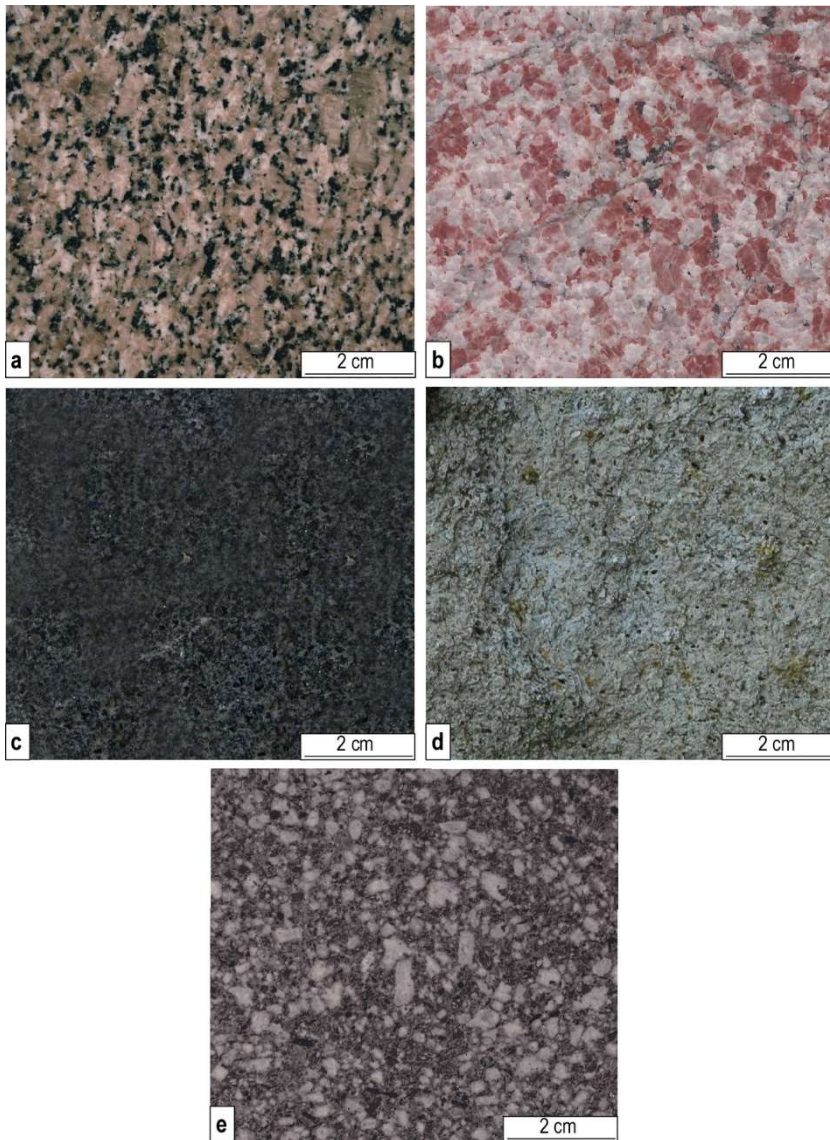


Figure 3.21: Macroscopic pictures of the most representative varieties of magmatic rocks of Canavese-Biellese district; **a.** *Balma Syenite*; **b.** *Pantheon Red Granite*; **c.** *Vico Diorite*; **d.** *Rongio Stone*; **e.** *Ponte Guelpa Stone*.

Balma Syenite (**Figure 3.21a**) is the most exploited stone of Canavese-Biellese district. The quarrying activity, at present, involves two quarries in the Cervo Valley: the Vej della Balma quarry (reactivated in 2003) and the Colombari quarry, both of which located in the San Paolo Cervo Municipality in the Biella Province.

This quartz-syenite has a typical grey-violet color and shows a weak anisotropy defined by the magmatic flow texture. Its mineralogical composition consists of K-feldspar (orthoclase), plagioclase (andesine), Mg-hornblende, biotite, diopside relict and rare quartz. Sphene is the distinctive accessory mineral; the others are apatite, zircon and opaques. K-feldspar typically occurs as crystals with Carlsbad twinning and perthitic exsolutions; its color mainly influences the color of the rock (Sandrone et al., 2004).

The *Balma Syenite* is widely used in Torino; among its employments it must be mentioned the Monument to Emanuele Filiberto Duca d'Aosta located in Piazza Castello in front of the Teatro Regio (*Figure 3.22*), the columns and paving of the San Damiano block in Via Roma, the columns of Porta Nuova Railway Station, the columns of Via Cernaia arcades, the paving of Vittorio Emanuele I and Umberto I bridges, the paving of the ancient roads for carriages of Piazza San Carlo, the steps and the architectural elements of Chiesa di San Massimo façade, the paving in front of Cathedral. It has also been adopted for architectural elements (e.g. the columns of the façade of the Basilica Nuova) of the Oropa Sanctuary (BI).

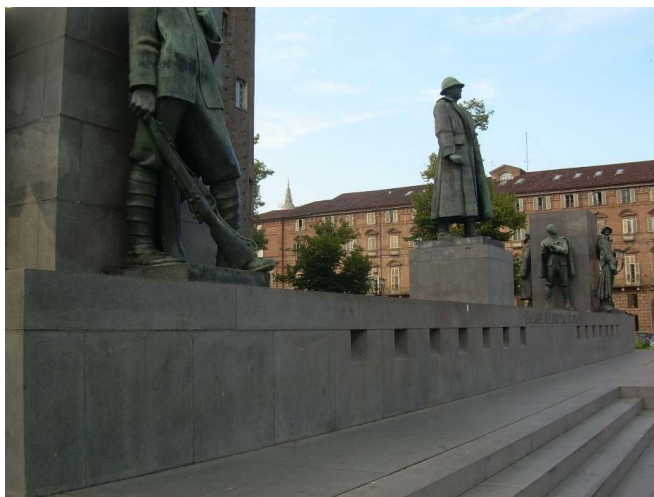


Figure 3.22: Monument to Emanuele Filiberto Duca d'Aosta located in Piazza Castello (Torino) made up of *Balma Syenite*.

The *Pantheon Red Granite* (**Figure 3.21b**) (Belmonte Granite or Valperga Granite) was extracted in the hamlet of Case Piandane, in the municipality of Pertusio, a few kilometres far from Valperga and the Belmonte Sanctuary (TO). Its exploitation was probably dated back to the mid of 20th century and it was completely abandoned around the '70s, possibly because of the unfavorable position of the site. This granite belongs to the Canavese Zone and is characterized by a medium grained texture and red color due to the presence of red orthoclase. The other main minerals phases are plagioclase, quartz and biotite partially replaced by chlorite.

In Torino it was used for the pavement of the hall of the National Social Welfare Institution building in Piazza C.L.N.

Traversella Diorite, *Vico Diorite* (**Figure 3.21c**) and *Brosso Diorite* crop out on the left side of Chiusella Valley (near Ivrea) at Laj quarry (Traversella, TO), Piancampiglia quarry (Vico Canavese, TO) and Brosso (TO) municipality, respectively. They belong to the Brosso-Traversella Pluton and consist of phaneritic magmatic intrusive rocks, with fine grained texture, made up of plagioclase, amphibole, biotite, rare quartz and K-feldspar. Compositionally they vary from quartz-diorite to quartz-monzonite. *Traversella* variety is light gray in color, *Vico* variety is dark gray in color with a very fine-grained texture and the *Brosso* one is gray in color with a coarser texture (Sandrone et al., 2004).

This kind of rocks are still exploited and, among the main uses in Torino, they were adopted for the paving of ancient roads for carriages of Piazza San Carlo, the columns of the S. Emanuele block in Via Roma (**Figure 3.23**) and the Vittorio Emanuele I and Umberto I bridges.

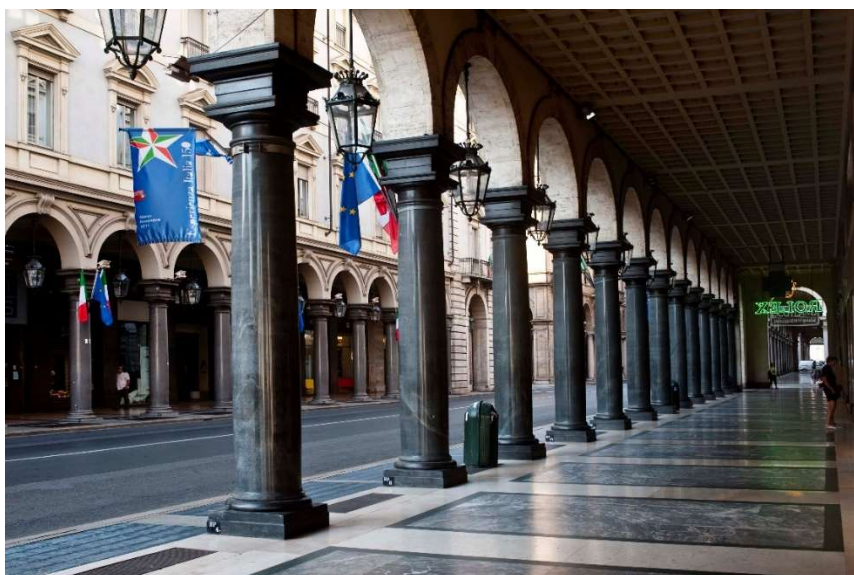


Figure 3.23: Columns of the S. Emanuele block in Via Roma (Torino) made up of *Vico Diorite*.

Rongio Stone (*Figure 3.21d*), exploited at Rongio Superiore (BI), is a quartz-diorite porphyry, a filonian rock with oligoporphyric structure and microcrystalline matrix. Its phenocrystals are idiomorphic plagioclase and lamellar brown biotite, often iso-oriented. It shows a medium- to fine-grained holocrystalline matrix composed by plagioclase, brown biotite, quartz and rare interstitial K-feldspar. In the 19th century, this stone was systematically exploited and widely used in the Vercelli and Biella areas, especially in the manufacture of plinths, slabs and shelves for balconies, sidewalk paving and other architectural elements. The quarry was gradually abandoned since 1880-1890.

Among its local uses it must be mentioned the church of S. Teonesto of Rongio Superiore, the arcades of the church of the Nativity of Brusnengo and the blocks priory masonry of San Pietro at Castelletto Cervo (BI) (*Figure 3.24*) (Piana et al., 2018).



Figure 3.24: External (a.) and interior arcades (b.) of priory masonry of San Pietro at Castelletto Cervo (BI).

Ponte Guelpa Stone (Figure 3.21e) crops out at Ponte Guelpa (BI) and it is a quartz-monzodiorite porphyry, a sub-volcanic rock with porphyritic structure. It presents phenocrysts of zoned plagioclase, biotite (replaced by chlorite), hornblende and quartz. It shows a holocrystalline matrix composed by quartz, K-feldspar, biotite and apatite. It was used for rural and local uses.

3.2.2.2 The gneiss

Verde Argento, Verde Selene (Figure 3.25a) and Verde Oropa (Figure 3.25b) belong to the Eclogitic Micaschists Complex of the Sesia-Lanzo Zone.

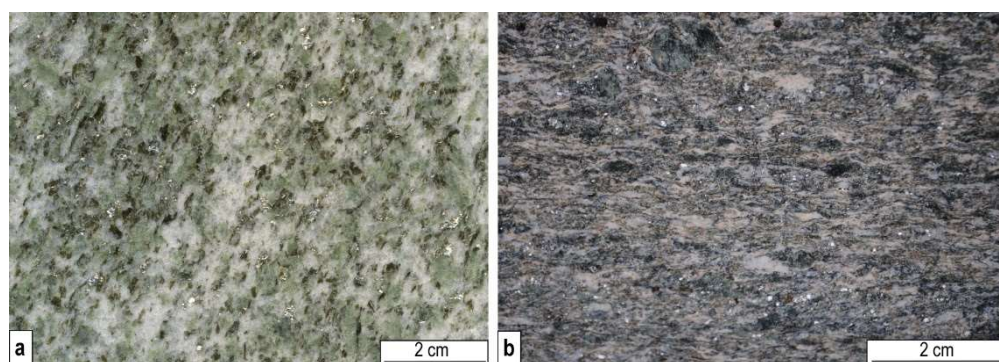


Figure 3.25: Macroscopic picture of *Verde Selene* (a.) and *Verde Oropa* (b.).

Verde Argento and *Verde Selene* (Figure 3.25a) are both giadeite orthogneiss, metagranitoid that recorded eclogitic facies conditions with isotropic texture.

Both are characterized by light-green color due to the occurrence of abundant giadeite replacing plagioclase and white mica pseudomorphs on biotite. Quartz and rare K-feldspar complete the paragenesis. *Verde Argento* is exclusively quarried in the Settimo Vittone Municipality (TO) with a production of about 1.500 m³/y of «workable stone» whereas *Verde Selene* is quarried in two quarries in the Tavagnasco Municipality (TO) with an overall production of about 20.000 m³/y (Sandrone et al., 2004).

They are both used as coating of few buildings in the Torino city center and for the Court building of Ivrea. Buildings, churches, cemeteries, sidewalks and supports of vineyards in the Municipalities of Borgofranco, Tavagnasco and Settimo Vittone, the structure of the underpasses of the Chivasso-Aosta railway, the stretch between Ivrea and Pont-Saint-Martin are all made up of these rocks. Applications are attested also in Aosta, Zermatt, Verbier, Crans-Montana (CH), Innsbruck (AT), Chamonix (FR).

Verde Oropa (**Figure 3.25b**) is a heterogeneous orthogneiss in which leucocratic domains alternate with melanocratic ones: the latter are green in colour and partially preserve eclogitic paragenesis. Its mineralogy is given by quartz, phengite, omphacite, garnet and epidote while sphene, apatite and zircon are present in accessory quantities. It was quarried right above the Oropa sanctuary in the province of Biella. As a consequence, it was used for many architectural elements of the Oropa Sanctuary such as the columns of the principal courtyard (see [Paragraph 3.3.6](#)).

Finally, *Verde Jaco* takes its name from the name of Giacomo Tibaldo, the biellese founder of the quarry at Pont Canavese (TO) in the lower Orco Valley. The peculiar name is due to the Biella surroundings dialectal contraction “Jaco” of the name Giacomo. It belongs to the Sesia-Lanzo Zone and it is a veined orthogneiss light gray to green in color. Its principal minerals are

quartz, albite, white mica, chlorite and epidote. It is characterized by abundant folded meta-aplitic intercalations (Gasco and Gattiglio, 2011). It is used for contemporary interior and external architectural elements for public and private buildings.

3.2.2.3 The marble

Pont Canavese Marble crops out at Pont Canavese (TO) and it belongs to the pre-triassic marble intercalation of the Sesia-Lanzo Zone. It is a dolomitic marble with isotropic, granoblastic and fine-grained texture, white to gray in color. It was employed in Torino during 18th and 19th centuries, for example for the statues of the Basilica di Superga and the statue of "Fama che incatena il Tempo" at Palazzo dell'Università (*Figure 3.26*).



Figure 3.26: Statue of "Fama che incatena il Tempo" at Palazzo dell'Università in Torino carved in *Pont Canavese Marble*.

3.2.3 Cottian Alps district

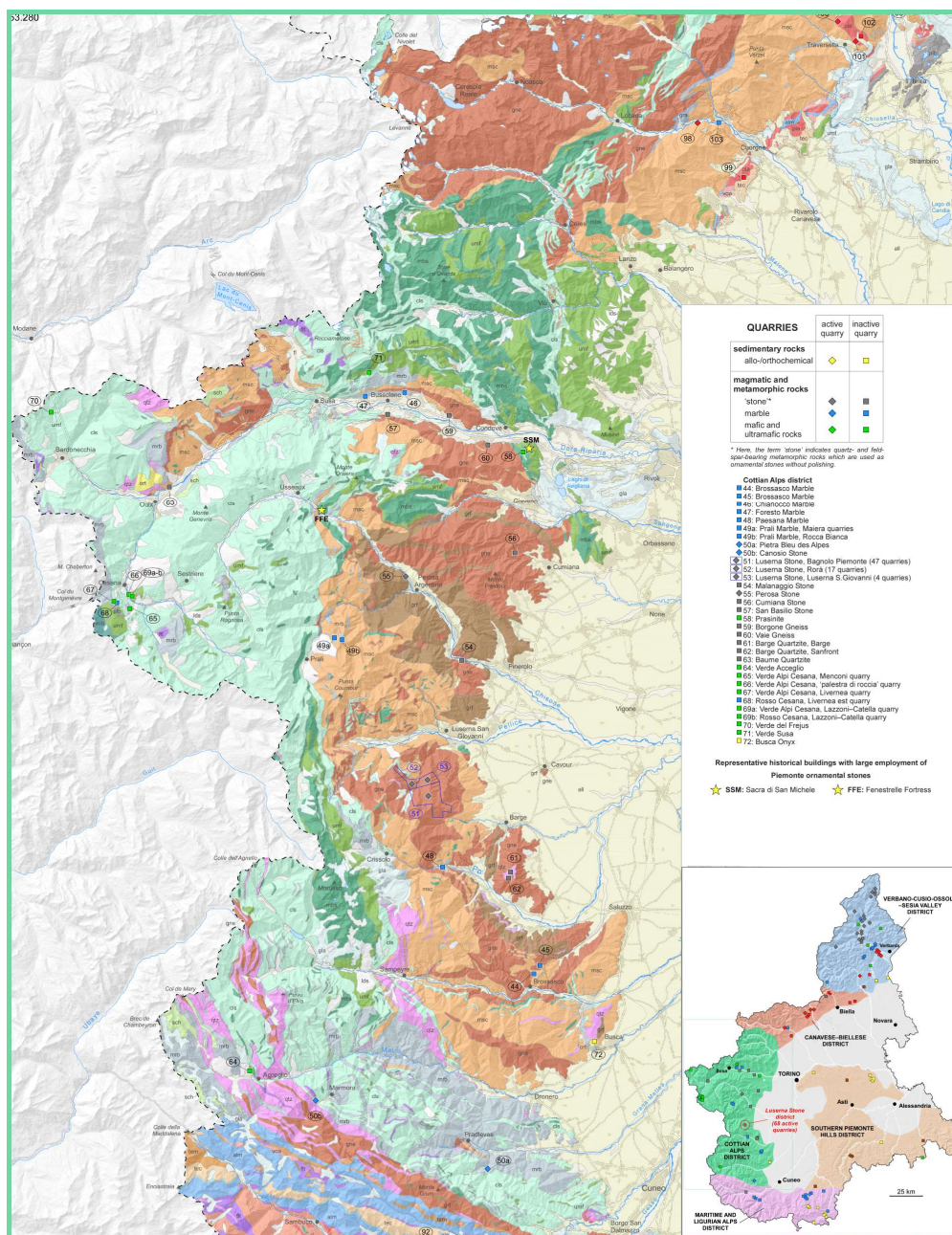


Figure 3.27: Cottian Alps district, detail of Geo-lithological map of ornamental stones of Piemonte region.

This quarry district is located in the inner part of the Cottian Alps (Figure 3.27) and its ornamental stones mainly belong to two different units of the Alpine

Axial Belt: the continental crust of the Dora Maira Unit (Penninic Domain) and the undifferentiated Liguria – Piemonte Oceanic Units. Due to the multitude of the lithotypes occurring in the area, the district, since Roman times, has been a source of ornamental stones over the centuries and still represents a reservoir of material used for architectural heritage (Borghetti et al., 2016).

The conspicuous mining activity in the Cottian Alps (Susa, Sangone, Chisone, Chisola, Germanasca, Pellice, Po, Varaita, Maira, and Grana valleys), is testified by all those buildings and monuments spread all over the Piemonte region built with “Cottian” rocks. Moreover, in the past, this activity represented one of the most important economic resource for the alpine valley’s inhabitants.

For instance, in the Susa Valley, for centuries the quarrying activity was led with simple and primitive techniques while, in the second half of the 19th century, important changes occurred. Indeed, thanks to the Industrial Revolution, the introduction of the explosive for mining purposes, and the arrival of the railway up to the upper Susa Valley, the transport of stone materials to Torino was remarkably improved. This first economic boom was followed by several periods of crisis, mainly related to the two war conflicts, which strongly damaged the region's economy. Currently the activity of extraction in these valleys has significantly reduced due to the competition of the international market and only the quarrying district of the Luserna Stone is able to resist well on the stone trade.

3.2.3.1 The Marble

Seven principal marbles can be recognized in the district: *Brossasco Marble*, *Chianocco Marble*, *Foresto Marble*, *Paesana Marble*, *Prali Marble*, *Bleu des Alps Stone* (**Figure 3.28**) and *Canosio Stone*. They belong to the Dora Maira Unit,

unless the Bleu des Alps Stone, which occurs in the Liguria–Piemonte Oceanic Domain.

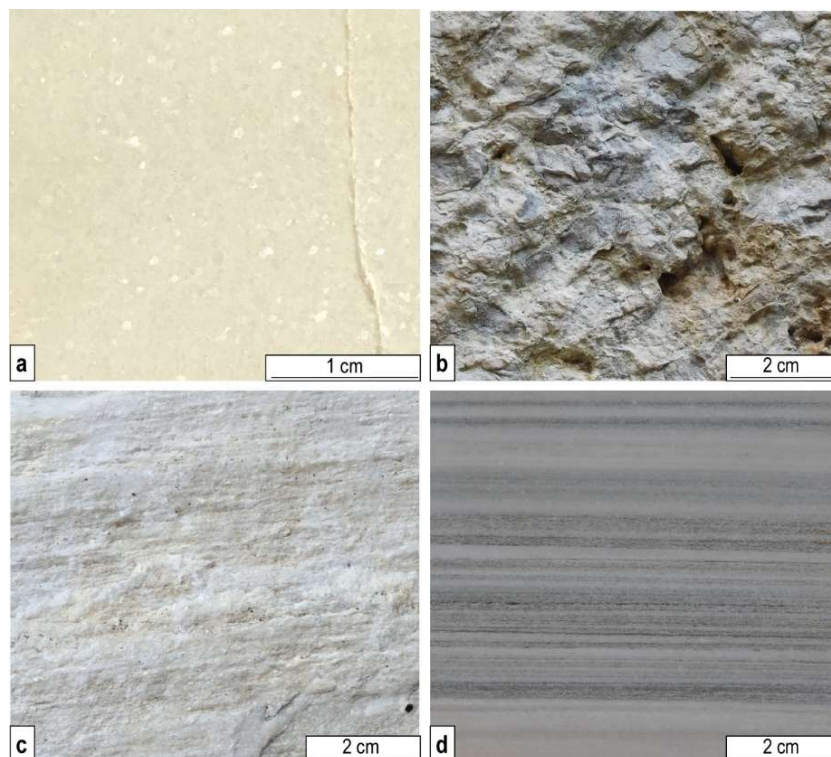


Figure 3.28: Macroscopic pictures of the most representative marbles of Cottian Alps district.
a. *Brossasco Marble* b. *Chianocco Marble* c. *Foresto Marble* d. *Prali Marble*.

The marbles of Dora Maira unit show different aspect, grain size, composition and workability, even though they were all adopted for buildings and statuary for both local uses and cultural heritage of the region. The Prali, Brossasco and Paesana Marble belong to the polymetamorphic basement of DM unit, whereas the *Foresto* and *Chianocco Marble* come from its Permian–Mesozoic metasedimentary succession, only affected by Alpine metamorphism.

Brossasco Marble (*Figure 3.28a*), cropping out in Rore (Varaita Valley, CN), belongs to the Brossasco-Isasca Complex, a thin slice of the Dora Maira Unit, which suffered ultra-pressure metamorphic conditions during Alpine age

(Compagnoni et al.,1995). It is a Triassic white coarsely crystalline isotropic marble consisting of calcite and minor dolomite and formed under high-grade metamorphic conditions (over 700°C). The marble has a massive, largely saccharoidal texture. Garnet (reddish brown), omphacite (light green), amphibole (dark green), white mica, and locally phlogopite (brown) associated with carbonate are also present. Among its principal uses, the statues and vases on top of the Juvarra façade of Palazzo Madama (*Figure 3.29*), the columns and architrave of the S. Filippo Neri Church façade, the corinthian capitals of the aedicule of the Superga Church in Torino Hill must be mentioned.

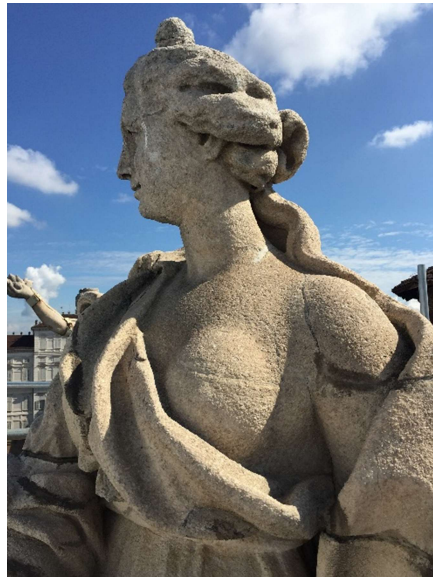


Figure 3.29: Statue in *Brossasco Marble* on top of the Juvarra façade of Palazzo Madama in Torino.

Paesana Marble was quarried in Calcinere Inferiore, a hamlet of Paesana (CN). It is a Paleozoic white marble characterized by isotropic structure, heteroblastic grain size, and granoblastic texture. The Paesana Marble belongs to the same unit of the Brossasco Marble and show quite similar petrographic features. Its quarry furnished a valuable white marble, widely used for aulic

buildings in Piemonte region during the 17th and the 18th century. Moreover, it was used for the portal of Casa Cavassa in Saluzzo (Borghi et al., 2005).

Prali Marble (Figure 3.28d) is a Paleozoic fine-grained calcitic marble. It is characterized by a banded structure, gray to green in color, with levels made up of femic minerals (amphibole, white mica and other silicates). It has been quarried in the Germanasca Valley since the 14th century and was also known as Perrero or Faetto Marble. The Rocca Bianca (a mountain 2,383 m a.s.l. located on the border between the municipalities of Prali and Perrero), from 1584 until 1968, was the most important quarry in terms of quantity of exploited material. Since 1981, the marble has been occasionally extracted in the Maiera quarry (western slope of the Rocca Bianca) with production rate of several hundred cubic meters per year (Borghi et al., 2016). This material shows some important uses: the pillars of the railing of Palazzo Reale (*Figure 3.30*), the statues of the Gran Madre di Dio Church, and the external sculptures of the Basilica Mauriziana.

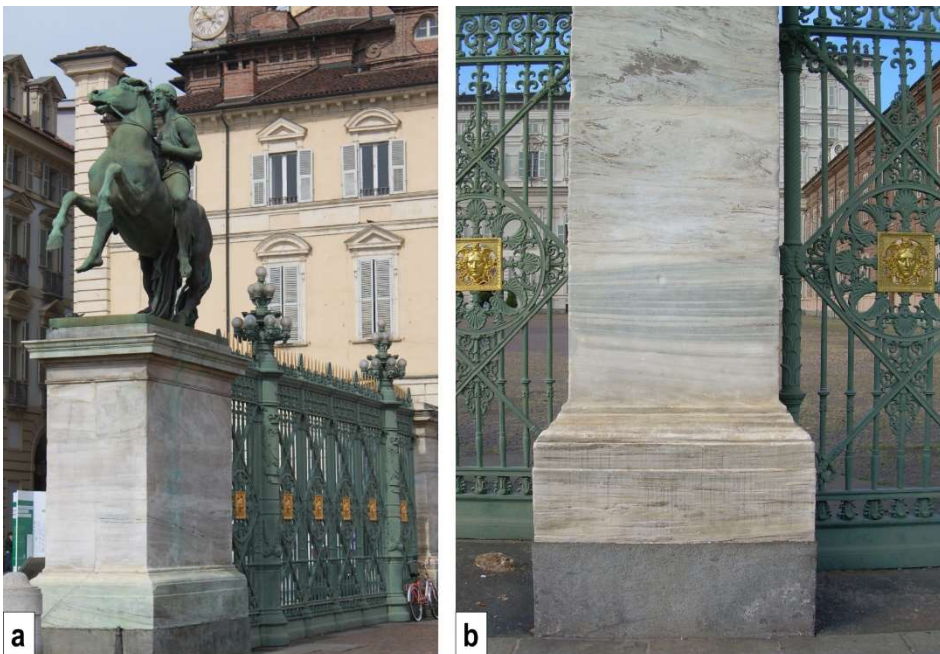


Figure 3.30: a. Pillars of the railing of Palazzo Reale in Torino made up of *Prali Marble*. b. Detail of banded structure of the marble.

Chianocco Marble (Figure 3.28b) crops out in Chianocco (Susa Valley, TO) and it is a Triassic dolomite brecciated marble, white to yellow in color, characterized by vuggy texture and weak foliation. In the past, the vacuolar structure was improperly attributed to the degradation in urban context (e.g. acid rains, pollution). Conversely, it has been demonstrated that it is a primary feature of the rock itself (Gambino et al., 2019).

It was used in Torino during the baroque era by the Savoy architect Filippo Juvarra (1678–1736) for historical buildings, such as the façade of Palazzo Madama, the plinths of the façade of the Cathedral, and the columns (now plastered) of the portico of Piazza San Carlo. It was also adopted for the Arch of Augustus (9-8 BC) in Susa (TO). The choice of this material was probably taken for two main reasons: the first was economic as the *Chianocco Marble* quarries were located closely to Susa; the second was political and related to the promotion of local materials by the Romans and the ruling family of the Cottian Alps (Agostoni et al., 2017).

Foresto Marble (Figure 3.28c) crops out in Foresto (Susa Valley, TO), close to Chianocco municipality. It shows a fine grain size, a planar fabric, and is white to ice-grey in color. It consists mostly of dolomite, although calcite crystals occur. White phengitic mica and chlorite define the anisotropy of the rock (Fiora and Audagnotti, 2001).

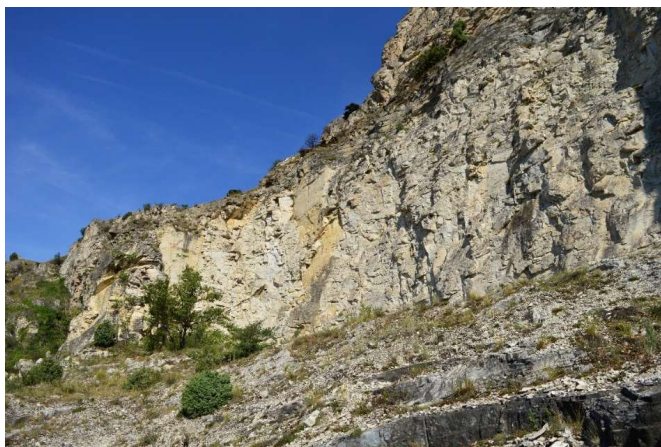


Figure 3.31: Ancient quarry of Foresto Marble.

As local uses, it was employed for the Arch of Augustus (Agostoni et al., 2017) (*Figure 3.32*), for the same reasons of *Chianocco Marble*, and for the portal of S. Francesco Church in Susa.



Figure 3.32: Arch of Augustus in Susa made up of *Foresto* and *Chianocco Marbles*.

In Torino it was used for some important buildings: the Cathedral façade (*Figure 3.33*), the pillars and plinths of the Sindone Chapel, the bases of the columns of the S. Carlo and S. Cristina churches, the interior of the S. Lorenzo Church.



Figure 3.33: Cathedral façade of Torino made up of *Foresto Marble*.

In the last decades, the similar chemical composition and the proximity between the Foresto and Chianocco quarries led to mistakenly merge these marbles in a unique lithotype. Recently, (Gambino et al., 2019) on the base of a detailed petrographic study, demonstrated that they are two distinct types of marble.

Bleu des Alpes Stone crops out in Saretto and Monterosso Grana (CN). It is a banded calcite marble, gray in color, with anisotropic structure, fine grained and granoblastic texture. It was adopted for public and private contemporary buildings and rural architecture of Piemonte region.

Finally, *Canosio Stone* crops out in Canosio (CN) and it is a calcitic marble, gray in color, with anisotropic structure. It was employed for local uses.

3.2.3.2 The Gneiss

From the past to the present day in the Cottian Alps district, the orthogneisses belonging to the Dora Maira Unit represent an important source of ornamental stones which can be gathered in seven varieties: *Luserna Stone*, *Borgone and Vaie Gneiss*, *San Basilio Stone*, *Cumiana Stone*, *Malanaggio* and *Perosa Stone* (Figure 3.34).

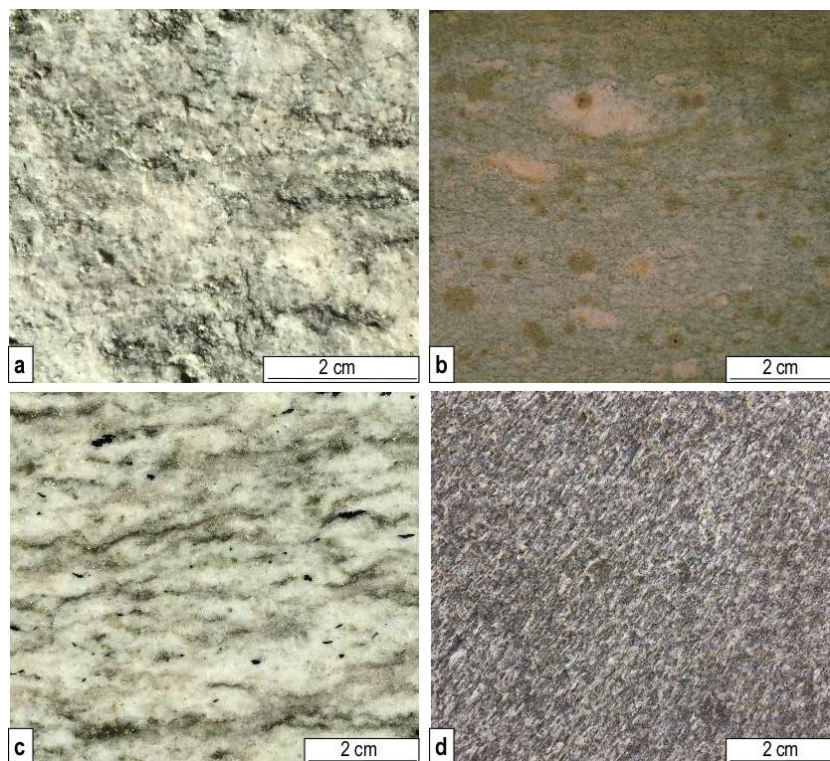


Figure 3.34: Macroscopic pictures of the most representative gneiss of Cottian Alps district. **a.** *Luserna Stone*; **b.** *Cumiana Stone*; **c.** *San Basilio Stone*; **d.** *Malanaggio Stone*.

Luserna Stone (Figure 3.34a) is one of the most representative and employed silicate stone in historical and current applications. It crops out over a large area (approximately 50 km²) along the border between Torino and Cuneo provinces. The *Luserna Stone* quarries are located in the Bagnolo Piemonte, Rorà and Luserna S. Giovanni municipalities. Nowadays, the *Luserna Stone* is the most important dimension stone quarried from the Dora-Maira Unit.

It shows a fissile texture and is easy to split along schistosity planes defined by the iso-orientation of phyllosilicates. The phyllosilicates are mainly represented by white mica crystallized under high pressure conditions and, in smaller quantities, biotite and chlorite. Magmatic porphyroclasts, represented by K-feldspar, in addition to quartz and albite, partially recrystallized during the Alpine metamorphic event, imparts a micro-augen texture to the rock (Sandrone et al. 2000). It is widely used for any kind of private and public buildings and architectural elements in the whole Piemonte region. Among the principal uses in Torino, it must be mentioned: the slabs covering the dome of the Mole Antonelliana (*Figure 3.35*), the paving of Piazza Castello and other squares of the city, the coverings of the old “Le Nuove” prison, the façade of the Historic Car Museum, the sidewalk of the Vittorio Emanuele I and Umberto I bridges.



Figure 3.35: Detail of the slabs covering the dome of the Mole Antonelliana made up of *Luserna Stone*.

In the past, the lower Susa Valley was characterized by the presence of numerous quarries designated to the exploitation of gneisses, namely the *Borgone* and *Vaie Gneiss*, and *San Basilio Stone*. *Borgone* and *Vaie Gneiss* were probably employed in the Bronze Age and certainly used during the Roman time. Currently, only the *San Basilio Stone* quarry is still active (Borghgi et al., 2016).

Borgone Gneiss crops out in Borgone municipality (TO) and it is an orthogneiss with augen texture characterized by centimeter-large porphyroclasts of K-feldspar embedded in a recrystallized matrix mainly consisting of quartz and albite, in addition to white mica and minor biotite. Epidote and rare garnet, representing the metamorphic products of magmatic plagioclase, are also present. Allanite, zircon, monazite and apatite occur as accessory minerals. It shows a weak foliation defined by white mica. In Torino, it was adopted for the Murazzi coatings and the new Wing of Palazzo Reale (columns, pilasters, cornices, capitals, rusticated basement).

Vaie Gneiss crops out in Vaie municipality (TO) and it is an orthogneiss with augen texture characterized by porphyroclasts of K-feldspar, quite similar to the Borgone gneiss. The main difference between these two stone varieties is the presence of primary muscovite (partially replaced by phengite) in the Vaie Stone (Cadoppi, 1990). It was employed in Torino for the columns, the plinths and the cornices of S. Cristina Church in Piazza San Carlo, the plinth of Palazzo Madama façade and the coating of the Basilica Mauriziana façade.

San Basilio Stone corresponds to the historic *Villar Focchiardo Gneiss* (Borghgi et al., 2016) and it is an orthogneiss light gray in color with a weakly defined foliation (*Figure 3.34c*). It is characterized by a lineation highlighted by tourmaline crystals, black in color. Its active quarry is located in Bussoleno (TO). In Torino it has been adopted for the basement of the pillars of the

Isabella bridge, the balustrade of staircase of Murazzi, the paved and the sidewalks. Moreover, in the Susa Valley (Sant'Ambrogio di Torino municipality), two sarcophagi of Savoy kingdom at the Sacra di San Michele are made up of this stone. Lastly, it is the material used for the 19th century artillery emplacements of Exilles fortress (TO).

The other important orthogneisses exploited in the Cottian Alps district in Chisone Valley are the *Cumiana Stone*, *Malanaggio Stone* and *Perosa Stone*; the latter is the only actively quarried gneiss at present.

Cumiana Stone (**Figure 3.34b**) crops out in Cumiana (TO) and it is an orthogneiss with augen texture characterized by millimeter-large porphyroclasts of pinkish K-feldspar and abundant white mica, which defines the foliation. It was adopted in Torino for the batteries coatings and the armlets of the arches of the Vittorio Emanuele I bridge (**Figure 3.36**, **Figure 3.37**), the skirting of Palazzo Carignano, and the coatings of Murazzi.



Figure 3.36: Vittorio Emanuele I bridge and Gran Madre di Dio Church on the right shore of the Po River.



Figure 3.37: Detail of batteries coatings and the armlets of the arches of the Vittorio Emanuele I bridge made up of *Cumiana Stone*.

Malanaggio Stone (**Figure 3.34d**) is an amphibole–biotite orthogneiss of quartz–diorite composition that intruded the Pinerolo Graphitic Complex of the Dora Maira Unit ca. 288–290 Ma (Bussy and Cadoppi, 1996). It is a medium-fine grained gneiss, dark gray in color due to abundance of biotite. It shows dark grey inclusions of mafic differentiates and sporadic white veins. Its quarrying activities began in the early 19th century with the opening of five quarries. Among the others, the F.lli Guglielminotti quarry in Malanaggio municipality was the most important and the most famous; despite this, because of the low demand of stone materials and the decreased availability of manpower after World War II, these quarries were closed.

This variety of stone was largely used in Torino for the columns of the façade of Gran Madre di Dio Church (**Figure 3.38**), the piers of the Umberto I bridge, the façade of the Basilica Mauriziana, the front steps of the Palace of Fine Arts

in the Valentino Park, the columns, the cornice, the crowning, the plates and the inner gallery of the Law Court Palace and for the lateral skirting of S. Cristina and S. Carlo churches (*Figure 3.39*).



Figure 3.38: Columns of the façade of Gran Madre di Dio Church made up of *Malanaggio Stone*.

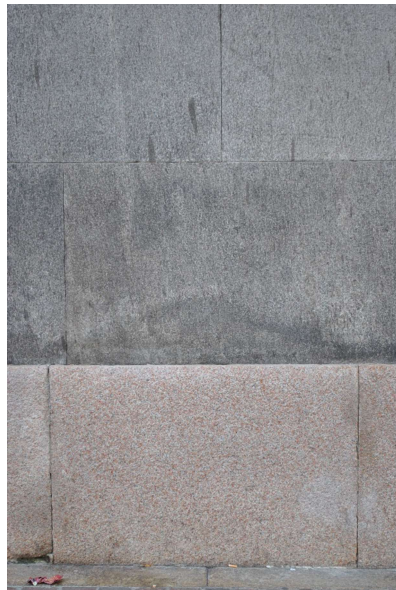


Figure 3.39: Detail of lateral skirting of S. Cristina and S. Carlo churches made up of *Malanaggio Stone* (upper part) and *Baveno Granite* (lower part).

Moreover, architectural elements of Castello di Racconigi (TO) and Fenestrelle Fortress (Fenestrelle, Chisone Valley) (see [Paragraph 3.3.4](#)) are made up of this stone.

Perosa Stone is a micro-augen gneiss similarly to the *Malanaggio Stone*. It is distinguished mainly by the presence of white mica (which is absent in the historic *Malanaggio* variety) which defines the main schistosity. The rock consists primarily of quartz, plagioclase, chlorite, biotite, hornblende, zoisite and clinozoisite; garnet, apatite and titanite occur as accessory minerals. The microstructure is weakly foliated; in places, the original sites of magmatic amphibole and plagioclase (mainly oligoclase/andesine) can still be recognized. The quarry is located in Brandoneugna, a village near Perosa Argentina (*Figure 3.40*).



Figure 3.40: *Perosa Stone* quarry.

In Torino it has been adopted for the plinth of the Modern Art Gallery and the external cladding of the Automobile Museum. It has also been used in

Sestriere ski station for the Church of S. Edoardo, and in Villar Perosa for the funeral chapel of the Agnelli family.

3.2.3.3 The Prasinite and the Ophicalcite

Commonly known as “Pietre Verdi”, the Prasinite and the ophicalcites of the Susa Valley belong to the Oceanic Units of the Western and Ligurian Alps and played a major role as ornamental rocks.

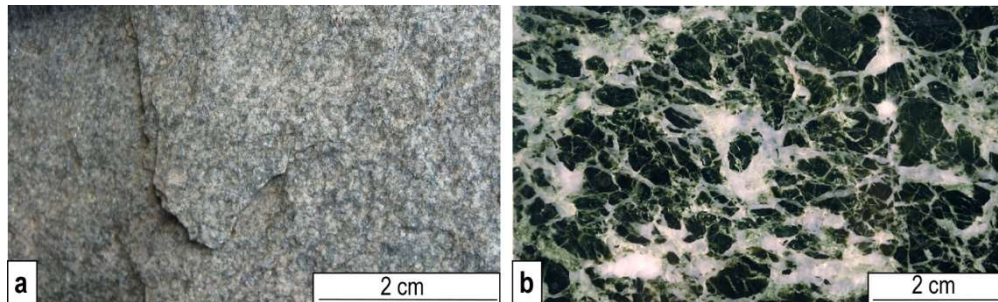


Figure 3.41: Macroscopic picture of (a.) *Prasinite* and (b.) *Verde Alpi Cesana*.

Prasinite is a green metabasite with tabular and fine-grained texture (*Figure 3.41a*). It is characterized by micro-augen texture due to peciloblastic albite. Its principal constituents are chlorite, amphibole, epidote, and albite. It crops out in the M. Pirchiriano, in the lower Susa Valley; on the top of this mount was erected the historic Sacra di San Michele (10th-13th century), an important abbey symbol of the Piemonte region, whose apses and flying buttresses are made up of this stone (see [Paragraph 3.3.1](#)).

Prasinite was also used in Torino, for example as architectural and decorative elements of the atrium and the 17th century façade of Palazzo Carignano, the skirting of the Regional Museum of Natural Sciences and the skirting of the Santissimi Martiri Church.

The meta-ophicalcites are known as “Marmi Verdi” (“Green Marbles”), and they represent a valuable and unique ornamental material. The *Verde Alpi Cesana* (*Figure 3.41b*) is the most famous, but it must be also mentioned the

Verde Acceglio, the *Verde del Frejus* and the *Verde Susa*. At present, all the quarries are inactive.

Verde Acceglio crops out near Acceglio (CN) and belongs to the Oceanic Units of Western and Ligurian Alps (**Figure 3.42**). It is a meta-ophicalcite with brecciated texture consisting of fragments of green serpentinite cemented by a fine system of white veins composed of pure calcite.



Figure 3.42: *Verde Acceglio* quarry.

Verde Alpi Cesana, even if part of a different geological unit (Chenaillet Unit; Ligurian – Piemonte domain, Polino, 1984), shows the same petrographic feature of *Verde Acceglio*.

The mining activity was localized within the Montgenevre - Chenaillet Massif, in the upper Susa Valley, at the border with the France, and involved an area of about ten square kilometers between the Val Gimot, the municipality of

Cesana Torinese, Monte Cruzeau, and Lago Nero. This material was firstly discovered at the end of the 19th century by Oreste Catella (a famous quarry owner) and was historically extracted from four quarries: Menconi, Palestra di roccia (“climbing wall”) (*Figure 3.43*), Livernea, and Lazzoni-Catella.

The Menconi quarry and the Liverna quarry were active from 1920 to 1970 and 1900 to 1976, respectively. *Verde Alpi Cesana* shows, at both sites, a remarkable heterogeneity in color. In both these sites the rock is characterized by chlorite, magnetite and calcite veins running almost parallel one the others. Palestra di roccia quarry had been exploited from the end of the 19th century up to 1930. Here, on the contrary of Menconi and Liverna quarries, the calcite veins characterizing the rock mass are almost perpendicular to each other. Iron and chromium oxides also occur.

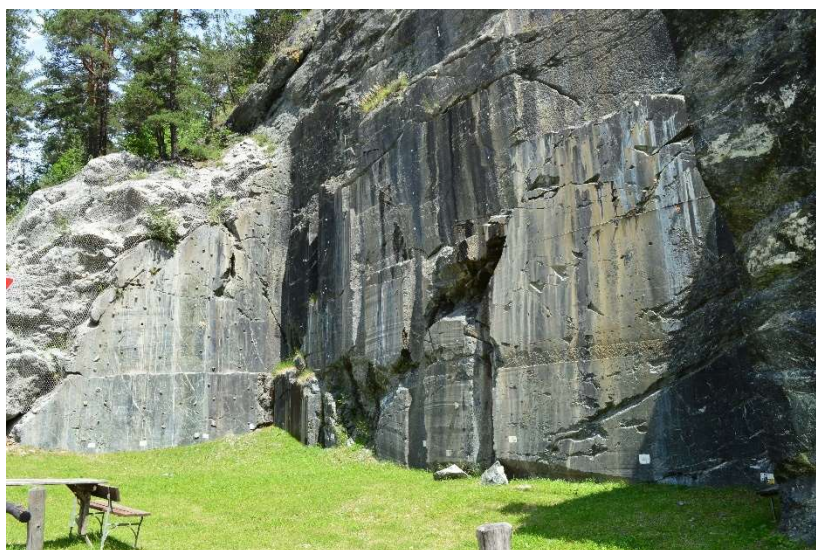


Figure 3.43: Palestra di roccia (“climbing wall”) quarry of *Verde Alpi Cesana*.

Finally, the material exploited in the Lazzoni-Catella quarry from the beginning of 1900 to 1940, shows also hematite and magnetite minerals (Di Pierro and Fiora, 1998).

This peculiar material shows many employments in Torino: the plinth of Palazzo di Città, Industria Sudalpina Gallery (internal and the external plinths, pavement, internal and external rounds, strips in exteriors) (*Figure 3.44*); the San Federico Gallery (pilasters, windowsill on balconies, jambs, frames, pavement); the hall of Sala degli Svizzeri at Palazzo Reale; the Beaumont Gallery; the Politecnico di Torino Faculty chair floor; the pavement of the foyer of the Teatro Regio; the decorations inside the chapels of the Cathedral; the internal flooring and other internal decorations of the Consolata Sanctuary.

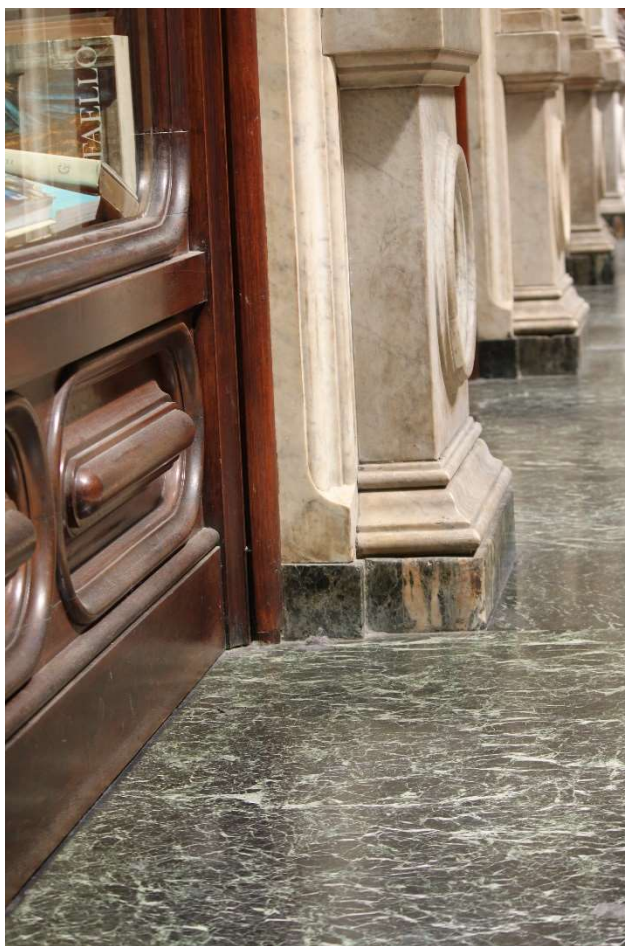


Figure 3.44: Detail of pavement of Sudalpina Gallery made up of *Verde Alpi Cesana*.

Moreover, it was also widely used in Cesana Torinese in several historical and ecclesiastical buildings. Finally, it presents another important employment for the internal architectural elements of the Vicoforte Sanctuary (CN). Finally,



Figure 3.45: Façade of Cartier jewellery store in Paris made up of *Verde Alpi Cesana*.

Verde Alpi Cesana has been adopted also out of Italy: it was very appreciated in France during the Empire (e.g. the portals and the plinth of the Annecy Cathedral and the exterior of the Cartier jewelery in Paris (**Figure 3.45**)).

)), in Belgium it was adopted for all the decoration of the Brussels Courthouse, in Bangkok for several buildings (Bonetto and Fornaro, 2005).

Alongside the extraction of the *Verde Alpi Cesana*, in the Livernea and Lazzoni-Catella quarries, *Rosso Cesana* was quarried too. This meta-ophicalcite differs from the *Verde Alpi* variety for its typical red-purple color due to a hematite groundmass.

Verde del Frejus crops out at Comba del Frejus, Bardonecchia (TO) and exploited from 1750 to 1915 and from 1929 to 1952 (Fiora and Gambelli, 2006). It belongs to the Internal Piemonte Zone in the middle Susa and consists of a meta-ophicalcite with a strongly brecciated texture made up of clasts of green

serpentinite cemented by a fine system of beige dolomite veins. Its principal minerals are abundant serpentine, dolomite, rare talc, chlorite and magnetite. The only ornamental use attested in literature (Fiora and Gambelli, 2016) are the windowsills, the benches and the jambs of the Railway station of Bardonecchia (TO).

Finally, *Verde Susa*, also known as “Verde Faussignana” or “Verde Fugera”, crops out in Falcemagna, a hamlet of Bussoleno (TO) in the middle Susa Valley. It is a meta-ophicalcite with a brecciated texture with fragments of serpentinite cemented by a fine system of veins composed of pure calcite. Its quarry is inactive now, but this stone was largely used in the Susa Valley for the founts and baptisteries. It also shows some important uses in Torino: the Sala degli Svizzeri of Palazzo Reale, the Beaumont Gallery, the Mole Antonelliana pavement. Furthermore, it was adopted for internal architectural elements in the Vicoforte Sanctuary (CN).

3.2.3.4 The Quartzite

Two quartzite rocks were exploited in this district: *Barge Quartzite* and *Baume Quartzite*.

Barge Quartzite (**Figure 3.46**) is another important dimension stone quarried in the Dora-Maira Unit, and it is exploited along the western slope of the Monte Bracco (in the Barge and Sanfront municipalities, east of Paesana village), in the lower Po Valley (Borghi et al., 2016). Geologically, it represents Permian–Triassic quartzarenite deposited during the post-Variscan marine transgression and subjected to Alpine-age metamorphism (Vialon 1966). It is a micaceous, fine-grained quartzite that displays a tabular and homogeneous appearance. It is a micaceous quartzite made up of quartz (>95%), yellow to gold in color, showing a fine-grained texture and well-defined foliation. Since prehistoric times it is known as “Bargiolina” and used as a substitute for flint

and celebrated by Leonardo da Vinci. It has been intensely exploited since the early 20th century (Borghini et al., 2016).

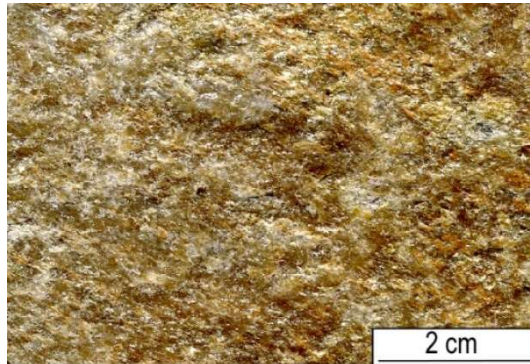


Figure 3.46: Macroscopic picture of *Barge Quartzite*.

Among its several uses in Torino, it must be cited the atrium of the S. Filippo Church, the paving of Via Roma (S. Casimiro and S. Costanza blocks), the roof coverings of the old “Le Nuove” prisons and some portions of the Via Po pavement.

Baume Quartzite crops out at Baume, Oulx (Susa Valley, TO) and it is a fine-grained micaceous quartzite with tabular texture and weak foliation (**Figure 3.47**). It was used for the steps in front of the presbytery and the roof covering of the church of Oulx, for the 18th century pavement of the Novalesa Abbey Church, and the roof covering of Exilles Fortress.

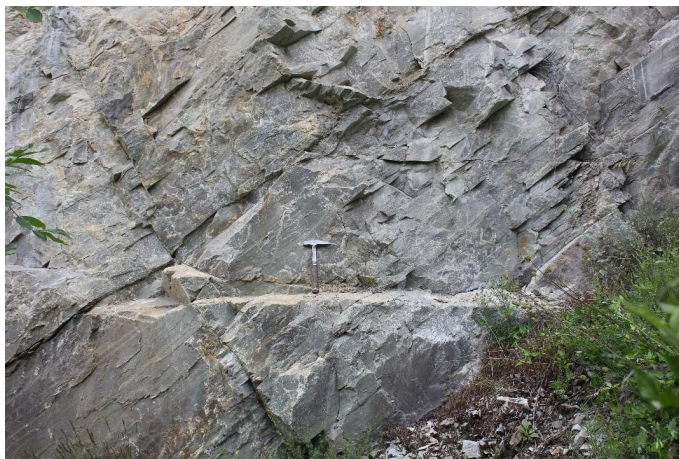


Figure 3.47: Detail of *Baume Quartzite* quarry.

3.2.3.5 The Alabaster

The only sedimentary rock, belonging to the undifferentiated sedimentary and metasedimentary units preserved along the main tectonic contacts, is the so-called *Busca Onyx* quarried at Eremo di Busca (CN), which is a very valuable stone material (*Figure 3.48*). It consists of a carbonate alabaster (speleothem) characterized by a translucent appearance and a regular alternation of yellow to light brown bands formed by calcite spar separated by thin sandy-pelite levels. The *Busca Onyx* was formed in veins systems within Triassic dolostone.



Figure 3.48: Macroscopic picture of *Busca Onyx*.

In Torino, it is employed for the S. Filippo Neri Church (altar and interiors), the Sala degli Svizzeri in Palazzo Reale, the Beaumont Gallery, and the interior of S. Francesco d'Assisi Church. It was also used in the interiors of the Basilica di Superga (TO) (see [Paragraph 3.3.2](#)), and the Vicoforte Sanctuary (see [Paragraph 3.3.5](#)) (CN) (Marengo et al, 2019).

3.2.4 Maritime and Ligurian Alps district

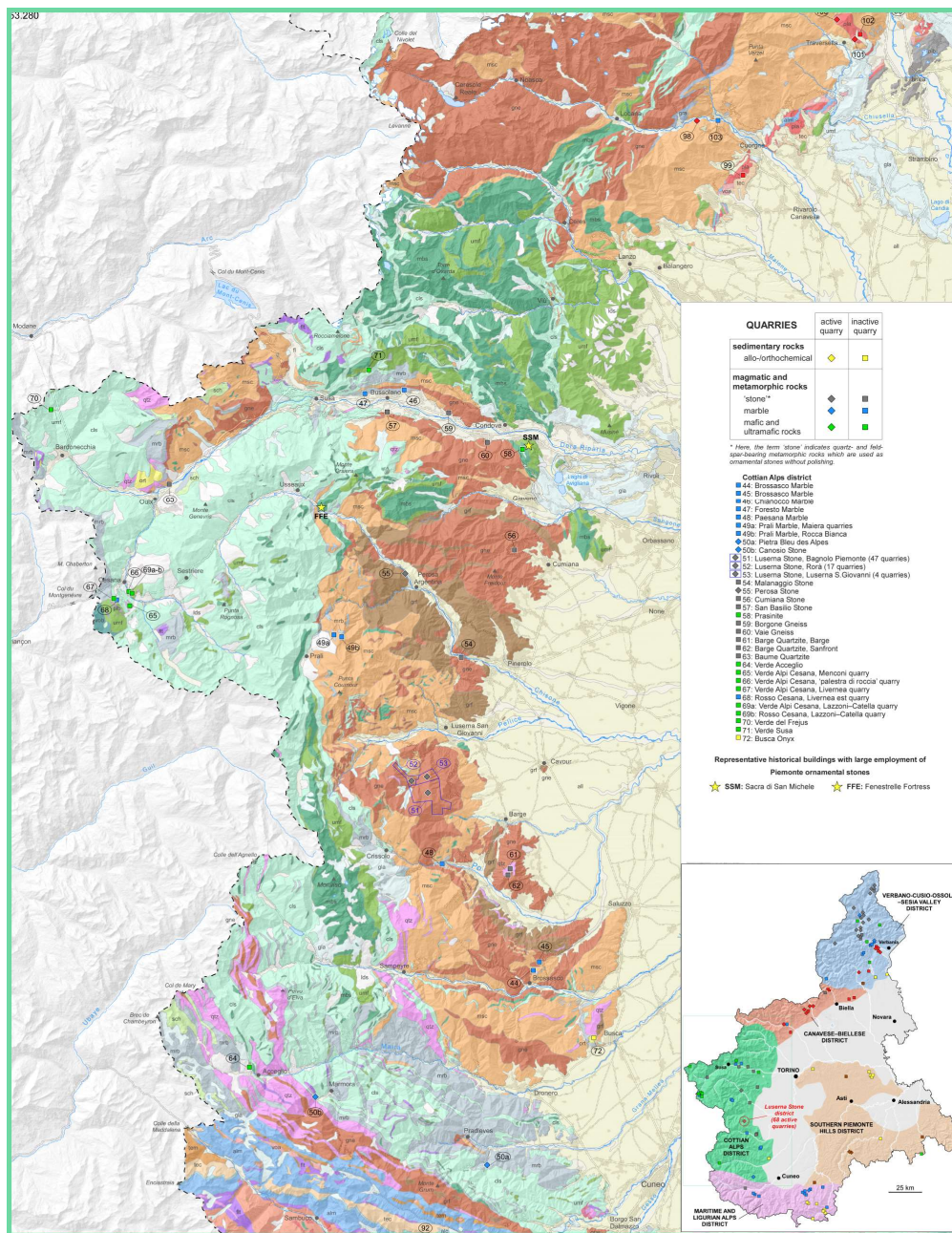


Figure 3.49: Maritime and Ligurian Alps district, detail of Geo-lithological map of ornamental stones of Piemonte Region.

This district includes the mountain area of southern Piemonte and, in particular, the Mondovì hinterland, historically known as “Monregalese”,

where a wide variety of marbles and sedimentary carbonate rocks was quarried (*Figure 3.49*). The marbles belong to the Internal Briançonnais units (Penninic Domain) of the Alpine Axial Belt, whereas the sedimentary carbonate rocks are part of the External Briançonnais successions of the Alpine External Belt.

It must be noted that all these rocks are historically commercialized as “marbles”.

The quarrying activity in the area flourished in the 17th and 18th centuries, when these materials, with their extraordinary chromatic variety, were used as structural elements (e.g. columns), for important buildings of the Piemonte Baroque (e.g. the Sindone Chapel in the Torino Cathedral and the Vicoforte Sanctuary). After this period of time, exploiting activity was considerably reduced and nowadays it is limited only to few quarries.

The feature of this district consists especially in the chromatic variety of the stone materials; in addition to black, grey and white “marbles” also purple, red, brecciated red, *Verzino* and yellow ones occur.

For over two centuries, the choice of different marble (and carbonate sedimentary rock) varieties from the Monregalese district just depended on the taste of the period and was not based on their geological feature. Marbles have always represented an exclusive material with an important symbolic value; and, even in modern times, the choice of marbles were directly linked to the central power. This is the reason why the colored “marbles” of this district, between the late 16th to middle 19th centuries, were used almost exclusively in Torino and in the headquarters of central power. With a few exceptions, local uses were allowed only when the marbles were no longer chosen by the kingdom.

These precious materials have been mainly used as small decorative elements, such as masonry ashlar, flooring, steps, inlays, balustrades and entablatures, although there are also examples of monolithic elements (mostly columns). Because of their unfavorable location (most of the quarries are located in mountain areas that are difficult to reach) and the limited volume of stone material that could be quarried, in the last centuries these “marbles” succumbed in the competition with the larger quarries in Toscana, Veneto and Lombardia (Badino et al., 2001).

3.2.4.1 The grey and black carbonate “marble”

The grey and black stones of this district (*Figure 3.50*) were mainly used during the 17th century in relation with the incoming of the famous architect Guarino Guarini in Torino. *Bigio di Frabosa* marble, for example, has never been used before the Guarini intervention in the dome of the Sindone Chapel. Five principal historical marbles can be recognized: *Bardiglio di Valdieri*, *Bigio di Moncervetto Marble*, *Bigio and Nero di Frabosa*, *Nero Nuvolato di Miroglio*, *Nero Vallone*.

In addition, *Nero di Ormea* and *Portoro di Nava*, two allochemical carbonate rocks historically known as “black marbles” (G.A.L. Mongioie, 2005), have to be cited.

Bardiglio di Valdieri (*Figure 3.50a*) crops out in San Lorenzo, Valdieri (CN) and it is a calcite marble with white mica, K-feldspar, and pyrite as accessory minerals. The *Bardiglio di Valdieri* began to be quarried in the Gesso Valley in the mid 18th century and in a few years, it replaced *Bigio di Frabosa*. Indeed, the resource of *Bardiglio* was considered the most valuable for the greater homogeneity of the material and the quarry of Valdieri, owned by the royal family, was more frequently used for those employment sponsored by the royal house.

It was employed in Torino for the Sala dei Medaglioni mantelpiece of Palazzo Reale and the central hall of the Town Hall; it was also adopted for the interior of the S. Filippo Neri Church, the Consolata Sanctuary, and the Spirito Santo Church. It is also one of the marbles employed for the interior of the Vicoforte Sanctuary (CN) (see [Paragraph 3.3.5](#)).

Bigio di Moncervetto marble was quarried at I Bassi locality, Moncervetto (CN) and it is a saccaroid marble gray in color characterized by large and white calcite veins. It is an heteroblastic marble consisting of calcite. Dolomite, white

mica, quartz and rutile occur as accessory minerals. It was widely used in Torino for interiors such as the halls of the Polytechnic. Another important use consists of the internal and external columns of the Crocetta Church.

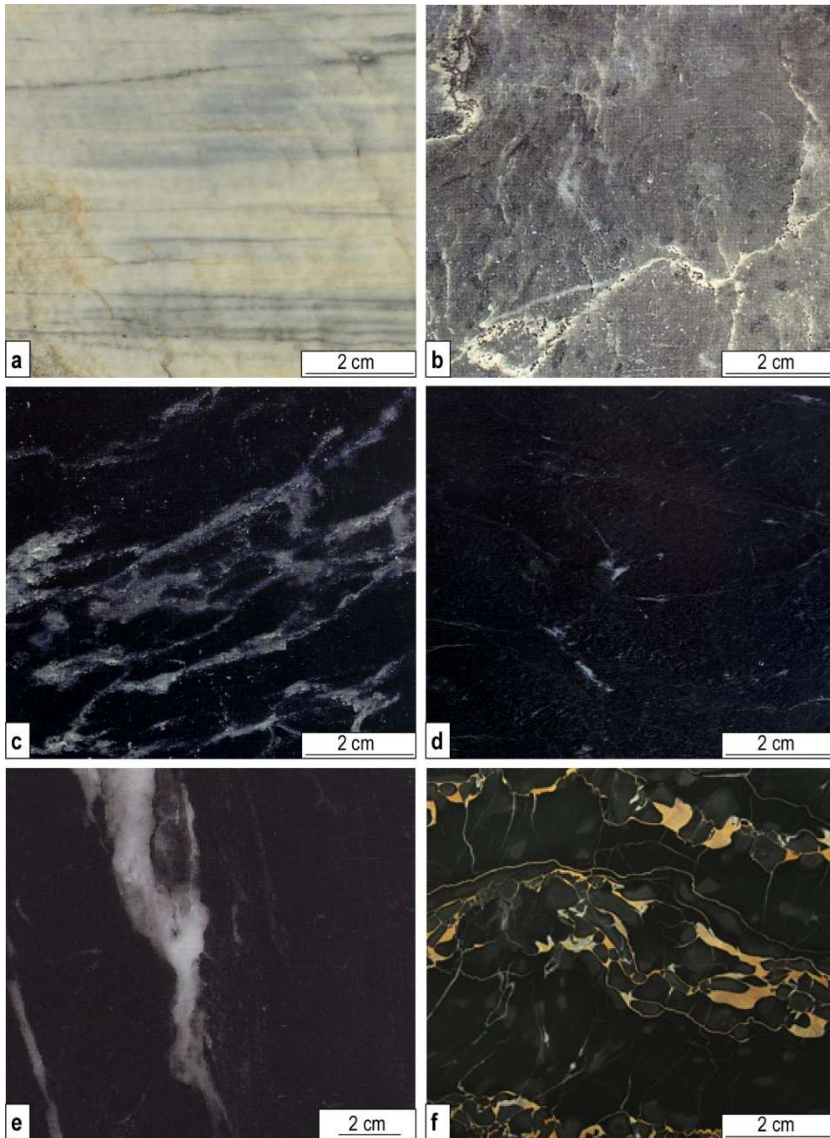


Figure 3.50: Macroscopic pictures of the most representative grey and black carbonate “marble” of Maritime and Ligurian district **a.** *Bardiglio di Valdieri*; **b.** *Bigio di Frabosa*; **c.** *Nero Miroglio* (G.A.L. Mongioie, 2005); **d.** *Nero Vallone* (G.A.L. Mongioie, 2005); **e.** *Nero Ormea*; **f.** *Portoro di Nava*.

For the Vicoforte Sanctuary (CN) it was adopted for the capitals and the bases of columns of the interior. Of international significance is the use of this rock

for the monolithic columns and other decorations in Annecy Cathedral (*Figure 3.51*) in France and for the Swiss National Bank in Lausanne (Catella, 1969).

Bigio and Nero Frabosa marble (Figure 3.50b), exploited in Frabosa (CN), is a calcite marble with fine grained texture, gray to black in color. It shows an heteroblastic grain size and anisotropic texture. The *Frabosa Marble* quarries were considered among the most important of the Southern Piemonte area. Their exploitation was particularly intense between the 17th and 18th centuries, especially for the construction the Vicoforte Sanctuary (CN), then for the entirely covering of the dome of the Sindone Chapel in Torino, and, in the following century, for stems and pedestals of the large interior columns of the Basilica of Superga (Torino Hill) (see [Paragraph 3.3.2](#)).



Figure 3.51: Monolithic columns and other decorations in Annecy Cathedral (France) made up of *Bigio di Moncervetto* marble.

Other important uses in Torino are the bases of the columns of the Gran Madre di Dio Church and the pediment and the tympanum of the S. Filippo Neri Church.

After the discovery of *Bardiglio di Valdieri* quarries, in the middle of the 18th century, *Bigio di Frabosa* was only used in secondary applications, such as skirting, steps and flooring.

Nero Nuvolato di Miroglio (**Figure 3.50c**) was exploited in Frabosa Sottana (CN) and its quarry was open at the beginning of the 20th century. It is a dark gray marble with several whitish, yellowish and reddish nuances (shaded). The most significant employments in Torino are the atrium of the Galileo Ferraris Institute and the internal decoration of Ossario dei Caduti of the Gran Madre di Dio Church.

Nero Vallone (**Figure 3.50d**) crops out at Frabosa Soprana (CN) and it is a black marble with fine grained texture and gray nuances (shaded). It was occasionally used during the 19th century and all along the 20th century. The altar of Montaldo Church in Mondovì (CN) is one of the most remarkable employment of this black marble.

Nero di Ormea (**Figure 3.50e**) is certainly the most significant sedimentary carbonate rock historically known as “black marble”. It was exploited at Isola Perosa, Ormea (CN) and it is a black fine-grained limestone where the color is due to the presence of organic matter; its texture can be uniform or veined. It was used for the steps and the portal of Santa Sindone Chapel in Torino and for the S. Rocco Chapel of the Vicoforte Sanctuary between the 20th and the 21th centuries (Badino et al., 2001).

Portoro di Nava (**Figure 3.50f**) crops out at Ponte di Nava in Tanaro Valley (CN) and it is a homogeneous black limestone characterized by a dense network of dolomite veins with subordinate light-yellow limonite (like *Portoro di Porto*

Venere). It was used during the 19th century for small interior decorative elements of the Vicoforte Sanctuary (CN) (Paragraph 3.3.5). It was also adopted for the high altar of S. Maria Assunta Church in Mondovì (CN).

3.2.4.2 The white marbles

Bianco and Verzino Frabosa marble (Figure 3.52) are known since Roman times (IV B.C.). It crops out at Frabosa Soprana (CN), and it is a white calcitic marble. It is characterized by a very fine grain, heteroblastic structure, sutured grain edges and anisotropic texture. Accessory minerals include quartz, white mica and dolomite.



Figure 3.52: Macroscopic picture of *Verzino Frabosa marble*.

In Torino it was used for the capitals and decorations of S. Carlo Church façade, for the decorations and statues of S. Cristina Church façade (*Figure 3.53*), for the capitals, the key masks and the crowning parapet of Palazzo Carignano. It was also employed in the Vicoforte Sanctuary (CN).



Figure 3.53: Statue of S. Cristina Church made up of *Frabosa Marble*.

Garessio white marble is a calcite marble with fine grained and anisotropic texture defined by white micas. It shows a strongly eteroblastic texture with sutured grains. It was exploited at Garessio (CN) as well as the *Bardiglio di Garessio* (dolostone dark gray in color with white veins). In Torino it was employed for the façade of the Corpus Domini Church.

3.2.4.3 The “persichini”

Thanks to the architect Filippo Juvarra, active in Torino since 1714, the standards of architectural decorations became close to the Roman style. The use of black marble was drastically reduced. In the early 1720s, the new King Vittorio Amedeo II designed a radical renovation finalized to the implementation of the Kingdom resources. In this context, new marble quarries were opened the road network for the transport of the materials improved, thus making them available for the Courts. Among the several new employed lithotypes, some varieties of the so-called “*persichini*” occur (*Figure*

3.54). They are polygenic and polychrome matrix to clast supported dolomite breccia with a reddish dolomitized matrix rich in iron oxides, showing different degrees of recrystallization. The distinctive red color and brecciated structure characterized the architectural style of the entire century (G.A.L. Mongioie, 2005).

Casotto Breccia, or *Persichino di Casotto*, coming from Casotto Valley, was employed in Torino for the inner columns of Gran Madre di Dio Church, for the columns of high altar and of two lateral one of the Basilica of Superga, for the royal tombs of Savoy, for the coatings of the Beaumont Gallery of Armeria Reale, for the coatings and the frames of S. Martiri Church.

Persichino di Corsaglia (Figure 3.54a), from Corsaglia Valley, is very similar to *Casotto Breccia* and it probably corresponds to the variety of "red persichino" mentioned by Juvarra in the instructions for the Superga pavement.

The "persichini" of Casotto and Val Corsaglia were significantly adopted, a few years earlier, in the construction of Sant'Uberto in Venaria Reale chapel (TO).

Persichino di Garessio (Figure 3.54b), also known as *Garessio red diaspro* and *Rosato di Rocca Rossa*, was exploited at Pian Bernardo quarry, in Trappa locality, Garessio (CN) and it was used in Torino for the portals of the Armeria Reale and for the decorations of the altars and the columns of S. Bernardino da Siena Church.

Villarchiosso Breccia (or *Persichino di Villarchiosso*) was quarried at Villarchiosso, Garessio (CN) and it was adopted for the Beaumont Gallery of the Armeria Reale in Torino and for the S. Maria Assunta Church in Montaldo Mondovì.

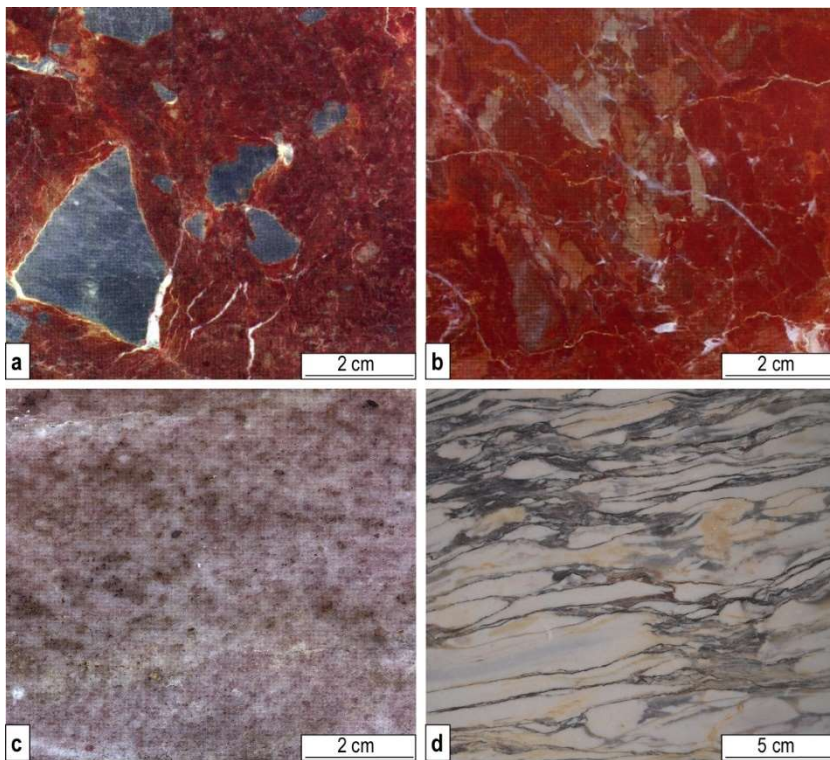


Figure 3.54: Macroscopic pictures of “persichini” and colored marbles of Maritime and Ligurian district. **a.** *Persichino di Corsaglia* (G.A.L. Mongioie, 2005); **b.** *Persichino di Garesio* (G.A.L. Mongioie, 2005); **c.** *Viola Piemonte* (G.A.L. Mongioie, 2005); **d.** *Cipollino di Valdieri*.

3.2.4.4 The colored marbles

The discovery of new materials lasted after the Juvarra death. Almost all the decorative works designed by the architect, but completed after his death, showed the use of marbles that he had never used before. His successor at court, Benedetto Alfieri (1699-1767), disposed the use of the most complete selection of Piemonte colored stone materials (G.A.L. Mongioie, 2005).

Seravezza di Moncervetto crops out at I Bassi, Moncervetto, Monastero Vasco (CN), in the same quarry of the *Bigio di Moncervetto Marble* (Figure 3.55).



Figure 3.55: Quarry of *Seravezza di Moncervetto* and *Bigio di Moncervetto*.

It is a calcite marble with a nodular aspect characterized by white portions alternated to violet to reddish parts with white mica. The grain is heterogeneous and the size is medium to fine. There is also dolomite, sometimes with perfect rhombohedra. The crystals are sutured with very embayed boundaries. Most crystals show polysynthetic gemination. The texture is anisotropic, in fact many calcite crystals are stretched according to a preferential direction of orientation. In Torino it constitutes the balustrades of the Gran Madre di Dio Church and interior uses of S. Teresa and S. Lorenzo churches. It is also employed for the S. Benedetto Chapel of Vicoforte Sanctuary (CN).

The last marble of the Moncervetto quarry is the *Viola Piemonte (Figure 3.54c)*, historically known as *Viola Val Corsaglia* or *Viola porpora antico*. It is a calcite marble, dark red to purple in color with pinkish spot and white calcite veins. It presents low percentage of phengite, dolomite, and quartz and its accessory minerals are apatite, fluoroapatite, magnetite, titanite, albite. *Viola Piemonte* is a medium grain marble with heteroblastic structure. The calcite crystals, tendentially sutured, have sharp to embayed boundaries and most of them show gemination. Overall, calcite has a rather deformed appearance. The

texture is anisotropic as it is characterized by a preferential orientation defined by white mica.

In Torino it was used for the pavement of the Polytechnic, for the interior coverings of the S. Teresa Church, and for interior uses of the S. Lorenzo Church. As the majority of the stones of this district, it was employed for interior uses in the Vicoforte Sanctuary.

Giallo Frabosa marble was exploited at Crevirola, Frabosa Soprana (CN), and it is a dolomite marble with homogeneous and granoblastic texture. Its accessory minerals are phengite, quartz, apatite, rutilo, and zircon and its yellow color is peculiar. It was occasionally used during the 17th century and continuously between 1700 and 1750. In Torino it was chosen for interior decorations of the S. Maria del Monte, S. Teresa and S. Lorenzo churches. It was also employed for the S. Uberto Chapel in Venaria Reale (TO) and the S.S. Apostoli Giacomo e Filippo Church in Frabosa Soprana (CN).

Val Tardita Breccia, despite its historical name, is a brecciated calcite marble gray in color with veins or lenses made up of white calcite. It shows a medium grained texture and presence of chlorite and quartz.

Cipollino di Valdieri (**Figure 3.54d**) was exploited in two quarries, Desertetto, Valdieri (CN) (**Figure 3.56a**) and Cima Cialancia, Demonte (CN) (**Figure 3.56b**), and it presents two varieties: *Cipollino dorato* and *Cipollino verde*.

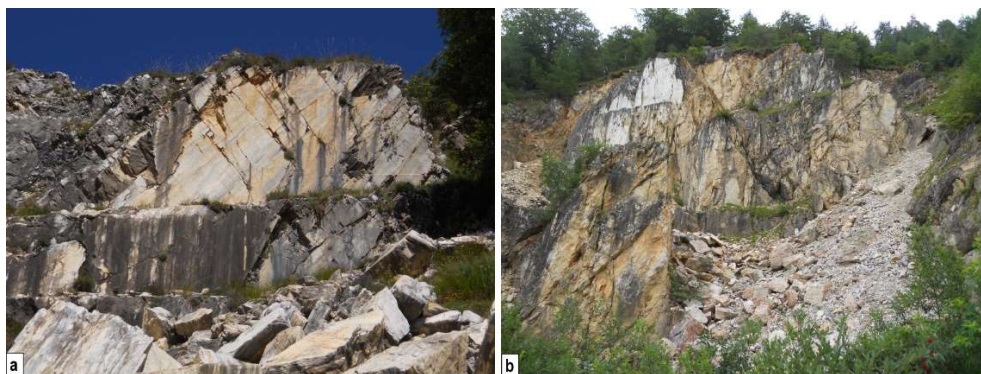


Figure 3.56: *Cipollino di Valdieri* quarries: **a.** Desertetto, Valdieri (CN) and **b.** Cima Cialancia, Demonte (CN)

It is a calcite marble with white mica, epidote, quartz, albite and chlorite. It displays heteroblastic grain size, granoblastic texture, and anisotropic structure. In Torino it was used for the Polytechnic graduation room and the Regio Theatre. It was also employed in Milano for the Madonna dei Poveri Church. Moreover, a column of *Cipollino Dorato* standing in an alcove overlooking the Westminster Cathedral Choir (Rogers, 2014).

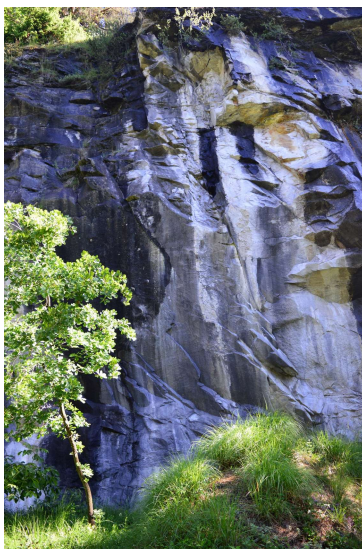


Figure 3.57: *Aisone Stone* quarry.

Finally, the *Aisone Stone*, quarried at Aisone (CN) (*Figure 3.57*), is an impure marble with abundant arenitic fraction made up of quartz, feldspars, white mica, and rare bioclasts (nummulitids, echinoid fragments); it was only adopted in the Stura valley for local and rural uses (Malaroda, 2000).

3.2.5 Southern Piemonte hills district

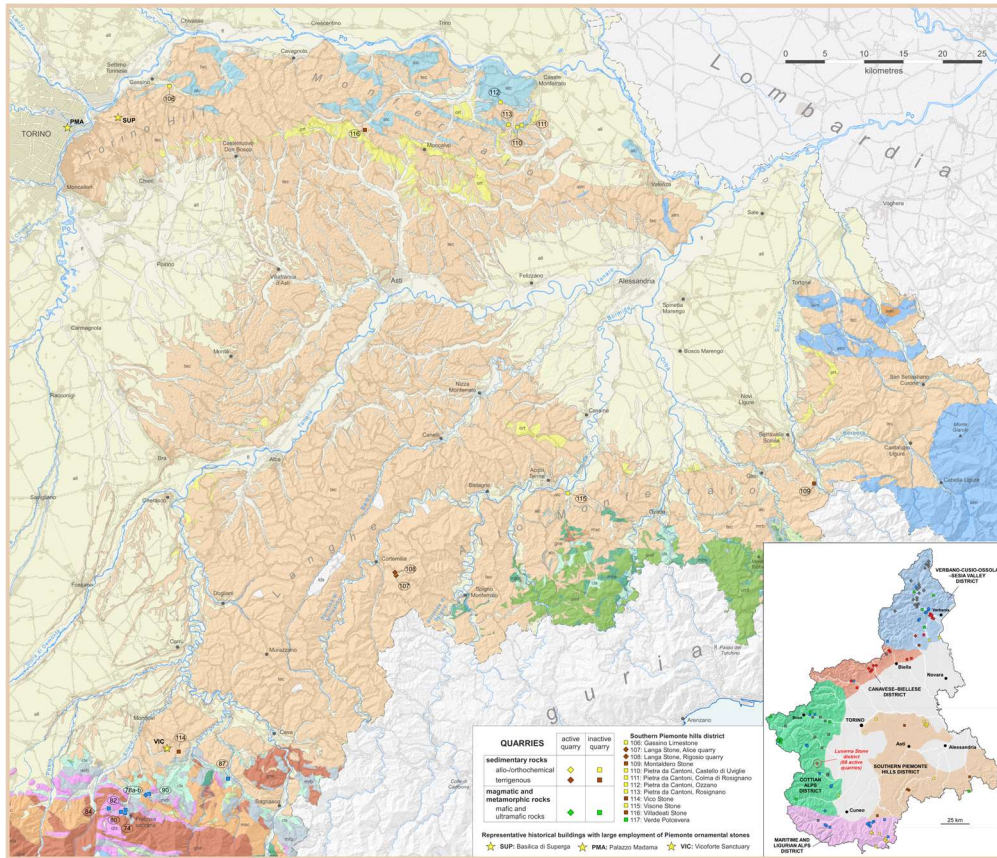


Figure 3.58: Southern Piemonte hills district, detail of Geo-lithological map of ornamental stones of Piemonte region.

This district corresponds to the hilly sector of the central and southeastern Piemonte, where some units of the Cenozoic sedimentary successions of the Tertiary Piemonte Basin were exploited as ornamental stones (*Figure 3.58*).

These lithotypes (carbonate rocks and sandstones), were mostly employed for the Romanesque churches disseminated in this huge area of Piemonte region in the High Middle Ages.

A metamorphic rock (*Verde Polcevera*) also belongs to the Southern Piemonte hills district. It was mainly used in the Liguria region.

3.2.5.1 Carbonate rocks

Gassino Limestone, *Pietra da Cantoni*, and *Visone Stone*, the carbonate rocks of this district, are very significant from the historical point of view.

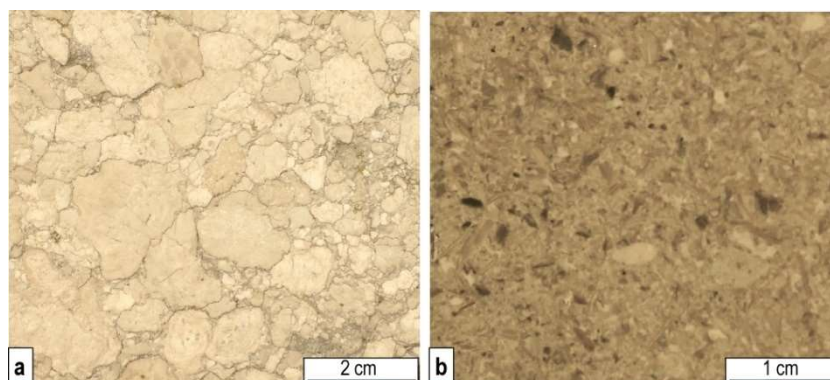


Figure 3.59: Macroscopic aspect of *Gassino Limestone* (a.) and *Visone Stone* (b.).

Gassino Limestone (*Gassino Stone* or *Gassino Marble*) (**Figure 3.59a**) is one of the most widely used carbonate rock in Piemonte. It was quarried in the Torino Hill area, near Bardassano and Gassino (TO), over three levels of banks – the De Filippi, the Caviglione and the “Bertot”- quarries (various authors used this term as synonym of “true Gassino limestones”).

This rock belongs to the Monte Piano Marl of Eocene age and consists of a whitish grain-supported biocalcirudite with a nodular structure. The grains are made up of lithoclasts and bioclasts (red algae, bryozoa, macroforaminifera, bivalve and echinoid fragments, corals, planktonic and benthonic foraminifera).

The quarry activity ended in the early decades of the 20th century, because of the complete exhaustion of the material and the insufficient mechanical properties. This rock is very susceptible to the atmospheric agents and pollution leading to the current deterioration of many buildings made up of *Gassino Limestone*.

It was widely used in the past, especially in the 17th century, by famous architects such as Amedeo di Castellamonte, Garove, Guarini, Juvarra,

Lanfranchi, and Vittozzi. The main works in Torino include the façade of S. Cristina Church in Piazza San Carlo; the cornice, the decorations, the ornaments and the columns of the portal and columns of the entrance hall of Palazzo Carignano; the cornice, the decorations and the columns of portal, columns of entrance, the balustrades of stairs of the Regional Museum of Natural Sciences; the columns of the arcades and the balustrades of Palazzo dell'Università (*Figure 3.60*); the basement of columns of the S. Filippo Neri Church façade; the external columns and the plinths of Basilica of Superga; the decorative elements of Palazzo dell'Accademia delle Scienze; the architectural elements of the Town Hall; the balustrade of the backside of Castello del Valentino. It was also adopted for several Romanesque churches of the Asti area (e.g. S. Martino Church in Buttigliera d'Asti; Alciati and Fiora, 2004; Campanino and Ricci, 1991).



Figure 3.60: Panoramic view (a.) and detail (b.) of columns of Palazzo dell'Università made up of *Gassino Limestone*.

Pietra da Cantoni, wrongly called “tuff”, is one of the most characteristic ornamental stone of Monferrato and was intensively quarried in the past. It is a glaucony-rich biocalcarenite rich in planktonic foraminifera that belongs to the *Pietra da Cantoni* Group of Burdigalian age. The term “Cantoni” indicates a half-meter large, cubic, “solid and elegant building material”. The *Pietra da*

Cantoni shows different varieties depending on the location of extraction. Such diversity is due to different grain sizes, the cohesion of elements related to the percentage of CaCO₃ in the matrix, and to the percentage of clay that, if abundant, may foster the meteorological deterioration of the material (Alciati and Fiora, 2004).

At the end of the 1960s, only few quarries exploited the raw material for the cement industry (Alciati and Fiora, 2004); nowadays, the production of this stone has ceased and most of the traces of the ancient quarries were totally obliterated by the vegetation. Some of these quarries were located at Castello di Uviglie, Colma di Rosignano, Ozzano, Rosignano (AL) (Timpanelli 2003). This ornamental stone was used from Roman times up to 1950-60. It was adopted for the S. Gaetano da Thiene Church in Torino, the Casale Monferrato Cathedral (AT), the Medieval houses of Ozzano Monferrato (AT), the S. Andrea Abbey in Vercelli and the S. Maria di Vezzolano Abbey (Albugnano, TO) (*Figure 3.61a-d*). Inside the rock were dug the so-called “infernot” (sort of winery) at Cella Monte, Rosignano Monferrato, Sala, Cereseto, Ottiglio, Moleto, Vignale (AL). The bell tower of S. Nazario and Celso Church in Montechiaro d'Asti is made up with alternation of Pietra da Cantoni and terracotta. It was also employed for the S. Secondo Church in Cortazzone and for many local buildings in Monferrato (AT) until 1950 (Sassone, 2005).

The *Visone Stone* (*Figure 3.59b*) is a whitish to grey biocalcarenite and biocalcirudite with macroforaminifera (*Operculina*, *Amphistegina*, *Miogypsina*), bivalves, echinoids, and red algae. It presents a scarce arenite to pelite siliciclastic fraction. It belongs to the Visone Formation (Burdigalian) and the quarries were located at Visone (AL).

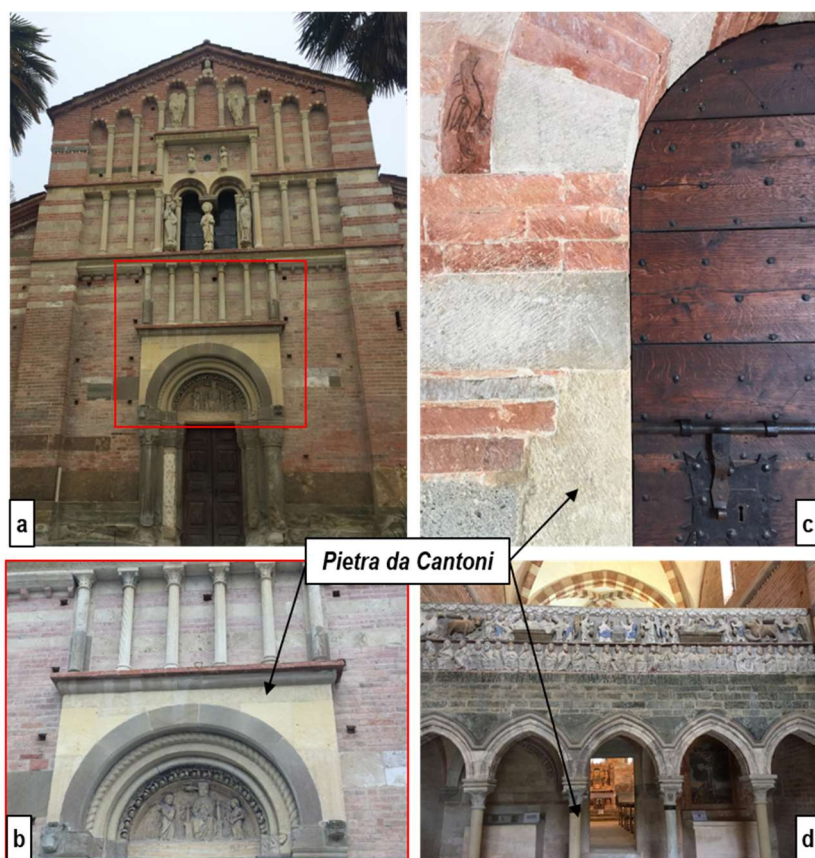


Figure 3.61: Abbazia di Vezzolano: **a. b.** Façade and detail of coating made up of *Pietra da Cantoni*; **c.** Wall of the courtyard in which *Pietra da Cantoni* is used; **d.** Columns in *Pietra da Cantoni* of the interior.

It was extracted from the Roman age and used over the centuries as dimension stone and for the production of lime. A discontinuous use of this rock emerges until the 20th century. An emblematic case of reuse of Roman material in medieval times has been identified in the Crypt of the Cathedral of Acqui Terme (AL, 11st century). Starting from the 15th century there is a reuse of this material. Indeed, it was frequently adopted for decorative apparatuses of mansions and churches. In the following century it was used in monumental complexes such as Santa Croce di Bosco Marengo (AL). It is often employed for the column as monolithic shaft, in the arcades and loggias, the

architectural elements characterizing the local courtly architecture (Allemani and Gomez Serito, 2018).

3.2.5.2 The sandstone

The large family of sandstone covers stones with different grain size, porosity, cement or matrix, compactness and composition. They were widely used as cladding stone, even in historic buildings. Four important rocks of Burdigalian-Langhian age (*Langa Stone*, *Montaldero Stone*, *Vico Stone* and *Villadeati Stone*) belong to this district.

Langa Stone is a quartz and mica-rich sandstone with calcite cement. It belongs to the Cortemilia Formation of Burdigalian-Langhian age and its principal active quarries are Alice and Rogosio, in Cortemilia area (CN).

It is a historic material for ornamental and construction applications. In ancient times, it was taken directly from the cultivated fields, there was no quarry. It is often a reused material. It was firstly employed by the Romans, as testified by headstones with epigraphs.

Over and above important historic uses, *Langa Stone* is still adopted in modern applications (e.g. local rural buildings); it was easy to work and offers fair durability characteristics. Among its uses, it must be mentioned the Churches of Roccaverano (AT), Calamandrana (AT) and Saliceto (CN) (G.A.L. Mongioie, 2005; Alciati and Fiora, 2004).

Montaldero Stone is a grey sandstone with bioclasts (bivalves, corals, gastropods) cropping out at Arquata (AL) and belongs to the Costa Montada Formation Burdigalian). During Roman times, at Arquata, the quarry work was the primary activity of the territory. Indeed, it was used for the construction of the ancient Libarna, especially for the large supporting structures such as columns, portals, paving slabs and aqueducts, the large pylons of the bridge that connected Libarna to the island of Precipiano, the S.

Maria and S. Antonio Abate churches and the Municipal Palace. It was also adopted for the Collegiate Church in Novi (AL), the Villa Caffarena in Serravalle Scrivia (AL) and, in Liguria, for the Marassi prison in Genoa.

Vico Stone is a yellow to grey quartz-feldspar rich sandstone with cross bedding, characterized by a strong dolomite cementation. It belongs to the San Paolo Formation (Burdigalian) and it was quarried near Vicoforte (CN). It was used for the external coating of the Vicoforte Sanctuary (*Figure 3.62*), the Mondovì Cathedral, and the Missione Church of Mondovì (CN) (G.A.L. Mongioie, 2005).



Figure 3.62: *Vico Stone* on the Vicoforte Sanctuary façade.

Villadeati Stone is a medium to coarse grain lithic greywacke with abundant matrix and dolomite cement; the clasts are made up of carbonate fragments, quartz, feldspar and serpentinite. It belongs to the Cardona Formation (early Oligocene) and it was quarried at Dietro Castello and Priocco quarries in Villadeati municipality (AL).

This rock was primarily used for the construction and decoration of the local houses, establishing a close connection between the resources of the territory

and the environment. Nowadays, only few traces of the main civil (castle and palaces) and religious architectures built with this sandstone remained. Indeed, most of them were demolished, remodeled and repeatedly plastered. The *Villadeati Stone* played a leading role in the Renaissance architecture of Monferrato. It constitutes a territorial specificity as its use characterised a significant phase in the history of the local marquisate. For this reason, the aforementioned *Pietra da Cantoni* was not the only local stone used both in the medieval period and in modern times. Compared to the *Pietra da Cantoni*, the *Villedati Stone* responds more effectively to the mechanic stresses (compression and shear) induced in the architectural use. This property may have led to its massive exploitation when the evolution of architectural proportions, during the 15th and 16th centuries, required columns with increasingly slended shafts, larger capitals and pieces of architraves for the entablatures.

Among its uses it must be mentioned the S. Maria Nuova Church in Lu Monferrato, the stones for the old sink in Ozzano, the wellhead near S. Agata Church in Pontestura, the portal of S. Martino Church in San Salvatore Monferrato, the Giovanni Giolito palace, the S. Caterina Church in Trino, the portal of S. Maria Church in Villadeati. Moreover, it was used in Casale Monferrato for the Town Hall, the S. Caterina monastery, the Gaspardone, Vurlando, Asinari, Del Carretto palaces and the portal of S. Domenico Church (Perin, 2016).

3.2.5.3 The ophicalcite

Verde Polcevera is the only metamorphic rock of this district. It is a serpentinite breccia of intense green color crossed by white carbonate veins. It was quarried at Cave di Pietra, Voltaggio (AL) and it belongs to the Voltri Massif. Two commercial varieties exist: a first quality «Verde Polcevera» with dark

green background and small white spots and branches fading into green; a second quality «Verde Polcevera», richer in white parts and branches.

In Piemonte it was used for the Vicoforte Sanctuary (CN). In Genova city center (Liguria, Cimmino et al., 2004) it was employed for the S. Lorenzo Cathedral façade of 11st century and Cristoforo Colombo Tunnel in Piazza Dante.

3.3 Representative monuments of Piemonte region

Stone resources have always been one of the main sources of material in the construction field and, in particular, an important cultural element as they were used as raw material to create works in the field of architecture that are now part of the cultural heritage. Even in Piemonte stone has always been used in historical and contemporary buildings, monuments and urban furniture, demonstrating the close link that exists between the urban area and natural stone resources and emphasizing the role that stone has had in culture and economic wealth of the cities.

The use of local stone resources since ancient times has also led to the construction of numerous military and religious buildings in the various Piemonte valleys. Among them six historic buildings have been reported on the Geo-lithological map, based on their historical and architectural significance, but also for the fact that they represent an example of the use of stone materials: *Sacra di San Michele, Superga Basilica di Superga, Palazzo Madama, Fenestrelle Fortress, Vicoforte Sanctuary* and *Oropa Sanctuary (Figure 3.63)*.

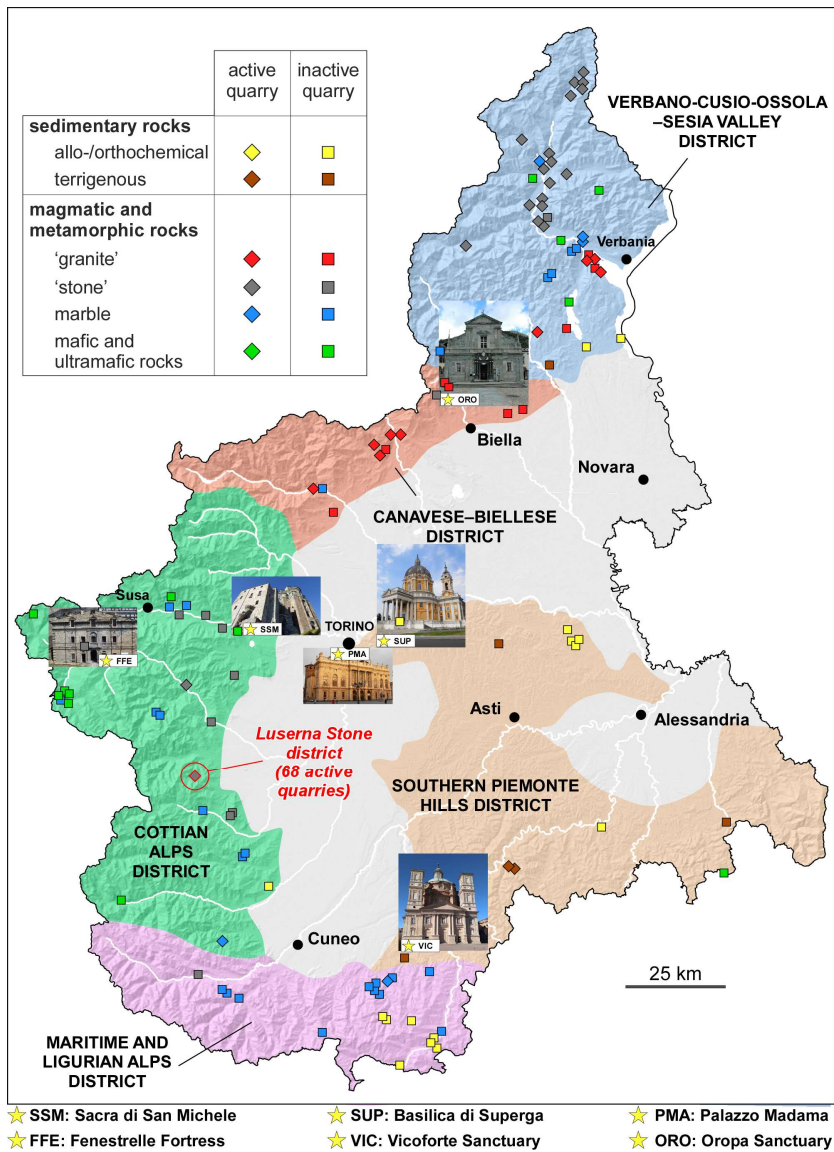


Figure 3.63: The six historic buildings represent an example of the use of stone materials in Piemonte region.

3.3.1 Sacra di San Michele

The Sacra di San Michele (*Figure 3.64*), symbol of Piemonte region, is an ancient abbey built between in the 10th century on the top of Pirchiriano Mount, at the outlet of Susa Valley 40 km from Turin. It is dedicated to the cult of the Archangel Michele, defender of the Christianhood, and is located along a route of pilgrim age which runs from Mont Saint-Michel in northern France to Monte Sant'Angelo in southern Italy. Nowadays, the Sacra di San Michele has become a destination for many visitors from all over Europe (www.sacradisanmichele.com).



Figure 3.64: Sacra di San Michele. Ph. Elio Pallard.

The peculiar characteristic of this building is that it was built around a rocky outcrop of serpentinites.

All the lithotypes used come from sectors of the Susa Valley close to the Sacra di San Michele, with the only exception of the *Luserna Stone* (*Figure 3.65a-d* and *Figure 3.66a* and *b*). This monument presents the use of the following

ornamental stones: *Prasinite*, *Vaie Stone*, *Foresto Marble*, *Baume Quartzite*. Other kind of lithotypes, that are not traditionally used as ornamental stones, were adopted: serpentinite, eclogite, calcschists, metagabbros, garnet-rich micaschist.

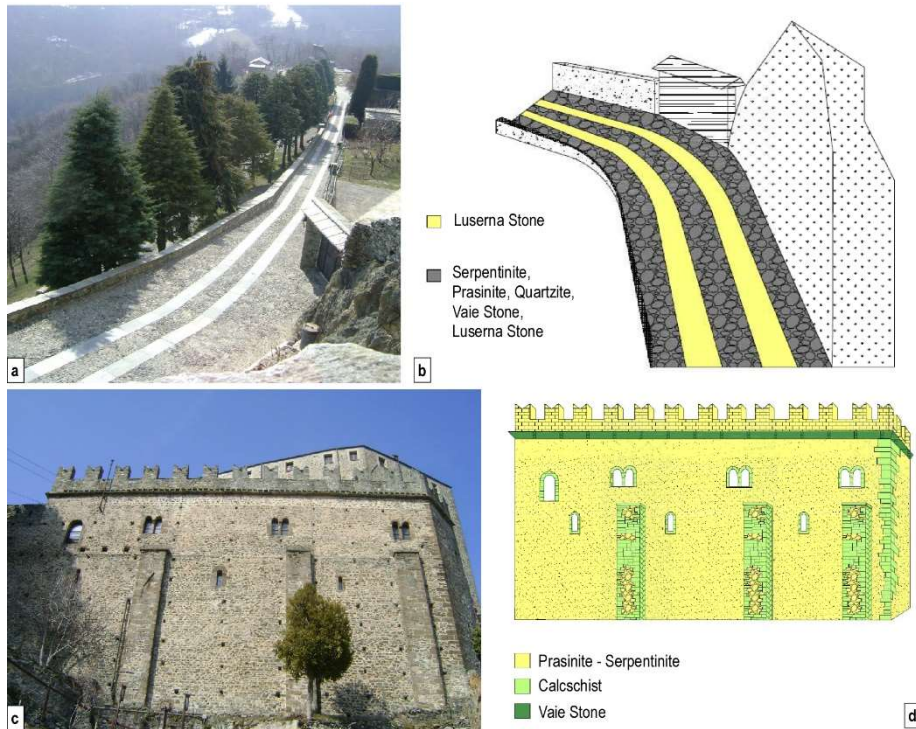


Figure 3.65: a. and c. Pictures of the access road to Sacra di San Michele and the “Foresteria Vecchia” building and their petro-architectonic relieves (b. and d.; Gambino, 2014) in which the used ornamental stones are highlighted.

The perimeter walls of the abbey consist essentially of irregular blocks of serpentinite, prasinite (Liguria-Piemonte Oceanic Units) and micaschist (Dora Maira Massif). The entrance door is made up of blocks of garnet and chloritoid calcschists as well as prasinite (*Figure 3.66c and d*).

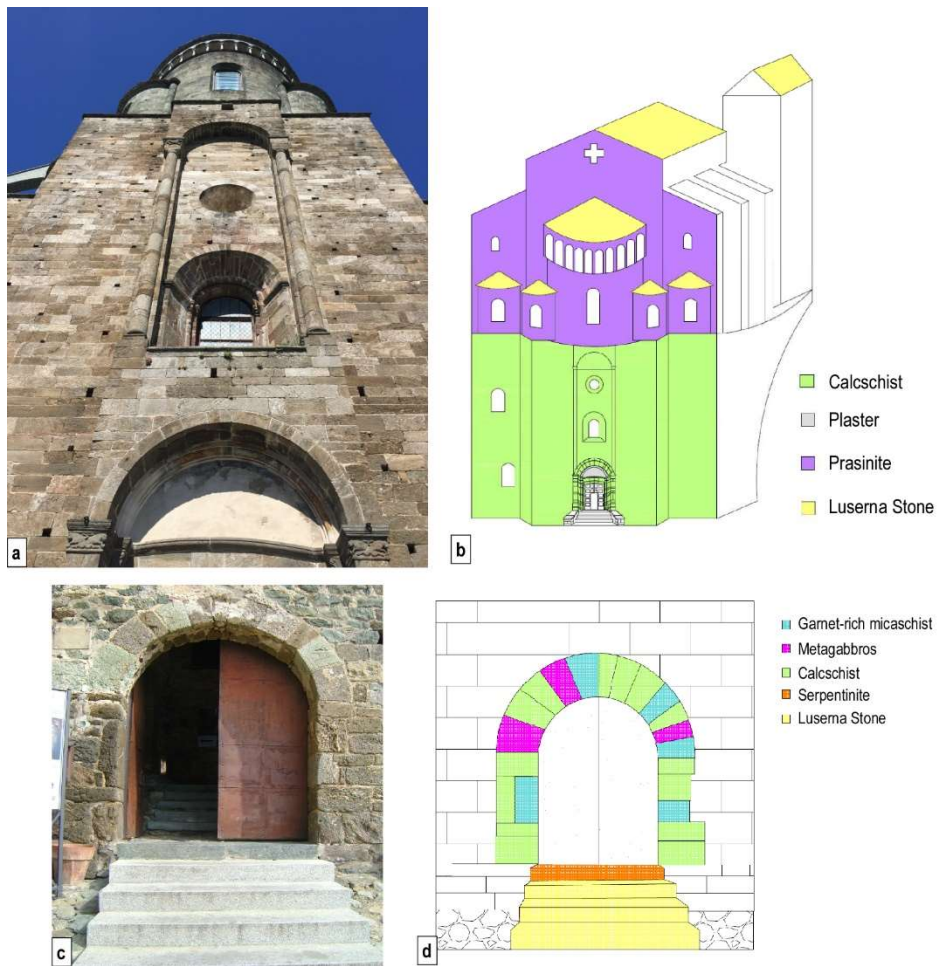


Figure 3.66: a. and c. Pictures of the East building of Sacra di San Michele and the entrance door and their petro-architectonic relieves (b. and d.; Gambino, 2014) in which the used ornamental stones are highlighted.

The internal staircase leading to the upper basilica, named Staircase of the Dead, has steps in augen-gneiss, replaced in the upper part by prasinite and micaschist (*Figure 3.67a-d*): it introduces the Portal of the Zodiac (*Figure 3.68a and b*), a great expression of the Romanesque art of the twelfth century. Columns and capitals are made of different varieties of marble.

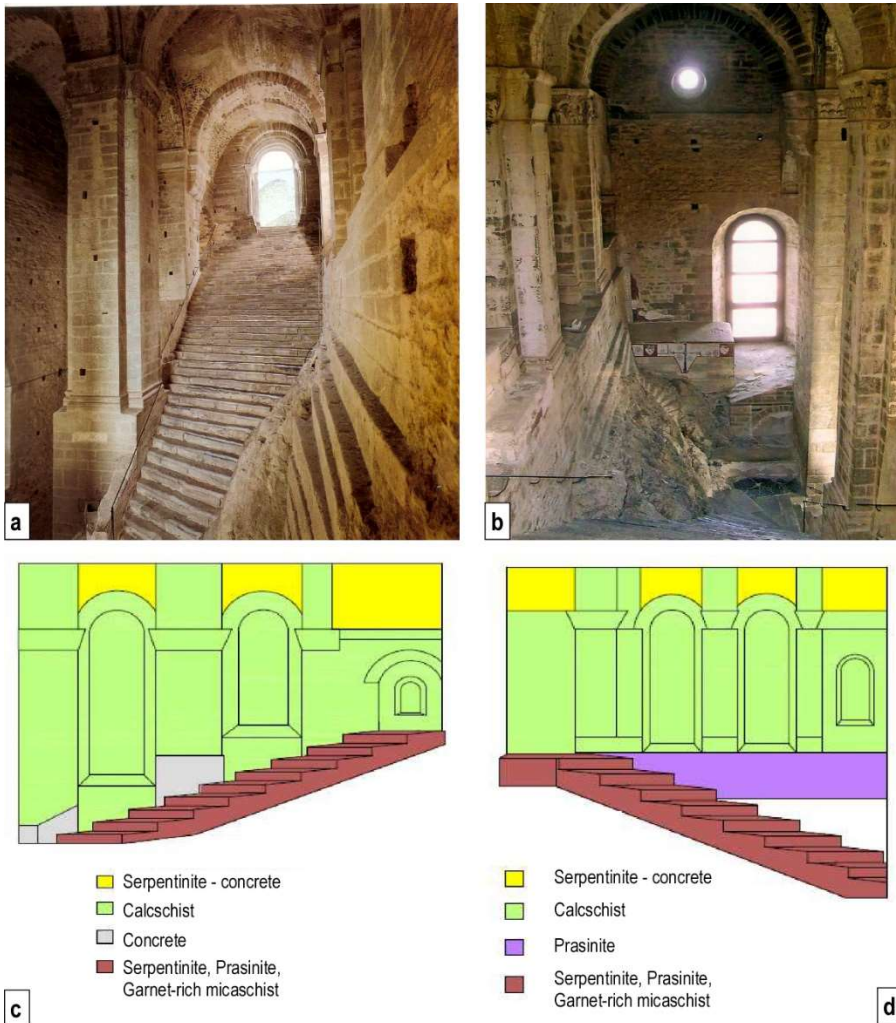


Figure 3.67: a. and b. Pictures of Staircase of the Dead and their petro-architectonic relieves (c. and d.; Gambino, 2014) in which the used ornamental stones are highlighted.

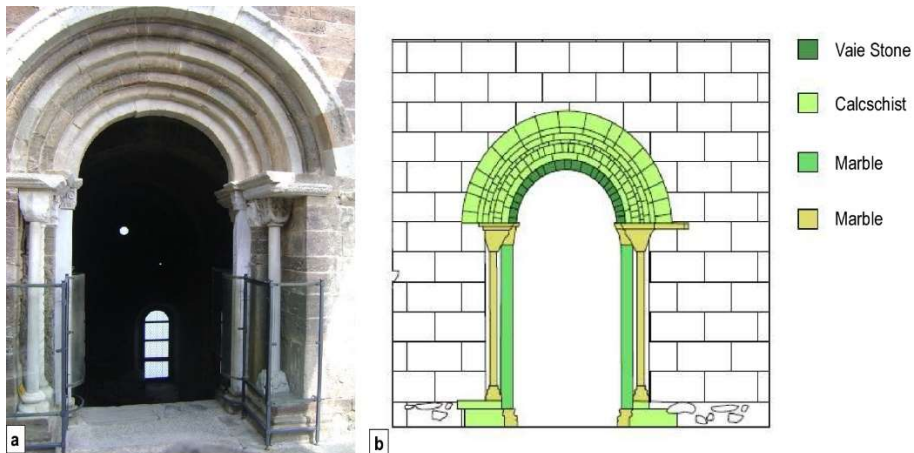


Figure 3.68: a. Picture of the Portal of the Zodiac at the top of the Staircase of the Dead and its petro-architectonic relief (b.; Gambino, 2014) in which the used ornamental stones are highlighted.

For the church portal prasinite, metagabbro and gneiss, were placed side by side to obtain a greater chromatic effect (*Figure 3.69a and b*). In 1836 a strong earthquake undermined the solidity of the building. The architect d'Andrade developed a series of flying buttresses and the crenellated crowning. The flying buttresses are all in prasinite (*Figure 3.69c, d and e*).

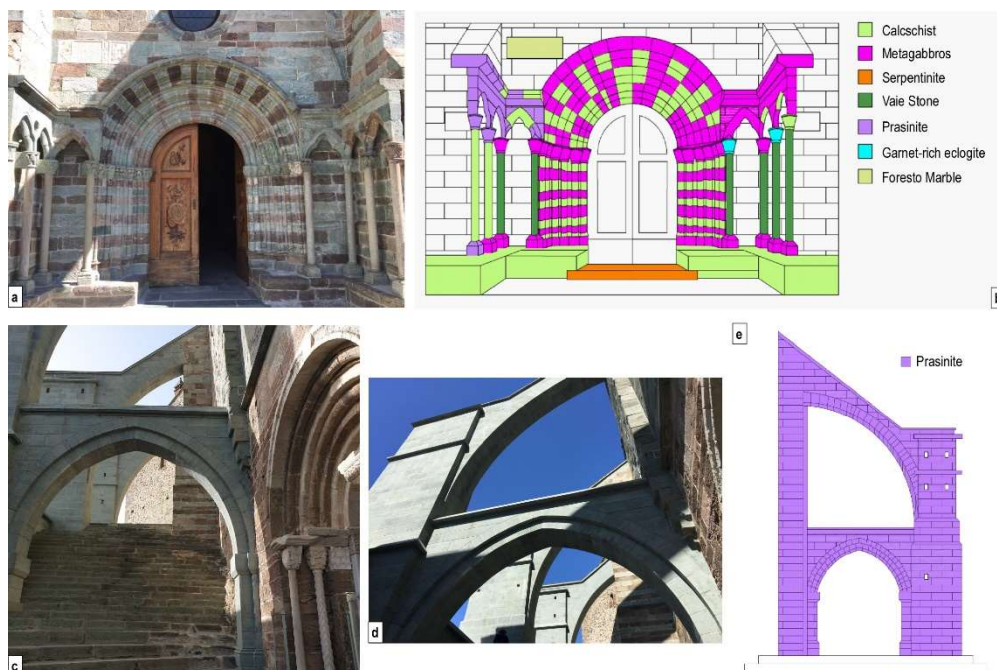


Figure 3.69: Pictures of the church portal (a.) and the flying buttresses (c. and d.) and their petro-architectonic relieves (b. and e.; Gambino, 2014) in which the used ornamental stones are highlighted.

This monument underwent several restorations and the stones used for these operations fit harmoniously into the existing architectural fabric.

The choice to adopt local materials, both during the construction phase and during the restoration sites, allowed to limit the degradation of the different lithotypes imputable to the difficult climatic conditions of the place.

3.3.2 Basilica di Superga

The Basilica di Superga (1731), located on the Torino Hill (672 m) and dedicated to the nativity of Mary, is a baroque complex designed by the famous architect Filippo Juvarra (*Figure 3.70*). It is a sort of "royal temple" where the remains of some members of the House of Savoy are buried (www.basilicadisuperga.com, www.museotorino.it).



Figure 3.70: Basilica di Superga façade.

For its construction numerous ornamental stones were used both from Piemonte and from other Italian regions. Ornamental stones quarried in Torino Hill, in the Susa Valley and in the Monregalese area have been used. As *Figure 3.71* highlights, *Gassino Limestone* was adopted for all the columns and for the pillars of the balustrade of the façade (*Figure 3.73a* and *b*); *Brossasco Marble* was used for the capitals of the columns and, furthermore, the pavement in front of the façade is made up of *Balma Syenite* and the staircase in *Vaie Stone*.

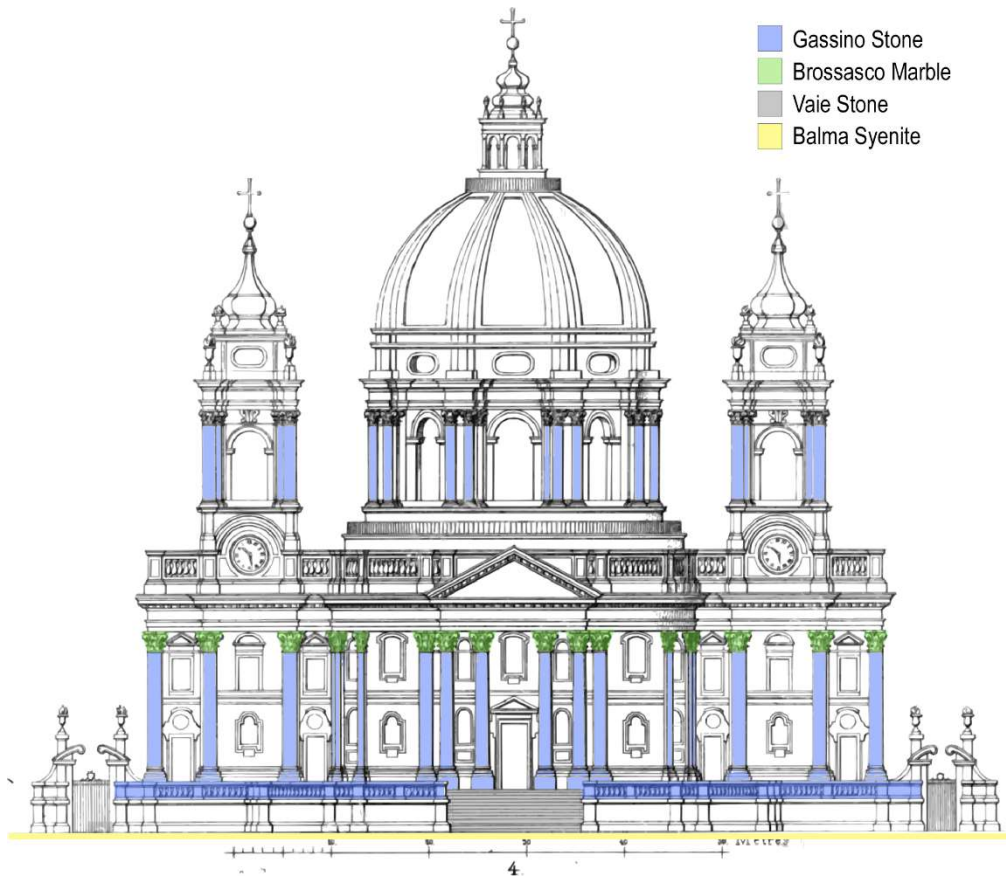


Figure 3.71: Petro-architectonic relief of Basilica di Superga façade (modified after Schulz and Denkmaeler der Kunst, 1860).

The Basilica has a circular plan with a longitudinal extension towards the presbytery. The dome rests on a majestic structure divided into two orders. The first consists of eight fluted columns in gray *Frabosa Marble* (*Bigio di Frabosa*) and base and capitals in *Foresto Marble*. Also, the basement of the columns is made up of *Foresto Marble* and *Busca Onyx* (**Figure 3.72a** and **b**). The second order consists of eight rudent limestone columns of *Gassino Stone* alternating with other eight columns of *Brossasco Marble*.

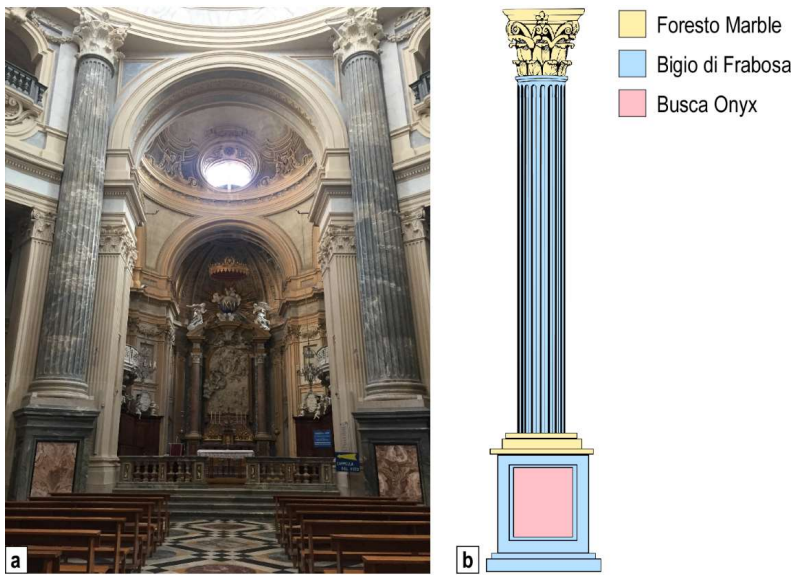


Figure 3.72: a. First order of the columns in the Basilica of Superga interior. b. Petro-architectonic relief of the column.

The interior is enriched by six chapels, four lateral altars and a Main Altar; the floor, sculptures and monuments are decorated with several ornamental stones, including *Bigio Frabosa Marble*, *Persichino di Corsaglia*, *Seravezza di Moncervetto*, *Busca Onyx* and *Verde Susa* (**Figure 3.73c and d**).



Figure 3.73: a. and b. Columns and pillars of balustrade of façade of the Basilica di Superga. c. and d. Interior pavement and balustrade of a chapel in which ornamental rocks used are highlighted.

3.3.3 Palazzo Madama

Palazzo Madama is an historical and architectural complex located in the centre of Torino. It was considerably embellished under the regency of the two Royal Ladies of Savoy kingdom also known as “Madame” (hence the name). The palace is an UNESCO World Heritage site and at present is the seat of the Ancient Art Museum. The famous architect Filippo Juvarra realized in 1718-1721 the great stone façade. This façade shows the employment of important ornamental stones outcropped in Susa Valley. Among these materials originally were used Chianocco Marble, for almost the whole façade, Brossasco Marble and Frabosa Marble. For the restorations through time Prali Marble and Malanaggio Stone were adopted too (see [Chapter 4](#); Gambino et al., 2019).

3.3.4 Fenestrelle Fortress

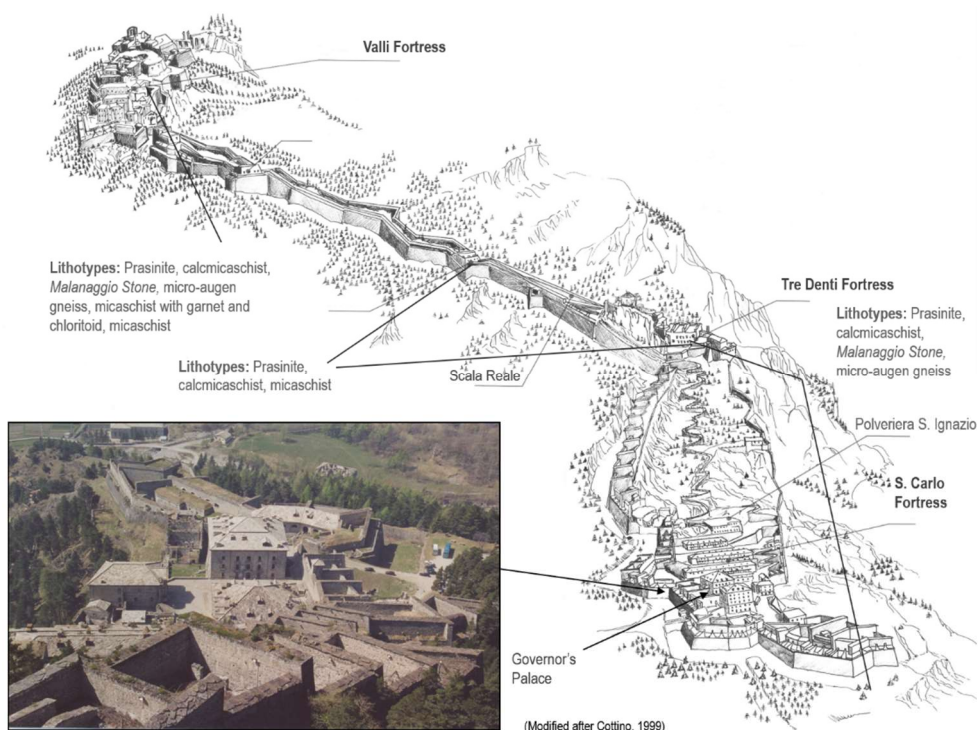


Figure 3.74: Simplified representation of the Fenestrelle Fortress with an illustration of the main buildings and the associated lithotypes used (modified after, Cottino, 1999).

The Fenestrelle Fortress (*Figure 3.74*) consists of a group of military constructions, built between the eighteenth and the nineteenth century in the middle part of the Chisone Valley (Piemonte, Italy), about 80 km West of Torino.

The fortified complex develops on the left orographic side of the middle Val Chisone on an area of approximately 1,300,000 m² between the elevations of 1150 and 1750 m s.l.m. for this reason it is also called the “Alpine Wall”. It includes three main nuclei, which follow one another from top to bottom and in chronological order of construction: Valli Fortress, Tre Denti Fortress and San Carlo Fortress (*Figure 3.76*). In the latter, the Governor's Palace is significant (shown in *Figure 3.75a* and *b*).

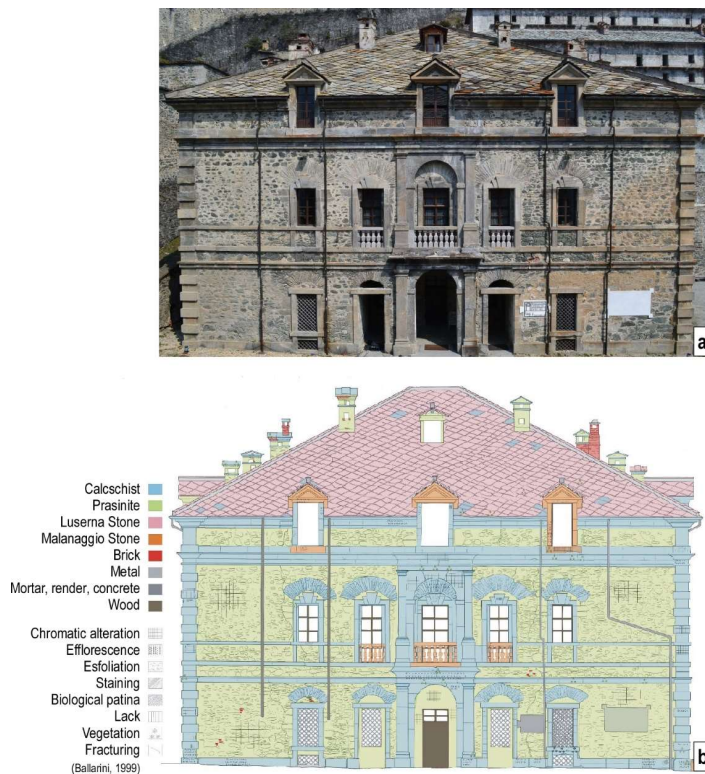


Figure 3.75: Façade (a.) and petro-architectonic and state of preservation relief (Fiora et al., 2006) (b.) of the Governor's Palace.

The work also consists of the longest Covered Staircase in Europe, consisting of 3996 stone steps: covered externally by the Risalti, it appears as a great wall connecting the upper and lower fortifications.

The fortress is entirely built on outcrops of metabasites (prasinite from massive to foliate) of the Orsiera-Rocciavrè Nappe (Liguria–Piemonte Oceanic Domain), which are an integral part of the defensive walls. It shows a general use of stone, from masonry to roof coverings, flooring, stairs, furnishing elements (fireplaces, ovens, sinks, shelves, wells). The cyclopean construction required the extraction and movement of at least 90,000 m³ of rock.

Most of the material is represented by lithotypes surfacing on site: these are mainly prasinite and calcschist, lithologies belonging to the Liguria-Piemonte Oceanic Unit, and, subordinately, of micaschist, augen gneiss, belonging to the Dora-Maira Massif. All these rocks were exploited in the building site itself or in the immediate vicinity. In addition, the dioritic ortogneiss named *Malanaggio Stone* also belonging to the Dora-Maira Massif, was used.



Figure 3.76: Detail of Porta Reale (San Carlo Fortress) in which calcschist is used for the pilasters and prasinite, metabasite and *Malanaggio Stone* for the wall.

3.3.5 Vicoforte Sanctuary



Figure 3.77: Vicoforte Sanctuary.

The Sanctuary of Vicoforte (*Figure 3.77*) is located in the homonymous municipality in Piemonte, on the orographic left of the Tanaro river, in correspondence with the first hill reliefs that fade, to the south, with the foothills of the Ligurian Alps.

The birth of the sanctuary as it is now known, is to be attributed to the Duke of Savoy Carlo Emanuele I, then ruler of those lands. He commissioned the construction to Ascanio Vitozzi and in May 1596 construction work began. Only in 1729, after a period marked by plagues, struggles of succession and death of those who had been the promoters of its construction, the work was resumed under the direction of the architect Francesco Gallo, who managed to complete it in just four years, completing it with the elliptical dome mounted in September 1732.

The rock used in the external construction was found to be a local sandstone (Vico Stone), extracted from the Pradera quarry in the locality of Candia in the neighboring municipality.



Figure 3.78: Detail of Vicoforte Sanctuary façade made up of *Vico Stone*.

The use of this sandstone is limited to the coating of the external part of the Renaissance-style Sanctuary, while the upper baroque part has seen the use of exposed bricks (*Figure 3.78*).

The interior of the Sanctuary is rich in important stone materials of Piemonte and extra-Piemonte origin. The Piemonte rocks include the main varieties of marble and carbonate breccias belonging to the Maritime and Ligurian Alps district as Frabosa Marble (Bigio, nuvolato and verzino variety), Seravezza di Moncervetto, Nero Ormea, Portoro, Bardiglio di Valdieri, Persichini and Busca Onyx (*Figure 3.79a-d*).

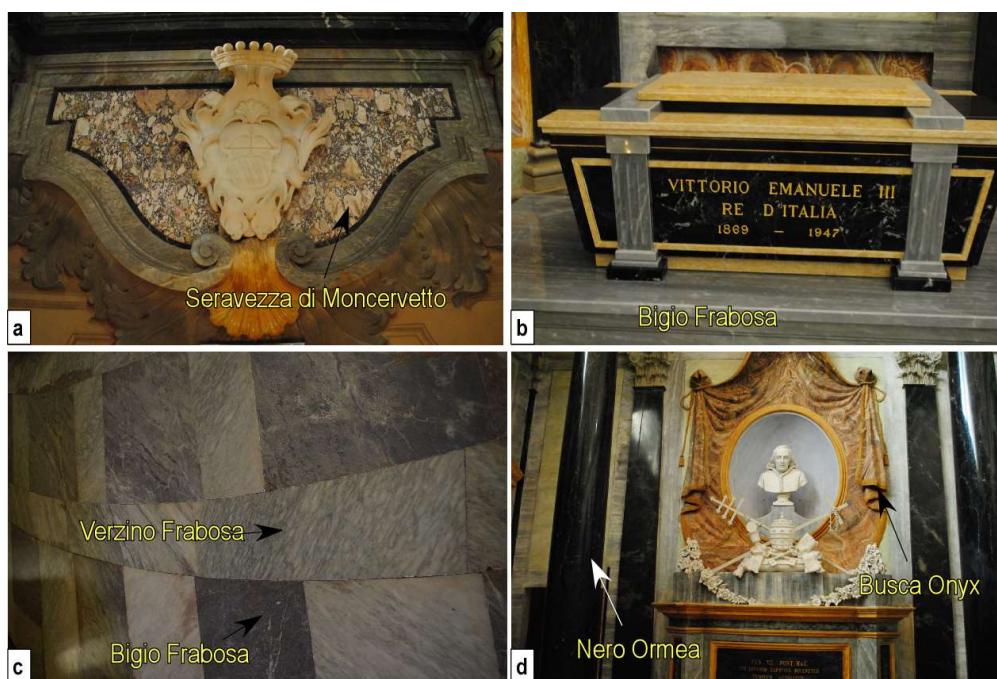


Figure 3.79: Details of interior of Vicoforte Sanctuary in which the main ornamental stones used are highlighted.

3.3.6 Oropa Sanctuary



Figure 3.80: Oropa Sanctuary.

The Oropa Sanctuary (*Figure 3.80*) is the largest Sanctuary dedicated to the Virgin Mary to be found in the Alps. It is located in a unique, natural and unspoilt setting at 1200 mt. a.m.s.l, close to the city of Biella. The monumental complex is made of three courtyards: the heart of the Sanctuary is the Old Basilica where the Black Madonna is kept. First documents concerning the sanctuary date back to the 13rd century. During the plague of 1599, the city of Biella made a vow to build this new church. The whole complex was later enriched by two squares built between 1600 and 1800. Beyond the square, stands the majestic new church (Basilica Superiore), characterized by a large dome visible in most of the territory of Biella. Work began in 1885 but was only partially completed in 1960. The complex is a UNESCO World Heritage Site and the entire territory became the "Sacro Monte di Oropa Special Nature Reserve". From 2017 to 2020 the Basilica Superiore was object of several

restorations. The *Verde Oropa* (Figure 3.81a and b) and the *Balma Syenite* are the two predominant stones used in this complex. Indeed, the columns of the first and the second courtyard, the façade of the Old Basilica (Figure 3.81c) are made up of *Verde Oropa*, a giadeite orthogneiss, belonging to the Sesia-Lanzo Zone, in which leucocratic domains alternate with melanocratic ones. The pavement and the balustrade of the entrance, as well as the columns of the Basilica Superiore are made up of *Balma Syenite*, a quartz-syenite gray to violet in color due to K-feldspar and belonging to the Biella Pluton (Cervo Valley). Furthermore, the *Porta Regia* shows the use of micaschists of the Sesia-Lanzo Zone and the Old Basilica displays the employment of serpentized peridotite for the columns of the façade (Figure 3.81d) and prasinite for the capitals.



Figure 3.81: Oropa Sanctuary: **a.** Columns made up of *Verde Oropa* of the first courtyard and its detailed picture (**b.**); **c.** Old Basilica with façade made up of *Verde Oropa* and columns of the entrance made up of serpentized peridotite (**d.**).

4. The case study of Palazzo Madama façade

Ancient buildings, artifacts and findings are mainly made of natural and materials obtained from geological resources. The development of geosciences as applied to cultural heritage highlights how the study of the genesis and characteristics of ornamental stones is primarily a geological matter and has to be solved by a geologic approach (Lazzarini, 2004). A proper characterization of these materials requires minero-petrographic studies for defining their provenance, conservation state, and application of good preservation strategies.

Often, the selection of stone materials in architecture is driven by specific values and meanings attributed to the different rocks; moreover, the use of specific lithotypes can be related to aesthetic values, technical progress or even economic circumstances. Because of the ease of laborability, marble has been widely employed in valuable buildings, from Roman times to the end of the eighteenth century (Borghi et al., 2015). In Piemonte, and in particular in Torino, stone has always been largely used for both constructions and decoration, becoming one of the distinctive elements of the local architectural heritage. Statues, city walls, floors, roofs, and other architectural elements, are often made of the many varieties of rocks belonging to the different geological units of the Western Alps (Sacco, 1907; Gambino et al., 2017). One of the most prestigious buildings in Torino is certainly Palazzo Madama (*Figure 4.1a*), a historical and architectural complex located in the center of the town. It is an UNESCO World Heritage site and at present is the seat of the city Ancient Art Museum. It is the testimony of two thousand years of history: originally built by the Romans as a gateway to the town, the building became first a defensive system, and then a symbol of power until the sixteenth century, when it was replaced by the Palazzo Reale as seat of the Duke of Savoy. With King Carlo

Alberto, politics also entered Palazzo Madama: in 1848, the king placed the Subalpine Senate in the large hall on the first floor, destined to become one of the places of politics in which Italy's unity was most strongly configured. Considerably embellished under the regency of the two Royal Ladies also known as "Madame" (hence the name): Maria Cristina of France and Maria Giovanna Battista of Savoy, the old medieval castle was retrained by the work of Filippo Juvarra, who realized (1718–1721) the great façade which dominates the square (Palazzo Madama Official Website <https://www.palazzomadamaTurin.it/en/node/1080>; Telluccini, 1928). He chose the *Chianocco Marble*, a yellowish grey marble from the Susa Valley, for coating the façade. The strong deterioration of this marble made necessary, over time, several restorations and replacements by different stone materials recalling the original one, but coming from different sources (Arnaldi di Balme, 2013; Fratini et al., 2018). As a consequence, many archaeometric studies carried out on the façade of Palazzo Madama resulted in contradictory and partially wrong conclusions in the attribution of the stones employed over the centuries (Berti, 1998; Berti and Gomez Serito, 1999).

For this reason, and because of many recent conservation issues, the Conservation and Restoration Foundation "La Venaria Reale", in collaboration with the Torino Musei Foundation and under the supervision of the Superintendence of Archeology, Fine Arts and Landscape for the Metropolitan City of Torino, promoted several technical and scientific investigations in order to develop a pilot project for the overall conservation and future maintenance of the historical façade (*Figure 4.1b*).

The purpose of this chapter is to provide a detailed petro-architectonic survey and a minero-petrographic characterization of the Chianocco Marble also aimed to define the causes of its degradation.

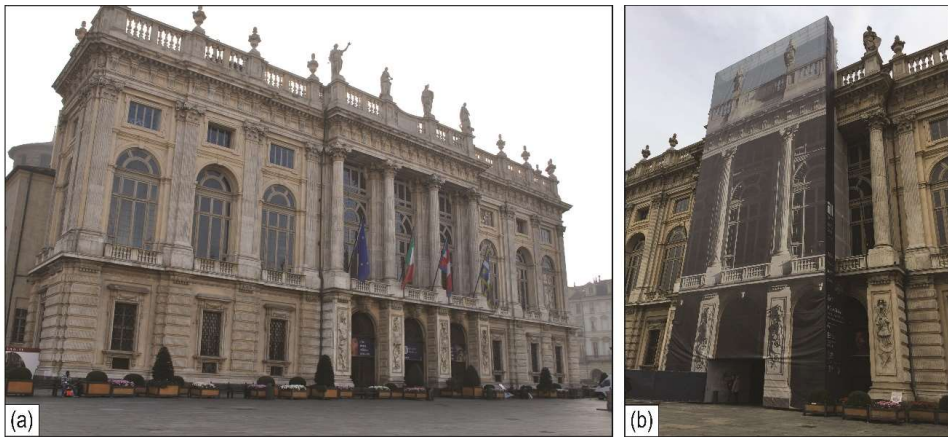


Figure 4.1: a. View of Palazzo Madama façade; b. Study site located in the central area of the façade.

4.1 Geological setting of the Chianocco Marble area

The *Chianocco Marble* crops out in the central area of the Susa Valley (NW Italy), in correspondence of the metamorphic stratigraphic cover of the Dora Maira Massif. The Dora Maira Massif is a continental crust unit belonging to the Penninic Domain of the Western Alps (*Figure 4.2a*) which was suffered by the Alpine orogeny about 50 Ma ago. The Dora Maira Massif is predominantly made up of Paleozoic micaschist, gneiss, and rare slices of dolomitic marble which derived from the Alpine metamorphism of Triassic to Early Jurassic carbonate sediments. The Alpine metamorphism developed under eclogitic conditions in a first event, when peak pressures (P) and temperatures (T) were reached, a retrograde metamorphic event under greenschist facies conditions followed. (Gasco et al., 2011). Historically, Susa Valley marbles have been distinguished as “Foresto and Chianocco Marbles” on the basis of their extraction site (Fiore and Audagnotti, 2001; Fiore and Gambelli 2006). Indeed, on the base of the present work, they are two different kinds of rocks with different petrographic features resulting from different geological processes. The *Foresto Marble* consists of massive whitish marble whereas the *Chianocco*

Marble is a brecciated marble that shows a vacuolar structure and a yellowish color.

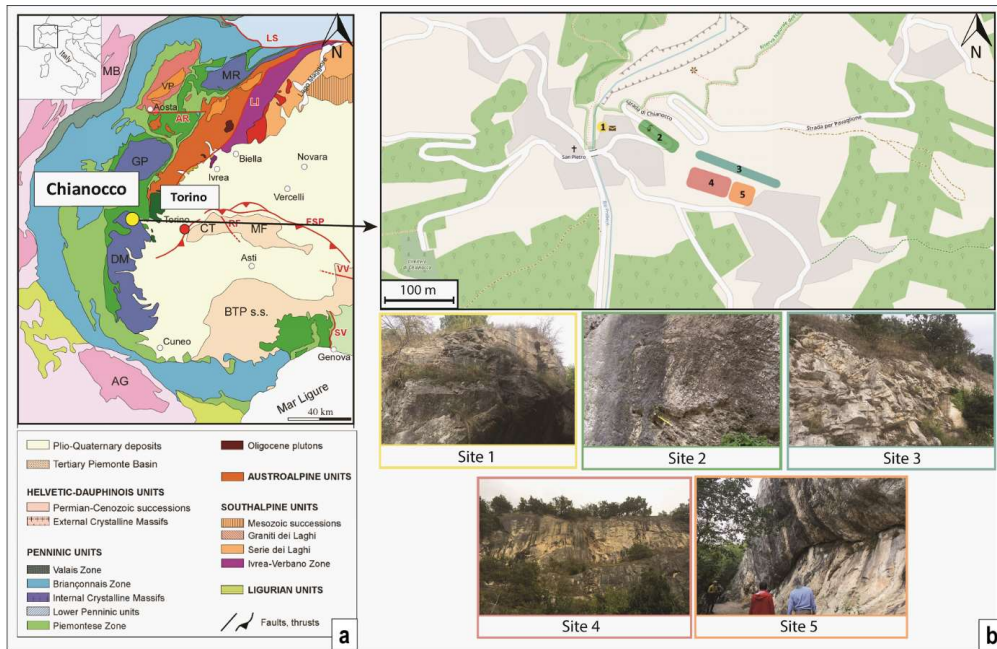


Figure 4.2: a. Geological setting of the Western Alps and location of the Chianocco marble; b. Location of the five historic quarry sites in the Chianocco municipality.

4.2 The Palazzo Madama façade

The façade of Palazzo Madama can be considered one of the masterpieces of the architect Filippo Juvarra. Classical and baroque decorative themes coexist; in fact, Juvarra designed a piano nobile with arch-headed windows linked to a mezzanine overhead by a colossal order of pilasters in a composite style. The central three arches are emphasized by the relief offered by the columns attached to the façade. The façade was surmounted by a spectacular balustrade decorated with vases and statues in white marble.

Juvarra's design choice consists in that the façade assumes the function of a transparent grid and through it the interior decorative development can be perceived, in a resulting composition based on the passage of light. Juvarra desired a completely open loggia but weather conditions in Turin had forced

him to protect the interior with the screen of large glazed windows (Palazzo Madama Official Website).

The petro-architectonic relief (*Figure 4.3*) resulted in the false color representation of the different categories of materials used originally (Chianocco Marble, Brossasco Marble, Frabosa Marble, and Vaje Stone), and in the restorations of the façade through time (Carrara Marble, Prali Marble, Botticino limestone, Malanaggio Stone and Bardiglio Marble) (original and restoration stones shown in *Table 4.1*).

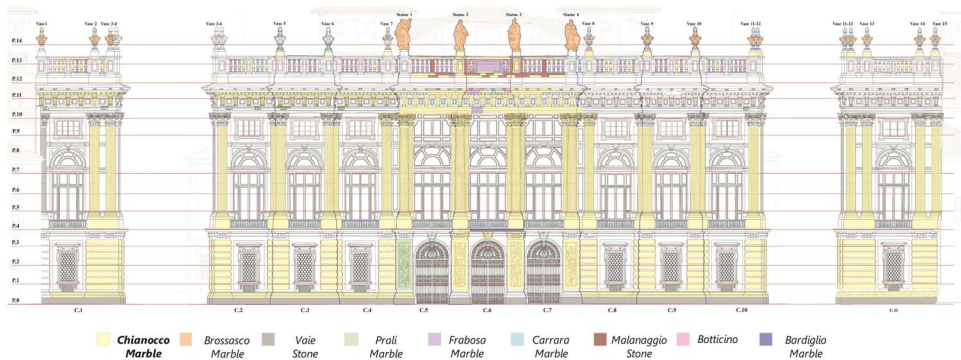


Figure 4.3: Petro-architectonic relief in false color representation of Palazzo Madama façade (architectural drawings courtesy of Foundation Torino Musei-Palazzo Madama). The A3 drawing can be found in [Appendix III](#).

(a)	Original Stones	Use	(b)	Replacement Stones	Replacement of	
					Chianocco Marble	Brossasco Marble
	Chianocco Marble	Columns, pilasters, ashlar, cornices, portals and summit balustrade		Prali Marble	Whole pillar under the first column on the left and slabs of the balcony between first and second column (?)	
	Brossasco Marble	Statues and bases on the summit balustrade, balustrade on the windows of the staircase		Carrara Marble		Several elements of the balustrades on the large windows of the staircase and parts of the vases on the summit balustrade
	Frabosa Marble	Staircase and elements of the summit balustrade		Botticino limestone	Elements of the cornice and of the upper part of the facade and slabs of the balcony between the third and fourth column	
	Vaie Marble	Base of façade		Malanaggio Stone	Elements of the great summit balustrade	
				Bardiglio Marble	Elements of lower balustrade	

Table 4.1: a. Original stone materials of architectural elements of the Palazzo Madama façade; b. Replacement stone materials of the architectural elements of the Palazzo Madama façade.

In particular, Chianocco Marble was employed for the entire marble decoration of the façade, including bas relief and ornaments, Brossasco Marble for the statues and the vases of the apex, and Vaje Stone for the base

of the building. Frabosa Marble was used for some pillars and the slab in the summit balustrade. The Carrara Marble, light gray in color, was employed for an extensive replacement that involved both parts originally made of Brossasco Marble and Chianocco Marble elements. Prali Marble was used for the first pillar on the left observing the façade and Malanaggio Stone replaces numerous elements (pillars, bases and cornices) of the central part of the large summit balustrade. Botticino limestone was employed for elements of the cornice and of the upper part of the facade and slabs of the balcony between the third and fourth column.

It is worth noting that the Gassino Stone, reported by previous authors as a replacement material for the capitals, ledge and balustrade (Berti, 1998; Berti and Gomez Serito, 1999), has not been found at Palazzo Madama.

All kinds of stone materials, both original and restoration ones, were exploited in the Piemonte region, except for Carrara marble, that crops out in Toscana, and Botticino limestone that crops out in Lombardia.

On the façade the following characteristics of the Chianocco Marble were observed: a strongly vacuolar structure (*Figure 4.4a*), a brecciated fabric with a pervasive vein network (*Figure 4.4b*), presence of mortars in the pores (*Figure 4.4c*), a reddish alteration of the columns (*Figure 4.4d*). Moreover, the local occurrence of a white soft powder on the stone suggests sulphation processes due to acid rains.

The so called Chianocco Marble therefore actually shows a more or less continuous range of fabrics and lithologies from veined marbles to a tectonic carbonate breccia characterized by a high porosity and a vacuolar appearance which is comparable to the *cargneules*, a historical Alpine term to indicate brecciated carbonate rocks with a vacuolar structure (Amieux and Jeanbourquin, 1989).

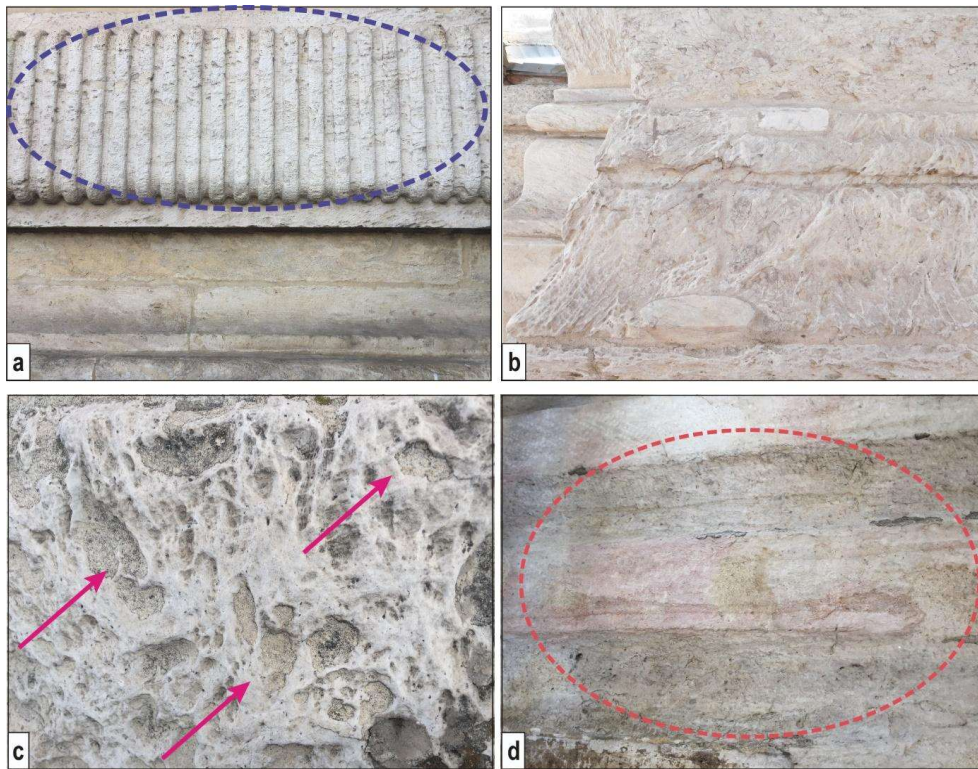


Figure 4.4: Characteristics of Chianocco Marble macroscopically observed on Palazzo Madama façade: **a.** Slab of the façade with a strongly vacuolar texture; **b.** Brecciated fabric with a pervasive vein network observed on a base of column of the façade; **c.** Presence of mortars in the pores of the stone; **d.** Detail of the reddish alteration of the column of the façade.

4.3 Materials ad Methods

The study of the Palazzo Madama façade consisted in the realization of an architectural-petrographic survey of the façade, in the characterization of its lithotypes, in the diagnosis of the state of preservation, in the study of the degradation causes, and in the definition of a model of the evolution of the marble of the façade from its formation to its employment.

For this kind of study related to buildings, monuments and artefacts constituted in marble (a precious material most used and traded in antiquity) a multi-analytical approach is necessary (Matthews, 1997; Gorgoni et al., 2002; Polikreti et al., 2007; Borghi et al., 2009).

Starting from the architectonic relief of the façade, a mapping of stone materials in false color, named “petro-architectonic relief” in this chapter, was achieved. The fragments detached from the façade were catalogued and, from the data collected, the most representative samples were selected for detailed studies.

In order to understand the properties of the material, the localization of the ancient quarries has been essential. Five significant sites in the Chianocco Municipality were individuated and sampling work has been conducted.

Petrographic studies on uncovered thin sections (30µm thick) were carried out by optical microscopy and cathodoluminescence (CL) at the Earth Sciences Department of the University of Turin.

CL observations were performed on polished thin sections using a CITL 8200 mk3 equipment (operating conditions of about 17 kV and 400 µA).

Representative polished thin sections of the marble were analyzed using the SEM-EDS system, with backscattered electron (BSE) and X-ray signals and it permitted to define the chemistry of selected minerals. In the BSE images the brightness signal is sensitive to differences among mean atomic number showing different grey levels for different phases (i.e., calcite and dolomite). In fact, the minerals with higher mean atomic numbers (e.g., calcite) are brighter than the ones with lighter forming elements (e.g., dolomite). In addition to carbonates, mica crystals have also been analyzed; a representative selection of mica composition is reported in the text

Determination of major elements was performed using a Scanning Electron Microscope (SEM; JEOL JSM-IT300LV) combined with an energy-dispersive X-ray spectrometer (EDX), with a silicon drift detector (SDD) from Oxford Instruments, installed at the Dipartimento di Scienze della Terra of the University of Turin. The following operative conditions were adopted: an

accelerating voltage of 15 kV, a counting time of 50 s, a process time of 5 μ s and a working distance of 10 mm. The measurements were performed in high vacuum conditions. A cobalt standard was analyzed for correction and calibration both in energy and in intensity of EDX acquired spectra. Enabling spectra visualization and elements recognition was done by the Microanalysis Suite Oxford INCA Energy 300. A ZAF data reduction program was used for spectra quantification. Astimex Scientific Limited standards were used to obtain full quantitative analyses. All the analyses were recalculated using the MINSORT computer program (Petraakis & Dietrich, 1985). Lastly, mass spectroscopy for the determination of stable isotope ratios was used. The stable isotope analyses (i.e., $\delta^{13}\text{C}$ and $\delta^{18}\text{O}$) have been performed on calcite and dolomite for the studied marble types. The protocol reported in McCrea (1950) was applied. An amount of 10 mg of powdered calcite or dolomite was reacted with 100% orthophosphoric acid under vacuum conditions. The oxygen and carbon isotopic composition produced by CO_2 was analyzed using a Finnigan MAT 250 mass spectrometer. The results are expressed as an isotopic ratio in relation to the PDB standard (Craig, 1957), following the convention defined by the International Atomic Energy Agency.

4.4 The Chianocco Marble

4.4.1 Petrography

Petrographic analyses have been conducted on façade samples and on outcrop ones. Specimens from the façade were not sampled directly in situ but they consist of fragments detached from the summit balustrade. Outcrop samples were collected from five sites in the surroundings of Chianocco village (*Figure 4.2b*) and four of them (Site 1, 2, 4, 5) resulted as analogous to the façade marble. Conversely, the marble of Site 3 is very massive, fine-

grained, white to gray and foliated at macroscopic observation. Similar features were not found in the marble used in the façade of Palazzo Madama. The marble from Site 3 (*Figure 4.5*) is characterized by a paragenesis consisting of major dolomite (Dol 80–90% in vol) and minor calcite (Cc 10–15% in vol) and some accessory minerals as quartz, white mica, apatite, rutile and opaque minerals. The rock shows a homogeneous grain ranging from homeo- to heteroblastic (average grain size 0.10–0.15 mm) grain. The texture is granoblastic characterized by a triple point structure; the single crystal shows lobed to irregular edges. It also has a weakly oriented texture defined by some crystals of white mica. A potassium mica characterized by high Si content (fengitic in composition) and a sodium mica (paragonite) was detected in this marble according to SEM-EDS analyses. This mineral assemblage is indicative of high pressure—low temperature metamorphic conditions. Potassium mica shows a strong zoning characterized by a compositional change in Si content between 6.63 and 7.37 atoms per formula unit (p.f.u.) on the basis of 22 O_x. (*Table 4.3*). Sodium mica is characterized by a compositional change in Si content between 5.98 and 6.14 atoms per formula unit (p.f.u.) based on 22 O_x. (*Table 4.4*). This implies that the mica has grown under metamorphic conditions of high pressure, typical for the Dora Maira Massif (Gasco et al., 2011). The zoning of phengite can be ascribed to the effects of partial retrogression of phengite towards muscovite during the second metamorphic event that involved the Dora Maira Massif, which took place in low pressure conditions (*Figure 4.5b, c, d*).

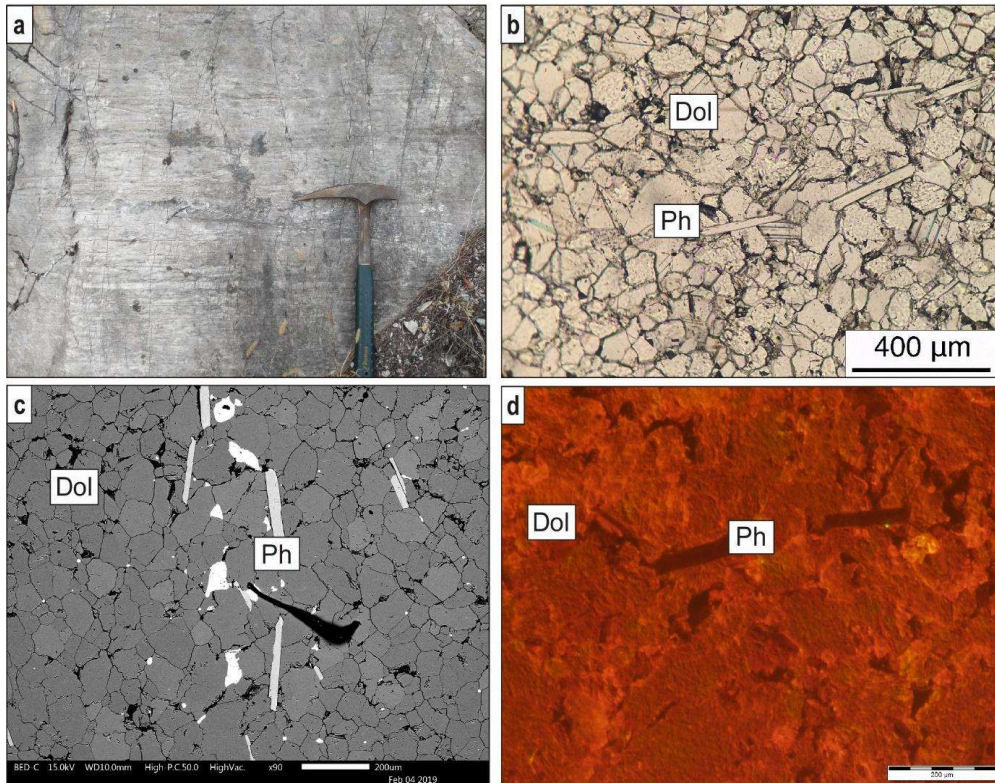


Figure 4.5: Petrography of the marble of Site 3; **a.** Macroscopic aspect of the marble at Site 3; **b.** Photo of optical microscope with only a polarizer, in which dolomite and phengite crystals are indicated; **c.** SEM backscattered image. Dolomite crystals are dark grey and phengite ones are light-grey; **d.** Cathodoluminescence image where dolomite crystals appear red and phengite crystals brown.

Based on microscopical observations, this marble, from the compositional and the textural point of view, is strictly comparable to the Foresto marble (Agostoni et al., 2017).

Conversely the Chianocco Marble (Sites 1, 2, 4, and 5) is characterized by a greater complexity in both structure and composition. Macroscopically it commonly shows a porous and vacuolar texture with irregularly shaped voids up to some centimeters large (*Figure 4.6a, b*). Microscopic analyses, and in particular SEM-BSE and cathodoluminescence (CL) imaging clearly show that the rock is dolomitic, but calcite may be very abundant (*Figure 4.6c-f*).

Calcite fills mm-large veins with commonly sharp edges. Crystals are equant, limpid and show an overall dull brown CL colour (*Figure 4.6e*).

However, a zoning is recognizable with the very first portion of crystals characterized by thin bands of bright to moderate yellow (*Figure 4.6e, f*). This zoning clearly documents a crystal growth in a void in static conditions. Calcite is also present in intimate association with dolomite, clearly distinguishable in CL for the orange colour. Calcite fills spaces among irregularly shaped fragments of dolomite, from few tens of microns to some millimetres large and shows the same zoning observed in veins. This demonstrates that the Chianocco Marble is a cataclasite where the original dolomitic marble was fractured and/or comminuted into fragments of heterogeneous grain size; successively the fractures and the open spaces in the cataclasite were cemented by sparry calcite. Moreover, in some portions of the rock, calcite septa that originally separated the dolomite clasts now surround the voids (*Figure 4.6g, h*).

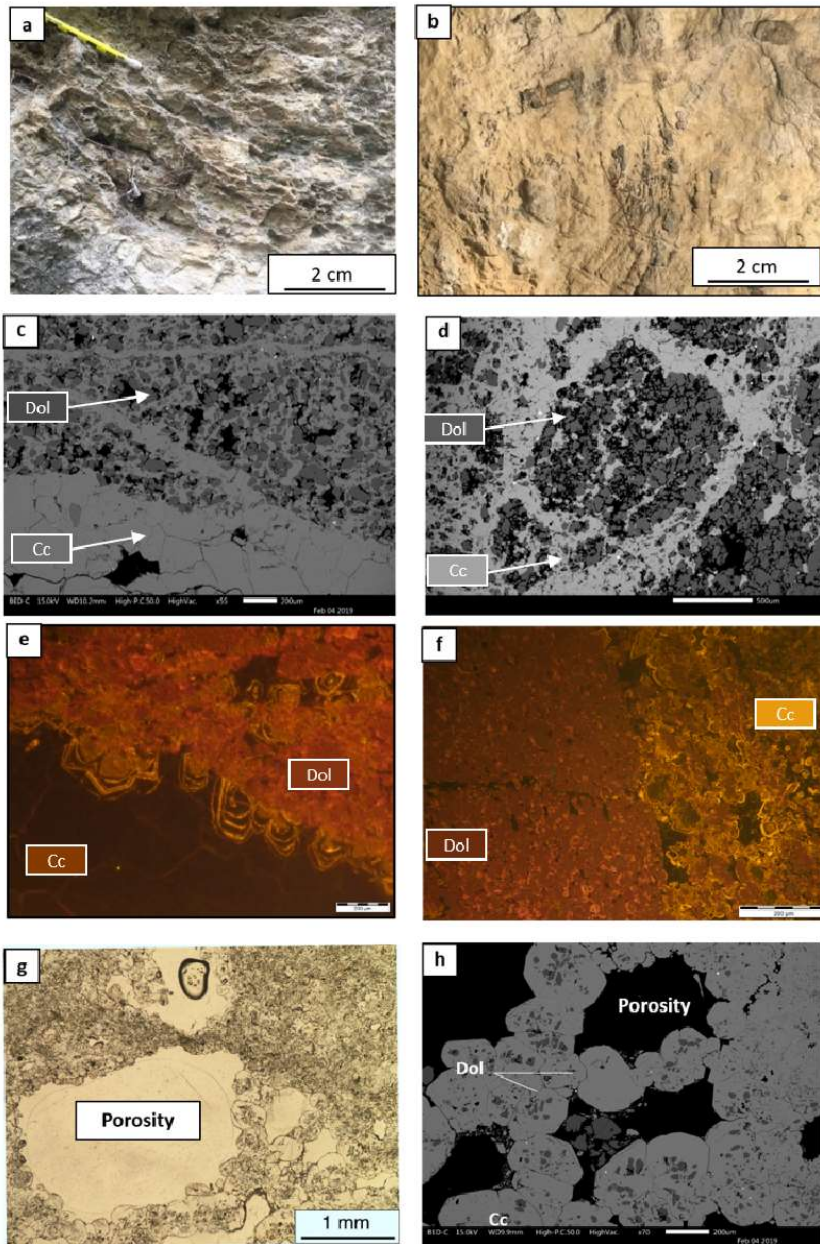


Figure 4.6: Petrography of Chianocco Marble: **a, b.** Macroscopic aspect of Chianocco Marble; **c.** SEM backscattered image where calcite veins are clearly visible; **d.** SEM backscattered image where cataclastic structure is evident; **e.** Cathodoluminescence image where in a calcite vein a zoning is recognizable with the very first portion of crystals characterized by thin bands of bright to moderate yellow; **f.** Cathodoluminescence image where different dolomite, in red, and calcite, in black and yellow, portions are recognizable; **g.** Optical microscope image with only polarizer, with evident vacuolar texture; **h.** SEM backscattered image where the voids are surrounded by calcite septa that originally separated the dolomite clasts.

Phengite and phlogopite occur in the Chianocco Marble and locally are broken and folded (*Figure 4.7*).

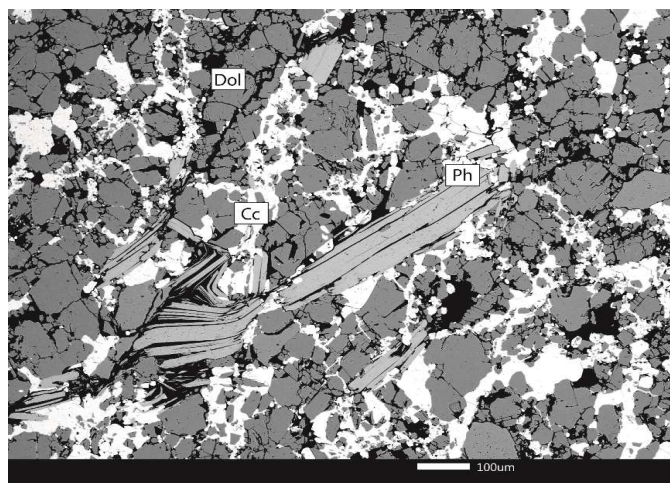


Figure 4.7: SEM backscattered image of Phengite crystal broken and folded.

Sample	Façade						Quarry					
							Site 3		Site 2-4			
Analysis number	Ph 1	Ph 2	Ph 3	Ph 4	Ph 5	Ph 6	Ph 7	Ph 8	Ph 9	Ph 10	Ph 11	Ph 12
SiO ₂	56.57	56.22	57.4	57.28	56.94	57.21	59.67	54.21	56.57	53.01	59.18	59.25
Al ₂ O ₃	26.83	27.39	25.8	26.05	26.42	26.06	22.64	30.89	26.77	32.52	23.24	23.32
FeO	0.00	0.00	0.00	0.00	0.00	0.00	0.00	0.00	0.00	0.00	0.00	0.00
MgO	5.45	5.35	5.75	5.66	5.61	5.78	7.37	3.79	5.34	3.42	6.99	6.95
CaO	0.00	0.00	0.00	0.00	0.00	0.00	0.00	0.00	0.00	0.00	0.00	0.00
Na ₂ O	0.00	0.00	0.00	0.00	0.00	0.00	0.00	0.00	0.00	0.72	0.00	0.00
K ₂ O	11.15	11.04	11.05	11.01	11.03	10.95	10.31	11.11	11.32	10.33	10.59	10.48
Total	97.05	96.27	96.86	97	95.77	96.05	95.98	96.47	97.03	95.62	96.07	95.9
Si	7.08	7.03	7.17	7.16	7.12	7.15	7.42	6.79	7.09	6.63	7.37	7.37
Al IV	0.92	0.97	0.83	0.84	0.88	0.85	0.58	1.22	0.92	1.37	0.63	0.63
Al VI	3.04	3.07	2.97	2.99	3.01	2.98	2.74	3.34	3.04	3.42	2.78	2.79
Fe	0.00	0.00	0.00	0.00	0.00	0.00	0.00	0.00	0.00	0.00	0.00	0.00
Mg	1.02	1.00	1.07	1.05	1.05	1.08	1.37	0.71	1.00	0.64	1.30	1.29
Ca	0.00	0.00	0.00	0.00	0.00	0.00	0.00	0.00	0.00	0.00	0.00	0.00
Na	0.00	0.00	0.00	0.00	0.00	0.00	0.00	0.00	0.00	0.18	0.00	0.00
K	1.78	1.76	1.76	1.76	1.76	1.75	0.00	1.77	1.81	1.65	1.68	1.66

Table 4.2: Representative SEM-EDS analysis of white mica from Palazzo Madama façade samples and Chianocco quarries recalculated on the basis of 22 Ox.

The white mica of façade and quarry samples, analyzed by SEM-EDS, plots in the field of phengite and displays a high content of Si, index of crystallization at high pressures (*Table 4.2; Figure 5.8*). More in detail, the Si amount, expressed as atoms per formula unit (p.f.u.) based on 22 oxygens, varies between 7.03 and 7.17 for façade samples, and between 6.63 and 7.42 for

quarry samples and falls in the field of phengite. The Mg content is between 1.00 and 1.08 atoms p.f.u. for façade samples and between 0.64 and 1.37 for quarry samples, whereas Fe was always absent, consistently with the carbonate system composition. The composition of phengite of Palazzo Madama samples partially corresponds to the mica of quarry marbles (*Figure 5.8a*). Notably the micas of historical quarry samples show a wider range of variation in the Si/Al ratio.

Phlogopite, which is characterized by a much higher Mg:Fe ratio than biotite, was also found. Phlogopite only rarely occurs in marbles and therefore it can be used to characterize the marble variety of Palazzo Madama façade from the mineralogical point of view. Phlogopite blasts occur rarely in the samples from the Chianocco quarries; *Figure 4.8* show representative SEM-EDS analyses of phlogopite.

Sample Analysis Number	Quarry (Site 3)			
	Pg 1	Pg 2	Pg 3	Pg 4
SiO ₂	50.57	49.11	50.13	49.64
TiO ₂	0.00	0.00	0.00	0.00
Al ₂ O ₃	40.67	42.04	41.07	41.53
FeO	0.00	0.00	0.00	0.00
MgO	0.62	0.00	0.48	0.00
CaO	0.00	0.28	0.00	0.00
Na ₂ O	7.50	8.17	7.73	7.90
K ₂ O	0.00	0.00	0.00	0.00
Total	95.53	96.06	96.78	96.38
Si	6.14	5.98	6.09	6.06
Al IV	1.86	2.02	1.91	1.95
Al VI	3.96	4.01	3.97	4.03
Fe	0.00	0.00	0.00	0.00
Mg	0.11	0.00	0.09	0.00
Ca	0.00	0.04	0.00	0.00
Na	1.77	1.93	1.82	1.87
K	0.00	0.00	0.00	0.00

Table 4.3: Representative SEM-EDS analysis of paragonite from Palazzo Madama façade samples and Chianocco quarries recalculated on the basis of 22 O_x.

Sample Analysis Number	Façade			Quarry (Site 2-4)				
	<i>Phl 1</i>	<i>Phl 2</i>	<i>Phl 3</i>	<i>Phl 4</i>	<i>Phl 5</i>	<i>Phl 6</i>	<i>Phl 7</i>	<i>Phl 8</i>
SiO ₂	46.17	46.51	46.21	47.55	47.27	46.33	46.88	46.46
TiO ₂	0.00	0.00	0.00	0.00	0.00	0.00	0.00	0.00
Al ₂ O ₃	14.87	13.42	13.62	12.67	12.68	14.66	14.41	13.32
FeO	0.00	0.00	0.00	0.00	0.00	0.00	0.00	0.00
MgO	28.79	29.61	29.30	29.77	29.81	28.34	28.30	30.01
CaO	0.00	0.00	0.00	0.00	0.00	0.00	0.00	0.00
Na ₂ O	0.00	0.00	0.37	0.00	0.00	0.00	0.00	0.00
K ₂ O	8.92	9.12	9.21	10.01	8.86	8.63	9.06	8.80
Total	96.84	97.00	96.55	96.70	93.69	95.02	96.68	96.62
Si	6.29	6.36	6.33	6.46	6.44	6.34	6.39	6.34
Al IV	1.71	1.64	1.67	1.54	1.56	1.66	1.61	1.66
Al VI	0.67	0.52	0.53	0.49	0.48	0.70	0.70	0.48
Fe	0.00	0.00	0.00	0.00	0.00	0.00	0.00	0.00
Mg	5.84	6.04	5.99	6.03	6.06	5.78	5.75	6.11
Ca	0.00	0.00	0.00	0.00	0.00	0.00	0.00	0.00
Na	0.00	0.00	0.10	0.00	0.00	0.00	0.00	0.00
K	1.37	1.39	1.41	1.67	1.35	1.31	1.38	1.34

Table 4.4: Representative SEM-EDS analysis of phlogopite from Palazzo Madama façade samples and Chianocco quarries recalculated on the basis of 22 Ox.

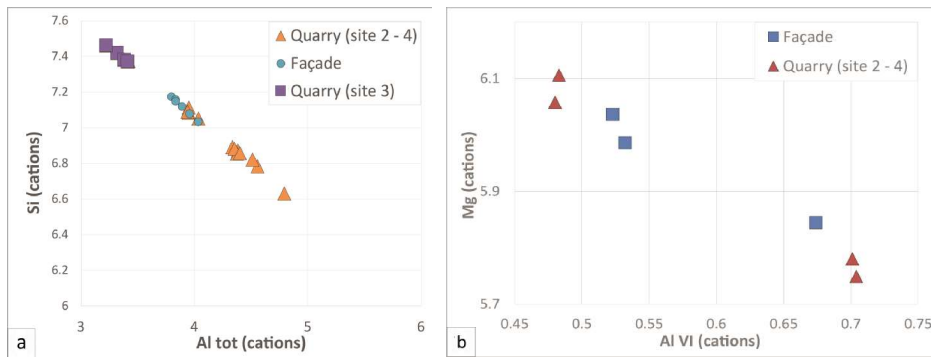


Figure 4.8: Representative diagrams of SEM-EDS analyses of white mica and of phlogopite of Chianocco Marble **a.** Si-Al tot classification diagram for white mica of the Chianocco Marble from Palazzo Madama façade and Chianocco quarry; **b.** Mg-Al VI classification diagram for phlogopite of the Chianocco Marble from Palazzo Madama façade and Chianocco quarry.

Finally, some samples are characterized by a red zone in calcite veins due to the presence of iron oxides inside calcite crystals (*Figure 4.9a, b*). This phenomenon is visible on the macroscopic scale in Site 4 (*Figure 4.9c*); the rock on the outcrop is similarly reddish as the column of the façade already mentioned (*Figure 4.4d*).

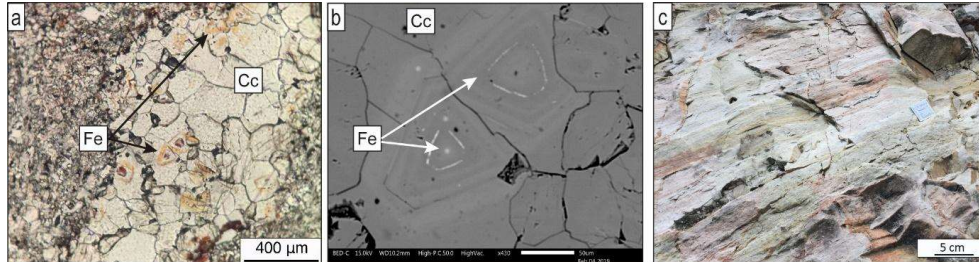


Figure 4.9: Reddish alteration phenomena: **a.** red zones in calcite veins observed by optical microscope with only a polarizer; **b.** SEM backscattered image where zones of iron oxides in calcite crystals are visible; **c.** reddish alteration phenomena visible at the Site 4 quarry.

SEM-EDS analysis also revealed in some areas superficial gypsum with spherical and “rose” morphology (*Figure 4.10a*). Also, intergranular gypsum was found (*Figure 4.10b, c*).

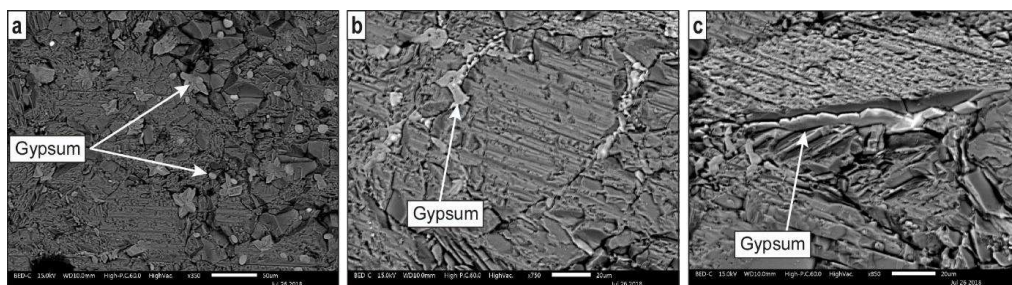


Figure 4.10: SEM backscattered image with superficial gypsum present in façade samples: **a.** spherical and “rose” morphology gypsum; **b.** and **(c)** intergranular gypsum.

4.4.2 C-O Stable Isotope Analysis

C-O stable isotope analyses have been carried out on two selected samples of Chianocco Marble where the characteristic brecciated structure is best represented. One consists of a piece detached from Palazzo Madama façade and the other comes from Site 4, in the surroundings of Chianocco village, where the rock are analogous to the façade marble. Values of $\delta^{18}\text{O}$ and $\delta^{13}\text{C}$ have been determined on calcite and dolomite of both samples. The results, referred to as the PDB standard, are plotted in *Figure 4.5* and *Figure 4.11* where data from the literature (Borghi et al., 2009), concerning the massive dolomitic marble, are also reported for comparison. These analyses were not aimed to be a complete archaeometric characterization and provenance of Palazzo Madama marble but only to verify the genetic relationships of calcite and dolomite which, on the basis of petrographic observations, are clearly not in equilibrium. Although the data set is not statistically highly significant, two points are relevant: 1) Isotopic data of dolomite samples coming from the façade and from Chianocco quarries compare well with data referred to the massive dolomitic marble of Chianocco and Foresto quarries (Borghi et al., 2009) with $\delta^{18}\text{O}$ values ranging between -7.06 and -6.00 and $\delta^{13}\text{C}$ ranging from 0.79 to 1.30 ; 2) Calcite is significantly more depleted in ^{18}O than dolomite, showing values of -9.2 and -10.8 ‰ PDB i.e., with a shift of up to -4.8 ‰ PDB

from dolomite to calcite in the same sample. This establishes marked differences in physico-chemical features of the fluids (temperature, nature and composition of fluids) and thus contrasting geological settings in which dolomite and calcite formed. In particular, the dolomite portion of the rock records the Alpine metamorphic overprint of Triassic sediments whereas the calcite portion is likely due to post-metamorphic evolution of the marble after exhumation and interaction with meteoric waters.

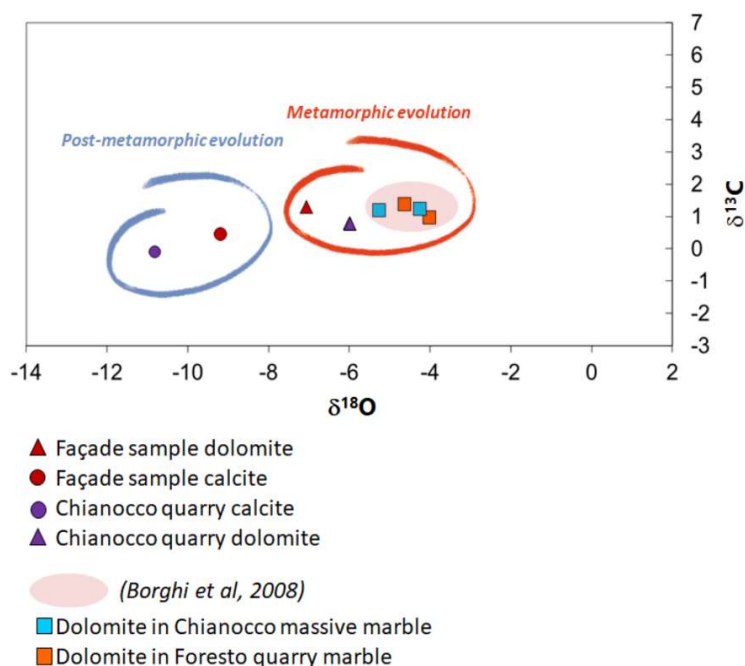


Figure 4.11: The $\delta^{18}\text{O}$ and $\delta^{13}\text{C}$ diagram of calcite and dolomite of the investigated Chianocco Marble. The isotopic reference of Chianocco and Foresto dolomite according to Borghi et al., 2008 is also reported.

Sample	Calcite		Dolomite	
	$\delta^{13}\text{C}$	$\delta^{18}\text{O}$	$\delta^{13}\text{C}$	$\delta^{18}\text{O}$
Façade sample	0.45	-9.20	1.30	-7.06
Chianocco quarry	-0.10	-10.82	0.79	-6.00

Table 4.5: Calcite and dolomite stable isotope (C, O) data of Palazzo Madama façade sample and Chianocco quarry sample.

4.5 Model evolution

The petrographic study of the quarry and façade samples allowed to define a model of the evolution of the rock from its formation to its employment. This model is articulated in six steps as shown in *Figure 4.12*, starting from deposition of the carbonate sediments, through Alpine metamorphism, brittle deformation and brecciation to superficial partial dissolution, with only the very last step being related to the recent exposure of the stone to atmospheric agents as a facing of Palazzo Madama. In the following, each step will be commented in detail.

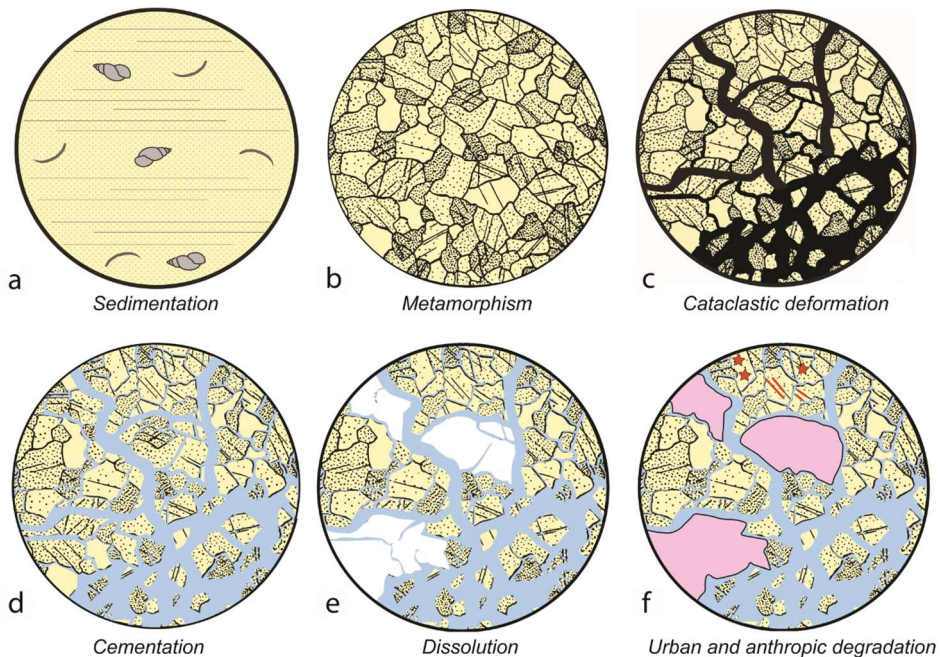


Figure 4.12: Representation of the evolution model of Chianocco Marble from its formation to its employment: **a.** Original carbonate sediments; **b.** Dolomite marble; **c.** Brittle deformation indicated by black fractures; **d.** Calcite cementation indicated in light blue color (tectonic carbonate breccia with a complex and pervasive cataclastic fabric); **e.** Selective dissolution of dolomite marble clasts indicated in white (vacuolar texture); **f.** Mortars in the pores indicated in pink and sulphation indicated in red stars, circles and lines in the upper part of the round.

4.5.1 Step 1

In the Triassic, a carbonate sediment was deposited in a peritidal environment and was very early dolomitized. No fossil nor sedimentary structures are preserved in the Chianocco Marble, but it is clearly established in the geological literature that an extensive carbonate platform existed in the Triassic in all the units presently involved in the Alpine chain.

4.5.2 Step 2

During the first part of the Alpine orogenesis (Late Cretaceous-Eocene) oceanic and continental units were involved in subduction processes. The presence of phengite indicates high pressure conditions in Site 3 sample, therefore attesting that it is a marble formed in a metamorphic process in a pressure and temperature range corresponding to eclogitic facies, the same conditions suffered by the *Foresto Marble*. These characteristics reveal that this marble variety is comparable to the *Foresto Marble*, extracted since ancient times a few kilometers from Chianocco, and used in 9 BC for the Arco di Susa (Agostoni et al., 2017) and for the façade of the Cathedral of Turin. It is in fact a fine-grained, very compact dolomite marble.

The proximity of Foresto quarries with Chianocco led to mistakenly merge *Foresto* and *Chianocco Marbles* in a unique lithotype.

4.5.3 Steps 3 and 4

In a later, post-metamorphic, stage which is not possible to date precisely, brittle deformation took place at high crustal levels, probably not far from the surface. This event caused a strong grain reduction of the dolomitic marble and its transformation into a tectonic carbonate breccia with a complex and pervasive cataclastic fabric. The $\delta^{18}\text{O}$ values of calcite veins and cement,

lighter than marble dolomite, possibly document meteoric waters percolating down and feeding a fracture-related circulation system.

4.5.4 Step 5

A process of selective dissolution of the dolomite marble clasts explains the origin of the vacuolar texture. This process took place when the calcite-cemented breccias were exposed to weathering at or very close to the topographic surface in a very recent past (possibly the Pleistocene) giving rise to a vacuolar structure comparable to that shown by the so called *cargneules* well known in the Alpine literature (Amieux and Jeanbourquin, 1989). In some portions of the rock, calcite septa that originally separated the dolomite clasts now surround the voids.

4.5.5 Step 6

Regarding the environmental degradation, superficial sulphation of carbonate rocks is typical of degradation due to acid rains, in particular for formation of gypsum crystals with spherical and “rose” morphology. The comparison with stone samples from outcrop shows that gypsum is not present in the Chianocco massive marble, insofar supporting the environmental degradation hypothesis.

Moreover, past restoration interventions carried out with not suitable materials (like cement-based mortars) contributed to accelerated deterioration.

4.6 Final considerations of use and conservation of Chianocco Marble

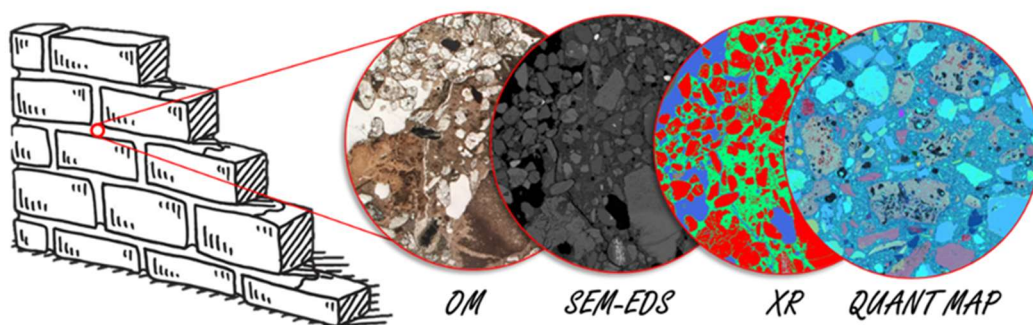
A multidisciplinary geological approach was applied to the façade of Palazzo Madama, which has been recently affected by environmental degradation. A detailed architectural-petrographic relief and minero-petrographic and

isotopic analyses were carried out comparing quarry samples coming from the historic sites of exploitation with selected fragments detached from the façade. The main results may be summarized as follows:

- the kind of ornamental stone used and their precise distribution on the façade were defined distinguishing the original stone materials from the ones used during historical restorations;
- the originally used material, the Chianocco Marble, is still the most abundant and the one which shows the greatest degradation;
- the minero-petrographic study of the Chianocco Marble and the comparison with the same material cropping out in the historical quarries shows that some features observed on Palazzo Madama façade such as a vacuolar structure and local reddening, usually absent in ornamental marbles, are primary features of the rock itself and are not due to degradation in an urban context. They are conversely related to the very complex history of the rock which started in the Triassic age as deposition of a carbonate sediment, evolved through Alpine metamorphism and subsequent brittle deformation, and finished with exposure at the surface where dissolution by meteoric waters generated the vacuolar structure. Only gypsum crystals grown in voids and the application of mortars in natural voids, enhancing the physical degradation of the stone, are due to pollution and human interventions.

This research highlights the importance of geological studies in conservation issues in cultural heritage by defining the characteristics of stone materials, and the reasons for their degradation. In particular, this is true for local heritage stones which can be studied not only on the historical buildings but also in the provenance areas.

5. Petrographic studies of mortars



The study of geomaterials in cultural heritage cannot be separated from the study of mortars. This chapter represents an important experimental and innovative section of this PhD research. The line of research of ancient and restoration mortars is not very diffused even though it provides many information about supply areas, variation of raw materials over the time, network/transportation systems, development and production processes. In particular, the characterization of mortar samples allows to investigate the production technology, to understand which kind of stone has been used to produce the lime, the ratio between binder and aggregate, the origin of the aggregate and its composition (Fratini et al., 2018). This study was focused on the original and restoration mortars of the Ancient Roman Theatre of Aosta (Aosta Valley, Italy).

The possibility of this research represented a unique opportunity in this field and allowed the development of a new analytical protocol. It consists in an original analytical protocol for the characterization of mortars based on automated acquisition and semi-automated processing of quantitative multi-elemental X-ray maps. The potential of this new protocol in the context of the petrographic study of mortars is significant because it allows to acquire objective data, not influenced by the operator. In particular, it regards the

determination of the binder / aggregate ratio and to the % determination of the macroporosity. Moreover, the study of the binder allows to evaluate its hydraulicity and its distribution in the section of the material under examination.

5.1 Historical background

Mortars, since ancient times, are an artificial and man-made product made up of natural materials typically obtained by the firing of carbonate or gypsum. By this process, the *binder* forms and, only after the mixing with an *aggregate* and *water*, it hardens becoming a mortar (Pecchioni et al., 2018).

Mortars are used to embed masonry units as well as wall finishing materials both internally (plaster) and externally (render). Mud was the first material adopted for these purposes and, although it is still used in earth construction, it is neither strong nor durable. To satisfy the demand for dependable structures, stronger and more durable binders have developed, the main ones being based on lime, cement and gypsum (Ingham, 2013).

Currently, according to NORMA UNI 10924, 2001 (the Italian standard to which this chapter refers), mortars are defined as a mixture of binders (organic or inorganic), aggregates (mainly of fine grain size) and water, to which it is possible to add one or more organic or inorganic additives, in order to improve and/or control the laying conditions of the mix, its physical characteristics (e.g. porosity, water permeability) and mechanical characteristics as resistance, deformability, adherence to surfaces, etc.

The *binder* can be principally differentiated into aerial (aerial lime and gypsum), where the hardening process takes place in contact with air, and hydraulic (hydraulic lime and cement), where the same process takes place in contact with water. The *aggregate* is used to reduce shrinkage phenomena and

to modify the mechanical properties of mortars and may derive from sediments or mechanically crushed rocks. The most appropriate aggregate is fine-grained, equidimensional and spherical. Its chemical composition is important because it may trigger chemical reaction with the binder that can decrease the physical and mechanical properties of the mortar.

The *water* is the last main component of a mortar and, as the previous ones, it plays a fundamental role. The quality, the quantity and the temperature of the water used in the mix influence the hardening process and the final result. In ancient times, it was better to use water with a limpid appearance, in minimum quantities in order to get a mixture with a homogeneous appearance and at room to hot temperature (in winter) to avoid subsequent disintegration due to increased volume caused by frost.

The use of mortars seems to have origin in prehistoric times. The discovery probably occurred as the result of an accidental event: the firing of a carbonate rock. It would have been reduced to a powder by heating (calcination process) then extinguished with water and then hardened in the air (Schiele & Berens, 1976).

In ancient times, people used different types of both binders and mortars for different purposes; these materials were known in Asia, Mesopotamia, Near East and Egypt. The Minoan civilization handed down to the Greeks the art of lime production that was in turn transmitted to the Etruscans. The Romans increased the Greeks' knowledge of mortars and began to spread out the use of these materials, improving their physical and chemical characteristics.

Thanks to the Romans, their writings and the study of the several Roman buildings still in good conditions, the advanced techniques of mortar production are nowadays known.

However, during history and especially in the Middle Ages, the techniques of building constructions changed considerably. Mortars with a totally different composition from the Roman parameters were found especially in Italy, France and England. In the medieval period, moreover, it seems that organic additives such as animal fat, linseed oil, albumen, blood and natural resins were used.

With the Industrial Revolution the first *cement*, called “Portland”, was introduced between the end of the 18th century and the beginning of the 19th century (the name Portland derives from the similarity with the rocks coming from the homonymous town in the southern peninsula of Great Britain).

Today's cement is obtained by baking mixtures of limestone and clay (*artificial cement*) or, rarely, marly limestone (*natural cement*) at very high temperatures (1450°C) allowing the complete combination of calcium oxide with silica and alumina in the molten state. The resulting material is called clinker.

This material has revolutionized the history of architecture and was used on a very wide scale throughout the 20th century (Tufani, 1987). Indeed, compared to traditional mortars, cement had a faster hardening and greater mechanical resistance. However, cement and concrete did not show the same durability as traditional mortars. This is the reason why, in recent years, many cement manufactures are developing materials with the same characteristics of traditional mortars.

5.2 The petrographic approach to the study of mortars

Until the beginning of the 1980s, the study of mortars was based on chemical studies, mainly analyzing ions in aqueous solution. However, these methods, due to the peculiar nature of the mortar made up of a binder and an aggregate

that are difficult to separate, did not answer all the questions necessary for a correct characterization of the compound. Later, mortars started to be considered as a rock, and mineralogic and petrographic studies were carried out in order to investigate the two different components separately.

Nowadays, several techniques are used to characterize mortars: wet chemical analysis, instrumental methods for characterization of organic and inorganic materials as thermal analysis (DTA, TGA, DSC) (Pires & Cruz, 2007) (UNI 11305, 2009) (Moropoulou et al., 1995, 2000) and infra-red spectroscopy (FTIR) (Derrick et al., 1999) (NORMA UNI 11135, 2009), physical and mechanical testing for durability and performance assessment respectively, radiocarbon dating (this technique has recently allowed to date mortars to an accuracy of about 30 years) and X-ray diffraction (XRD) (NORMA UNI EN 13925-1, 2006; NORMA UNI EN 13925-2, 2006; NORMA UNI EN 13925-3; NORMA UNI 11135, 2009) Other instrumental techniques for the analysis of organic materials are also adopted (gas chromatography with mass spectrometry; ion, liquid and thin layer chromatography).

For this topic, a petrographic approach was adopted involving optical microscopy (OM) and Electron Microscopy with X-ray analysis (SEM-EDS). Indeed, in the field of the Science and Conservation of Cultural Heritage, the petrographic characterization of mortars is the methodology that better allows to obtain the greatest amount of information on the nature of these materials, despite it is not still the most adopted technique.

Mortars characterization has been performed by combining macroscopic observations, minero-petrographic and micro-chemical techniques as shown in several works focused on this topic (Cagnini et al. 2013; Cantù 2015; Lezzerini et al., 2017; Lezzerini et al. 2018; Miriello et al., 2010; Pecchioni et al. 2018; Riccardi et al., 2007).

The preliminary thin section studies performed by optical microscope are useful to get basic information on the main characteristics and properties of these artificial materials. Data obtained by SEM-EDS and X-ray mapping complement the information obtained by the petrographic studies (Karkanis, 2007, Bany Yaseen, 2013). SEM-EDS analysis allows to perform elemental analysis of samples and is used for characterization of textural and compositional interrelationships of mortar components. Quantitative X-ray mapping, when used, furnish the point-by-point chemical composition of the analyzed area of the thin section.

This analytical approach allows to get archaeometric data. At first, it allows to recognize the type of binder and the nature of the aggregate providing many answers about supply areas, variation of raw materials over the time, network/transportation systems, development and production processes. Consequently, it is possible to understand which kind of stone has been used to produce the lime, the binder/aggregate ratio, the geographic and geologic origin of the aggregate and its composition.

In this context, two fundamental parameters were considered in detail. Firstly, the ratio binder/aggregate (B:A) has great relevance for the mechanical properties of the mortar and its durability. It also allows to qualitatively discriminate whether a mortar is modern or historical: the former generally have a B:A ratio of 1:3, while historical mortars may have values of 1:1, 1:2.

The other important parameter is the Hydraulic Index (HI). This index is strictly related to the amount of clayey minerals or hydraulic materials (e.g. *cocciopesto*) that are present in the original composition of the binder. It is identified by the formula:

$$HI = \frac{SiO_2 + Al_2O_3 + Fe_2O_3}{CaO + MgO}$$

The numerator indicates the acidic components of the binder, while the denominator, its basic components.

Based on the value of the Hydraulic Index, binders can be distinguished according to the following classification reported in **Table 5.1** (Mariani, 1976).

Binder	Aerial lime	Weakly hydraulic lime	Moderately hydraulic lime	Hydraulic lime	Eminently hydraulic lime	Cement
HI	0 – 0.10	0.10-0.16	0.16-0.31	0.31-0.42	0.42-0.50	0.50-0.65

Table 5.1: Classification of binders based on Hidraulicity Index values (Mariani, 1976)

5.3 The case study

The minero-petrographic approach was applied to mortar samples belonging to the **Ancient Roman Theatre of Aosta** (Aosta Valley, Italy). These samples represent the target of a new and original analytical protocol for the study of mortars based on optical microscopy, SEM-EDS analysis and automated acquisition and semi-automated processing of quantitative multi-elemental X-ray maps. Through the KMeans Cluster Analysis, mineral phases of the aggregate and the composition of the binder are classified in a representative area (in this case 16 mm²). The described methodology represents an upgrade of the standard archaeometric and minero-petrographic procedure typically performed by optical microscope and by SEM-EDS and it allows to investigate the composition of the binder and the aggregate, provenance of raw materials, “dating” of mortar samples and comparison of different samples.

In addition, by simple algebraic operations, pixel by pixel full quantification of each EDS spectrum of the elemental maps (expressed as oxides) was performed in order to calculate the distribution of Hydraulicity Index (HI),

with its statistical error, within the investigated domains. Interestingly, also within altered mortars, the HI values can be precisely defined.

The outcome of this methodology consists in the constitution of an analytic protocol that can be applied for every kind of mortar, plaster and cement by a minero-petrographic point of view.

In this Thesis the description of mortars has been done according to the Standard NORMA UNI 11176.

5.3.1 Mortars of the Roman Theatre of Aosta

The focus of this research is the study of mortars of the Roman Theatre of Aosta (*Figure 5.1*). The analyzed samples are of roman age as well as different subsequent restoration phases.

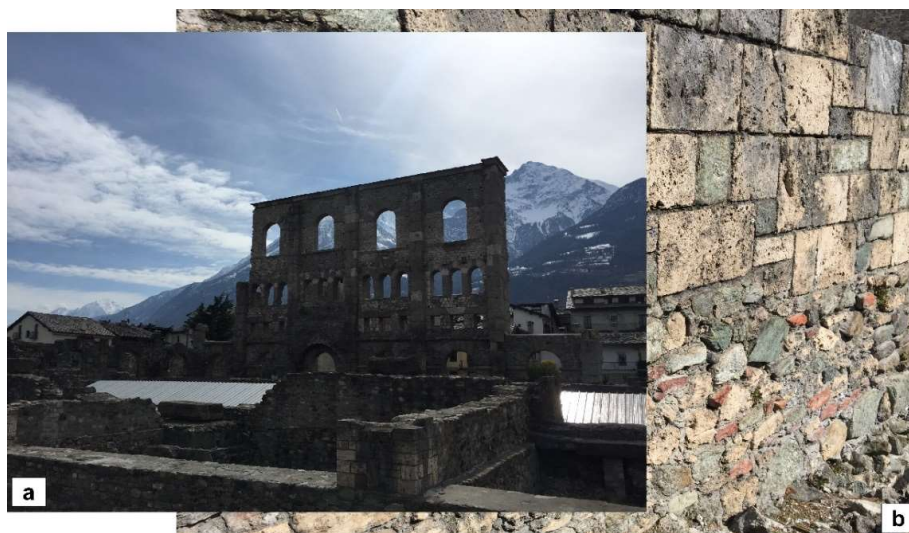


Figure 5.1: a. Panoramic view of the Roman Theatre of Aosta and b. a detail of a wall of the Theatre.

In this chapter, a brief historical introduction about the Theatre and the different phases of restoration will be illustrated. Furthermore, the geological setting of Aosta Valley is also described in order to provide the fundamental background to interpret the results in terms of supply areas of raw materials.

After the description of the study materials, particular attention will be given to the methodology adopted in the study of the mortars as it represents an innovative upgrade of the standard method typically adopted in the study of these materials. Indeed, a minero-petrographic-based analytical protocol for the characterization of the mortars, both ancient and restoration ones, has been developed.

Finally, due to the application of this protocol to the studied samples, the results and their interpretation will be discussed.

5.3.2 The Roman Theatre of Aosta

The city of Aosta, the ancient *Augusta Prætoria*, was founded in the 25 B.C., whereas the buildings for public performances such as the Theatre and the Amphitheatre, located in the north-eastern corner of the town plan, were built a few decades later, as the remains of pre-existing buildings discovered in the area demonstrate.

The Roman Theatre of Aosta, as every roman theatre of the same period, is composed by the *cavea*, the *orchestra*, the *pulpitum*, the *scænæ frons* and the *post scænam*. The part behind the *cavea* is generically called *façade* (**Figure 5.2**).

The Theatre is one of the masterpieces of the Roman provincial architecture of the High Empire. Besides the *façade*, the most visible and easily recognizable architectural component inside the Theatre Roman Area is certainly the *cavea*. Its remaining lower semicircular steps (*ima cavea*) and *præcinctiones*, are today entirely covered with blocks of local travertine.

The *pulpitum*, the curved and rectangular architectural component that precedes the *scæna* originally clad with marble of different colours, was then reconstructed with cement-bounded terracotta bricks; this technique was

used in the Aosta Valley for other architectural restorations from the end of the 19th century onward.

On the other hand, *frons scænæ* and *post scænæ*, have different construction techniques and show various materials.

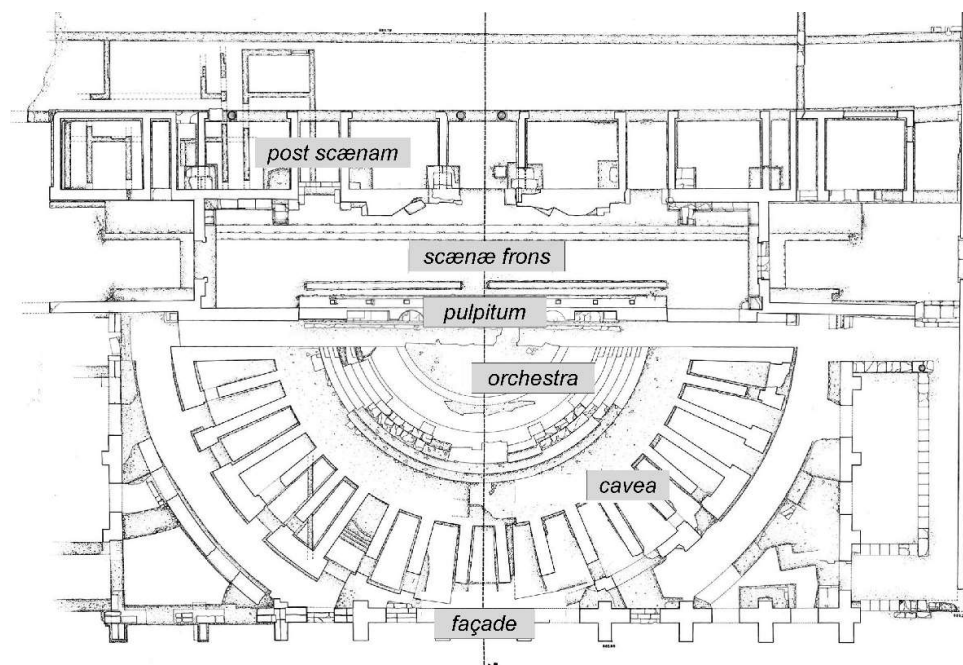


Figure 5.2: Plan of the Roman Theatre of Aosta (modified after Pedeli, 2009) showing the main constituting sectors.

The masonry structure of the area behind the cavea is largely constituted by fluvial pebbles, whole or split in half, of quartzite, schist and granite. Travertine was also widely used. Rarely grey marble, conglomerate and brick were also employed. Instead, conglomerate with different granulometry and travertine was adopted for the façade. During several restorations the use of the same materials has been encouraged. In some cases, the intervention is perfectly recognizable. All these aspects are observable in *Figure 5.3*.

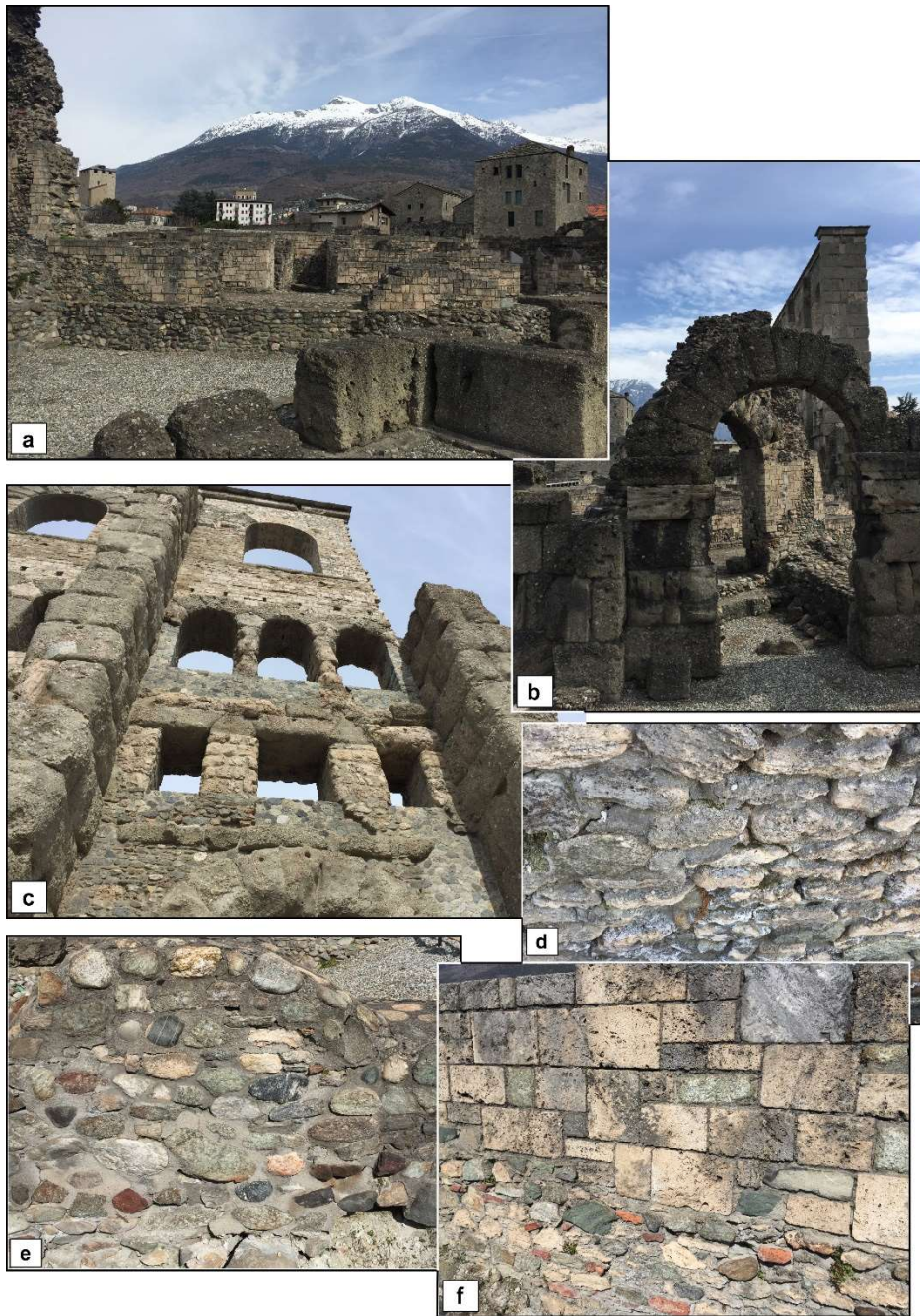


Figure 5.3: Different aspects of the Roman Theatre of Aosta: **a.** The area behind the cavea. **b.** Arches behind the façade of the theatre. **c.** Façade of the theatre made up of different building materials as conglomerate characterized by different granulometry and travertine. **d. e.** Walls constituted by pebbles. **f.** Wall with blocks of travertine highlighting a restoration intervention.

These structures were built by the so-called *rubble masonry* technique using blocks of conglomerate (**Figure 5.4**). This technique consists of two specular vestments made up of river pebble (sometimes fragments or blocks of travertine also appear) binded by a first kind of mortars or cements. The cavity in between the two walls is filled with macro-inerts (pebbles, lithic scales, etc.) drowned in a second mortar. It is a recurring construction technique in Roman times, similar to the one used for the construction of the walls of Aosta.

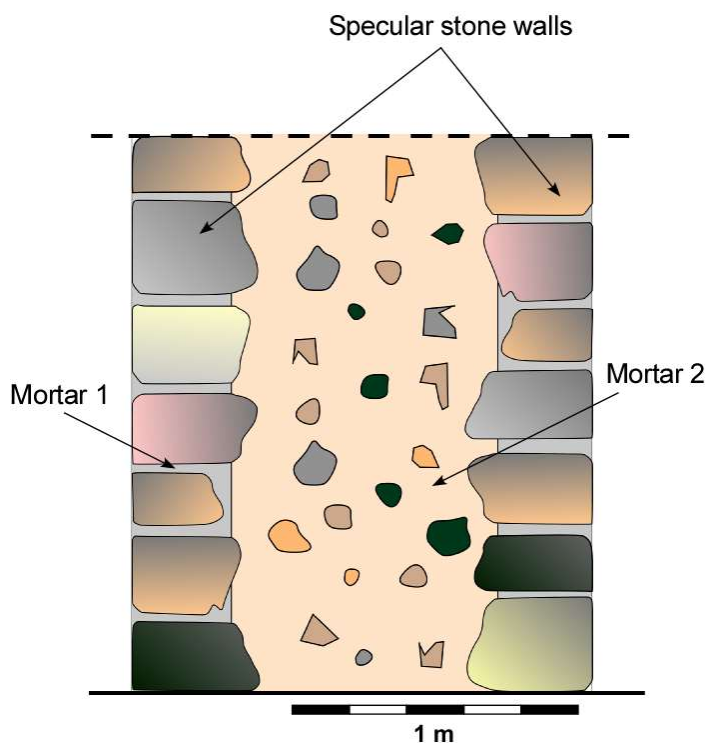


Figure 5.4: Sketchy representation of the rubble masonry technique in which the space between two specular stone walls cemented by a first type of mortar (1) is filled with a second type of cement/mortar (2).

5.4 Geological setting of Aosta Valley

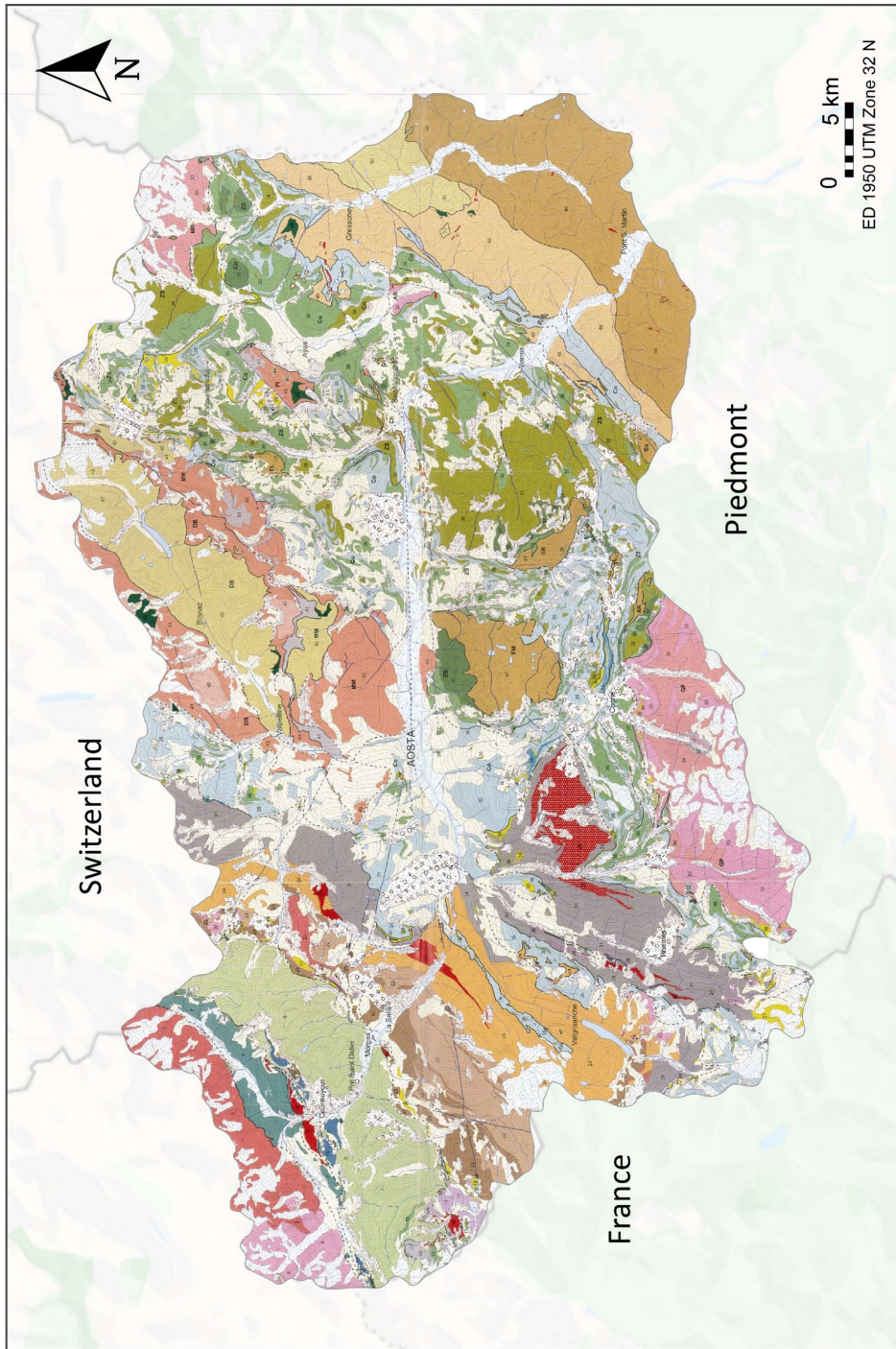


Figure 5.5: Geo-tectonic map of Aosta Valley (De Giusti et al., 2004). The Legend is shown in *Figure 5.6*



Figure 5.6: Legend of geo-tectonic map of Aosta Valley (modified after De Giusti et al., 2004).

As shown in

Figure 5.5 and in Figure 5.6 the Aosta Valley region consists mainly of continental units derived from the European (Helvetic, Pennidic) and

Adriatic/African (Austroalpine) palaeomargins, and of oceanic units derived from the closure of the interposed Mesozoic Alpine Tethys (Piedmont and Valaisan ophiolites), mainly characterised by a polyphasic Alpine metamorphic imprint.

In the Aosta Valley all the main structural domains of the Alpine belt are exposed, with the exception of the chain of the Franco-Swiss Giura, the Eocene-Neogene successions of the Alpine Foreland Basin, the penultimate Klippen of the French Prealps and Chiabrese and, on the opposite side, the Southern Alps (De Giusti et al., 2004 and references therein).

The Austroalpine domain consists of the Sesia Lanzo Zone, which extends in the lower valley, between Verres and the Canavese Line, and represents the innermost (eastern) unit of the Alpine chain. It can be divided in three main lithological complex, named Eclogitic Micaschists Complex (mainly metamorphosed under eclogite – facies conditions), Gneiss Minuti Complex (pervasively re-equilibrated under greenschist – facies conditions) and the Second Dioritic – Kinzigitic Complex, which mainly preserves pre-Alpine H-T metamorphic conditions.

In addition to the Sesia Lanzo Zone, the Austroalpine Domain also includes a group of external elements (Dent Blanche nappe of Argand s.l.). They are divided into eclogitic lower units (M. Emilius, Glacier-Rafray, Chatillon, Etirol-Levatz, etc.) and non-eclogitic upper units (Dent Blanche s.s., M. Mary, Pillonet): the former are located between the Combin and Zermatt-Saas units, or within the Zermatt-Saas unit, the latter lies over the Piedmont Zone, at the same structural level as the Sesia-Lanzo Zone (De Giusti et al. 2004, and references therein). All tectonic units referred to the Austroalpine domain consist of continental – derived pre-Alpine basement with minor slices of Mesozoic carbonate cover (Roisan Zone).

In addition to the external units (Sion-Courmayeur, Versoyen) derived from Mesozoic sediments, the Penninic Zone is dominated by the composite nappe of the Great St. Bernard and by the Internal Penninic Massifs of Monte Rosa and Gran Paradiso, tectonically overthrust by the main ophiolitic units of the Piedmont Zone.

The Piedmont Zone consists of several tectonic units of oceanic pertinence and Mesozoic age, recording a polyphasic Alpine metamorphic history. These tectonic units may be distinguished into two tectono-metamorphic groups of ophiolitic units (Zermatt-Saas in the lower position and Combin Zone in the upper position) according to their tectonic positions, lithological association and contrasting metamorphic imprint. The Zermatt–Saas Zone disappears under the Mischabel and Gran Nomenon backfolds and is dominated by metamorphic ophiolites derived from oceanic mafic and ultramafic protoliths characterized by an eclogitic imprint of Eocene age and a subsequent retrogression towards greenschist facies conditions (Ernst and Dal Piaz 1978; Beltrando et al. 2010). The upper part of the Piedmont nappe stack (Combin Zone) mainly consists of Mesozoic metasediments (carbonate to terrigenous calcschists and impure marbles) alternating with tabular beds of greenschist facies tholeiitic metabasalts (prasinities) and including lenses of serpentinites and minor metagabbros; relics of sodic amphiboles and lozenge-shaped pseudomorphs after lawsonite document the existence of a blueschist facies event before the pervasive greenschist facies overprint of late Eocene – early Oligocene age (Caby 1981; Baldelli et al. 1983; Sartori 1987; Marthaler and Stampfli 1989; Burri et al. 1998; Dal Piaz 1999; De Giusti et al. 2004; Dal Piaz et al. 2010). Exotic sheets of continental origin discontinuously occur near the base of the Combin Zone, both on the southern (Faisceau de Cogne; Elter 1971, 1972) and northern sides (Pancherot – Cime Bianche unit; Dal Piaz 1999 and

references therein) of the Aosta Valley. These tectonic sheets consist of Permian silvery quartzite schists, Lower Triassic tabular quartzites followed by metadolostones and marbles (Middle–Late Triassic), slope breccias with metadolostone fragments probably of Jurassic age and ophiolite free calcschists considered to be Cretaceous in age.

The Gran Paradiso and Monte Rosa nappes represents the metamorphic product of pre-Mesozoic continental units equilibrated under eclogite – facies metamorphic conditions. They mainly consist of mono- and poly-metamorphic silicate-bearing rocks as micaschists and orthogneisses and minor meta-carbonate cover of Mesozoic age (e.g., Govi 1975; De Giusti et al. 2004; Malusà et al. 2005).

The Great St. Bernard composite nappe consists of a polymetamorphic continental basement, a monometamorphic basement of Carboniferous - Permian age and a mainly meta-carbonate cover of Mesozoic age. In the more external position of the Penninic domain, the Sion–Courmayeur Zone outcrops (Elter and Elter 1965), interpreted as an outer oceanic unit with respect to the Piedmont Zone (Loprieno et al. 2011 and references therein). In the Aosta Valley, the Sion–Courmayeur Zone consists of two main geological units: the Roignais Versoyen Unit and the Brèches de Tarentaise Unit. The first is composed of oceanic metasediments, metabasites and serpentinitized lherzolites of Mesozoic age. The presence in the metabasites of high-pressure metamorphic assemblages is reported by Cannic et al. 1996; Beltrando et al. 2010 and references therein.

Finally, the Helvetic Domain is a large tectonic unit that occurs north-west of Penninic Front and crop out in the Italian territory only marginally, forming the massif of Mont Blanc. It consists of a continental basement, characterized by polymetamorphic schists, orthogneiss and Permian granites, and Mesozoic

units represented by weakly metamorphosed predominantly carbonate rocks (Von Raumer, 1987).

5.5 The original and restoration phases of the Roman Theatre

The combination of different materials, along with the overlapping construction techniques, maintenance and restoration phases, confer to the Roman Theatre Area a very heterogeneous aspect. Indeed, it is characterized by several building material and, for this reason, it shows very diversified preservation conditions (Pedeli, 2009).

Up to the 18th century, the whole knowledge about the original function of the building was lost and its remains were recognized only recently.

Carlo Promis, Inspector of Monuments of Antiquity of the State Regions in 1837, performed the first investigations on the monument. From 1838 the Roman Theatre was then studied and surveyed by scientific methods. In 1864 some excavations revealed a series of walls, while in the 20s of the twentieth century an initial arrangement of the monument started by the demolition of the houses that surrounded it. However, it was completely brought to light between 1933 and 1941, when important restoration and integration works were carried out.

In the 1960s, the east and southwest areas (insulae 31 and 32) were investigated, where remains of dwellings emerged; between 1997 and 2000, a series of investigations allowed to get the complete knowledge of the construction phases of the monument. (Appolonia and Fazari, 2005).

The last conservative restoration work, preceded by a series of studies, was completed in 2009.

5.5.1 Original phase

The parts of the residual masonry of the ancient theatrical structure, discovered in the 1930's and which have not been subject of subsequent reconstructions, can be attributed to the so-called "original phase". They were found in the original nucleus and in the lower parts of the vestments. The mortars of this phase macroscopically appear very degraded, disintegrated and often almost pulverised.

5.5.2 First restoration phase

The first phase of restoration was carried out in the 1930's and involved a major renovation of the masonry, which was rebuilt in its missing parts. This intervention was performed respecting the original constituents (e.g. reusing the same materials found out of context in the same excavation) that allow an easy identification of the original parts. This is the most extensive and homogeneous restoration work recognizable in the theatre area and is the only one that also affects the upper part of the walls (Studio Costruzioni Terrezza, 2008).

5.5.3 Second restoration phase

The first restoration work was followed by others of minor importance, clearly recognizable in the vertical stratigraphy of the masonry. This phase, conventionally called "second restoration phase", is characterized by a limited extension and non-homogeneity of both the materials and techniques adopted. This phase, on the contrary to the previous one, is not the result of a unitary project of intervention (Studio Costruzioni Terrezza, 2008).

5.5.4 Third restoration phase

From a stratigraphic point of view, and following the heterogeneous interventions described above, there is a "third phase of restoration", which is widespread, uniform and clearly recognizable. In this case the presence of a basic technical and aesthetic project for the reconstruction of the deteriorated portions of the masonry is evident. Another characteristic of this phase is the exclusive use of pebbles for the facing, which are regularly arranged and homogeneously sized (Studio Costruzioni Terrezza, 2008).

5.5.5 Fourth restoration phase

The last recognizable phase is represented by a series of occasional reconstructions in cement mortar carried out at different times in order to close small open voids in the facing. As for the second phase, this "fourth restoration phase" does not show a unitary design of intervention but seems to be the result of extraordinary maintenance following localized degradation phenomena (Studio Costruzioni Terrezza, 2008).

In *Figure 5.9* sampling of original mortar and restoration ones have been reported.

In *Figure 5.10* Wall 6 has been represented. It can be possible to observe the relative chronology of the different restoration phases (from the first one date back to the 30's to the fourth one characterized by the use of modern cement), although there are also samples from the Roman era.

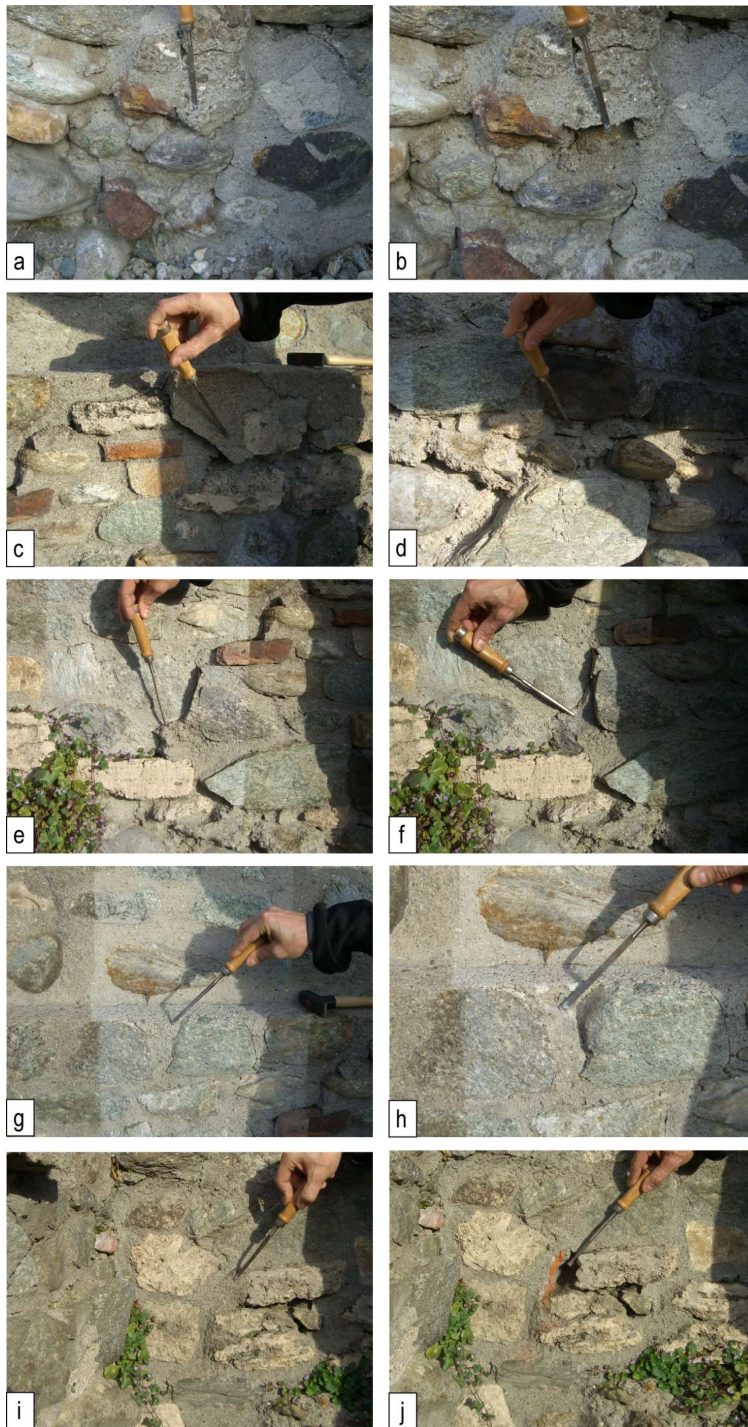


Figure 5.7: Sampling sites of original and restoration mortar before and after the sampling. **a.** and **b.** Sample AAM37 (original mortar) **c.** and **d.** Sample AAM33 (first restoration phase) **e.** and **f.** Sample AAM34 (second restoration phase) **g.** and **h.** Sample AAM35 (third restoration phase) **i.** and **j.** Sample AAM36 (fourth restoration phase).

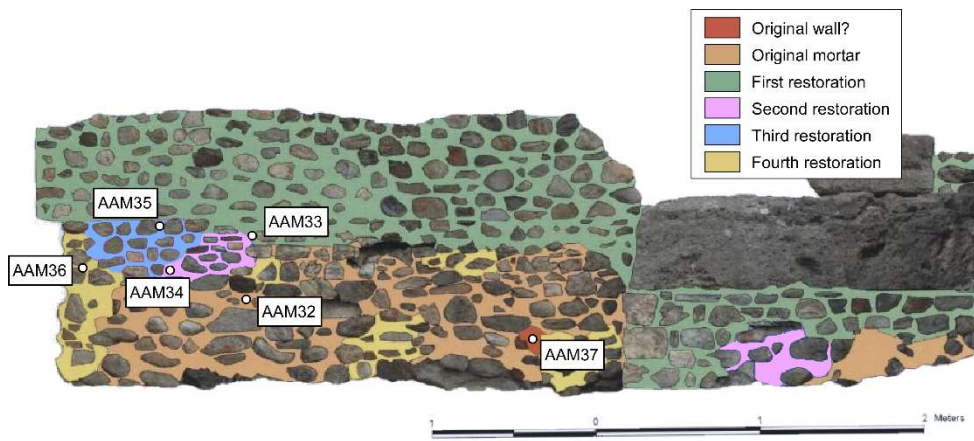


Figure 5.8: Frontal view of the Wall 6. The colors, representing the different mortars used to build and restore the wall through time, allows to highlight the several interventions spanning from the first one dated back to the 30's to the fourth one characterized by the use of modern cement. The location of the samples AAM32, AAM33, AAM34, AAM35, AAM36, AAM37 is also illustrated. From Appolonia et al. (2010) modified.

5.6 Materials and Methods

In this paragraph, in addition to the investigated materials, the applied methodology, which represents the focus and the innovation of this research, will be described in detail.

5.6.1 The samples



Figure 5.9: Sampling of centimeter-sized mortars specimen performed by a chisel.

Forty-two centimetric samples of mortars were taken by a chisel as shown in *Figure 5.9*.

They come from two different restoration investigation campaign performed in 2008 (first phase) and in 2009 (second phase), when archaeological and preliminary archaeometric studies were also performed. The samples were collected at the walls shown in *Figure 5.10*. A detailed description of the sampling is given in *Figure 5.11*. Thin sections of these samples were prepared in order to perform observation by optical microscope and SEM-EDS analyses.

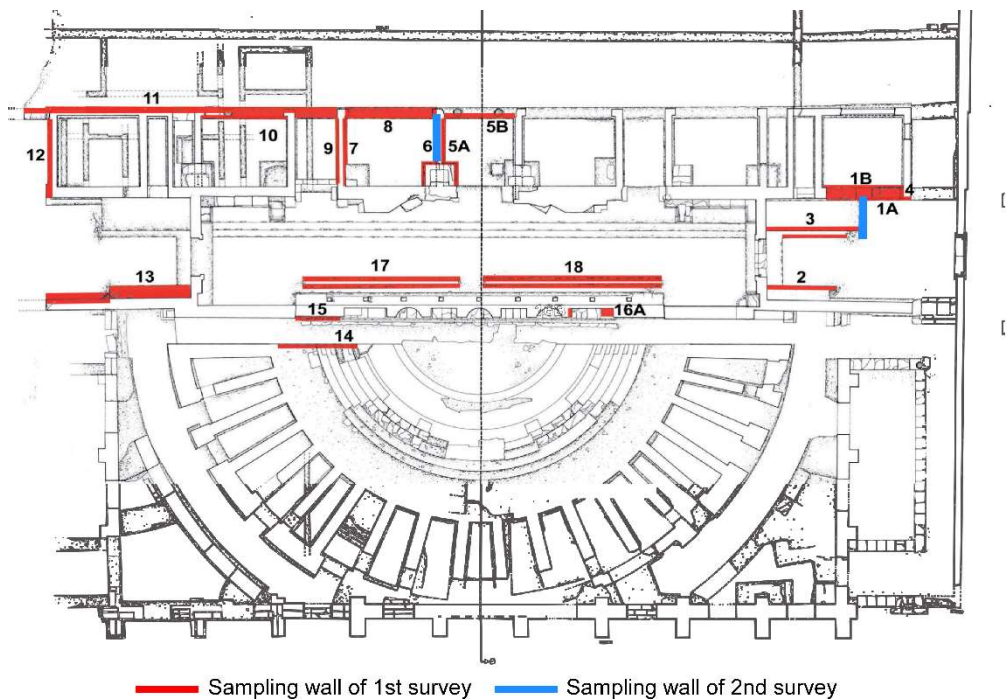


Figure 5.10: Plan of the Roman Theatre of Aosta. The first sampling survey focused on the walls highlighted in red whereas the light blue ones were sampled during the second survey (Pedeli, 2009).

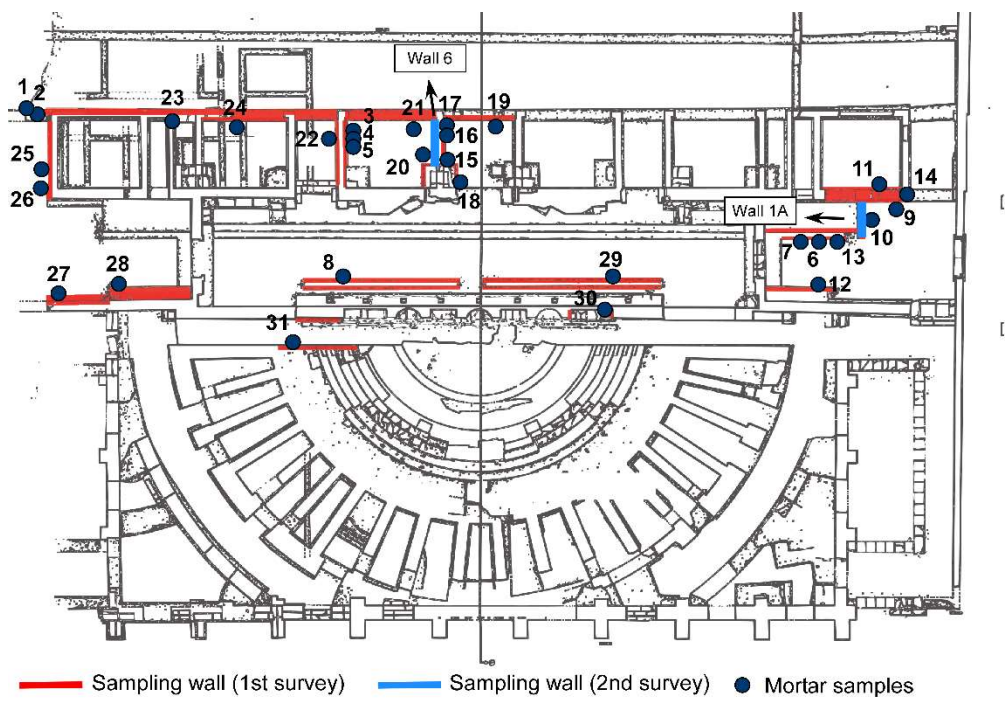


Figure 5.11: Plan of the Roman Theatre of Aosta with the sampling areas of first (2008) and second (2009) investigation campaigns (Appolonia et al., 2010)



Figure 5.12: Thin section of the samples of Roman Theatre of Aosta, Optical Microscope, // pol.

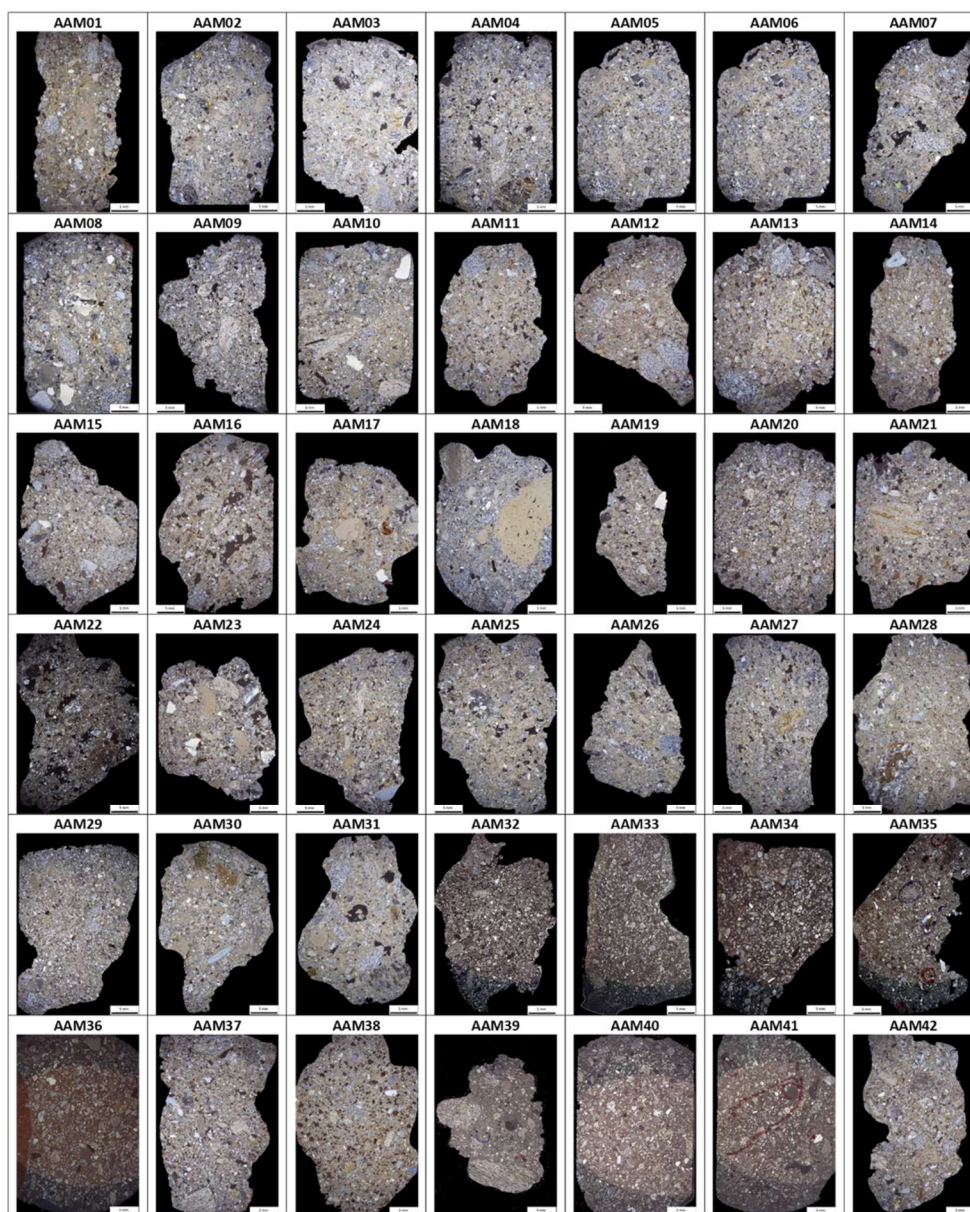


Figure 5.13: Thin section of the samples of Roman Theatre of Aosta, Optical Microscope, X pol.

Photos by optical microscope with only polarizer and crossed polarizers have been reported in *Figure 5.12* and in *Figure 5.13*. The samples from AAM01 to AAM31 are part of the so-called "first phase", i.e. according to the archaeometric analyses carried out by the laboratory of Aosta and according to the evidence from the archaeological excavations, these samples are to be

considered original, dating back to Roman times (1st century AD). The complete list of analyzed samples is reported in **Table 5.2**. From the chemical analyses carried out in 2008 (Applonia et al., 2010), a wide variability of data can be deduced, especially with regard to the calcimetry data. The minero-petrographic approach to the study of these mortars makes it possible to characterize the mortar samples, to investigate the production technology, and therefore to complete the studies undertaken on these samples.

The samples from AAM32 to AAM42 are instead representative of the relative chronology of the different restoration phases, although there are also samples from the Roman era. In this case the study was useful to highlight the differences of the different mortars, original and cementitious.

Sample	Original/restoration mortar	Number of wall
<i>First campaign of investigation (2008)</i>		
AAM01	Original	11
AAM02	Original	12
AAM03	Original	7
AAM04	Original	7
AAM05	Original	7
AAM06	Original	6
AAM07	Original	6
AAM08	Original	17
AAM09	Original	1B
AAM10	Original	1A
AAM11	Original	1B
AAM12	Original	2
AAM13	Original	6
AAM14	Original	1B
AAM15	Original	5A

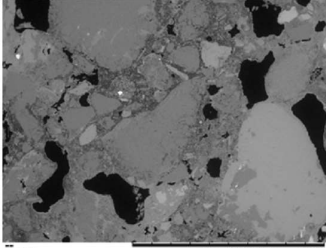
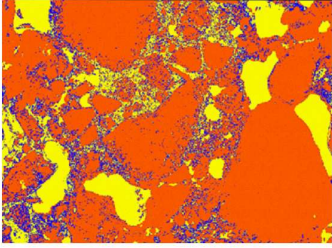
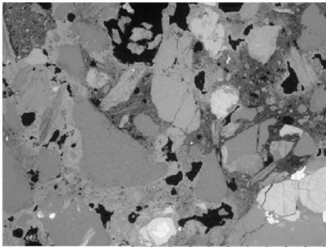
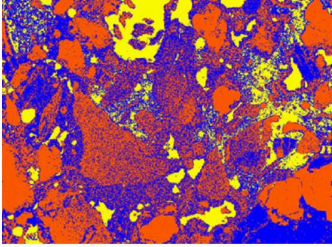
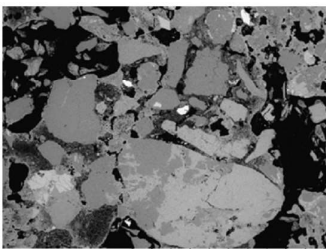
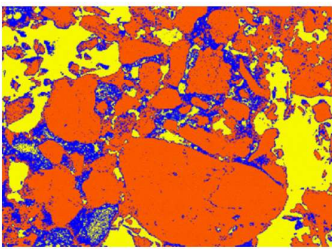
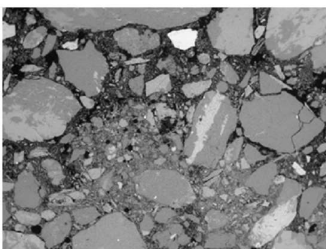
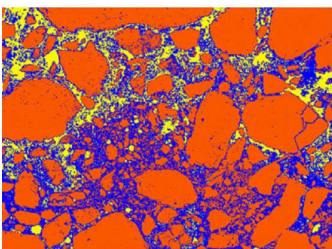
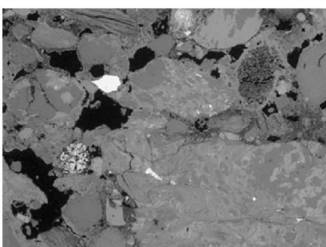
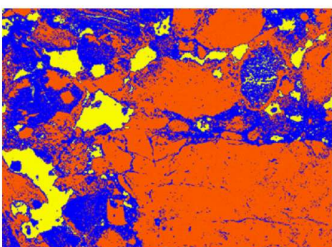
AAM16	Original	5A
AAM17	Original	5A
AAM18	Original	5A
AAM19	Original	5B
AAM20	Original	6
AAM21	Original	8
AAM22	Original	9
AAM23	Original	11
AAM24	Original	10
AAM25	Original	12
AAM26	Original	12
AAM27	Original	13
AAM28	Original	13
AAM29	Original	18
AAM30	Original	16A
AAM31	Original	14

Second campaign of investigation (2009)

AAM32	Original	6
AAM33	First restoration	6
AAM34	Second restoration	6
AAM35	Third restoration	6
AAM36	Fourth restoration	6
AAM37	Original	6
AAM38	Third restoration	1A
AAM39	Second restoration	1A
AAM40	Fourth restoration	1A
AAM41	First restoration	1A
AAM42	Original	1A

Table 5.2: Samples of mortars of first and second campaign (Appolonia et al., 2010)

All samples have been observed by optical microscope. For some representative samples of first campaign imaging analysis was performed in order to obtain the percentage of aggregate, binder and porosity (*Table 5.3*).

Sample	Backscattered photo	False-color image	Aggregate (A) Binder (B) Porosity (P)
AAM11			A 66% B 14% P 20%
AAM12			A 45% B 41% P 14%
AAM13			A 57% B 21% P 22%
AAM14			A 60% B 28% P 12%
AAM15			A 56% B 34% P 10%

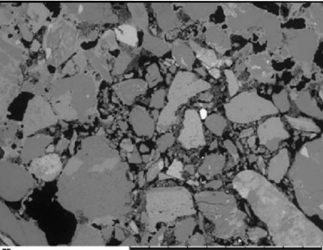
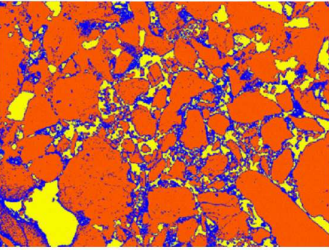
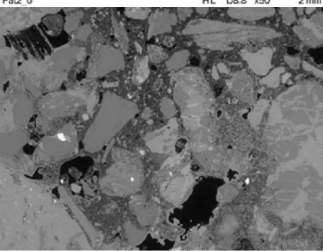
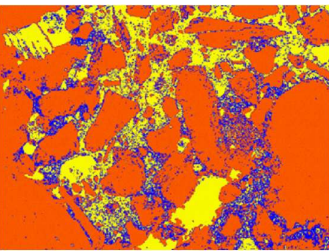
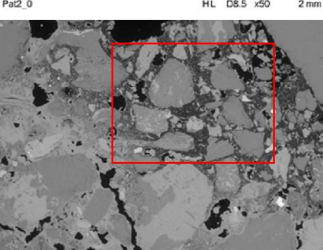
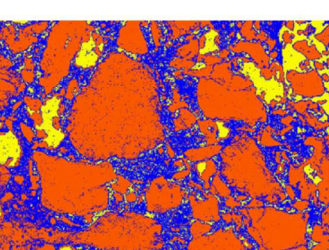

Sample	Backscattered photo	False-color image	Aggregate (A) Binder (B) Porosity (P)
AAM20			A 64% B 21% P 15%
AAM21			A 63% B 17% P 20%
AAM22			A 57% B 31% P 12%
			Aggregate 58% ± 6% Binder 27% ± 8% Porosity 16% ± 4%

Table 5.3: Imaging analysis of representative orinal samples of first campaign of investigation (AAM01, AAM11, AAM12, AAM13, AAM14, AAM16, AAM17, AAM20, AAM21, AAM22). Percentage of aggregate, binder and porosity is reported.

Nevertheless, eight samples, belonging to first and second campaign of investigation, were selected to apply the analytical protocol described in the following paragraph.

The *original mortars* of Roman age were chosen based on their representativeness and on the quantity of binder still present. Indeed, of the binder of these samples showed a poor state of preservation to the point that,

in some cases, the binder resulted almost absent. They are the following: **AAM01, AAM17, AAM25, AAM37.**

Mortars of restoration phases are selected from the same wall 6 represented in *Figure 5.8* to maintain a coherence between sampling and analysis. They are the following: **AAM33, AAM34, AAM35, AAM36.**

5.6.2 Analytical protocol

A new analytical protocol for the study of these geomaterials has been developed and tested on the above-mentioned samples. It consists of a combination of standard petrographic tools and an innovative semi-automated investigative method by quantitative X-ray mapping that, following five steps, leads to a complete characterization of mortars (*Figure 5.14*).

The first step consists in the characterization by optical microscope of thin sections of mortars, the second one in the SEM- EDS X-ray mapping acquisition, followed by their elaboration (third step). For this purpose, a new specific software called "**Geomaterials Mapping (GeoMatMap)**" has been developed. The fourth step consists of SEM-EDS quantitative spot analysis acquisition, to calibrate the results obtained by the X-ray data set. Lastly, the fifth step is aimed to the interpretation of the acquired data.

In the following paragraphs each of these steps will be described in detail.

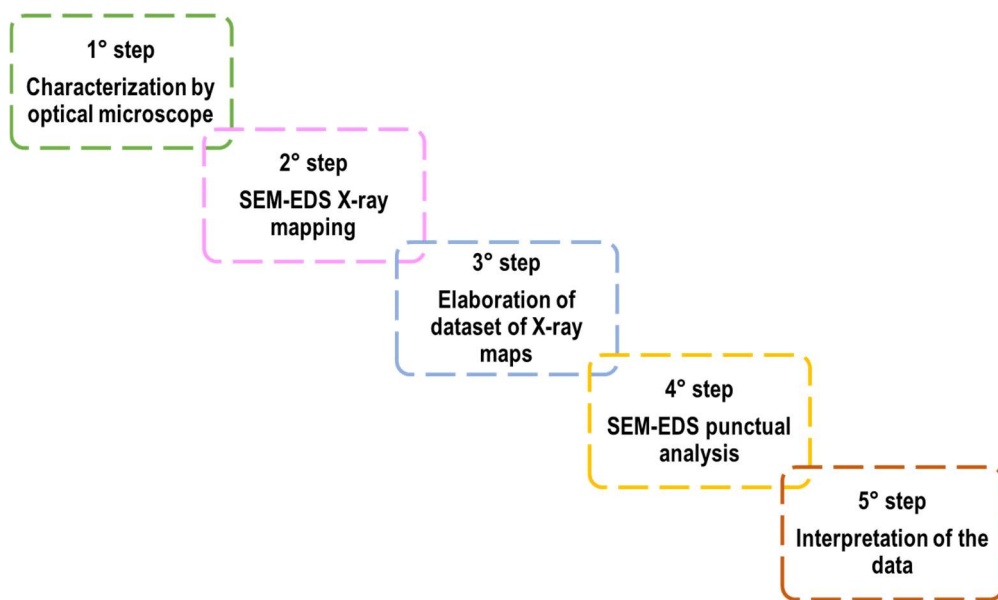


Figure 5.14: The five steps of the analytical protocol adopted in this Thesis for the study of mortars through a petrographic approach.

5.6.2.1 1° step: Characterization by optical microscope

Based on the protocol reported in Pecchioni et al., 2018, the observation by optical microscope allowed to investigate the principal texture-compositional characteristics of the mortars (*Figure 5.15*). Qualitative considerations can be then confirmed or refuted by the SEM-EDS analysis. Concerning the aggregate, it is possible to assume the minero-petrographic characterization, the granulometry and the shape of clasts/grains, their distribution within the binder as well as their orientation. Relating to the binder, optical microscopy allows to define its composition and texture (presence of lumps and fragments of uncooked stone, presence of crystalline phases distinctive of some types of binder), the porosity, the binder/aggregate ratio, the presence of recrystallization process and the state of preservation.

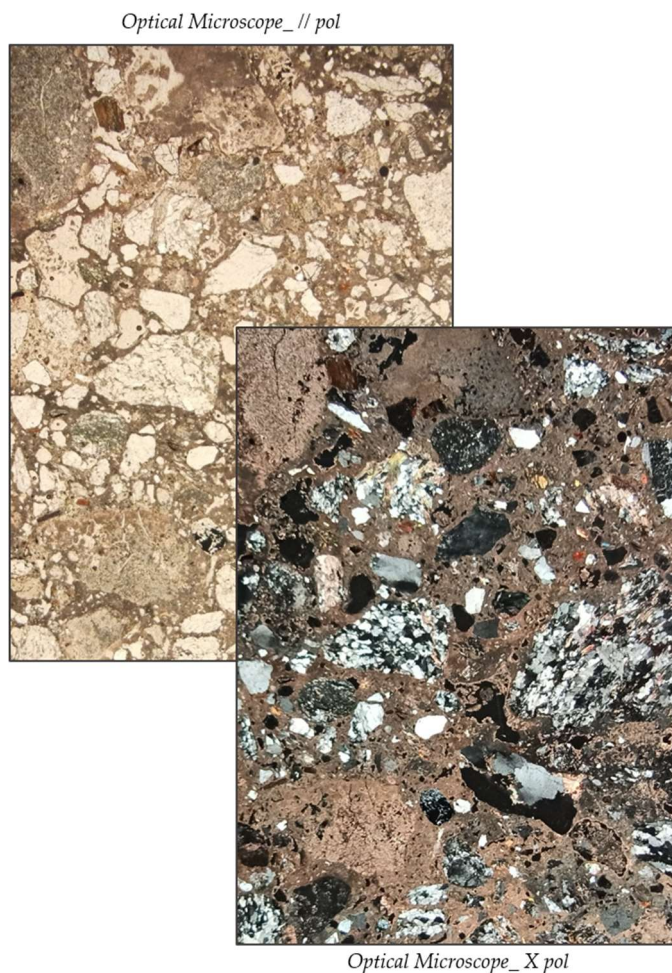


Figure 5.15: Example of thin section of a Roman mortar (AAM17) observed by optical microscope (//pol and X pol).

5.6.2.2 2° step: SEM-EDS Quantitative X-ray mapping

The focus of this step is the identification and classification of the different mineral phases using the point-by-point chemical composition thanks to the acquisition of X-ray quantitative maps. For this purpose, *Aztec Software*© has been used (*Figure 5.16*).

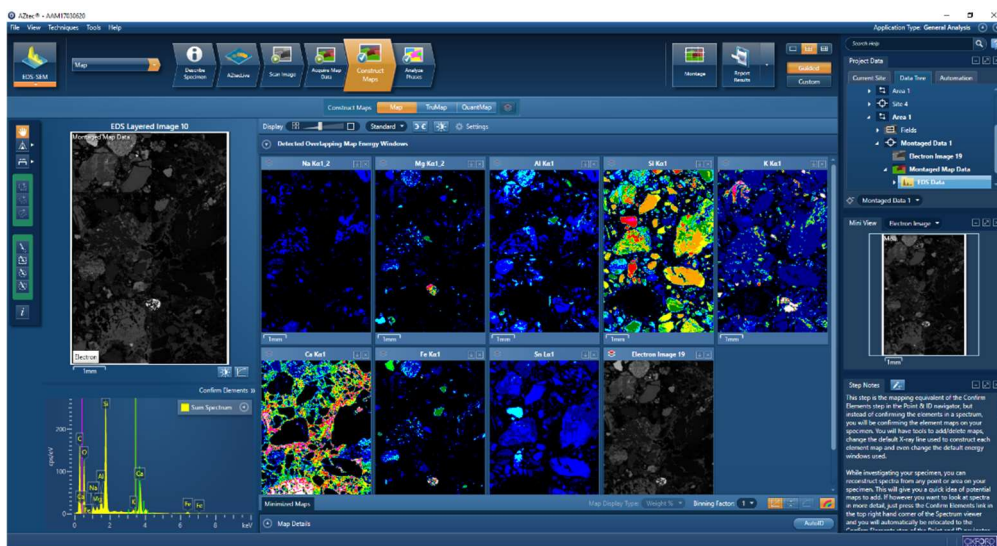


Figure 5.16: Aztec software interface during the acquisition of quantitative maps.

Several works already focused on this topic and furnish fundamental knowledge (Belfiore et al., 2016; Cossio and Borghi, 1998; Cossio et al., 2002; Hugo et al. 2015; Lanari et al., 2014; Ortolano et al., 2014; Ortolano et al., 2018; Parish and Brewer, 2010; Seddio and Carpenter, 2017; Teng and Gauvin, 2020).

In order to obtain sufficiently representative quantitative maps, it is necessary to have a volume of the signal source X minor than the smallest detail to analyze (lateral resolution) and a low noise level that allows to highlight contrast points with different concentrations. Concerning the first point, the X-ray source volume with a beam of 15 KeV (which depends on the density and the average atomic number of the sample) is between 1 and 2 μm ; for this reason, it is useless to select a beam pitch smaller than this value. Secondly, to decrease statistical noise and increase contrast, many counts at each point of the spectrum are required: it can be obtained by the combination of high counting efficiency (CPS) and/or high residence time at each point (Dwell Time).

Obviously, working with high counting efficiency conditions (with the same solid angle as the detector) requires a high probe current which generally worsens the beam resolution; however, since the required resolution is related to the X-ray origin volume (not to the secondary electrons: two orders of magnitude higher) the loss of resolution is negligible.

The question that arises with this type of process is how large the scanned area must be in order to be representative of the entire sample. The largest possible area is, generally, the best answer. This depends on the minimum and maximum size of the objects to highlight and classify: if the objects are large in size compared to the scanned area, in a single frame they are likely to fall on the edge and therefore the percentage classification may be distorted for that class.

Modern microanalytical techniques try to solve the problem by acquiring several adjacent (or slightly overlapping) frames to allow the software to accurately align the individual frames.

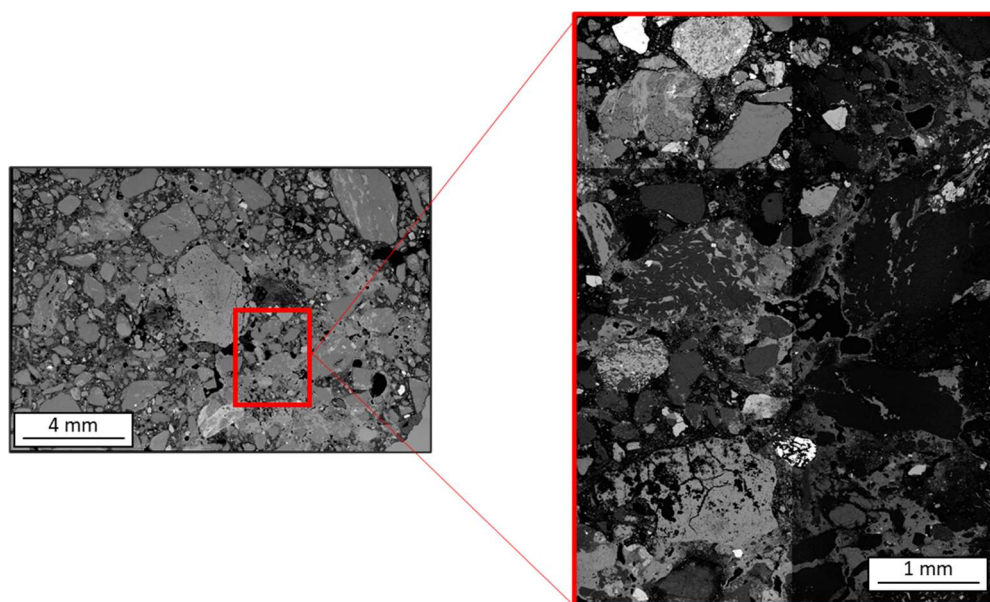


Figure 5.17: Representative area for X-ray map on sample AAM17.

To scan a very large sample area many frames are used, or alternatively, magnification is reduced (increasing the scanned area per frame); in this case it is important to be careful to use the correct number of pixels to get the maximum resolution achievable with X-rays (1 -2 μm). Working at a low working distance (WD of about 10mm) is difficult to achieve low magnification (<100x) without edge distortion: this generally prevents the signal level from being uniform throughout the scanned area of the frame; this can be improved by using a large final collimation aperture (> 100 μm).

In this work, with WD = 10 mm and E = 15 KeV, a magnification of 50X for each frame can be successfully reached (2.55 * 1.9 mm of scanned area); indeed, selecting a scan of 1024 X 768 pixels results in a step of 2.5 μm .

A beam energy of 15 keV and a probe current of 5nA was used, using a process time of 1 μs ; these conditions allowed to reach about 10^6 counts per second (CPS) with a dead time of 30%.

The total acquisition time depends on the total number of pixels and the Dwell-Time (DT): it is reasonable to assume an interval minor of 24 hours; typically a remote nightly acquisition of 16 h was selected, resulting a suitable time to reach a multi-user instrument.

In the case of a geological sample, thin sections with real sample size of 40x20 mm are often used; in this case, to reach a lateral resolution of 2.5 μm a total of 120 MPixels should be scanned: to maintain a total time of 16 hours a DT = 500 μs must be selected. These operative conditions get 50 counts for each spectrum: this is reasonable for a qualitative distribution map, but a quantitative map needs more counts.

Operative conditions adopted consist in DT = 7 ms, which imply a total time of acquisition of about 16 h for 8 frames scanned at 50X magnification and

1024 * 768 pixels spatial resolution for a total of about 6.5 MPixels on 40 mm² (Figure 5.17).

5.6.2.3 3° step: Elaboration of the acquired data

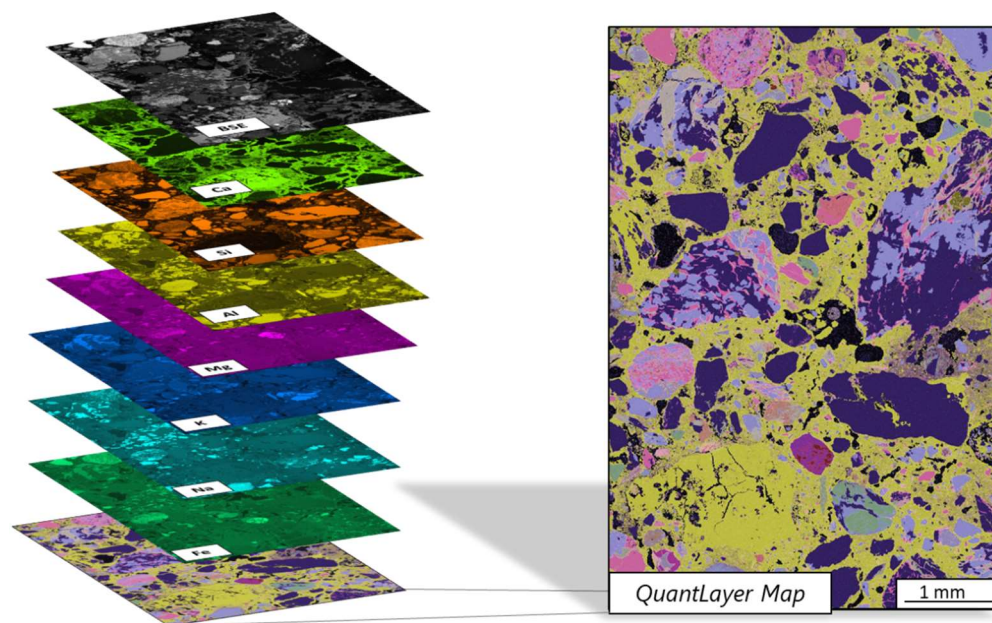


Figure 5.18: Backscattered image, smart maps and quant layer maps obtained from X-ray Map on sample AAM17.

Generally, an acquisition of several hours is affected by the characteristic instabilities of the instrument: with W source, the variation of the filament emission is the most important one; this is displayed by a slow and linear decrease of the signal (luminosity) during the acquisition; nevertheless, in the phase of heating and saturating the filament a minimum of 1% / hour loss of emission can be obtained.

Carbon, coated evenly on all points of the map, can be used to highlight the points with bad closure. By semi-automatic reprocessing, only for these points, an estimate of the carbon can be calculated by difference, comparing the previous analysis with low closure. The introduction of semi-quantitative carbon in the list of analyzed elements for the phase map calculation

significantly improves the separation between clusters and, therefore, the accuracy and velocity of convergence of the K-Means calculation. Thanks to this operation and to the quantitative dataset for each element, it has been fundamental to establish the finest method in order to obtain, point by point, their classification into single homogeneous cluster (mineralogical phases).

In this regard, the cluster analysis is certainly the most appropriate statistical method of multivariate analysis. It will not be described here in detail, but some considerations concerning the selected options must be done.

Cluster Analysis construct systematic structures in large numbers of variables and observations. For samples of small dimension, Hierarchical Cluster Analysis is the most appropriate: when the sample (n) is large, the algorithm may be very slow to reach a solution. In general, users should consider K-Means Cluster when the sample size is larger than 200 μm .

K-Means Cluster Analysis is used to classify observations through K number of clusters: the idea is to minimize the distance between the data and the corresponding cluster centroid. K-means analysis is based on one of the simplest clusters solving problem algorithms, and it is faster than Hierarchical Cluster Analysis: in this case the quickness of the method is very important because the quantitative maps contain a few millions of pixels.

Nevertheless, it is notable that the process of K-means cluster analysis assumes that the user already knows the centroid of the observations, or, at least, the number of groups to be clustered. There is no way to set the number of clusters for the analysis. In order to obtain a good cluster solution, it may be necessary to examine the characteristics of the clusters and then modify incrementally the number of them. Generally, the number of clusters must not be less than the number of statistic observables: in this instance 11 quantitative elements were analyzed (*Figure 5.18*).

For **GeoMatMap Software**, the freely available "Accord.MachineLearning" package (<http://accord-framework.net/>) was used. Even in the case of a map with a greater number of pixels (6.5^6) with 11 observables the total processing time for K-Means is less than 200 seconds.

When the clusters are obtained, it is important to check if they are homogeneous; to do this, various methods are available:

- to observe the false color image (clusters) resulting from K-Means processing;
- to extract the EDS spectra, for each point of the cluster, summed to form the average spectrum for each class; in this way by qualitatively and quantitatively analyses of the spectrum of each cluster, it is possible to identify single mineralogical phases;
- additional information comes from the BSE image acquired simultaneously with the X map and spatially superimposed: it is possible to extract a BSE image for each cluster (it contains only the image points belonging to that cluster). The BSE image information consists in an average atomic number: if this image is transformed in a histogram, the peaks will be centered on the average atomic number of each phase. From the analyses of the number and shape of the peaks, considerations on the homogeneity of the cluster can be formulated.

If one or more clusters are not homogeneous, the K-Means processing with a greater number of clusters can be repeated.

After different attempts, imposing a high initial number of clusters and then grouping together phases characterized by an identical stoichiometry, a correct separation into single homogeneous phases can be reached. The best results have been achieved by imposing a number of clusters 3-4 times the number of mono-elemental maps (30-40 clusters).

Finally, the Hierarchical Cluster Analysis, shown in *Figure 5.19* as example, represents the most suitable method to group phases with similar chemical composition, given the low number of observables, using as input the centroid (11 dimensions) of the individual clusters calculated with K- Means.

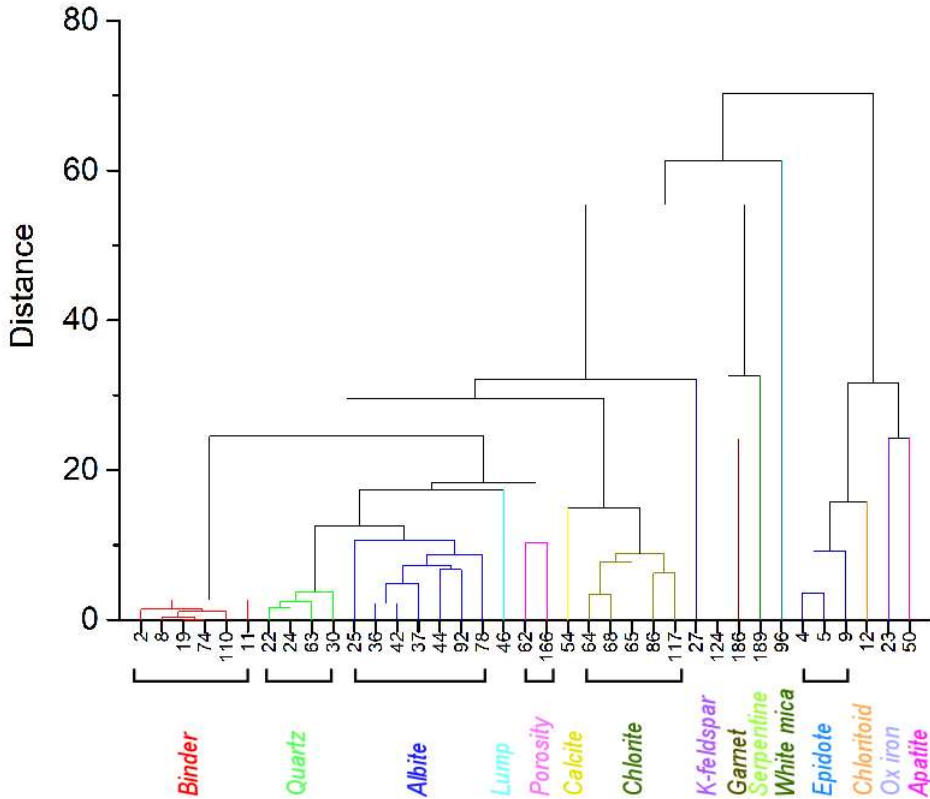


Figure 5.19: Example of Hierarchical Cluster Analysis graph (sample AAM17).

At the end of this process of elaboration of the data coming from the SEM-EDS X-ray mapping, the available output is the following:

- a) quantitative chemical analyses for each point of the map for the fixed list of elements (Na, Mg, Al, Si, P, S, K, Ca, Ti, Fe) based on an element calculated by stoichiometry (Oxygen) and expressed as Wt%, Oxide%, At%, App% (apparent concentration not normalized) (*Figure 5.18a*);
- b) quantitative false colors (based on 8 concentration class) Image Map for each element (*Figure 5.18b*);

c) false color image of the K-Mean clusters, where each phase is identified by a different false color (*Figure 5.20*);

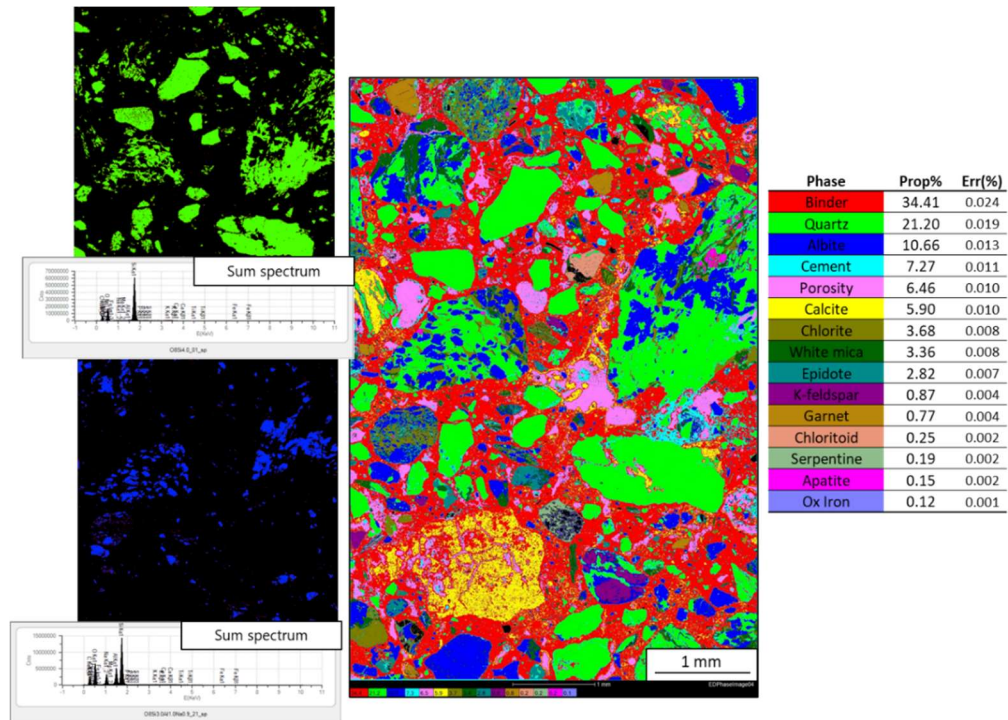


Figure 5.20: False color image of the K-Mean clusters of sample AAM17 where each mineral phase is identified by a different false color. For every mineral phase there is a corresponding EDS sum spectrum.

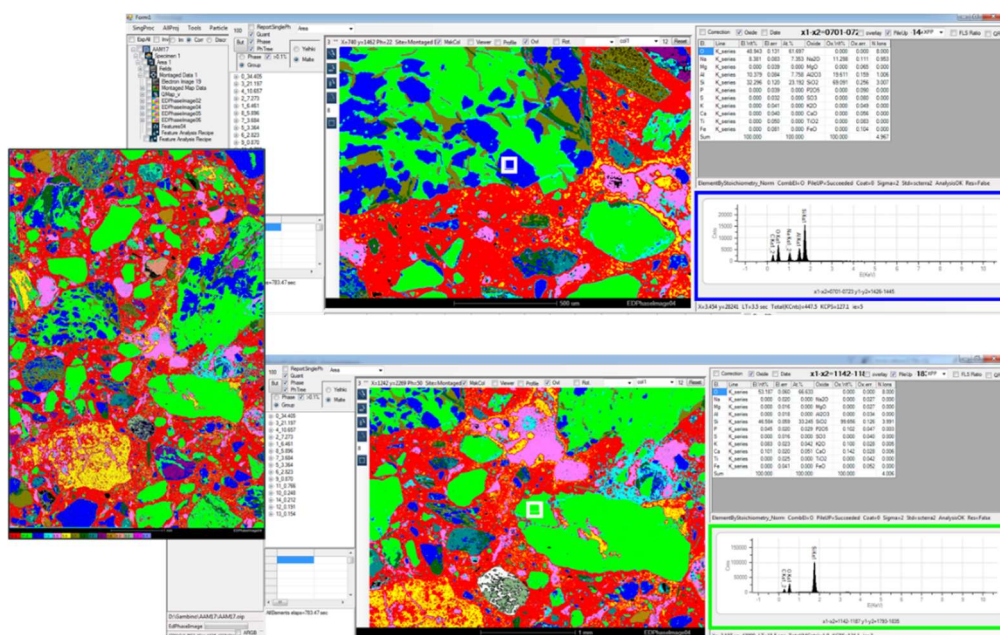


Figure 5.21: False color image of the K-Mean clusters of sample AAM17 where each mineral phase is identified by a different false color. By selecting a small area (white square), it is possible to visualize the spectrum of the mineral phase (blue and green rectangles).

- d) table with centroid of each cluster expressed as Wt% of the acquired elements and modal % of the mineralogical phases;
- e) average EDS spectrum for selected area of each cluster (**Figure 5.21**);
- f) quantitative analysis for selected area of each cluster based on a fixed number of oxygen for that mineralogical phase;
- g) Hidraulicity Index (HI) calculation using the quantitative X-ray maps compound of SiO_2 , Al_2O_3 , Fe_2O_3 , Ca_2O_3 and MgO expressed as discrete color class image (**Figure 5.22**).

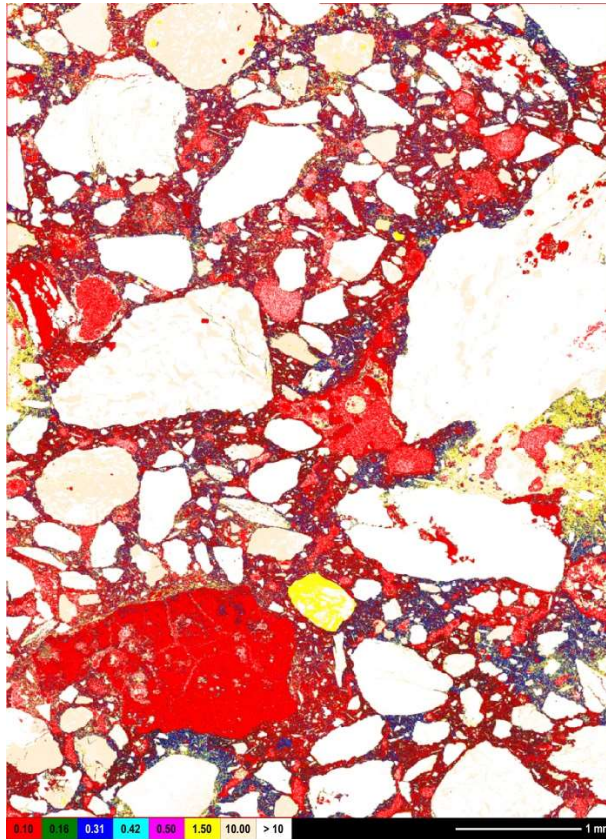


Figure 5.22: Example of Hydraulicity Index $((\text{SiO}_2+\text{Al}_2\text{O}_3+\text{Fe}_2\text{O}_3)/(\text{CaO}+\text{MgO}))$ false color map (sample AAM17).

5.6.2.4 4^o step: Quantitative SEM-EDS spot analyses

The method described above has been calibrated by quantitative spot EDS analysis in order to confirm K-means data as shown in *Figure 5.23*.

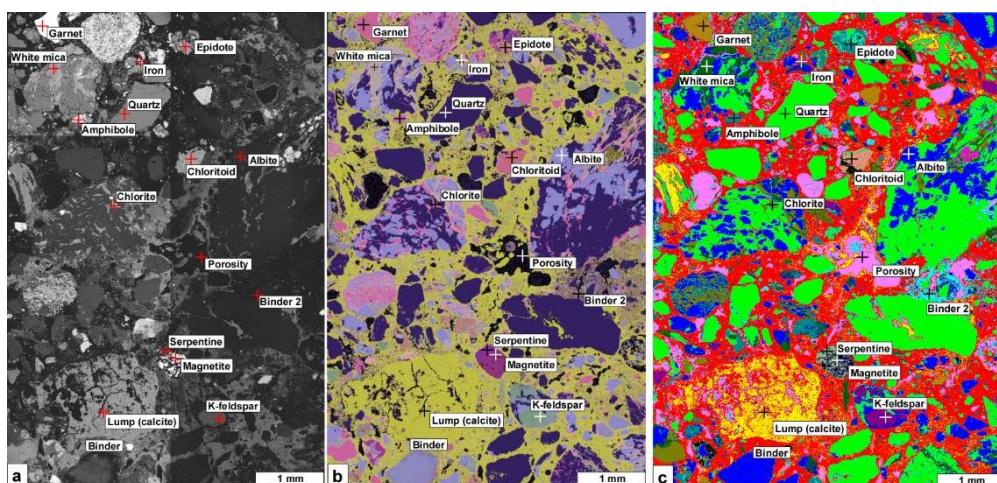


Figure 5.23: Example of spot analysis by SEM-EDS on sample AAM17 performed to calibrate the GeoMatMap protocol. **a.** Backscattered image **b.** Quantlayer map **c.** False color image of the K-Means clusters.

5.6.2.5 5° step: interpretation of the acquired data

The correct interpretation of the collected data allows to make several assumptions regarding both the *aggregate* and the *binder*. Concerning the former, it allows to assume:

- Information on the supply areas of raw materials;
- Information of possible sieving or grinding of the aggregate;
- Indication on the accuracy in the mixing process of the mortar;

Relating to the *binder* the following informations may be achieved:

- type of material used for the preparation of lime;
- information on the quantity of mixing water used or possible problems in the mixing inlet phase due to too fast drying;
- definition of the mixture (lean or greasy);
- values of Hydraulicity Index;
- State of preservation.

An extended flow-chart of the method is provided in *Figure 5.24*.



Figure 5.24: Flow chart of analytical protocol for the petrographic study of mortars.

5.7 Results

5.7.1 Petrography and X-ray maps

5.7.1.1 Original Roman mortars

The mortars sampled in the first (from AAM1 to AAM31) and second surveys (AAM32, AAM37, AAM42), according to archaeological and archaeometric data (Appolonia. et al., 2010), belong to original bedding mortars of Roman age.

Based on detailed characterization by optical microscope, SEM-EDS analysis and X-ray map analysis, despite the several sampling sites (e.g. different walls of the Theatre; *Figure 5.8*), all the samples have been gathered in one single group. Indeed, they show very similar grain size, sorting, composition of both aggregate and binder and A/B ratio. Furthermore, all the samples are characterized by a poor state of preservation due to the scarce amount of binder leading to the aggregate detachment.

The aggregate

The grain size of the aggregate is fine, from 0.5 to 4 mm and moderately sorted. The samples show a bimodal grain size distribution highlighted by fine and coarse grains occurring in variable ratio depending to the observed section. The clasts are spherical in shape and display a sub-angled to sub-rounded rounding. Reaction edges with the binder have not been detected. The general aspect of a thin section has been displayed in *Figure 5.25a* and *b*. Petrographically, the aggregate is typically made up of lithic fragments of quartzite, micaschist, calcschist, marble and prasinite, with the only exception of monomineralic clasts of quartz and biotite that have also been individually found.

Quartzite elements mostly have subspherical shapes and subrounded to rounded edges. They are fine and very fine-grained (*Figure 5.25c*).

Micaschist elements are subangular in shape and consist of lamellar micas and quartz crystals (*Figure 5.25d*). Some of them can be classified as graphitic micaschists and some others also contain garnet crystals (around 200 μm in size) (*Figure 5.25e*).

Calcschist elements are subangular in shape and consist of fine-grained carbonate, fine-grained white mica arranged in sub-millimeter and continuous oriented levels and minor fine-grained quartz (*Figure 5.25f*).

The marble fragments show a sub-rounded to rounded shape and consist of calcite crystals with lobed edges and triple joints (*Figure 5.25g*).

Prasinite elements are subangular in shape and consist of lamellar chlorite, amphibole, albite and epidote crystals (*Figure 5.25f*).

Quartz elements are present especially in the fine-grained fraction of the aggregate. Edges can be either angular or rounded. Locally it exhibits the classic undulose extinction due to deformation (*Figure 5.25g*).

Biotite presents the typical lamellar shape and pleochroism from light brown to dark brown (*Figure 5.25h*).

Neither additions nor additives such as straw, wood or other substances have been found.

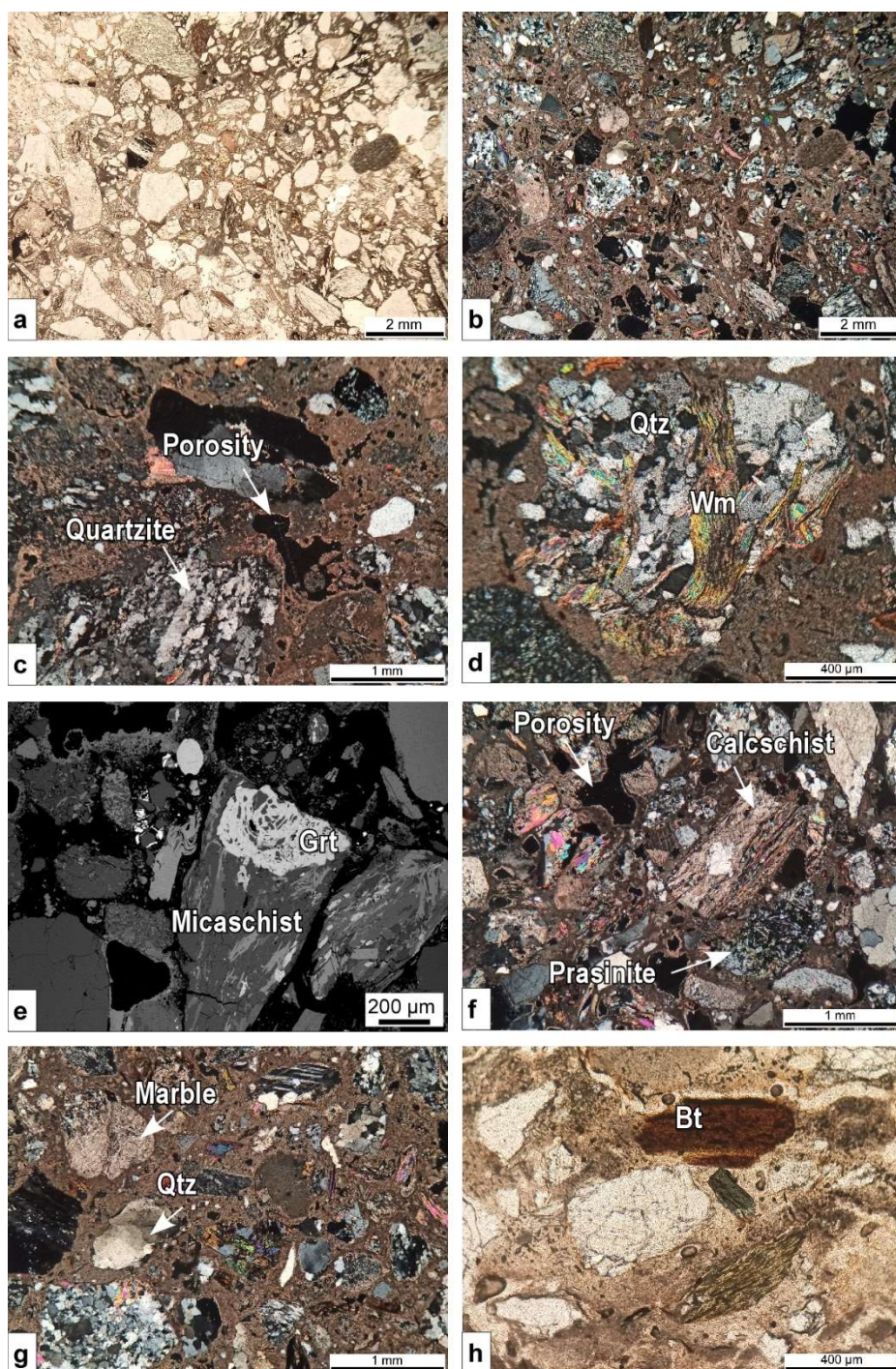


Figure 5.25: Microphotographs of Roman mortars. General aspect of roman mortar by optical microscope, //pol (a.) and X pl (b.). Note the fine grain size of the aggregate, from 0.5 to 4 mm, moderately sorted. The clasts are sub-angled to sub-rounded rounding in shape c. Detail of a quartzite clast and an irregularly shaped pore (X pol). d. Detail of a micaschist element made up of quartz and iso-oriented white mica (X pol). e. Detail of a micaschist clast with a garnet

crystal (SEM backscattered image). **f.** Detail of calcschist and prasinite clasts. Note also the irregular shape of porosity (X pol). **g.** Detail of sub-rounded clast of marble and monomineralic element of quartz with classic undulose extinction due to deformation (X pol). **h.** Detail of a clast made up of single crystal of pleochroic biotite (// pol). Qtz: quartz, Wm: White mica, Grt: garnet, Bt: biotite.

The binder

The binder, light brown in color, shows a micritic texture according to the definition of Standard NORMA UNI 11176. It is homogeneous even though there is a widespread presence of lumps (*Figure 5.26a-d*). These lumps, millimetric in size, generally have rounded shapes. They are mostly homogeneous, dark brown in color, and some of them are characterized by fractures due to the phenomenon of shrinking (*Figure 5.26a* and *c*).

The porosity is widespread, with an irregular to rounded shape, essentially due to the detachment of the aggregate from the binder and shrinking phenomena. There is also a micro-porosity due to the loss of binder over time, which has brought the samples to their current poor state of preservation.

The Binder/Aggregate ratio is around 1/2.

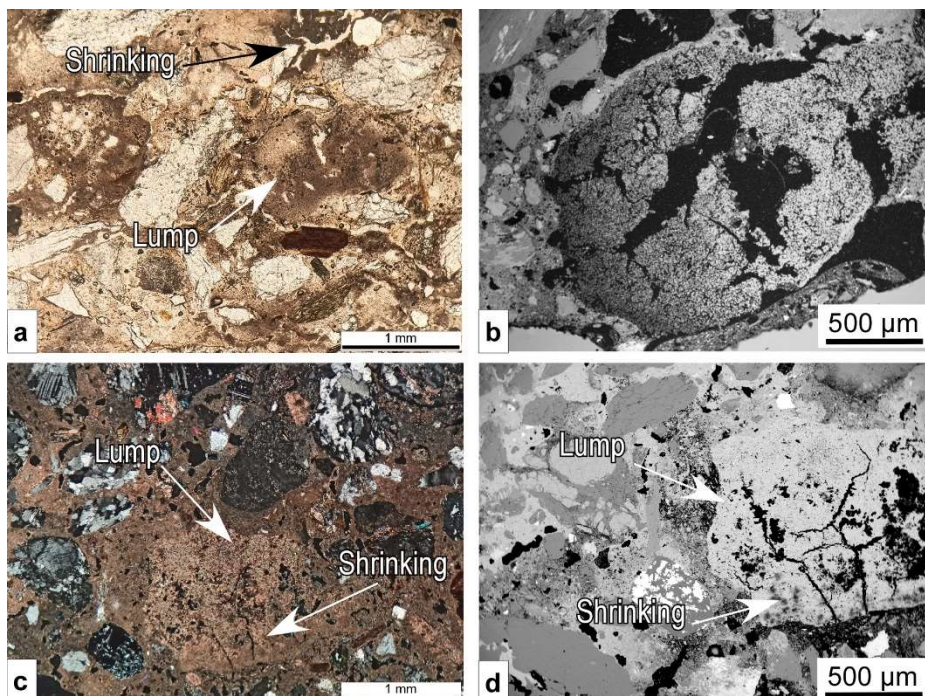


Figure 5.26: Microphotographs of Roman mortars. **a.** Detail of the micritic binder characterized by the occurrence of a lump. Widespread shrinking phenomena are also recognizable throughout the thin section (*// pol*). **b.** Detail of rounded lump characterized by fractures due to shrinking. **c.** (*X pol*) and **d.** (SEM backscattered image) Detail of a lump with thin fractures due to shrinking phenomena.

As already explained in the previous [Paragraph 5.6.1](#), and given the aforementioned compositional and textural features, four representative samples (AAM01, AAM17, AAM25, AAM37) have been chosen. The false-color X-ray maps and the amount percentages of their mineral phases are respectively displayed in *Figure 5.27*, *Figure 5.28*, *Figure 5.29*, *Figure 5.30*, and in *Table 5.4*, *Table 5.5*, *Table 5.6*, *Table 5.7*.

False- color quantitative X-ray maps expressed in oxides processed using Aztec Software are shown in **Appendix IV**.

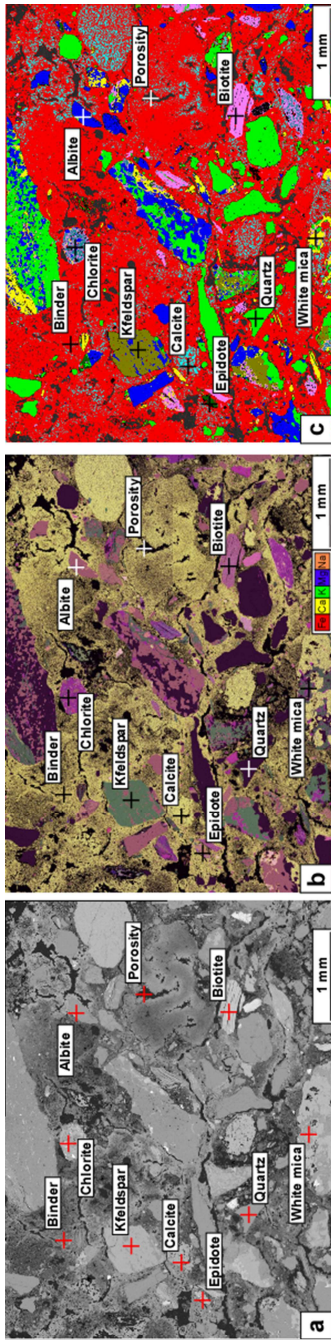


Figure 5.27: Representative area of sample AAM01 **a.** Backscattered image **b.** Quant layer map **c.** False color GeoMatMap.

Mineral phase	Prop%	O Wt	Fe Wt	Ti Wt	Ca Wt	K Wt	Si Wt	Al Wt	Mg Wt	Na K Wt
Binder	58.76	37.09	0.18	0.03	19.01	0.07	1.83	0.42	0.10	0.03
Quartz	11.56	50.97	0.25	0.02	0.14	0.07	45.56	0.51	0.11	0.10
Porosity	7.04	0.00	0.00	0.00	0.00	0.00	0.00	0.00	0.00	0.00
Albite	6.18	47.80	0.09	0.02	0.34	0.29	33.14	10.81	0.03	7.46
Calcite	4.84	57.66	0.05	0.02	41.99	0.02	0.19	0.04	0.02	0.01
Biotite	2.97	46.87	14.02	0.42	2.19	1.45	18.01	10.55	6.39	0.10
White mica	2.44	49.25	1.34	0.10	0.40	6.47	25.20	16.28	0.81	0.15
K-feldspar	2.15	46.38	0.06	0.01	0.02	11.23	31.87	10.19	0.02	0.21
Epidote	1.16	51.73	1.46	0.11	14.83	1.76	18.34	10.67	0.33	0.78
Chlorite	0.57	45.04	18.11	0.13	0.26	0.05	14.50	11.09	10.81	0.01
Total	97.67									

Table 5.4: Percentage amount, listed in order of abundance, of mineral phases, porosity and binder and the relative chemical composition expresses as single element wt% obtained by GeoMatMap software (AAM01 sample).

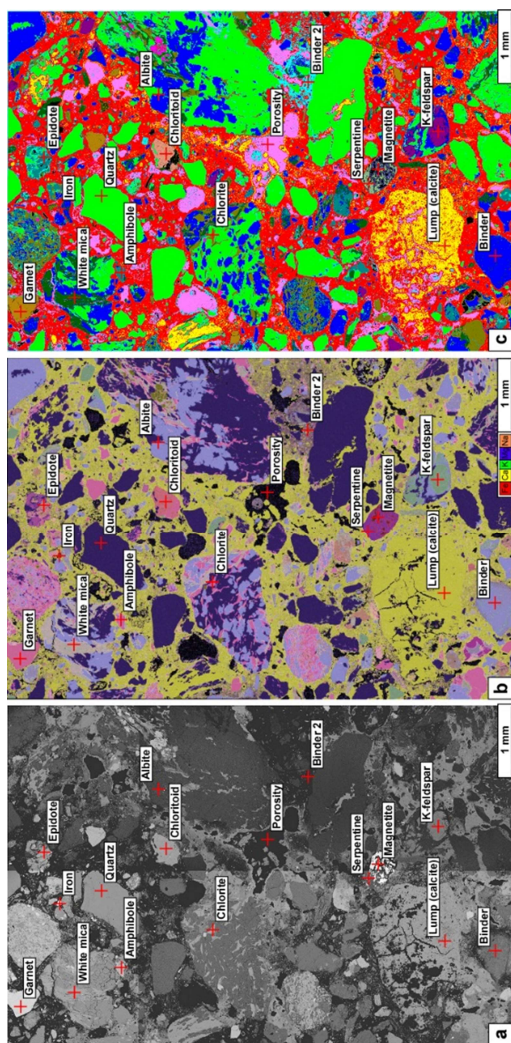


Figure 5.28: Representative area of sample AAM17 **a.** Backscattered image **b.** Quant layer map **c.** False color GeoMatMap.

AAM17 - Roman mortar

Mineral phase	Prop%	O Wt	Fe Wt	Ti Wt	Ca Wt	K Wt	Si Wt	Al Wt	Mg Wt	Na K Wt
Binder	34.41	32.39	0.31	0.06	58.15	0.17	6.78	1.17	0.18	0.07
Quartz	21.20	53.24	0.02	0.01	0.02	0.00	46.60	0.01	0.00	0.01
Albite	10.66	48.81	0.17	0.02	0.60	0.52	31.64	10.93	0.08	7.17
Binder 2	7.27	0.00	0.00	0.00	0.00	0.00	0.00	0.00	0.00	0.00
Porosity	6.46	18.50	0.31	0.13	2.82	0.39	13.89	0.87	0.20	0.19
Calcite	5.90	28.57	0.00	0.00	71.32	0.02	0.04	0.01	0.01	0.01
Chlorite	3.68	42.43	17.36	0.07	0.80	0.58	18.00	12.14	8.46	0.12
White mica	3.36	47.15	1.30	0.07	0.26	7.63	26.56	15.68	1.06	0.24
Epidote	2.82	44.41	4.96	0.13	12.53	1.18	21.90	12.86	1.68	0.30
K-feldspar	0.87	46.89	0.02	0.01	0.03	11.82	31.12	10.01	0.00	0.05
Garnet	0.77	41.74	21.94	0.01	1.09	0.03	18.87	11.88	4.41	0.01
Chloritoid	0.25	41.48	22.86	0.01	0.01	0.01	13.06	22.31	0.19	0.01
Serpentine	0.19	46.94	0.39	0.01	0.04	0.01	25.23	0.11	27.24	0.01
Apatite	0.15	39.91	0.02	0.02	42.17	0.01	0.09	0.01	0.01	0.01
Ox Iron	0.12	29.00	56.51	0.02	42.72	0.03	6.96	0.71	5.90	0.02
Total	98.11									

Table 5.5: Percentage amount, listed in order of abundance, of mineral phases, porosity and binder and the relative chemical composition expresses as single element wt% obtained by GeoMatMap software. (sample AAM17).

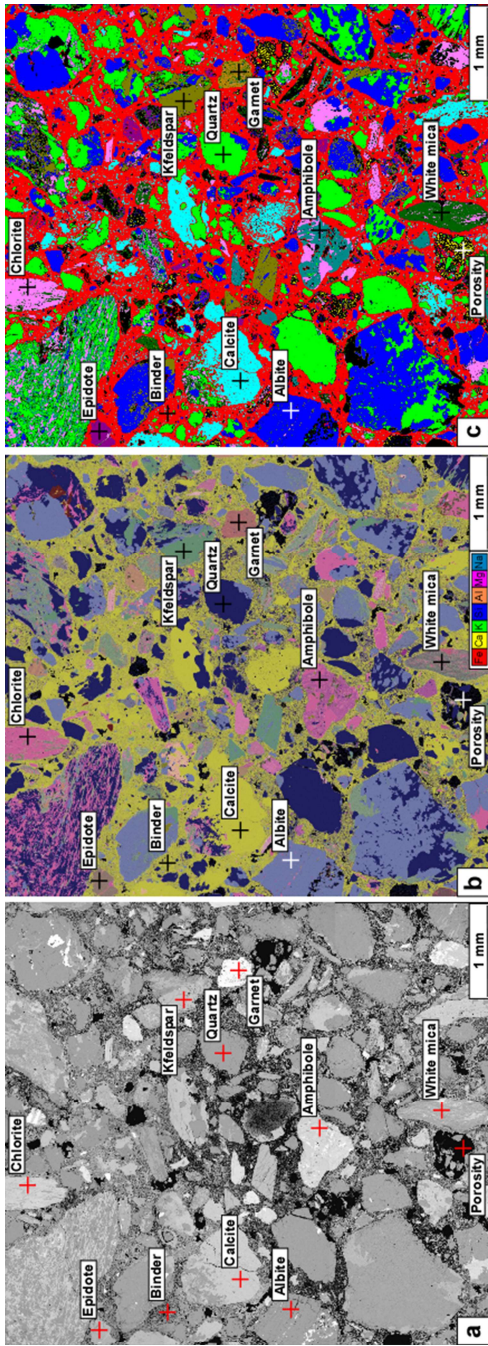


Figure 5.29: Representative area of sample AAM25 a. Backscattered image b. Quantlayer map c. False color GeoMatMap.

Mineral phase	Prop%	O	Wt	Fe	Wt	Ti	Wt	Ca	Wt	K	Wt	Si	Wt	Al	Wt	Mg	Wt	Na	K	Wt	
Binder	36.65	36.27	0.16	0.29	2.26	13.42	0.28	45.98	0.10	0.51											
Quartz	15.46	52.94	0.08	0.21	0.31	45.84	0.05	0.24	0.01	0.26											
Albite	15.23	48.91	7.95	0.02	10.49	32.07	0.07	0.36	0.02	0.05											
Calcite	6.72	28.71	0.01	0.03	0.02	0.29	0.02	70.86	0.02	0.02											
Chlorite	4.29	41.80	0.04	8.58	12.15	17.03	0.56	0.33	0.18	19.30											
Porosity	3.48	7.10	0.13	0.09	0.23	5.24	0.23	1.08	0.11	0.12											
K-feldspar	3.34	47.70	1.45	0.15	11.75	30.54	7.84	0.23	0.03	0.26											
White mica	3.13	46.54	0.39	1.65	16.66	24.16	4.84	1.42	0.32	3.96											
Amphibole	2.81	44.94	0.13	7.13	2.96	28.17	0.28	5.97	0.05	10.33											
Epidote	1.47	45.16	0.37	0.15	15.18	21.95	1.29	13.68	0.05	2.13											
Garnet	0.26	42.28	0.01	0.07	12.69	20.37	0.06	5.81	0.03	18.66											
Total	92.83																				

Table 5.6: Percentage amount, listed in order of abundance, of mineral phases, porosity and binder and the relative chemical composition expresses as single element wt% obtained by GeoMatMap software (sample AAM25).

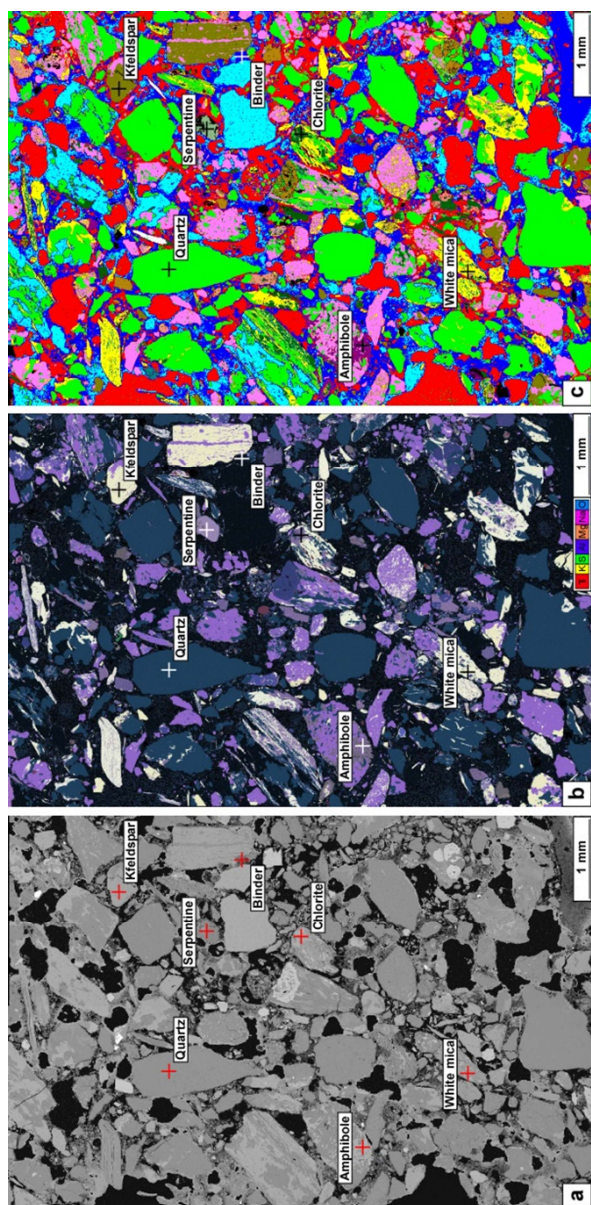


Figure 5.30: Representative area of sample AAM37 **a.** Backscattered image **b.** Quantlayer map **c.** False color GeoMatMap.

Mineral phase	Prop%	O Wt	Fe Wt	Ti Wt	Ca Wt	K Wt	Si Wt	Al Wt	Mg Wt	Na K Wt
Porosity	22.86	24.00	0.31	0.36	1.77	16.61	0.48	5.99	0.24	0.68
Quartz	22.12	43.53	0.01	0.00	0.01	38.11	0.00	0.01	0.07	0.01
Binder	19.91	30.60	0.05	0.15	0.78	4.16	0.13	62.04	0.07	0.30
Calcite	9.61	28.60	0.01	0.03	0.01	0.08	0.02	71.18	0.02	0.03
Albite	9.28	48.90	7.89	0.04	10.63	31.96	0.10	0.30	0.02	0.09
White mica	5.55	47.19	0.46	0.82	16.65	25.85	6.80	0.65	0.15	1.37
K-feldspar	3.20	47.29	0.89	0.08	11.23	30.56	9.64	0.07	0.03	0.17
Chlorite	1.58	40.60	0.02	9.21	12.88	14.47	0.09	0.10	0.03	22.57
Biotite	1.31	43.50	0.26	5.85	13.68	19.78	2.39	0.63	0.22	13.65
Amphibole	1.23	44.08	0.23	6.89	4.12	25.97	0.25	6.72	0.19	11.51
Garnet	0.91	40.67	0.01	1.95	11.55	18.26	0.02	3.41	0.02	24.08
Epidote	0.53	44.36	0.04	0.02	16.02	19.60	0.05	17.66	0.02	2.19
Serpentine	0.13	46.64	0.02	23.87	8.56	20.26	0.00	0.02	0.01	0.57
Paragonite	0.11	48.67	5.28	0.00	22.26	23.60	0.04	0.02	0.01	0.03
Total	98.11									

Table 5.7: Percentage amount, listed in order of abundance, of mineral phases, porosity and binder and the relative chemical composition expresses as single element wt% obtained by GeoMatMap software (sample AAM37).

5.7.1.2 Restoration mortars

Most of the mortars sampled in the second surveys (AAM33, AAM34, AAM35, AAM36, AAM38, AAM39 AAM40, AAM41 – see *Table 5.2*) belong to the different restoration phases of the Roman Theatre ([Paragraph 5.5](#)).

Based on a detailed characterization by optical microscope, SEM-EDS analysis and X-ray map analysis, and according to archaeological data (Appolonia et al., 2010), the samples have been gathered in four groups referring to each restoration phase.

First restoration

Mortars of the first restoration are represented by AAM33 and AAM41 samples.

The aggregate

The grain size of the aggregate is fine (< 4 mm), in particular ranging from 200 µm to 2 mm and the grains are well sorted. The samples show a heterogeneous grain size distribution. The clasts are low-spherical and display an angular to sub-angular shape. Reaction edges with the binder have never been detected. The general aspect in thin section has been displayed in *Figure 5.31a* and *b*. Petrographically, the aggregate is made up of lithic fragments of quartzite, quartz-micaschists, chloritoschists and calcschists belonging to the coarser grain fraction (1.5 – 2 mm).

Quartz-micaschists elements are angular in shape and consist of lamellar white mica and quartz crystals (*Figure 5.31c*).

Quartzite elements have subspherical shapes and subrounded to rounded edges. They show a fine grain size (*Figure 5.31d*).

Chloritoschist elements are sub-angular in shape and composed of fine-grained chlorite, rare white mica and quartz iso-oriented in levels.

Calcschist elements are angular in shape and consist of fine-grained calcite, fine-grained white mica arranged in sub-millimeter and continuous oriented levels and minor fine-grained quartz.

Monomineralic clasts of quartz, 400 – 600 μm in size, sub-angular to angular in shape are present. They locally exhibit the classic undulose extinction typical of those crystals that suffered tectonic deformation (*Figure 5.31d*). Other monomineralic elements belonging to the finest grain fraction (200 – 300 μm) have been found: lamellar chlorite and sub-angular albite.

The binder

The binder is homogeneous, light brown in color and shows a micritic texture according to Standard NORMA UNI 11176.

The porosity, scarcely developed, is rounded in shape, as shown in *Figure 5.31e*, and possibly due to bubbles formation during mortar firing.

The difference between this set of samples and the Roman ones is evident; the binder is very dense, little shrinking phenomena have been observed (*Figure 5.31f*) but aggregate is not separating from the binder.

The Binder/Aggregate ratio is around 1\1.

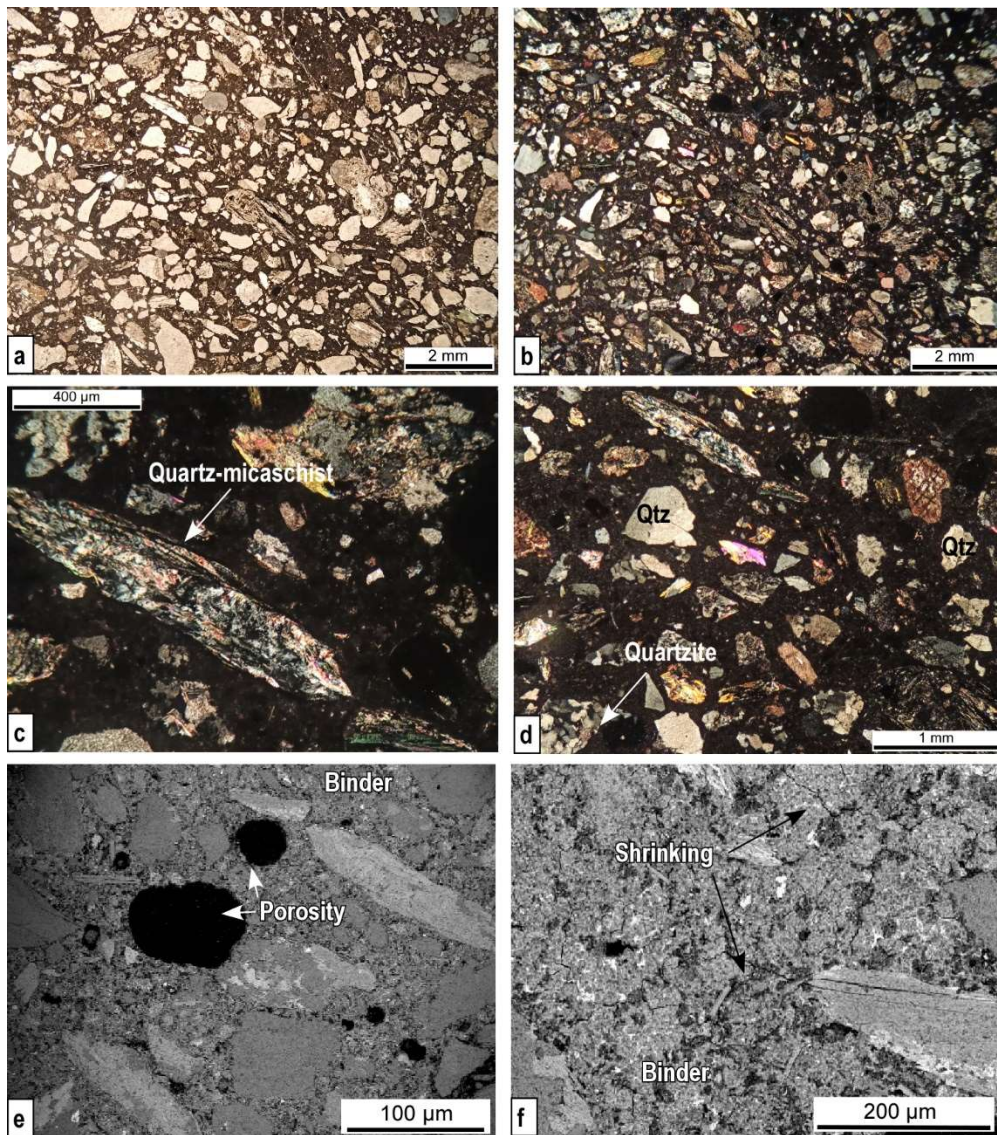


Figure 5.31 Microphotographs of the first restoration phase. **a.** General aspect of mortars by optical microscope with // (**a.**) and X pol (**b.**). Note the fine grain size of the aggregate, 200 μm to 2 mm, which is also well sorted. The clasts are low-spherical and display an angular to sub-angular shape **c.** Detail of a quartz-micaschist clast, angular in shape (X pol). **d.** Detail of monomineralic element of quartz, 400 to 600 μm in size. Note, in the bottom left corner of the microphotograph, a sub-rounded quartzite element made up of fine-grained quartz (X pol). **e.** Detail of rounded pores, possibly due to bubbles formation during mortar firing (SEM backscattered image). **f.** Detail of thin shrinking of the binder (SEM backscattered image). Qtz: quartz.

Second restoration

Mortars of second restoration are represented by AAM34 and AAM39 samples.

The aggregate

The grain size of the aggregate is fine, from 200 μm to 2 mm in size and well sorted. The grain size distribution is heterogeneous and the samples show three grain size classes: from 200 to 400 μm , from 400 to 600 and from 1 –to 2 mm evenly distributed. The clasts are sub-spherical and display a sub-angular to sub-rounded shape. Reaction edges with the binder have not been detected. The general aspect of a thin section has been provided in *Figure 5.32a*.

Compositionally, the aggregate is made up of lithic fragments of micaschist, granite, marble, serpentinite, chloritoschist and aggregates of vein-filling minerals belonging to the coarse-grained fraction (1 – 2 mm).

Micaschist elements are sub-angular in shape and consist of lamellar white mica and quartz crystals.

Granite elements are sub-angular in shape and characterized by the following minerals: geminated K-feldspar in which albitic perthites are recognizable, quartz and albite crystals.

Marble elements are rounded in shape and around 1 mm in size. Calcite crystals show the typical high birefringence and sutured edges (*Figure 5.32b*).

Serpentinite elements are made up of acicular serpentine crystals.

Chloritoschist elements are sub-angular in shape and composed by iso-oriented chlorite with fine-grained white mica.

The clasts made up of aggregate of vein-filling minerals are typically composed by quartz, calcite, dolomite and pyrite. They show an irregular shape and are rare.

Monomineralic elements of K-feldspar have been observed. They are characterized by their typical tabular shape and they present a grain size around 2 mm (*Figure 5.32c*).

Monomineralic clasts of quartz have been also found, sub-angular to sub-rounded in shape characterized by undulose extinction; they are present especially in the fraction of the aggregate from 400 to 600 μm in size.

Lamellar white mica is the monomineralic element belonging to the fraction from 200 to 400 μm in size.

The binder

The binder is homogeneous, dark brown in color and shows a micritic texture according to Standard NORMA UNI 11176 (*Figure 5.32e*).

The porosity is widespread and characterized by rounded shape (*Figure 5.32f*).

As for the samples of the first restoration phase, the binder is very dense. Shrinking phenomena have been observed even though the aggregate is not separating from the binder (*Figure 5.32g*).

The Binder/Aggregate ratio is around 1/1.

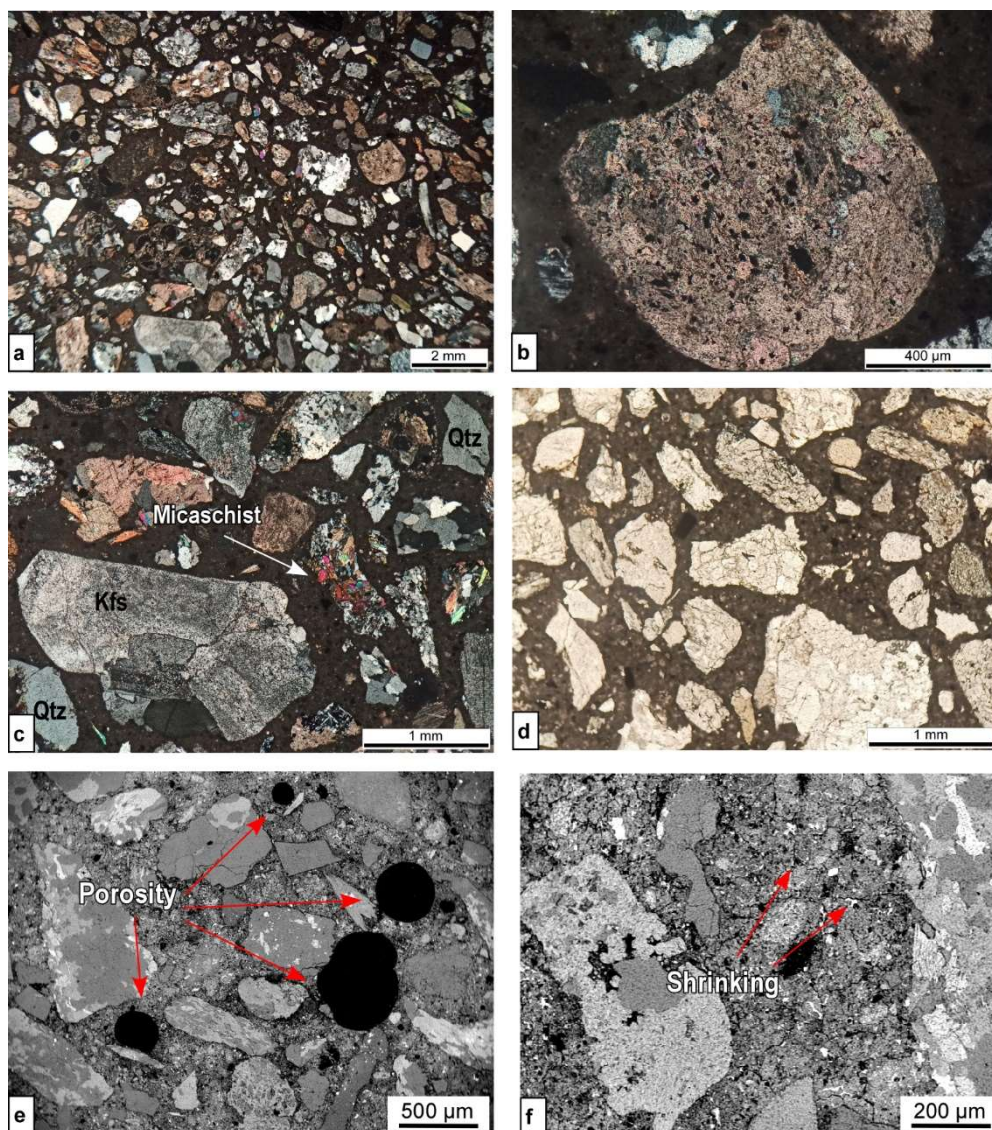


Figure 5.32: Microphotographs of the second restoration phase. **a.** General aspect of mortars by optical microscope, X pol. Note the fine grain size of the aggregate, 200 μm to 2 mm, with heterogeneous distribution. The clasts are sub-spherical and display a sub-angular to sub-rounded shape. **b.** Detail of a marble element, rounded in shape and around 1 mm in size. Note calcite crystals with typical high birefringence and sutured edges (X pol). **c.** Detail of a sub-angular micaschist clast, a monomineralic element of K-feldspar (around 2 mm long) and single crystals of quartz widespread throughout the thin section, 400 – 600 μm in size (X pol). **d.** Detail of the micritic texture of the binder, dark brown in color (// pol). **e.** Detail of the widespread porosity characterized by a rounded shape (SEM backscattered image) **f.** Detail of thin shrinking of the binder. Qtz: quartz, Kfs: K-feldspar.

Third restoration

Mortars of the third restoration are represented by AAM35 and AAM38 samples.

The aggregate

The grain size of the aggregate is fine, from 200 μm to 2 mm, and well sorted. The samples show three grain size classes evenly distributed: from 200 to 400 μm , from 400 to 600 μm and from 1 to 2 mm. The clasts are sub-spherical and display a sub-angular to sub-rounded shape. The general aspect of a thin section has been provided in *Figure 5.33a*.

Petrographically, the aggregate is made up by blast-furnace slags, lithic fragments of serpentinite, gneiss, calcschist, micaschist, chloritoschist and monomineralic clasts of quartz and calcite.

Blast-furnace slag displays the typical composition of this kind of material and a very characteristic morphology. Indeed, these elements, belonging to the fraction from 1 to 2 mm in size, present crystals of needle olivine surrounded by a glassy matrix. They show many rounded pores and a thick edge suggesting reaction with the binder and detachment from it. Shrinkage phenomena have also been observed around these elements (*Figure 5.33b, c, and d*).

Serpentinite elements are sub-rounded in shape, composed by fine-grained serpentine, and belong to the fraction around 1 mm in size.

Gneiss elements are composed by albite, quartz and K-feldspar. They are sub-rounded in shape and belong to the fraction around 1 mm in size.

Micaschist elements are elongated (up to 2 mm long) in shape and consist of lamellar micas and quartz crystals.

Chloritoschist elements are sub-angular in shape and they are composed by fine-grained chlorite oriented in levels and minor white mica. They belong to the fraction around 1 mm in size (*Figure 5.33e*).

Monomineralic clasts of quartz, sub-angular to sub-rounded in shape, are present in the fraction of the aggregate from 400 to 600 μm in size and from 200 to 400 μm one. They locally exhibit the classic ondulose extinction of quartz due to deformation.

Calcite elements are sub-angular in shape and belong to the fraction from 200 to 400 μm in size too.

The binder

The binder is homogeneous distributed, light to dark brown in color and shows a micritic texture according to Standard NORMA UNI 11176.

The porosity is widespread and characterized by rounded in shape.

As for the samples of the first and second restoration, the binder is very dense, but in this case shrinking phenomena have been observed around the blast-furnace slags (*Figure 5.33f*). On the contrary, no lumps have been observed.

The Binder/Aggregate ratio is around 1\1.

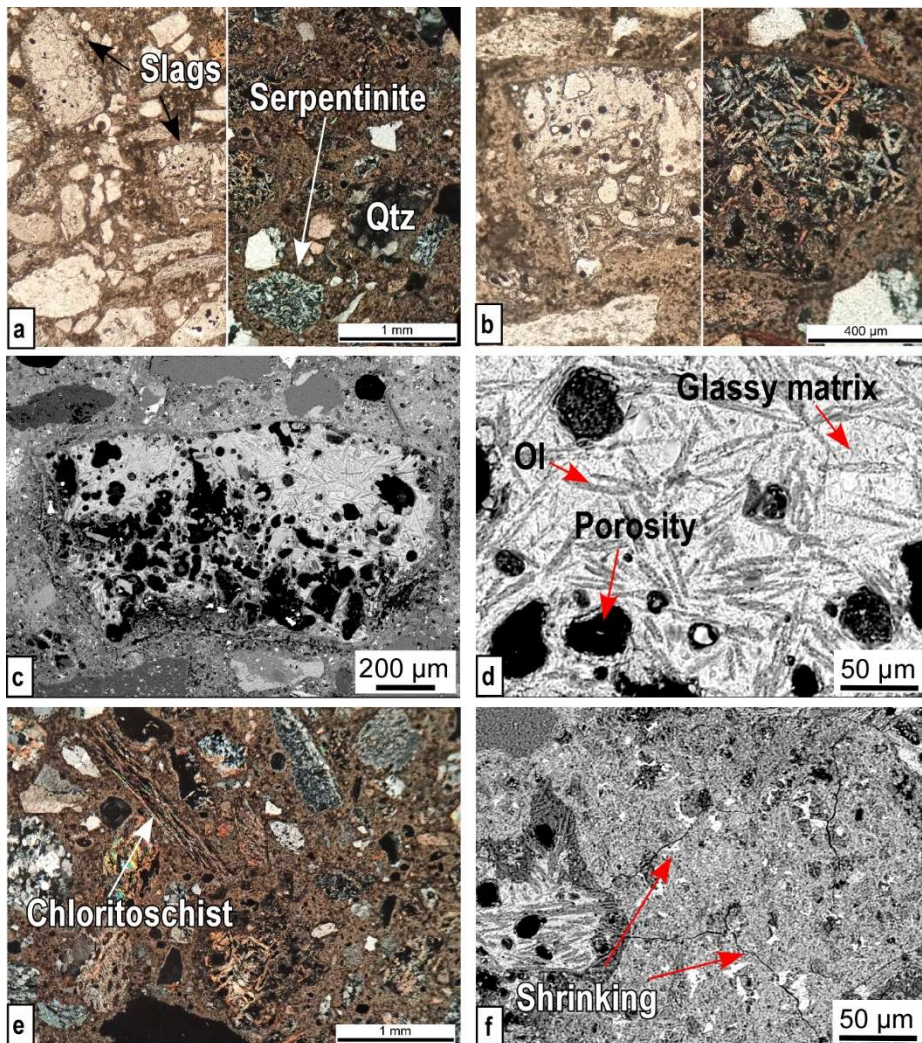


Figure 5.33: Microphotographs of the third restoration phase. **a.** Comparison of // and X pol images of the same mortar sample. Note the presence of blast-furnace slags, rounded lithic fragments of serpentinite and monomineralic element of quartz. **b.** Detail of a slag comparing // and X pol. **c.** SEM backscattered image of the slag previously shown. Note the several rounded pores within the slag and its thick outer edge suggesting a chemical reaction with the binder. **d.** Detail of slag with crystals of acicular olivine surrounded by a glassy matrix (SEM backscattered image). **e.** Detail of a chloritoschist element, sub-angular in shape, and the micritic texture of the binder (X pol). **f.** Detail of shrinking phenomenon observed around the blast-furnace slag.

Fourth restoration

Mortars of fourth restoration are represented by AAM36 and AAM40 samples.

The aggregate

The grain size of the aggregate is fine, from 200 μm to 2 mm, and well sorted. The samples show three grain size classes evenly distributed: from 200 to 400 μm , from 400 to 800 μm and from 1 to 2 mm in size. The clasts are sub-spherical and display a sub-angular, sub-rounded and rounded shape. The general aspect has been provided in *Figure 5.34a*.

Petrographically, the aggregate is made up of lithic fragments of granitoid, phengite-rich micaschist, calcschist, chloritoschist, rare vein-filling minerals and monomineralic clasts of quartz.

Granitoid elements are made up of quartz, plagioclase, muscovite, K-feldspar (sometimes altered) and show a sub-rounded shape. They belong to the fraction from 1 to 2 mm and to the fraction from 400 to 800 μm (*Figure 5.34a*).

Calcschist elements are sub-rounded in shape and consist of coarse-grained calcite, minor fine-grained quartz and crystals of white mica. They belong to the fraction from 1 to 2 mm (*Figure 5.34b*).

Chloritoschist elements are sub-angular in shape and they are composed by fine-grained chlorite oriented in levels and minor white mica. They belong to the fraction from 1 to 2 mm.

Micaschist elements are sub-rounded in shape and consist of lamellar white mica and quartz crystals.

Vein-filling minerals are composed by quartz, calcite and rare white mica, they show a sub-rounded shape and they belong to the the fraction from 1 to 2 mm (*Figure 5.34c*).

Monomineralic clasts of quartz, sub-angular to sub-rounded in shape and with a undulose extinction, are present in the fraction from 200 to 400 μm .

A single crystal, 70 μm large, of biotite has also been found.

The binder

The binder, inhomogeneously distributed and characterized by light to dark brown areas, shows a micritic texture according to Standard NORMA UNI 11176.

The porosity is irregular in shape and shrinking phenomena are diffused in all sections (*Figure 5.34d*).

In the binder, belite, ettringite and tetracalcium aluminoferrite occur. They are micrometer remains that had not reacted with the binder during the firing. All of them are only recognizable by SEM-EDS analysis (see [Paragraph 5.7.2](#)). Belite (*Figure 5.34e*) and tetracalcium aluminoferrite are bright and rounded in shape observed by backscattered image. Instead, ettringite is fractured and shows a circular shape that is detached from the binder (*Figure 5.34f*).

The Binder/Aggregate ratio is around 1/1.

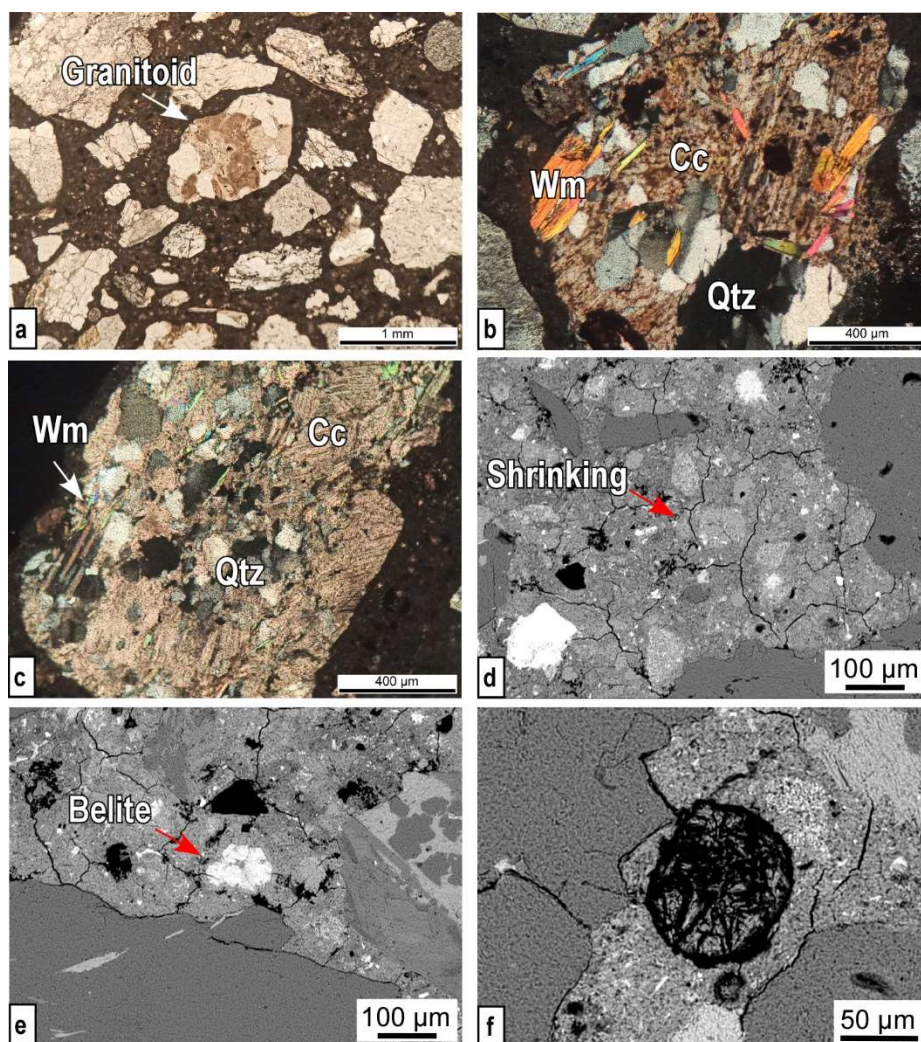


Figure 5.34: Microphotographs of the fourth restoration phase. **a.** General aspect of the mortar, by optical microscope, // pol. Note the presence of granitoid lithic fragment. **b.** Detail of sub-rounded calcschist elements (1 mm in size) made up of coarse-grained calcite, minor fine-grained quartz and white mica (X pol). **c.** Detail of sub-rounded aggregate of vein-filling minerals composed by quartz, calcite and rare white mica crystals (X pol). **d.** Detail of inhomogeneous binder characterized by lighter and darker areas as highlighted by the SEM backscattered image. **e.** Detail of bright and rounded in shape belite (SEM backscattered image). **f.** Detail of ettringite grown on original voids; note the circular shape (SEM backscattered image). Cc: calcite, Wm: white mica, Qtz: quartz.

As already explained in the previous Paragraph, and given the aforementioned compositional and textural features, four representative samples for each phase of restoration have been chosen: AAM33 for the first restoration, AAM34 for the second, AAM35 for the third and AAM36 for the

fourth one. The false-color X-ray maps and the amount percentages of their mineral phases are respectively displayed in *Figure 5.35*, *Figure 5.36*, *Figure 5.37*, *Figure 5.38*, and in *Table 5.8*, *Table 5.9*, *Table 5.10* and in *Table 5.11*.

False-color quantitative X-ray maps expressed in oxides processed using Aztec Software are shown in **Appendix IV**.

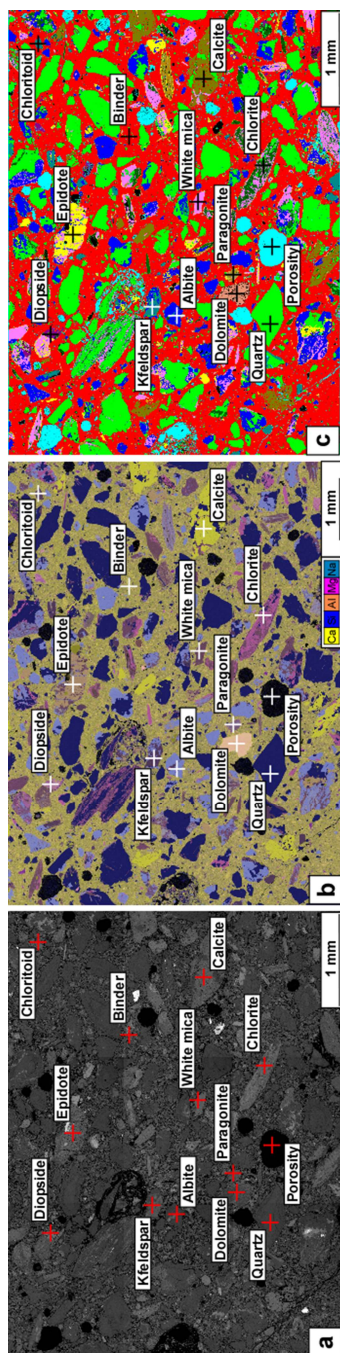


Figure 5.35: Representative area of sample AAM33 **a.** Backscattered image **b.** Quantlayer map **c.** False color GeoMatMap.

Mineral phase	Prop%	O Wt	Fe Wt	Ti Wt	Ca Wt	K Wt	Si Wt	Al Wt	Mg Wt	Na Wt
Binder	50.52	39.30	0.39	0.04	38.65	0.05	18.36	2.71	0.39	0.03
Quartz	19.17	52.80	0.13	0.02	0.56	0.13	45.28	0.81	0.07	0.11
Albite	7.77	48.94	0.10	0.02	0.87	0.39	31.95	10.77	0.04	6.86
Porosity	5.77	21.64	0.42	0.10	8.29	0.34	13.66	1.87	0.82	0.22
White mica	4.21	47.35	0.67	0.03	0.60	7.44	26.04	17.17	0.49	0.15
Epidote	2.99	45.27	2.29	0.15	12.35	1.78	22.75	14.23	0.62	0.51
Calcite	2.31	28.91	0.17	0.02	70.09	0.02	0.67	0.06	0.03	0.01
Chlorite	2.18	43.29	14.42	0.09	0.85	1.39	18.36	14.45	7.03	0.08
K-feldspar	1.12	46.84	0.03	0.01	0.30	11.67	31.02	9.98	0.01	0.08
Diopside	0.57	44.57	5.85	0.12	12.85	0.15	27.02	2.97	6.22	0.21
Paragonite	0.36	48.82	0.08	0.04	0.66	0.47	24.35	21.59	0.06	3.86
Dolomite	0.29	32.93	0.11	0.02	43.75	0.02	0.29	0.07	22.77	0.01
Chloritoid	0.16	48.14	1.90	0.16	1.01	2.04	24.08	20.28	1.04	1.30
Total	97.43									

Table 5.8: Percentage amount, listed in order of abundance, of mineral phases, porosity and binder and the relative chemical composition expresses as single element wt% of obtained by GeoMatMap software (sample AAM33).

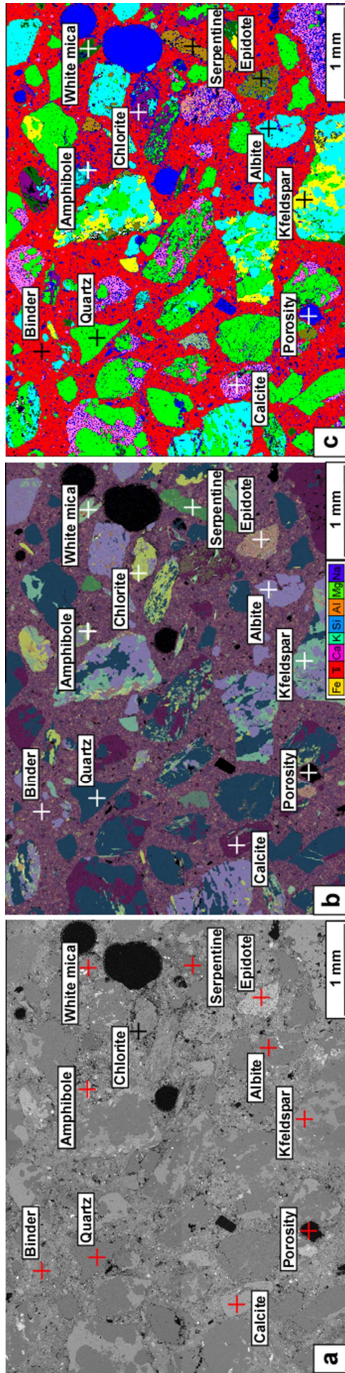


Figure 5.36: Representative area of sample AAM34 a. Backscattered image b. Quantlayer map c. False color GeoMatMap.

Mineral phase	Prop%	O Wt	Fe Wt	Ti Wt	Ca Wt	K Wt	Si Wt	Al Wt	Mg Wt	Na Wt
Binder	39.521	55.78	0.53	0.03	29.36	0.02	11.25	2.69	0.33	0.01
Quartz	17.664	53.79	0.06	0.01	0.17	0.12	45.14	0.52	0.03	0.16
Porosity	12.723	32.19	0.97	0.15	14.71	0.13	4.95	1.23	0.67	0.08
Albite	10.159	49.72	0.07	0.02	0.51	0.33	31.1	10.64	0.03	7.57
Calcite	4.448	57.78	0.07	0.02	41.63	0.02	0.39	0.03	0.06	0.01
K-feldspar	2.61	47.73	0.02	0.01	0.09	11.69	30.5	9.88	0	0.08
Epidote	2.373	50.92	3.07	0.11	17.97	0.58	17.93	8.26	0.73	0.43
White mica	2.167	50.82	1.29	0.05	1.17	6.67	23.65	15.47	0.57	0.31
Amphibole	1.845	53.09	1.25	0.15	12.61	0.26	28.31	2.13	1.53	0.68
Chlorite	1.405	48.16	17.22	0.01	0.24	0.04	12.95	11.48	9.87	0.02
Serpentine	0.708	53.78	0.28	0.01	0.22	0.01	20.92	0.05	24.72	0.01
Dolomite	0.298	58.59	0.12	0.02	27.11	0.01	0.26	0.3	13.58	0.01
Diopside	0.234	47.17	0.4	0.02	17.41	0	25.03	0.09	9.86	0.01
Biotite	0.134	43.52	19.82	0.1	0.55	6.02	17.07	9.8	3.09	0.02
Total	96.289									

Table 5.9: Percentage amount, listed in order of abundance, of mineral phases, porosity and binder and the relative chemical composition expresses as single element wt% obtained by GeoMatMap Software (sample AAM34).

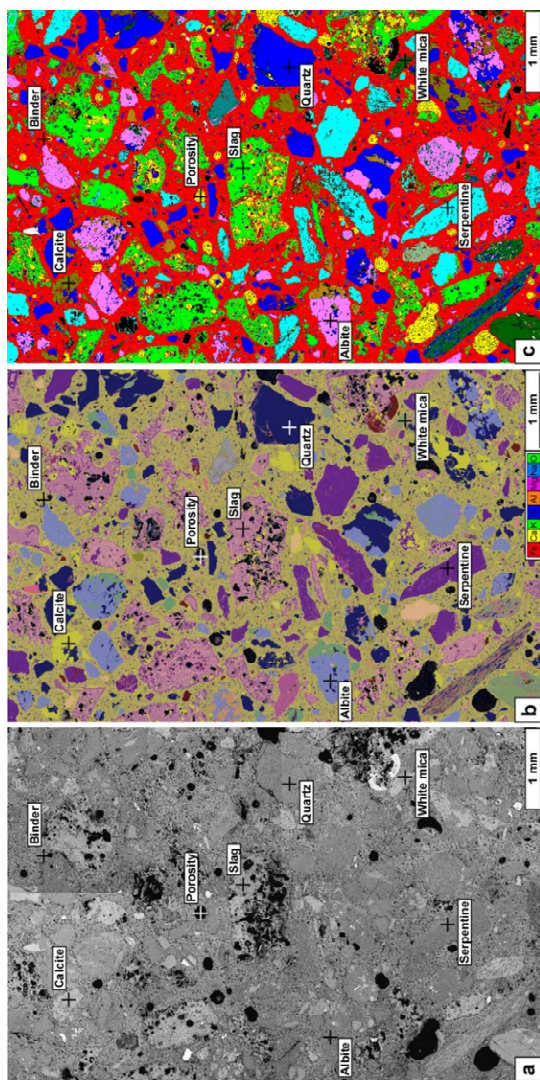


Figure 5.37: Representative area of sample AAM35 a. Backscattered image b. Quantlayer map c. False color GeoMatMap.

Mineral phase	Prop%	O Wt	Na Wt	Mg Wt	Al Wt	Si Wt	K Wt	Ca Wt	Ti Wt	Fe Wt
Binder	45.22	37.73	0.10	1.27	2.45	15.40	0.17	41.92	0.05	0.71
Slag	12.89	44.36	0.03	16.21	3.49	21.62	0.05	13.80	0.03	0.18
Quartz	10.72	52.52	0.25	0.30	1.43	44.22	0.12	0.89	0.02	0.14
Serpentine	6.51	46.74	0.01	27.41	0.90	24.27	0.01	0.21	0.02	0.40
Albite	5.41	49.04	7.84	0.01	10.64	32.18	0.05	0.14	0.01	0.02
Porosity	3.89	16.78	0.16	0.75	0.54	11.35	0.27	5.34	0.17	0.14
Calcite	2.18	28.63	0.01	0.07	0.04	0.11	0.02	71.07	0.02	0.02
White mica	2.17	46.66	0.30	1.20	17.82	23.96	5.39	0.52	0.16	3.94
Plagioclase	1.44	48.11	2.36	0.16	14.42	28.09	2.03	4.12	0.06	0.57
Olivine	1.12	46.29	0.01	22.91	2.80	23.64	0.03	4.17	0.02	0.08
K-feldspar	0.89	46.88	0.04	0.00	10.08	31.04	11.81	0.06	0.01	0.02
Amphibole	0.53	36.38	0.10	6.36	3.93	13.87	0.19	10.21	0.60	26.30
Dolomite	0.35	33.04	0.01	23.38	0.07	0.30	0.02	43.01	0.02	0.14
Chlorite	0.22	40.22	0.02	7.90	13.43	14.07	0.04	0.12	0.04	24.14
Total	93.54									

Table 5.10: Percentage amount, listed in order of abundance, of mineral phases, porosity and binder, and the relative chemical composition expressed as single element wt% obtained by GeoMatMap Software (sample AAM35).

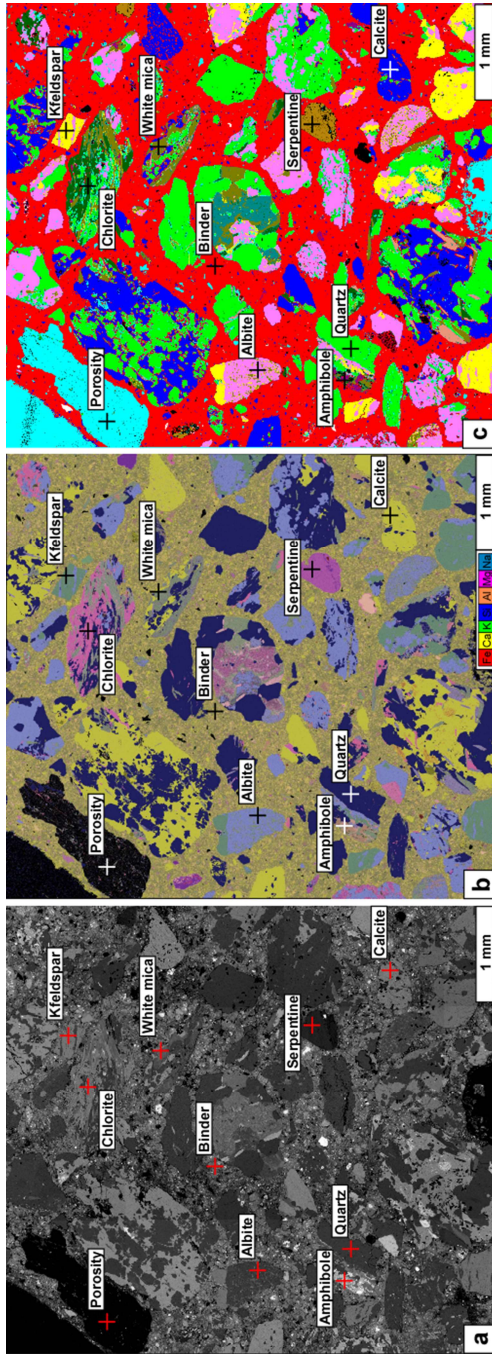


Figure 5.38: Representative area of sample AAM36 **a.** Backscattered image **b.** Quantlayer map **c.** False color GeoMatMap.

Mineral phase	Prop%	O Wt	Na Wt	Mg Wt	Al Wt	Si Wt	K Wt	Ca Wt	Ti Wt	Fe Wt
Binder	43.71	38.08	0.04	0.47	3.20	15.68	0.09	41.39	0.07	0.78
Quartz	14.26	53.24	0.01	0.00	0.01	46.62	0.00	0.03	0.01	0.01
Calcite	9.65	28.70	0.02	0.04	0.05	0.30	0.04	70.26	0.03	0.52
Porosity	9.06	2.13	0.08	0.06	0.49	1.12	0.06	0.28	0.04	0.06
Albite	8.77	49.01	7.68	0.01	10.74	32.11	0.18	0.19	0.01	0.03
K-feldspar	4.56	47.06	0.29	0.06	10.75	30.72	10.82	0.13	0.02	0.13
White mica	2.66	47.32	0.06	0.44	17.62	25.82	8.02	0.14	0.02	0.52
Chlorite	1.61	42.09	0.05	10.19	12.42	16.61	0.69	0.52	0.05	17.35
Biotite	1.42	47.63	0.21	2.39	17.69	24.87	3.41	0.50	0.06	3.20
Amphibole	1.03	45.23	1.37	0.86	10.05	25.30	1.92	13.26	0.19	1.75
Serpentine	0.64	46.63	0.01	24.93	7.45	20.57	0.01	0.04	0.01	0.31
Paragonite	0.40	48.88	4.47	0.00	22.36	23.95	0.15	0.09	0.01	0.03
Plagioclase	0.37	48.42	5.76	0.22	9.98	31.33	0.18	3.50	0.08	0.47
Diopside	0.14	43.60	0.03	7.92	1.40	25.09	0.05	19.21	0.08	2.56
Total	98.27									

Table 5.11: Percentage amount, listed in order of abundance, of mineral phases, porosity and binder and the relative chemical composition expresses as single element wt% obtained by GeoMatMap Software (sample AAM36).

5.7.2 Mineral Chemistry

Mortars forming minerals have been analysed by SEM-EDS and their formulae were recalculated using Minsort software (Petraakis & Dietrich, 1995). The elements values reported in the following will be given as atoms per unit formula (a.p.u.f.). Amphibole have been recalculated based on 23 oxygens, distinguishing between A=0 and A≠0, according with Hawthorne et al. (2012), for the ideal formula, and with Petraakis & Dietrich (1995) for the chosen recalculation method.

Potassic white mica have been always distinguished in its phengite and muscovite end-members. For practical reasons, high- to medium-Si Wm is considered phengite for values >3.35 a.p.u.f., while medium- to low-Si Wm is considered muscovite for values <3.35 a.p.u.f.

Garnet and talc have been recalculated based on 12 oxygens, pyroxene based on 6 oxygens, white mica on 11 oxygens, biotite on 22 oxygens, feldspars on 8 oxygens, chlorite on 28 oxygens, epidote on 25 oxygens. Mineral abbreviations are given according with Whitney & Evans (2010).

5.7.2.1 Principal minerals

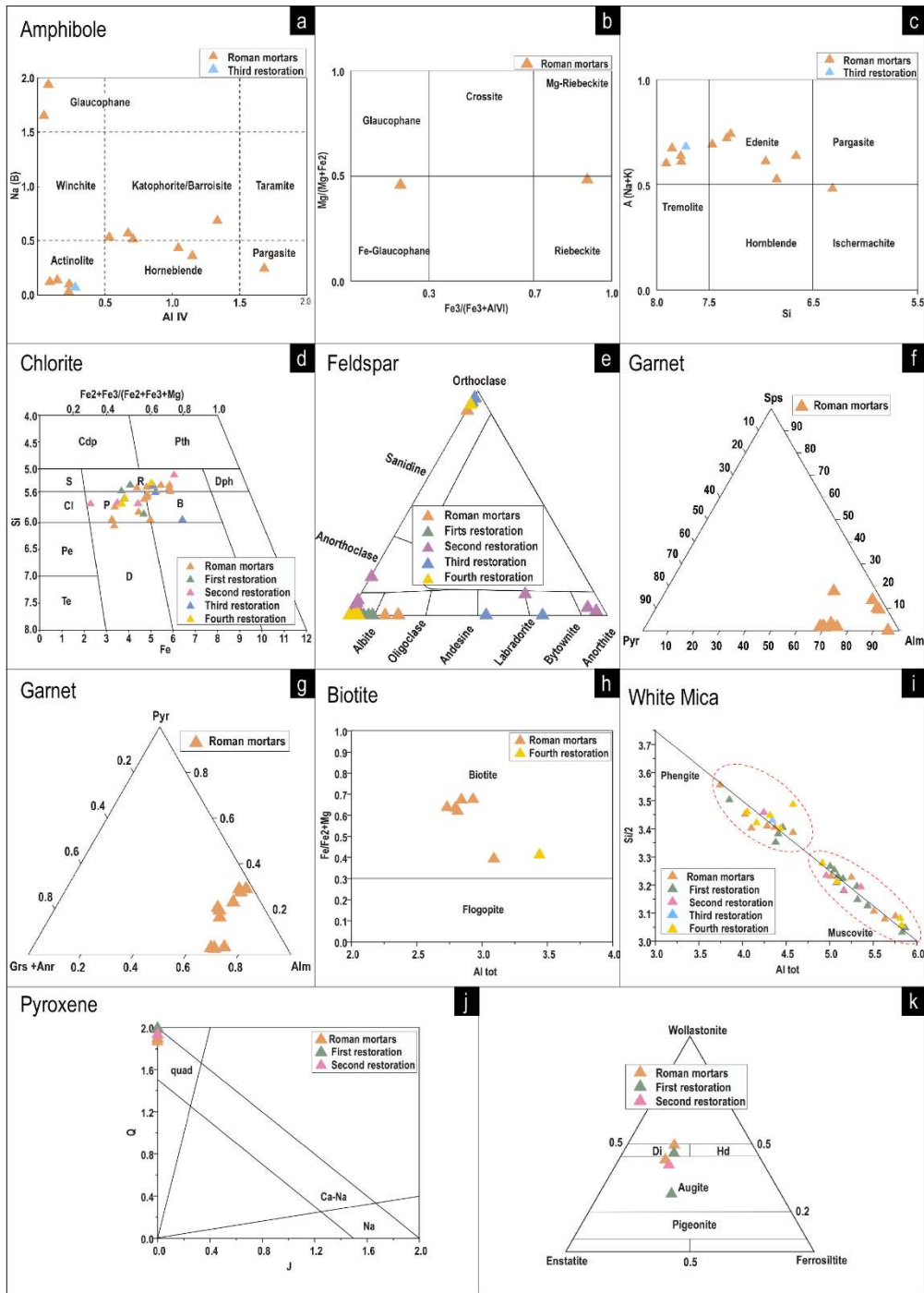


Figure 5.39: Mineral Chemistry of Roman and restoration samples. **a.** Al IV vs Na (B) classification diagram for Amphibole. **b.** Na-Amphibole classification diagram. **c.** Na-Ca-Amphibole classification diagram. **d.** Chlorite classification diagram, after Hey (1954) **e.**

Feldspar ternary classification diagram. **f.** Alm, Sps, Pyr ternary Garnet diagram. Alm: almandine, Sps: Spessartine, Pyp: Pyrope. **g.** Sps, Pyp, Grs+Adr ternary Garnet diagram. Grs: grossular, Adr: andradite. **h.** Biotite classification diagram (Guidotti C.V., 1984) **i.** K-White Mica classification diagram. **j.** Q-J Pyroxene classification diagram, after Morimoto (1988). **k.** Ca-Mg-Fe Pyroxene ternary classification diagram.

5.7.2.1.1 Amphibole

All the analyzed amphiboles come from the Roman mortar samples with the only exception of a single sample belonging to the third restoration (sample AAM35). The results are reported in *Table 5.12*. The diagram Al IV vs Na(B) (*Figure 5.39a*) shows the composition of all the analyzed amphiboles.

The amphiboles in the Roman samples show a variable composition as evidenced by the dispersion of the analysis points. These points are included in the field of glaucophane, actinolite, hornblende, barroisite and pargasite.

The amphibole of the third restoration sample has been classified as actinolite. The diagram of *Figure 5.39b* shows the composition of the Na-Amphiboles ($A=0$; $B_{Na}>1.50$) that fall in the fields of Fe-rich glaucophane and between Mg-rich Riebeckite and Riebeckite.

Based on the classification Na-Ca Amphibole diagram (*Figure 5.39b*), the Ca-rich amphiboles of the Roman samples show a variable composition as evidenced by the dispersion of the analysis points. These points occur in the field of tremolite and edenite. Only one sample is included in the field of tschermakite. Ti and Mn are absent.

Amphibole

<i>Anal.</i>	1	2	3	4	5	6	7	8	9	10	11	12
SiO ₂	56.27	41.79	55.03	52.31	53.99	55.12	46.38	46.35	47.07	52.35	51.49	51.13
TiO ₂	0.00	1.32	0.00	0.00	0.00	0.00	0.00	0.00	0.00	0.00	0.00	0.00
Al ₂ O ₃	9.89	10.09	1.99	1.95	1.82	1.08	8.61	10.97	7.98	5.27	5.63	5.39
Cr ₂ O ₃	0.00	0.00	0.00	0.00	0.00	0.00	0.00	0.00	0.00	0.00	0.00	0.00
FeO	17.28	23.64	15.75	15.36	17.12	14.95	22.47	21.53	20.25	16.42	17.18	16.94
MnO	0.00	0.00	0.00	0.00	0.00	0.00	0.00	0.00	0.00	0.00	0.00	0.00
MgO	6.69	7.76	13.63	14.18	13.38	14.99	8.52	8.81	9.79	13.16	13.13	13.44
CaO	0.26	10.85	11.81	11.58	12.33	12.19	10.37	8.54	9.89	8.87	8.70	9.25
Na ₂ O	7.60	1.54	0.44	0.00	0.50	0.54	1.20	2.39	1.52	1.93	2.07	1.86
K ₂ O	0.00	1.03	0.00	0.00	0.00	0.00	0.45	0.00	0.00	0.00	0.00	0.00
Total	98.00	98.02	98.65	95.37	99.15	98.87	98.00	98.58	96.50	98.00	98.20	98.00
Si	7.920	6.316	7.909	7.769	7.764	7.853	6.850	6.664	6.954	7.467	7.328	7.290
Al IV	0.080	1.684	0.091	0.231	0.236	0.147	1.150	1.336	1.046	0.533	0.672	0.710
Al VI	1.561	0.114	0.247	0.110	0.072	0.035	0.349	0.523	0.343	0.354	0.272	0.196
Ti	0.000	0.150	0.000	0.000	0.000	0.000	0.000	0.000	0.000	0.000	0.000	0.000
Cr	0.000	0.000	0.000	0.000	0.000	0.000	0.000	0.000	0.000	0.000	0.000	0.000
Fe 3+	0.366	1.105	-0.034	0.121	0.226	0.242	1.094	1.516	1.136	0.712	0.971	1.028
Mn	0.000	0.000	0.000	0.000	0.000	0.000	0.000	0.000	0.000	0.000	0.000	0.000
Mg	1.405	1.748	2.919	3.141	2.869	3.184	1.876	1.889	2.155	2.799	2.785	2.857
Fe 2+	1.668	1.882	1.868	1.628	1.833	1.540	1.681	1.073	1.366	1.135	0.972	0.919
Fe 2+	0.000	0.000	0.059	0.158	0.000	0.000	0.000	0.000	0.000	0.111	0.102	0.072
Ca	0.039	1.756	1.819	1.842	1.899	1.861	1.640	1.315	1.566	1.356	1.327	1.414
Na	1.961	0.244	0.122	0.000	0.101	0.139	0.360	0.685	0.434	0.533	0.571	0.514
Na	0.114	0.209	0.000	0.000	0.039	0.010	-0.017	-0.018	0.001	0.000	0.000	0.000
K	0.000	0.199	0.000	0.000	0.000	0.000	0.084	0.000	0.000	0.000	0.000	0.000
X _{mg}	0.457	0.482	0.602	0.637	0.610	0.674	0.527	0.638	0.612	0.692	0.722	0.742
Fe ₂ O ₃	2.283	11.648	-0.313	1.150	2.074	2.223	9.702	14.356	10.556	7.295	10.088	10.460
FeO	9.356	17.849	16.092	15.215	15.164	12.750	13.420	9.143	11.421	11.496	10.033	9.078

Table 5.12: Microprobe analysis of Amphibole for Roman mortars and Third restoration ones.

5.7.2.1.2 Chlorite

The analyzed chlorites come from the original samples of the Roman period and from those of the different restoration phases and have been plotted on the classification diagram of Hey M.H. (1954) (**Figure 5.39d**). The analyses are reported in *Table 5.13* and *Table 5.14*.

The compositions of all examined chlorites are on average homogeneous. Chlorites of roman samples belong to ripidolite and pycnochlorite fields and some of them are on the limit with diabanite, brunsvigite and ripidolite fields. Chlorites of first restoration, second and fourth samples belong to ripidolite and pycnochlorite fields. Chlorites of third restoration samples show ripidolite and brunsvigite composition.

Chlorite																
Roman mortars																
Anal.	1	2	3	4	5	6	7	8	9	10	11	12	13	14	15	16
SiO ₂	24.17	24.71	24.65	25.00	26.88	28.29	29.70	27.84	30.18	25.51	26.28	25.75	24.74	24.97	25.95	24.91
Al ₂ O ₃	20.69	21.95	19.82	19.81	19.19	19.14	16.37	17.20	19.53	22.05	19.93	19.66	18.62	19.17	22.59	21.93
FeO	33.09	31.68	33.21	30.22	25.93	21.46	21.02	29.16	21.16	26.25	27.83	28.53	27.07	33.73	29.28	29.28
MnO	0.91	0.00	0.00	0.00	0.00	0.52	0.33	0.45	0.00	0.00	0.00	0.00	0.00	0.00	0.46	0.38
MgO	9.36	10.33	10.02	12.49	13.41	19.89	20.60	13.35	19.67	14.20	13.99	14.06	13.35	12.06	12.72	11.47
Total	88.23	88.67	87.70	87.52	85.41	89.29	88.02	88.00	90.55	88.01	88.03	88.00	83.79	89.93	91.01	87.98
Si	5.316	5.317	5.432	5.431	5.817	5.721	6.074	5.961	5.955	5.366	5.579	5.500	5.544	5.377	5.354	5.345
Al ^{IV}	2.684	2.683	2.568	2.569	2.183	2.279	1.926	2.039	2.045	2.634	2.421	2.500	2.456	2.623	2.646	2.655
Al ^{VI}	2.678	2.883	2.581	2.501	2.713	2.283	2.019	2.302	2.497	2.831	2.563	2.449	2.463	2.243	2.849	2.890
Ti	0.000	0.000	0.000	0.000	0.000	0.000	0.000	0.000	0.000	0.000	0.000	0.000	0.000	0.000	0.000	0.000
Cr	0.000	0.000	0.000	0.000	0.000	0.000	0.000	0.000	0.000	0.000	0.000	0.000	0.000	0.000	0.000	0.000
Fe	6.086	5.701	6.121	5.489	4.694	3.630	3.595	5.221	3.491	4.618	4.940	5.098	5.074	6.075	5.054	5.254
Mn	0.170	0.000	0.000	0.000	0.000	0.088	0.058	0.082	0.000	0.000	0.000	0.000	0.000	0.000	0.081	0.070
Mg	3.068	3.315	3.291	4.045	4.327	5.996	6.281	4.263	5.787	4.452	4.426	4.479	4.460	3.871	3.915	3.669
Z	8.000	8.000	8.000	8.000	8.000	8.000	8.000	8.000	8.000	8.000	8.000	8.000	8.000	8.000	8.000	8.000
Y	12.003	11.900	11.993	12.034	11.735	11.998	11.953	11.869	11.774	11.901	11.929	12.025	11.997	12.190	11.898	11.883
X _{Mg}	0.335	0.368	0.350	0.424	0.480	0.623	0.636	0.449	0.624	0.491	0.473	0.468	0.468	0.389	0.436	0.411
A _(mu)	0.227	0.236	0.215	0.210	0.213	0.192	0.166	0.186	0.197	0.232	0.210	0.205	0.205	0.197	0.234	0.237
A _(or)	0.227	0.236	0.215	0.210	0.213	0.192	0.166	0.186	0.197	0.232	0.210	0.205	0.205	0.197	0.234	0.237

Table 5.13: Microprobe analysis of Chlorite for Roman mortars.

Chlorite															
Anal.	First restoration				Second restoration				Third restoration			Fourth restoration			
	1	2	3	4	1	2	3	4	1	2	3	1	2	3	
SiO ₂	27.49	25.41	26.68	26.38	23.10	28.77	26.74	27.76	26.62	24.69	25.28	27.34	26.21	24.62	
TiO ₂	0.00	0.00	0.00	0.00	0.00	0.00	0.00	0.00	0.00	0.00	0.00	0.00	0.00	0.00	
Al ₂ O ₃	21.99	22.50	20.05	22.19	21.42	21.28	19.45	20.39	15.40	20.49	19.63	18.57	18.12	21.72	
Cr ₂ O ₃	0.00	0.00	0.00	0.00	0.00	0.00	0.00	0.00	0.00	0.00	0.00	0.00	0.00	0.00	
FeO	27.66	24.66	23.11	22.78	33.91	15.39	26.37	22.03	35.62	29.63	30.15	22.75	23.00	29.32	
MnO	0.00	0.00	0.00	0.00	0.00	0.00	0.00	0.00	0.00	0.00	0.00	0.00	0.00	0.00	
MgO	8.08	14.68	16.38	16.39	8.21	22.24	13.87	18.07	9.69	13.12	12.94	18.60	17.63	12.36	
CaO	1.65	0.76	1.33	0.58	1.37	1.01	1.60	0.85	0.00	0.00	0.00	0.74	1.81	0.00	
Na ₂ O	0.00	0.00	0.00	0.00	0.00	0.00	0.00	0.00	0.00	0.00	0.00	0.00	0.00	0.00	
K ₂ O	1.14	0.00	0.00	0.00	0.00	0.00	0.00	0.00	0.66	0.00	0.00	0.00	0.00	0.00	
Total	88.00	88.01	87.55	88.32	88.00	88.70	88.03	89.10	88.00	87.93	88.01	88.00	86.77	88.01	
Si	5.853	5.312	5.575	5.427	5.128	5.663	5.658	5.639	5.957	5.320	5.455	5.669	5.564	5.279	
Al IV	2.147	2.688	2.425	2.573	2.872	2.337	2.342	2.361	2.043	2.680	2.545	2.331	2.436	2.721	
Al VI	3.371	2.857	2.514	2.808	2.733	2.598	2.510	2.521	2.019	2.524	2.447	2.207	2.097	2.769	
Ti	0.000	0.000	0.000	0.000	0.000	0.000	0.000	0.000	0.000	0.000	0.000	0.000	0.000	0.000	
Cr	0.000	0.000	0.000	0.000	0.000	0.000	0.000	0.000	0.000	0.000	0.000	0.000	0.000	0.000	
Fe	4.925	4.313	4.040	3.919	6.295	2.533	4.667	3.742	6.665	5.339	5.441	3.944	4.083	5.258	
Mn	0.000	0.000	0.000	0.000	0.000	0.000	0.000	0.000	0.000	0.000	0.000	0.000	0.000	0.000	
Mg	2.563	4.575	5.104	5.028	2.717	6.525	4.376	5.473	3.234	4.216	4.161	5.748	5.577	3.950	
Ca	0.375	0.171	0.298	0.127	0.325	0.214	0.362	0.185	0.000	0.000	0.000	0.164	0.412	0.000	
Na	0.000	0.000	0.000	0.000	0.000	0.000	0.000	0.000	0.000	0.000	0.000	0.000	0.000	0.000	
K	0.309	0.000	0.000	0.000	0.000	0.000	0.000	0.000	0.189	0.000	0.000	0.000	0.000	0.000	
Z	8.000	8.000	8.000	8.000	8.000	8.000	8.000	8.000	8.000	8.000	8.000	8.000	8.000	8.000	
Y	10.858	11.745	11.657	11.755	11.744	11.656	11.554	11.735	11.917	12.078	12.049	11.898	11.758	11.976	
Xmg	0.342	0.515	0.558	0.562	0.301	0.720	0.484	0.594	0.327	0.441	0.433	0.593	0.577	0.429	
A(mu)	0.235	0.238	0.213	0.231	0.237	0.214	0.212	0.209	0.150	0.214	0.206	0.190	0.190	0.230	
A(or)	0.258	0.238	0.213	0.231	0.237	0.214	0.212	0.209	0.164	0.214	0.206	0.190	0.190	0.230	

Table 5.14: Microprobe analysis of Chlorite for restoration mortars.

5.7.2.1.3 Feldspar

The analyzed feldspars belong to the original samples of the Roman period and from those of the different restoration phases and refer to aggregate elements consisting of lithic fragments or single feldspar clasts. Representative analyses are reported in *Table 5.15*, *Table 5.16* and in *Table 5.17* and are plotted in the diagram of *Figure 5.39e*.

The composition of feldspars is variable as two main categories occur:

Albite: the feldspars of the Roman mortar samples, of the third and fourth restorations fall into this class;

K-feldspar: the K-feldspar of the first, second and third restoration belong to this category.

Two feldspars of roman samples are classified as oligoclase whereas those of the second restoration show one sample between the labradorite and bytownite fields and two samples of anorthitic composition. Finally, labradorite and bytownite occur for two samples of third restoration.

Plagioclase														
Anal.	Roman mortars								First restoration					
	1	2	3	4	5	6	7	8	1	2	3	4	5	6
SiO ₂	62.47	68.72	70.08	69.56	69.56	69.44	69.52	68.89	67.99	68.75	69.55	69.04	69.35	68.89
TiO ₂	0.00	0.00	0.00	0.00	0.00	0.00	0.00	0.00	0.00	0.00	0.00	0.00	0.00	0.00
Al ₂ O ₃	21.08	19.20	19.02	19.13	19.25	19.36	19.73	19.44	19.87	19.30	19.26	19.25	19.22	19.08
FeO	1.84	0.00	0.00	0.00	0.00	0.00	0.00	0.00	0.00	0.00	0.00	0.00	0.00	0.00
MgO	0.00	0.00	0.00	0.00	0.00	0.00	0.00	0.00	0.00	0.00	0.00	0.00	0.00	0.00
CaO	4.15	0.00	0.00	0.00	0.00	0.00	0.00	0.00	1.85	1.51	0.80	0.31	0.90	1.14
Na ₂ O	9.75	12.07	10.90	11.31	11.18	11.20	11.32	11.66	10.30	10.45	10.39	11.39	10.53	10.89
K ₂ O	0.00	0.00	0.00	0.00	0.00	0.00	0.00	0.00	0.00	0.00	0.00	0.00	0.00	0.00
Total	99.29	99.99	100.00	100.00	99.99	100.00	100.57	99.99	100.01	100.01	100.00	99.99	100.00	100.00
Si	2.813	3.003	3.041	3.026	3.025	3.020	3.008	3.004	2.971	2.999	3.023	3.010	3.018	3.007
Al	1.119	0.989	0.973	0.981	0.986	0.992	1.006	0.999	1.023	0.992	0.986	0.989	0.986	0.981
Ti	0.000	0.000	0.000	0.000	0.000	0.000	0.000	0.000	0.000	0.000	0.000	0.000	0.000	0.000
Fe	0.069	0.000	0.000	0.000	0.000	0.000	0.000	0.000	0.000	0.000	0.000	0.000	0.000	0.000
Mg	0.000	0.000	0.000	0.000	0.000	0.000	0.000	0.000	0.000	0.000	0.000	0.000	0.000	0.000
Ca	0.200	0.000	0.000	0.000	0.000	0.000	0.000	0.000	0.087	0.071	0.037	0.014	0.042	0.053
Na	0.851	1.023	0.917	0.954	0.943	0.944	0.950	0.986	0.873	0.884	0.875	0.963	0.888	0.922
K	0.000	0.000	0.000	0.000	0.000	0.000	0.000	0.000	0.000	0.000	0.000	0.000	0.000	0.000
Z	3.932	3.992	4.014	4.007	4.011	4.012	4.014	4.003	3.994	3.992	4.009	3.999	4.003	3.988
X	1.052	1.023	0.917	0.954	0.943	0.944	0.950	0.986	0.959	0.955	0.913	0.977	0.930	0.975
an	0.190	0.000	0.000	0.000	0.000	0.000	0.000	0.000	0.090	0.074	0.041	0.015	0.045	0.055
ab	0.810	1.000	1.000	1.000	1.000	1.000	1.000	1.000	0.910	0.926	0.959	0.985	0.955	0.945
or	0.000	0.000	0.000	0.000	0.000	0.000	0.000	0.000	0.000	0.000	0.000	0.000	0.000	0.000

Table 5.15: Microprobe analysis of Plagioclase for Roman mortars and First restoration ones.

Petrographic studies of mortars

Plagioclase															
Anal.	Second restoration						Third restoration				Fourth restoration				
	1	2	4	5	6	7	1	2	3	4	1	2	3	4	5
SiO ₂	70.75	70.03	68.10	68.98	70.02	67.55	67.70	69.21	56.38	54.04	68.66	69.04	67.34	68.81	69.12
TiO ₂	0.00	0.00	0.00	0.00	0.00	0.00	0.00	0.00	0.00	0.00	0.00	0.00	0.00	0.00	0.00
Al ₂ O ₃	18.67	19.01	19.71	19.68	18.76	18.88	19.90	19.43	25.60	27.24	19.15	19.48	20.39	19.38	19.56
FeO	0.00	0.00	0.00	0.00	0.00	0.00	0.00	0.00	0.00	0.00	0.00	0.00	0.00	0.00	0.00
MgO	0.00	0.00	0.00	0.00	0.00	0.00	0.00	0.00	0.00	0.00	0.00	0.00	0.00	0.00	0.00
CaO	0.62	1.06	1.01	0.64	1.29	3.68	0.72	0.30	12.06	15.76	0.64	0.00	0.77	0.52	0.31
Na ₂ O	9.96	9.91	11.18	10.69	9.93	9.89	11.67	11.05	5.96	2.96	11.55	11.48	11.50	11.29	11.00
K ₂ O	0.00	0.00	0.00	0.00	0.00	0.00	0.00	0.00	0.00	0.00	0.00	0.00	0.00	0.00	0.00
Total	100.00	100.01	100.00	99.99	100.00	100.00	99.99	99.99	100.00	100.00	100.00	100.00	100.00	100.00	99.99
Si	3.062	3.038	2.978	3.002	3.041	2.969	2.965	3.012	2.552	2.456	3.001	3.008	2.949	3.002	3.008
Al	0.952	0.972	1.016	1.010	0.960	0.978	1.027	0.997	1.366	1.459	0.986	1.000	1.052	0.996	1.003
Ti	0.000	0.000	0.000	0.000	0.000	0.000	0.000	0.000	0.000	0.000	0.000	0.000	0.000	0.000	0.000
Fe	0.000	0.000	0.000	0.000	0.000	0.000	0.000	0.000	0.000	0.000	0.000	0.000	0.000	0.000	0.000
Mg	0.000	0.000	0.000	0.000	0.000	0.000	0.000	0.000	0.000	0.000	0.000	0.000	0.000	0.000	0.000
Ca	0.029	0.049	0.047	0.030	0.060	0.173	0.034	0.014	0.585	0.768	0.030	0.000	0.036	0.024	0.014
Na	0.836	0.834	0.948	0.902	0.836	0.843	0.991	0.932	0.523	0.261	0.979	0.970	0.976	0.955	0.928
K	0.000	0.000	0.000	0.000	0.000	0.000	0.000	0.000	0.000	0.000	0.000	0.000	0.000	0.000	0.000
Z	4.015	4.010	3.993	4.012	4.001	3.947	3.992	4.009	3.918	3.916	3.987	4.008	4.001	3.998	4.012
X	0.865	0.883	0.995	0.932	0.896	1.016	1.025	0.946	1.108	1.028	1.009	0.970	1.012	0.979	0.943
an	0.033	0.056	0.048	0.032	0.067	0.171	0.033	0.015	0.528	0.746	0.030	0.000	0.036	0.025	0.015
ab	0.967	0.944	0.952	0.968	0.933	0.829	0.967	0.985	0.472	0.254	0.970	1.000	0.964	0.975	0.985
or	0.000	0.000	0.000	0.000	0.000	0.000	0.000	0.000	0.000	0.000	0.000	0.000	0.000	0.000	0.000

Table 5.16: Microprobe analysis of Plagioclase for Second, Third and Fourth restoration mortars.

K-feldspar										
Anal.	Roman mortars			Second restoration			Third restoration		Fourth restoration	
	1	2	3	1	2	3	1	2	1	
SiO ₂	66.81	65.36	65.54	68.92	66.32	66.79	65.28	65.99	66.28	
TiO ₂	0.00	0.00	0.00	0.00	0.00	0.00	0.00	0.00	0.00	
Al ₂ O ₃	18.26	18.37	18.00	17.98	18.97	18.21	17.92	18.09	18.24	
FeO	0.00	0.00	0.00	0.00	0.00	0.00	0.00	0.00	0.00	
MgO	0.00	0.00	0.00	0.00	0.00	0.00	0.00	0.00	0.00	
CaO	0.00	0.00	0.00	1.58	0.62	0.35	0.00	0.00	0.00	
Na ₂ O	0.89	0.36	0.39	2.56	0.61	0.37	0.58	0.33	0.65	
K ₂ O	14.03	15.91	16.07	8.96	13.49	14.29	16.22	15.59	14.83	
Total	99.99	100.00	100.00	100.00	100.01	100.01	100.00	100.00	100.00	
Si	3.042	3.010	3.022	3.071	3.014	3.042	3.016	3.030	3.032	
Al	0.980	0.997	0.978	0.944	1.016	0.978	0.976	0.979	0.983	
Ti	0.000	0.000	0.000	0.000	0.000	0.000	0.000	0.000	0.000	
Fe	0.000	0.000	0.000	0.000	0.000	0.000	0.000	0.000	0.000	
Mg	0.000	0.000	0.000	0.000	0.000	0.000	0.000	0.000	0.000	
Ca	0.000	0.000	0.000	0.075	0.030	0.017	0.000	0.000	0.000	
Na	0.079	0.032	0.035	0.221	0.054	0.033	0.052	0.029	0.058	
K	0.815	0.935	0.945	0.509	0.782	0.830	0.956	0.913	0.865	
Z	4.022	4.008	4.000	4.016	4.030	4.020	3.992	4.009	4.015	
X	0.893	0.967	0.980	0.806	0.866	0.880	1.008	0.943	0.923	
an	0.000	0.000	0.000	0.094	0.035	0.019	0.000	0.000	0.000	
ab	0.088	0.033	0.036	0.274	0.062	0.037	0.052	0.031	0.062	
or	0.912	0.967	0.964	0.632	0.903	0.943	0.948	0.969	0.938	

Table 5.17: Microprobe analysis of K-feldspar for Roman and restoration mortars.

5.7.2.1.4 Garnet

The chemical composition of the analyzed garnets, part of the Roman mortar samples, have been reported in the Alm, Sps, Pyr ternary Grt diagram (*Figure 5.39f*) and in the Sps, Pyr, Grs+Adr ternary Grt diagram (*Figure 5.39g*).

Representative analyses reported in *Table 5.18*.

This mineral displays a composition of a solid solution of almandine (71% - 54%), pyrope (30%-3%), spessartine (3% - 0%), andradite (6% - 3%), grossular (2%-0%) and have no uvarovite.

The tetrahedral site of the studied samples is close to the ideal value of 3.000 atoms per unit formula (a.p.u.f.) and varies between 2.915 and 3.013 (a.p.u.f.), with almost total Si; the octahedral site is close to the optimum of 2.000 (a.p.u.f.) and varies between 1.803 and 1.939 (a.p.u.f.). The X site is close to the ideal value of 3.000 (a.p.u.f.) and varies between 2.800 and 3.036 (a.p.u.f.).

Garnet											
Roman mortars											
<i>Anal.</i>	1	2	3	4	5	6	7	8	9	10	11
SiO ₂	37.99	38.51	38.19	38.30	36.80	37.51	36.89	37.42	39.02	35.94	37.19
TiO ₂	0.00	0.00	0.00	0.00	0.00	0.00	0.00	0.00	0.00	0.00	0.00
Al ₂ O ₃	20.98	20.99	20.16	20.28	20.61	21.12	20.28	20.69	19.89	20.06	20.55
Cr ₂ O ₃	0.00	0.00	0.00	0.00	0.00	0.00	0.00	0.00	0.00	0.00	0.00
FeO	28.96	28.12	30.69	32.21	33.14	31.01	32.83	25.75	28.62	30.88	27.77
MnO	0.56	0.62	1.25	0.60	0.00	0.79	0.75	6.56	3.06	3.03	4.40
MgO	5.05	5.30	5.84	7.42	0.95	7.39	7.07	3.64	0.74	0.69	0.77
CaO	6.47	6.46	3.87	1.19	8.51	2.17	2.19	5.93	8.68	9.39	9.33
Total	100.01	100.00	100.00	100.00	100.01	99.99	100.01	99.99	100.01	99.99	100.01
Si	2.985	3.013	3.007	3.003	2.968	2.940	2.915	2.977	3.101	2.917	2.991
Al IV	0.015	0.000	0.000	0.000	0.032	0.060	0.085	0.023	0.000	0.083	0.009
Al VI	1.929	1.935	1.871	1.874	1.927	1.892	1.803	1.917	1.863	1.835	1.939
Cr	0.000	0.000	0.000	0.000	0.000	0.000	0.000	0.000	0.000	0.000	0.000
Ti	0.000	0.000	0.000	0.000	0.000	0.000	0.000	0.000	0.000	0.000	0.000
Fe 3+	0.075	0.062	0.128	0.125	0.080	0.123	0.201	0.089	0.135	0.169	0.063
Fe 2+	1.828	1.778	1.893	1.987	2.155	1.910	1.968	1.624	1.767	1.927	1.805
Mn	0.037	0.041	0.083	0.040	0.000	0.052	0.050	0.442	0.206	0.208	0.300
Mg	0.592	0.618	0.685	0.867	0.114	0.864	0.833	0.432	0.088	0.083	0.092
Ca	0.545	0.541	0.326	0.100	0.735	0.182	0.185	0.505	0.739	0.816	0.804
Z	3.000	3.013	3.007	3.003	3.000	3.000	3.000	3.000	3.101	3.000	3.000
Y	2.003	1.997	1.998	1.999	2.008	2.014	2.004	2.006	1.998	2.004	2.002
X	3.002	2.979	2.988	2.994	3.005	3.009	3.036	3.003	2.800	3.035	3.001
alm	0.609	0.597	0.633	0.664	0.717	0.635	0.648	0.541	0.631	0.635	0.601
sps	0.012	0.014	0.028	0.013	0.000	0.017	0.017	0.147	0.074	0.069	0.100
pyr	0.197	0.208	0.229	0.290	0.038	0.287	0.274	0.144	0.031	0.028	0.031
grs	0.144	0.151	0.045	-0.029	0.205	-0.001	-0.038	0.124	0.192	0.186	0.237
anr	0.037	0.031	0.064	0.063	0.040	0.061	0.099	0.044	0.072	0.083	0.031
uvr	0.000	0.000	0.000	0.000	0.000	0.000	0.000	0.000	0.000	0.000	0.000
Xmg	0.244	0.258	0.266	0.304	0.050	0.311	0.297	0.210	0.047	0.042	0.049
A	0.286	0.288	0.266	0.247	0.302	0.260	0.252	0.321	0.334	0.323	0.339
Fe ₂ O ₃	1.266	1.050	2.155	2.119	1.324	2.079	3.387	1.485	2.256	2.764	1.038
FeO	27.821	27.175	28.751	30.303	31.948	29.139	29.783	24.414	26.590	28.393	26.836

Table 5.18: Microprobe analysis of K-feldspar for Roman mortars.

5.7.2.1.5 Trioctahedral Mica

The analyzed trioctahedral mica belongs to the Roman mortars and one from the fourth restoration samples. They have been plotted in the 'biotite plane' classification diagram by Guidotti C. V. (1984) (*Figure 5.39h*) and belong to the field of biotite. The analyses are shown in *Table 5.19*.

The biotite of the Roman samples is characterized by Al VI contents of 0.265 to 0.560 (a.p.u.f.) and Ti contents of 0.287 to 0.366. The XMg value ranges from 0.324 to 0.606, the Si and Al IV contents from 5.423 to 5.670 and 2.330 to 2.577 (a.p.u.f.) respectively. The Ca values range from 0.108 to 0.262. The sodium component is absent.

Biotite has a value of $X = Na + Ca + K$ that varies between 1.025 and 1.494, much lower than the theoretical value of 2.000 (a.p.f.u.), a typical characteristic of several biotite minerals.

The biotite of the fourth restoration sample is characterized by Al VI value of 0.867 (a.p.u.f.), whereas Ti is absent. The Xmg value is 0.588, the Si and Al IV contents 5.428 and 2.527 (a.p.u.f.) respectively. The Ca value is 0.384 and the sodium component is absent.

Biotite							
	<i>Roman mortars</i>						<i>Third restoration</i>
<i>Anal.</i>	1	2	3	4	5	6	1
SiO ₂	36.43	34.56	37.48	37.68	36.47	36.73	36.58
TiO ₂	3.16	2.43	2.61	3.36	3.04	2.99	0.00
Al ₂ O ₃	15.54	15.37	15.78	18.07	16.27	15.25	19.66
Cr ₂ O ₃	0.00	0.00	0.00	0.00	0.00	0.00	0.00
FeO	25.81	28.09	25.05	16.13	27.47	26.87	15.80
MnO	0.00	0.00	0.00	0.00	0.00	0.00	0.00
MgO	8.35	7.64	8.61	13.92	7.40	8.56	12.63
CaO	1.43	1.18	1.36	1.50	0.66	1.61	2.42
Na ₂ O	0.00	0.00	0.00	0.00	0.00	0.00	0.00
K ₂ O	5.41	6.47	5.31	5.28	4.70	4.44	8.94
Total	96.12	95.75	96.20	95.93	96.01	96.46	96.02
Si	5.562	5.423	5.670	5.469	5.572	5.584	5.428
Al IV	2.438	2.577	2.330	2.531	2.428	2.416	2.572
Al VI	0.358	0.265	0.484	0.560	0.502	0.316	0.867
Ti	0.362	0.287	0.297	0.366	0.349	0.342	0.000
Cr	0.000	0.000	0.000	0.000	0.000	0.000	0.000
Fe	3.295	3.686	3.169	1.957	3.510	3.416	1.961
Mn	0.000	0.000	0.000	0.000	0.000	0.000	0.000
Mg	1.901	1.786	1.942	3.013	1.685	1.941	2.793
Ca	0.234	0.199	0.220	0.233	0.108	0.262	0.384
Na	0.000	0.000	0.000	0.000	0.000	0.000	0.000
K	1.053	1.295	1.025	0.977	0.917	0.862	1.693
Z	8.000	8.000	8.000	8.000	8.000	8.000	8.000
Y	5.917	6.023	5.893	5.897	6.046	6.015	5.621
X	1.287	1.494	1.245	1.211	1.025	1.124	2.077
X _{mg}	0.366	0.326	0.380	0.606	0.324	0.362	0.588
A(μ)	-0.036	-0.105	-0.026	0.016	0.017	0.013	-0.209
A(or)	0.144	0.124	0.149	0.175	0.162	0.149	0.155

Table 5.19: Microprobe analysis of Biotite for Roman mortars.

5.7.2.1.6 White mica

The investigated white mica crystals from the original samples of the Roman period and from those of the different restoration phases have been plotted on the Si/Al tot classification diagram. Representative analyses are reported in *Table 5.20* and *Table 5.21*.

The composition of this mineral varies according with two distinct classes represented in *Figure 5.39j*: a first high- to medium-Si phengite (3.30-3.55 Si), a second low-Si muscovite (3.11-3.25 Si). Only samples from the third restoration show phengite exclusively. Paragonite was identified in two Roman mortar samples (analysis in *Table 5.20*).

Concerning Roman samples, the value of the octahedral sites is higher than the theoretical value of 4,000 (a.p.u.f.) and ranges between 4.105 and 4.234 (a.p.u.f.). The XMg value varies between 0.471 and 0.850 whereas the Ti content is absent.

The value of the octahedral sites of the restoration samples, respectively from the first to the fourth, vary between 3.193 and 4.155, 3.957 and 4.129, 4.107, 3.916 and 4.159 (a.p.u.f.).

The Xmg value ranges between 0.396 and 0.667, 0.480 and 0.708, 0.654, 0.258 and 0.778 respectively.

	White mica								Paragonite			
	Roman mortars											
Anal.	1	2	3	4	5	6	7	8	9	1	2	
SiO ₂	49.78	50.76	50.64	51.42	52.62	46.74	48.57	48.74	51.70	48.26	48.10	
TiO ₂	0.00	0.00	0.00	0.00	0.00	0.00	0.00	0.00	0.00	0.00	1.02	
Al ₂ O ₃	25.45	27.64	26.99	25.48	23.51	35.15	33.52	32.12	29.66	38.14	37.35	
Cr ₂ O ₃	0.00	0.00	0.00	0.00	0.00	0.00	0.00	0.00	0.00	0.00	0.00	
FeO	6.41	4.77	5.21	5.50	5.21	1.91	1.60	2.92	1.09	0.65	0.50	
MnO	0.00	0.00	0.00	0.00	0.00	0.00	0.00	0.00	0.00	0.00	0.00	
MgO	2.92	2.39	2.63	3.12	3.63	0.98	1.12	2.03	3.46	0.00	0.41	
CaO	0.00	0.00	0.00	0.00	0.00	0.00	0.00	0.00	0.00	0.00	0.15	
Na ₂ O	0.00	0.00	0.00	0.00	0.00	0.63	0.96	0.60	0.55	6.85	6.44	
K ₂ O	10.44	9.46	9.52	10.60	9.79	9.78	8.17	8.91	8.54	1.10	1.05	
Total	95.00	95.01	95.00	96.12	94.75	95.20	93.94	95.31	95.00	95.00	95.01	
Si	6.805	6.811	6.820	6.902	7.110	6.212	6.454	6.460	6.774	6.178	6.158	
Al IV	1.195	1.189	1.180	1.098	0.890	1.788	1.546	1.540	1.226	1.822	1.842	
Al VI	2.906	3.182	3.105	2.933	2.854	3.718	3.705	3.477	3.356	3.934	3.792	
Ti	0.000	0.000	0.000	0.000	0.000	0.000	0.000	0.000	0.000	0.000	0.098	
Cr	0.000	0.000	0.000	0.000	0.000	0.000	0.000	0.000	0.000	0.000	0.000	
Fe	0.733	0.535	0.587	0.617	0.588	0.212	0.177	0.323	0.120	0.070	0.053	
Mn	0.000	0.000	0.000	0.000	0.000	0.000	0.000	0.000	0.000	0.000	0.000	
Mg	0.594	0.477	0.528	0.624	0.731	0.194	0.222	0.401	0.675	0.000	0.078	
Ca	0.000	0.000	0.000	0.000	0.000	0.000	0.000	0.000	0.000	0.000	0.020	
Na	0.000	0.000	0.000	0.000	0.000	0.163	0.247	0.154	0.141	1.700	1.598	
K	1.821	1.619	1.635	1.815	1.688	1.659	1.385	1.506	1.428	0.180	0.172	
Z	8.000	8.000	8.000	8.000	8.000	8.000	8.000	8.000	8.000	8.000	8.000	
Y	4.234	4.194	4.220	4.175	4.173	4.124	4.105	4.201	4.151	4.004	4.022	
X	1.821	1.619	1.635	1.815	1.688	1.822	1.631	1.661	1.568	1.880	1.790	
Xmg	0.448	0.471	0.474	0.503	0.554	0.477	0.556	0.554	0.850	0.000	0.595	
mu	1.000	1.000	1.000	1.000	1.000	0.910	0.849	0.907	0.910	0.096	0.096	
pg	0.000	0.000	0.000	0.000	0.000	0.090	0.151	0.093	0.090	0.904	0.893	
ma	0.000	0.000	0.000	0.000	0.000	0.000	0.000	0.000	0.000	0.000	0.011	

Table 5.20: Microprobe analysis of white mica and paragonite for Roman mortars.

5.7.2.1.7 Pyroxene

The investigated pyroxene crystals come from the original samples of the Roman period and from those of first and second restoration phases and have been plotted on the classification diagrams of Morimoto N. (1988). The analyses can be consulted in *Table 5.22*.

All the analyzed pyroxenes, plotted on the diagram in *Figure 5.39j*, show a calcitic composition, given by a solid solution between the enstatitic, wollastonitic and ferrosilitic end members. In addition, the composition is homogeneous for the individual samples.

The ternary classification diagram of the Ca-Fe-Mg pyroxenes by Morimoto N. (1988) in *Figure 5.39k* allows to classify the examined clinopyroxenes.

The clinopyroxenes of the Roman samples fall into the diopside field. The pyroxenes from the first restoration vary in composition between diopside and augite. The pyroxenes from the fourth restoration sample show a predominantly augitic composition.

In the Roman samples, the M(1) site has a Mg content that varies between 0.477 and 0.874 (a.p.u.f.), the Fe₂ content varies between 0.045 and 0.336 (a.p.u.f.) and the Fe₃ content varies between 0.063 and 0.000 (a.p.u.f.). In the samples from the first restoration, the M(1) site shows an Mg content that varies between 0.255 and 0.543 (a.p.u.f.), the Fe₂ content varies between 0.282 and 0.532 (a.p.u.f.) while the Fe₃ content varies between 0.113 and 0.116 (a.p.u.f.). The sample from the second restoration shows a Mg value of 0.924, an Fe₂ value of 0.041 and an Fe₃ value of 0.000. The sodium component is absent in all samples.

The X_{Mg} values vary between 0.618 and 0.951 for the Roman samples, between 0.324 and 0.658 for the samples from the first restoration and the pyroxene from the second restoration has a value of 0.958.

Pyroxene							
Anal.	Roman mortars				First restoration		Second restoration
	1	2	3	4	1	2	1
SiO ₂	50.95	49.51	53.46	52.11	49.40	47.45	55.63
TiO ₂	0.00	0.00	0.00	0.00	0.00	0.00	0.00
Al ₂ O ₃	0.90	8.24	1.63	2.94	1.85	2.90	0.61
Cr ₂ O ₃	0.00	0.00	0.00	0.00	0.00	0.00	0.00
FeO	13.55	15.47	12.00	1.52	13.28	19.62	1.36
MnO	0.00	0.00	0.00	0.00	0.00	0.00	0.00
MgO	11.32	14.03	11.72	16.66	9.54	4.32	17.29
CaO	23.28	11.28	20.93	23.07	25.94	25.71	25.11
Na ₂ O	0.00	0.00	0.00	0.00	0.00	0.00	0.00
K ₂ O	0.00	0.00	0.00	0.00	0.00	0.00	0.00
Total	100.00	98.53	99.75	96.30	100.01	100.00	100.00
Si	1.938	1.862	2.008	1.951	1.887	1.874	2.009
Al IV	0.040	0.138	-0.008	0.049	0.083	0.126	-0.009
Fe 3+	0.022	0.000	0.000	0.000	0.030	0.000	0.000
Al VI	0.000	0.227	0.080	0.081	0.000	0.009	0.035
Ti	0.000	0.000	0.000	0.000	0.000	0.000	0.000
Cr	0.000	0.000	0.000	0.000	0.000	0.000	0.000
Fe 3+	0.062	0.000	0.000	0.000	0.113	0.116	0.000
Fe 2+	0.329	0.295	0.336	0.045	0.282	0.532	0.041
Mn	0.000	0.000	0.000	0.000	0.000	0.000	0.000
Mg	0.609	0.477	0.584	0.874	0.543	0.255	0.924
Fe 2+	0.018	0.191	0.041	0.003	0.000	0.000	0.000
Mn	0.000	0.000	0.000	0.000	0.000	0.000	0.000
Mg	0.033	0.309	0.072	0.056	0.000	0.000	0.006
Ca	0.949	0.455	0.842	0.926	1.062	1.088	0.971
Na	0.000	0.000	0.000	0.000	0.000	0.000	0.000
K	0.000	0.000	0.000	0.000	0.000	0.000	0.000
T	2.000	2.000	2.000	2.000	2.000	2.000	2.000
M1+M2	2.000	1.955	1.956	1.984	2.000	2.000	1.978
Xmg	0.649	0.618	0.635	0.951	0.658	0.324	0.958
Fe ₂ O ₃	1.764	0.000	0.000	0.000	2.491	1.620	0.000
FeO	6.562	10.200	7.930	1.650	4.439	6.662	1.020

Table 5.22: Microprobe analysis of Pyroxene for Roman, first and second restoration mortars.

5.7.2.1.8 Epidote

The analyzed epidotes, coming from the Roman samples, refer to those crystals included in lithic clasts and to rare monomineralic clasts. The analyses are shown in *Table 5.23*. Despite the composition of the epidotes is variable,

but it never presents the pistacitic component. They are characterized by a solid solution of epidote and zoisite with values varying between 48%-80% in epidote and 20%-51% in zoisite respectively.

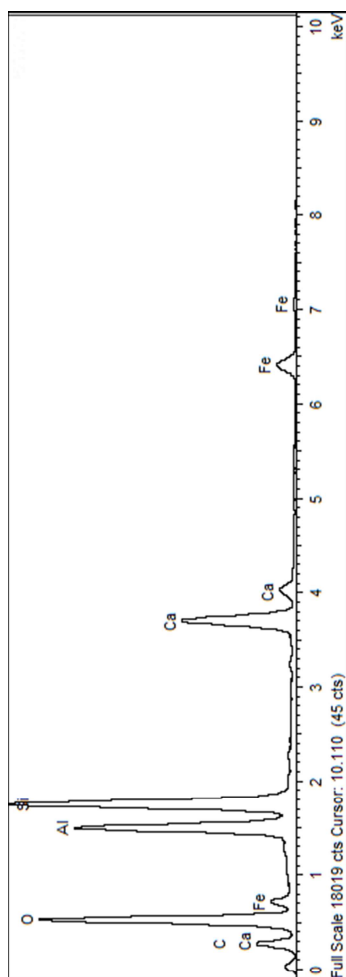


Figure 5.40: EDS Spectrum of epidote of Roman sample

Epidote

<i>Roman mortars</i>			
<i>Anal.</i>	1	2	3
SiO ₂	39.43	38.32	38.55
TiO ₂	0.00	0.00	0.00
Al ₂ O ₃	24.03	27.22	27.70
Cr ₂ O ₃	0.00	0.00	0.00
FeO	13.16	11.46	7.46
MnO	0.00	0.00	0.00
MgO	0.00	2.77	0.75
CaO	21.40	18.98	23.08
Total	98.02	98.75	97.53
Si	6.131	5.855	5.976
Al IV	0.000	0.145	0.024
Al VI	4.404	4.758	5.038
Ti	0.000	0.000	0.000
Cr	0.000	0.000	0.000
Fe 3+	1.596	1.242	0.962
Mn 3+	0.000	0.000	0.000
Fe 2+	0.115	0.223	0.004
Mn 2+	0.000	0.000	0.000
Mg	0.000	0.630	0.172
Ca	3.565	3.108	3.833
Z	6.131	6.000	6.000
Y	6.000	6.000	6.000
X	3.680	3.961	4.010
zo	0.202	0.379	0.519
ep	0.798	0.621	0.481
pi	0.000	0.000	0.000
Fe ₂ O ₃	13.837	7.340	4.426
FeO	0.899	1.185	0.017
Mn ₂ O ₃	0.000	0.000	0.000
MnO	0.000	0.000	0.000

Table 5.23: Microprobe analysis of Epidote for Roman mortars.

5.7.2.2 Other minerals

The *Figure 5.41* shows the EDS spectra of the minor mineral and accessory phases found and partly described in *Paragraph 5.7.1* concerning the petrography of the samples. These include calcite, quartz and serpentine (mainly Roman mortar and first restoration), dolomite and iron oxides (second restoration), glassy matrix and olivine (third restoration), belite, ettringite and tetracalcium aluminoferrite (fourth restoration).

EDS analysis of serpentine are reported in *Table 5.24*.

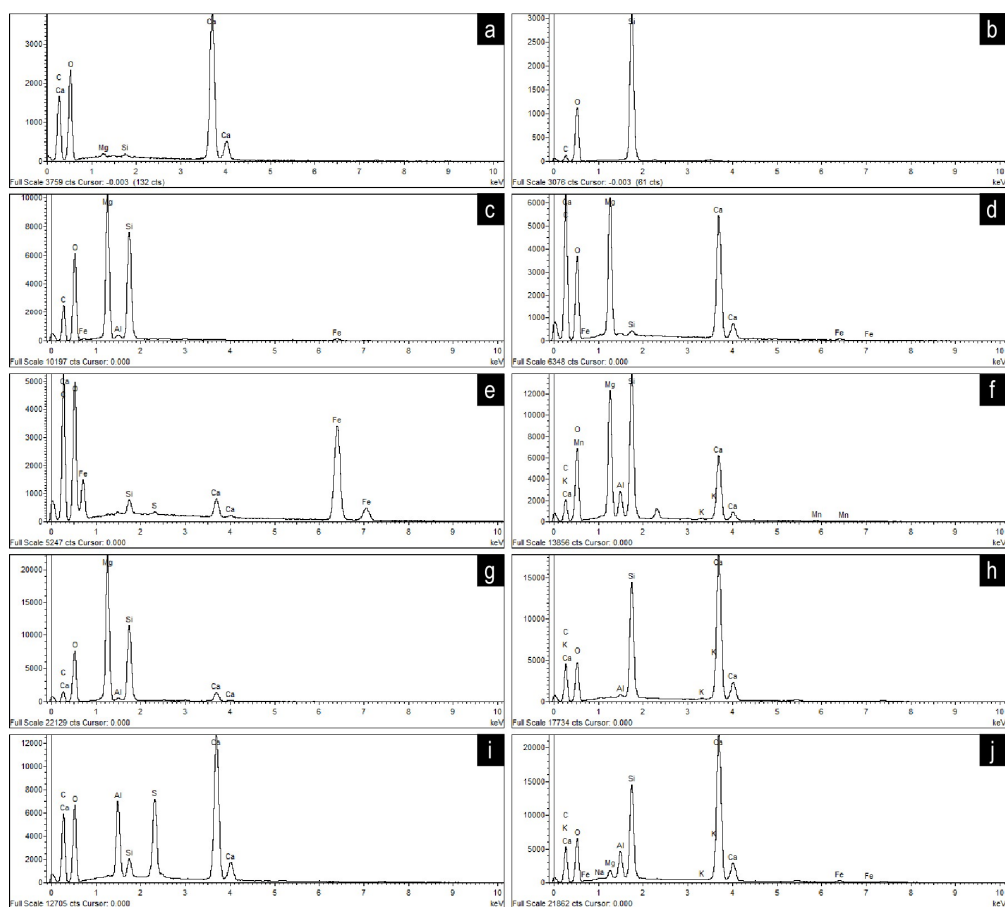


Figure 5.41: Examples of EDS spectra of **a.** calcite **b.** quartz, **c.** serpentine, **d.** dolomite, **e.** iron oxides, **f.** glassy matrix of furnace inclusion, **g.** olivine, **h.** belite, **i.** ettringite and **j.** tetracalcium aluminoferrite.

Serpentine						
Anal.	Roman				1° rest	2° rest
	1	2	3	4	1	1
SiO ₂	45.31	44.93	44.78	46.55	45.19	45.34
TiO ₂	0.00	0.00	0.00	0.00	0.00	0.00
Al ₂ O ₃	1.10	1.06	0.99	1.67	2.77	1.08
Fe ₂ O ₃	3.06	3.29	3.02	3.53	1.97	1.75
MnO	0.00	0.00	0.00	0.00	0.00	0.00
MgO	38.53	38.72	39.20	37.83	36.41	39.83
CaO	0.00	0.00	0.00	0.00	1.67	0.00
Na ₂ O	0.00	0.00	0.00	0.00	0.00	0.00
K ₂ O	0.00	0.00	0.00	0.00	0.00	0.00
Total	88.00	88.01	88.00	89.57	88.01	88.00
Si	2.079	2.066	2.058	2.097	2.068	2.069
Al	0.059	0.058	0.054	0.088	0.149	0.058
Ti	0.000	0.000	0.000	0.000	0.000	0.000
Fe	0.118	0.127	0.116	0.133	0.075	0.067
Mn	0.000	0.000	0.000	0.000	0.000	0.000
Mg	2.635	2.655	2.686	2.540	2.483	2.709
Ca	0.000	0.000	0.000	0.000	0.000	0.000
OH	4.891	4.905	4.915	4.859	4.858	4.902

Table 5.24: Microprobe analysis of serpentine for Roman, first and second restoration mortars.

5.7.3 Hidraulicity Index (HI)

The Hidraulicity Index, as explained in the [Paragraph 5.2](#), is an important parameter to be referred when analyzing mortars. This index is closely related to the amount of clay minerals or hydraulic materials that is present in the starting composition of the binder.

The Roman mortar samples AAM01, AAM17, AAM25, AAM37 and the samples from the first (AAM33), second (AAM34), third (AAM35) and fourth (AAM36) restorations were selected.

Figure 5.42 and *Figure 5.43* show, respectively, the false-color maps of the Roman mortar samples and the different restoration phases. Each false-color map is completed by a histogram where the calculation of HI (from 0 to 10) and all the values of the percentage calculated on the total number of pixels

for each image (Freq(cnts)%) are given along the abscissa (500 values) and the ordinate, respectively. Regarding the false-color maps of the hydraulicity index, it is necessary to point out that in the first color interval (red: from 0 to 0.1) there are many points with HI=0, i.e. points where the numerator oxides give sum 0 (very evident in AAM25 and AAM35). It should also be specified that the calcite elements of the aggregate (mainly present in lithic fragments) also belong to the red areas and are more concentrated in the areas where lumps occur and where the concentration of CaO is therefore higher.

Within the area of the analyzed section, the elaboration of these maps allows to better and more quickly evaluate not only the average value of the hydraulicity index but also its distribution and composition, which is not always homogeneous. It also allows an easier comparison of samples of different mortars.

The Roman mortar samples present an aerial to moderately hydraulic lime binder (Mariani et al., 1976).

The false-colour map of sample AAM25 (*Figure 5.42b*) shows an optical effect that turns to light beige and differs from the average HI value. This is mainly due to the scarcity of binder. As far as ancient samples subject to archaeological studies are concerned, it is always necessary to remember that they have suffered an invasive process of degradation over time, which leads to a change in their original characteristics. In particular, the binder of sample AAM01 is quite homogeneous with values of the HI ranging between 0.00 and 0.10 that falls in the field of aerial lime. Sample AAM17 is more inhomogeneous than the previous one and mainly presents values from 0.00 to 0.10, but it also presents areas where values range between 0.16 and 0.31 (in blue in the false-color HI map in *Figure 5.42c*) and other areas, rarer, where this value ranges between 0.50 and 1.50 (in yellow in the false-color HI map

in *Figure 5.42c*). The average HI value, due to these inhomogeneities, is above 0.10, placing this binder in the field of weakly hydraulic lime.

Sample AAM25, as already mentioned, is characterized by a low quantity of binder, however, from the histogram in *Figure 5.42b* it is evident that the HI of the binder belongs to the range between 0.00 and 0.20, collocating the binder in the moderately hydraulic range.

Finally, sample AAM37, as sample AAM01, is homogeneous and the HI values fall in the range between 0.00 and 0.10; therefore, it can be defined as aerial lime.

Table 5.25 shows spot analyses carried out in different areas of thin sections in which binder is more abundant. They all show a calcic composition. The sample AAM01 presents HI values from 0.04 to 0.16 (Mean=0.08), the sample AAM17 from 0.01 to 0.34 (Mean=0.16), the sample AAM25 from 0.05 to 0.25 (Mean=0.17) and finally the sample AAM37 from 0.03 to 0.24 ((Mean=0.09).

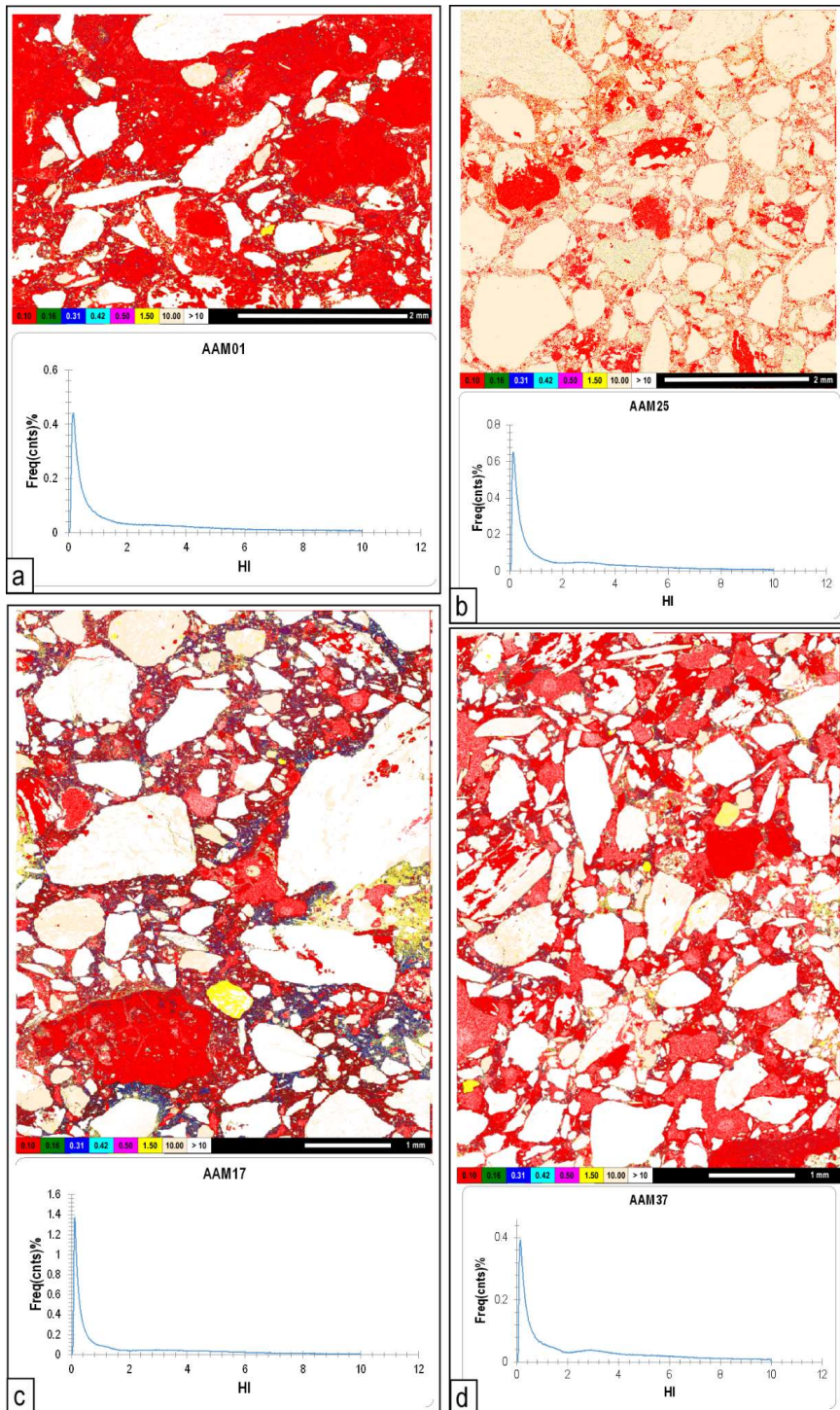


Figure 5.42: False-color maps of the Roman mortar samples and related histogram whose abscissa (500 values) shows the calculation of HI (from >0 to <10) and the ordinate all the values of the percentage calculated on the total number of pixels for each image (Freq(cnts)%). **a.** AAM01 sample **b.** AAM25 sample **c.** AAM17 sample **d.** AAM37 sample.

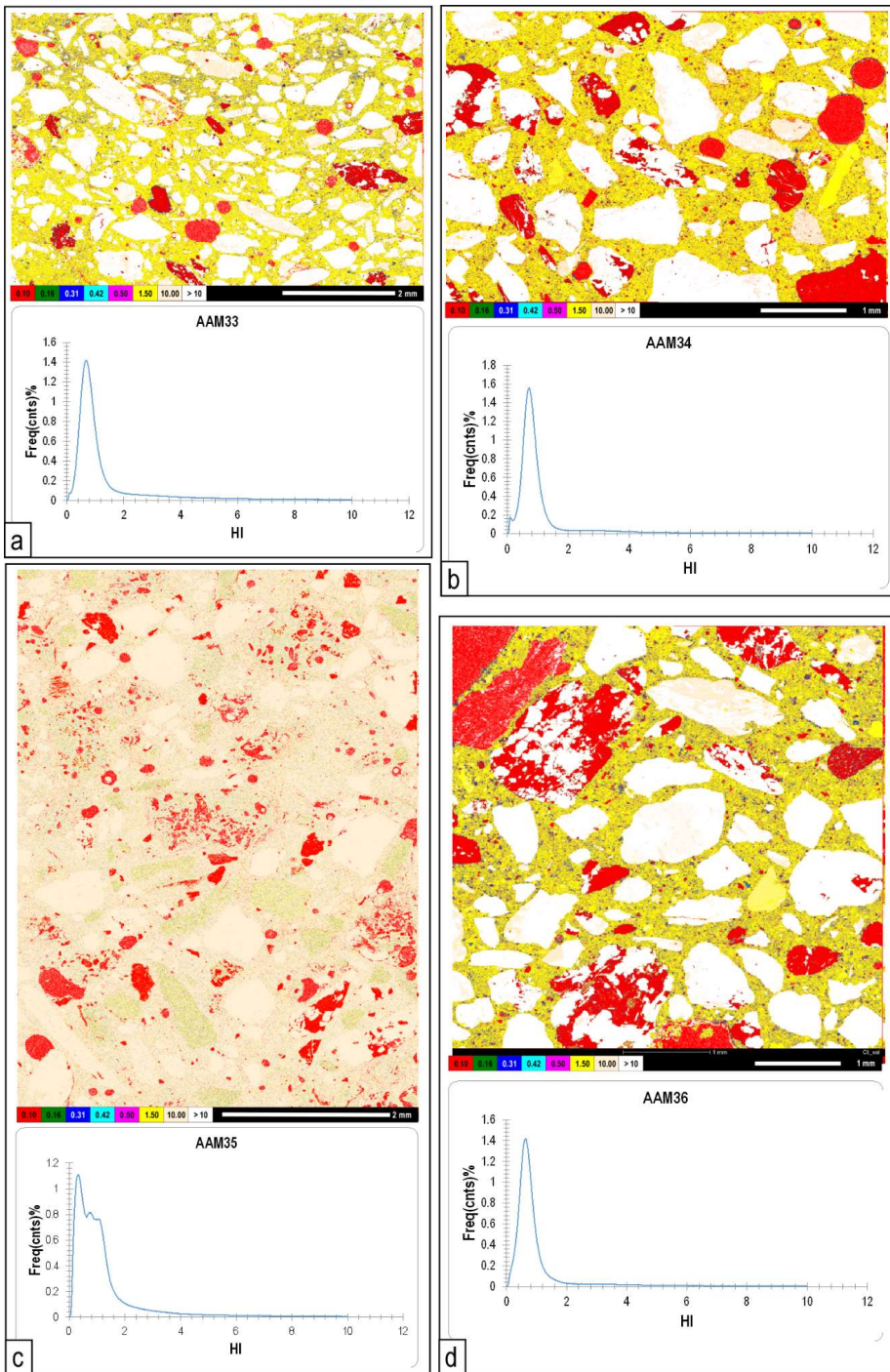


Figure 5.43: False-color maps of the restoration mortar samples and related histogram whose abscissa (500 values) shows the calculation of HI (from >0 to <10) and the ordinate all the values of the percentage calculated on the total number of pixels for each image (Freq(cnts)%). **a.** First restoration (AAM33 sample) **b.** Second restoration (AAM34 sample) **c.** Third restoration (AAM35 sample) **d.** Fourth restoration (AAM36 sample).

The binder of the first (AAM33), second (AAM34), third (AAM35) and fourth restoration (AAM36) presents an eminently hydraulic lime. They show HI values between 0.50 and 1.50.

In contrast to Roman mortars, the false-colour maps of HI show homogeneity in all samples. Also, in this case they are all calcic binders, although the % of MgO is slightly higher than Roman ones. *Table 5.26* shows the spot analyses carried out in different areas of thin sections. The sample AAM33 presents HI values from 0.85 to 0.95 (Mean=0.88), the sample AAM34 from 0.87 to 1.02 (Mean=0.94), the sample AAM35 from 0.45 to 0.77 (Mean=0.58) and finally the sample AAM36 from 0.73 to 1.27 (Mean=0.87).

Sample	SiO ₂	Al ₂ O ₃	Fe ₂ O ₃	MgO	CaO	HI
AAM01_1	9.33	2.83	1.73	1.02	85.08	0.16
AAM01_2	5.81	0.69	0.47	0.64	92.39	0.07
AAM01_3	7.38	1.1	0.92	1.39	89.22	0.10
AAM01_4	2.99	0.85	0.39	0.99	94.79	0.04
AAM01_5	3.9	0.7	0.6	0.9	93.9	0.05
AAM01_6	4.65	1.39	1.92	0.79	91.25	0.09
AAM01_7	4.47	0.76	0.71	0.52	93.54	0.06
AAM01_8	4.27	0.27	0.66	0.56	94.24	0.05
AAM01_9	5.37	2.01	1.34	0.31	90.98	0.10
AAM01_10	3.38	0.62	0.44	0.45	95.11	0.05
AAM01_11	4.09	0.73	1	0.14	94.04	0.06
AAM01_12	4.24	1.12	1.9	0.4	92.34	0.08
AAM01_13	4.24	1.12	1.9	0.4	92.34	0.08
AAM01_14	4.14	1.61	1.32	1.17	91.75	0.08
AAM01_15	3.66	1.44	0.47	1.18	93.24	0.06
AAM01_16	4.39	1.61	1.34	1.27	91.39	0.08
Mean						0.08
AAM17_1	15.89	2.88	1.38	0.57	79.28	0.25
AAM17_2	5.65	1.02	0.47	0.3	92.56	0.08
AAM17_3	0.54	0.27	0.02	0.46	98.71	0.01
AAM17_4	8.52	2.3	0.74	0.51	87.93	0.13
AAM17_5	16.46	7.43	1.67	0.9	73.54	0.34
Mean						0.16
AAM25_1	1.59	1.15	1.82	0.86	94.58	0.05
AAM25_2	15.8	3.28	0.83	0.47	79.61	0.25
AAM25_3	10.88	1.88	0.62	0.64	85.98	0.15
AAM25_4	9.67	2.48	0.73	0.71	86.41	0.15
AAM25_5	12.53	5.7	0.64	2.18	78.96	0.23
Mean						0.17
AAM37_1	1.51	0.45	7.48	7.34	83.22	0.10
AAM37_2	2.78	0.96	0.25	0.11	95.9	0.04
AAM37_3	1.89	0.43	0.23	0.15	97.31	0.03
AAM37_4	3.5	1.78	0.56	0.17	93.99	0.06
AAM37_5	6.14	0.85	0.65	0.15	92.21	0.08
AAM37_6	11.23	7.56	0.55	0.59	80.07	0.24
Mean						0.09

Table 5.25: Representative microprobe analysis of Roman mortars.

Sample	SiO ₂	Al ₂ O ₃	Fe ₂ O ₃	MgO	CaO	HI
AAM33_1	36.78	6.4	2.66	2.54	51.62	0.85
AAM33_2	36.38	6.66	4.2	3.93	48.83	0.90
AAM33_3	39.94	5.48	2.18	3.16	49.24	0.91
AAM33_4	37.83	4.99	1.13	2.85	53.2	0.78
AAM33_5	40.11	5.29	1.54	1.55	51.51	0.88
AAM33_6	36.78	7.27	4.63	2.69	48.63	0.95
Mean						0.88
AAM34_1	39.99	4.74	1.87	1.75	51.66	0.87
AAM34_2	35.94	8.86	2.78	1.75	50.67	0.91
AAM34_3	37.61	8.59	2.79	1.49	49.52	0.96
AAM34_4	36.99	8.05	5.46	2.57	46.93	1.02
AAM34_5	36.04	8.94	3.58	1.52	49.93	0.94
AAM34_6	35.44	9.48	3.64	2.09	49.35	0.94
Mean						0.94
AAM35_1	28.94	5.03	2.7	3.29	60.03	0.58
AAM35_2	24.17	4.41	2.47	3.82	65.13	0.45
AAM35_3	31.28	3.33	2.41	4.53	58.46	0.59
AAM35_4	23.39	4.47	2.14	2.47	67.53	0.43
AAM35_5	30.48	6.07	2.1	3.22	58.14	0.63
AAM35_6	32.36	8.19	2.88	3.85	52.72	0.77
AAM35_7	29.96	4.58	2.57	3.21	59.68	0.59
Mean						0.58
AAM36_1	31.75	8.23	2.26	1.94	55.82	0.73
AAM36_2	35.68	6.6	3.53	1.83	52.35	0.85
AAM36_3	38.11	6.37	2.05	2.37	51.09	0.87
AAM36_4	33.29	9.21	2.28	2.16	53.06	0.81
AAM36_5	34.06	7.03	4.24	2.1	52.57	0.83
AAM36_6	31.49	7.92	3.44	2.14	55.01	0.75
AAM36_7	40.12	13.57	2.31	1.37	42.63	1.27
Mean						0.87

Table 5.26: Representative microprobe analysis of restoration mortars.

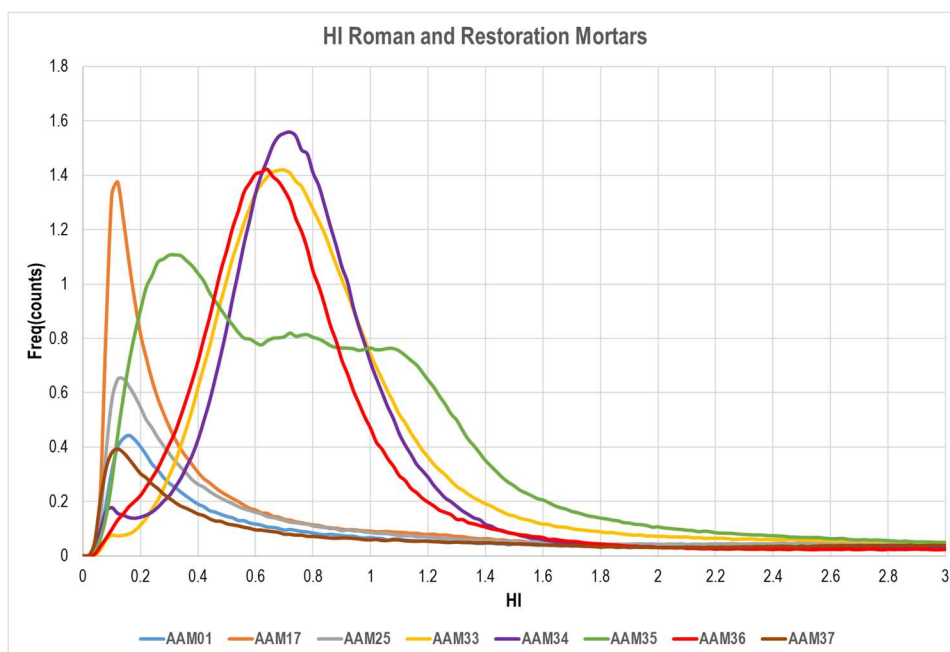


Figure 5.44: Histograms of Roman (AAM01, AAM17, AAM25, AAM37) and restoration (AAM33, AAM34, AAM35, AAM36) mortars whose abscissa (500 values) shows the calculation of HI (from >0 to <10) and the ordinate all the values of the percentage calculated on the total number of pixels for each image (Freq(cnts)%).

In *Figure 5.44* it is possible to observe the comparison of the histograms of the hydraulicity index of the mortars studied. It is very evident how the Roman mortars (AAM01, AAM17, AAM25 and AAM37) have a corresponding peak around a value of 0.1, although the number of counts is different, while the restoration mortars (AAM33, AAM34, AAM35, AAM36) shift their peak towards higher hydraulicity values with a main value around 0.7. They also have a more symmetrical histogram pattern, whereas those of Roman mortars are more asymmetrical and show a Gaussian with a curve tailing towards higher values. The sample AAM35 shows a more irregular pattern probably due to the reaction edges between the binder and the slags.

5.8 Discussion

The results reported in the [Paragraphs 5.7.1](#) and [5.7.2](#) allow to propose archaeometric interpretations, both in strict sense and in wider-ranging terms, on the analytical study of geo-materials. Indeed, it is possible to obtain data that provide information regarding the production technology of mortars, both Roman and restoration, and regarding the supply areas of raw materials. Concerning the analytical study of geo-materials, the proposed analytical protocol (see [Paragraph 5.6.2](#)) represents an upgrade in the analytical research of ancient mortars (Roman mortars) and more modern mortars (restoration mortars). It is potentially applicable to other geo-materials such as plasters, cements and also ceramics.

5.8.1 Production technology

In order to investigate the production technology of the studied mortars, it is necessary to interpret the optical microscopy data focusing on the distribution of the aggregate elements, their shape, size and sorting. In addition, as regards the elements of the aggregate it is important to check the presence of reaction edges with the binder.

Binder data can also provide several useful information. The presence, morphology and distribution of lumps, as well as evidence of shrinking and porosity can be identified by optical microscopy and backscattered SEM images.

5.8.1.1 Roman mortars

The grain size of the aggregate, from 500 μm to 4 mm, the moderate sorting and the bimodal grain size distribution highlighted by fine and coarse grains confirm the archaeological data (Appolonia, 2010) that placed the analyzed

samples as bedding mortars. Furthermore, the sub-angular to sub-rounded shape of the clasts shed light on their provenance possibly related to fluvial erosional processes.

As far as the binder is concerned, its composition and HI values suggest that it is a calcic aerial to moderately hydraulic lime (Mariani et al., 1976). This type of binder is entirely in accordance with its function as a bedding material.

On the base of the distribution of HI in the false color maps, it will be here proposed a different interpretation of the hydraulicity classification of the studied binders, especially concerning the two samples falling on the edge across the weakly to moderate hydraulic fields (AAM17 and AAM25, respectively). Taking as main example the mortar AAM17 (*Figure 5.42c*), it is possible to observe how the more hydraulic portions (blue and yellow color in *Figure 5.42c*) are strictly localized along the clasts edges and not randomly dispersed throughout the examined area. Such distribution could be related to chemical interactions between the aggregate and the binder during the mixing stage, the hardening of the mortar or both of them (Appolonia, *pers. comm.*). On the other hand, the raw material used as lime stone (in Aosta Valley marble, travertine or calcschist) may not have been pure and therefore may have given a silicate component to the mixture (Appolonia, *pers. comm.*). Given these assumptions, the higher hydraulicity of the samples AAM17 and AAM25 is not an intentional characteristic of their binders but, respectively, the product of subsequent processes affected the mortars or a pristine feature of the rocks adopted for the lime. As a consequence, these two binders can be classified as calcic aerial lime. In the study of mortars, especially for ancient specimens, it is then strongly recommended to perform detailed observation on as large as possible false color HI maps as proposed in the protocol adopted in this Thesis.

The widespread presence of lumps is due to a non-advanced traditional lime production technology. Indeed, the aspect and morphology of these lumps, which are often fissured, suggest that the binder is not totally mixed with the mixture, pointing to a lack of care during the mixing phase. The shrinkage phenomena observed in the binder, on the other hand, can be attributed to a shortage of binder in the mix. The widespread porosity, with an irregular to rounded shape, also indicates defects in the mixing of the mortar. Conversely, the micro-porosity is due to a loss of binder over time and bringing the samples to their current poor state of preservation.

5.8.1.2 Restoration mortars

For the restoration mortars, their difference with the ancient Roman mortars is evident. In all samples the grain size of the aggregate is finer (200 microns to 2 mm), and the distribution more homogeneous and denser. Also, the ratio binder/aggregate (B/A) is different; Roman mortars generally show a lower quantity of aggregate than restoration mortars. Indeed, the former have a B/A ratio of around 1/2 with the exception of sample AAM01 where the ratio is 2/1. Restoration mortars, on the contrary, show a quite constant ratio around 1/1 (*Table 5.27*).

	Samples	Binder (%)	Aggregate (%)	Porosity (%)	Ratio B/A
Roman mortars	AAM01	59	34	7	2/1
	AAM17	34	60	6	1/2
	AAM25	37	60	3	1/2
	AAM37	20	57	23	1/2
Restoration mortars	AAM33 (1° rest.)	51	43	6	1/1
	AAM34 (2° rest.)	40	47	13	1/1
	AAM35 (3° rest.)	45	51	4	1/1
	AAM36 (4° rest.)	44	47	9	1/1

Table 5.27: Percentage of binder, aggregate, porosity and ratio B/A of Roman and restoration mortars.

Furthermore, in the third restoration is remarkable the presence of blast-furnace slag used in addition to lithic fragments. These slags display a very characteristic morphology. Indeed, these elements, belonging to the coarse-grained fraction (1 – 2 mm), are made up of crystals of needle olivine embedded in a glassy matrix. They show many rounded pores and a thick edge suggesting reaction processes with the binder. Shrinking phenomena have also been observed around these elements.

The binder, on the other hand, is much more compact, less degraded, and hydraulic. The HI value, ranging between 0.50 and 1.50, places all the restoration specimens in the range of cement mortars. Indeed, in the samples of the first, second and third restorations, the porosity, rounded in shape (*Figure 5.31e* and *Figure 5.32e*), is possibly due to bubble formation during mortar firing. Shrinking phenomena were also observed in the samples of the first and second restorations (*Figure 5.31f* and *Figure 5.32f*), which were plausibly due to the rapid hardening of the hydraulic mortars.

In the samples of the third restoration, the shrinking is not only limited to the hardening of the binder but also related to the reaction occurring between the slags and the binder itself highlighted by the occurrence of reaction edges around the individual slags (see *Figure 5.33c*).

The binder used in the fourth restoration is more inhomogeneous and shows an irregular porosity. In contrast to the samples of the previous restoration phases, this is possibly due to an original lack of material during the preparation of the mortar. So that, in this case the porosity is not related to bubble formation during the firing but is a former property of the mixture. Shrinking phenomena, diffused in all samples, testify to the excessive quick hardening of the cement decreasing the mechanical performance of the material. In particular, in the binder of sample AAM36 (fourth restoration),

belite, ettringite and tetracalcium aluminoferrite (C_4AF) occur. While belite and ettringite are residues that can be found in any type of cement, C_4AF is specific of Portland cement.

5.8.2 Supply areas

Based on Optical Microscope observations (see Paragraph 5.7.1) and Mineral Chemistry data (see Paragraph 5.7.15.7.2) it is possible to identify the supply areas of the raw materials used as aggregate in both Roman and restoration mortars.

5.8.2.1 Roman mortars

Compositionally, the aggregate of Roman mortars is made up of lithic fragments of quartzite, micaschist, calcschist, marble and prasinite with the exception of monomineralic clasts of quartz and biotite that have also been individually found. They are all lithic materials consistent with the geology of the area (see Paragraph 5.4) leading to the assumption the sources of the materials were local.

In *Table 5.28* it is possible to review the main lithologies and minerals constituting the aggregate of the Roman mortars.

Sample	Quartz	White mica	Biotite	Quartzite	Albite	K-feldspar	Marble	Calcschist	Micaschist	Garnet	Prasinite
<i>Roman mortars</i>											
AAM01	x	x	x	x	x	x	x	x	x		x
AAM02	x	x	x		x			x	x	x	
AAM03	x	x	x	x	x			x	x		
AAM04		x			x			x	x		
AAM05	x	x			x	x		x	x		x
AAM06	x	x	x	x	x			x		x	
AAM07	x	x	x		x			x	x	x	
AAM08	x	x		x	x			x	x	x	
AAM09	x	x	x		x				x		
AAM10	x	x	x	x	x	x		x	x		
AAM11	x	x	x		x	x		x	x		x
AAM12	x	x	x	x	x			x	x		
AAM13		x	x		x	x		x			
AAM14	x	x			x			x	x		
AAM15	x	x			x				x		
AAM16		x	x		x	x		x	x	x	
AAM17	x	x	x		x	x		x	x		
AAM18	x	x			x	x		x	x		
AAM19	x	x	x	x	x			x	x		
AAM20	x	x	x	x	x	x		x	x		
AAM21	x	x	x	x	x			x	x		
AAM22		x			x			x	x		x
AAM23	x	x	x		x				x		
AAM24	x	x	x		x			x	x		
AAM25	x	x	x		x	x		x	x	x	
AAM26	x	x			x			x	x	x	x
AAM27	x	x	x			x		x	x	x	
AAM28	x	x		x	x			x	x		
AAM29	x	x	x	x	x			x	x		x
AAM30	x	x	x		x			x		x	
AAM31	x	x			x	x		x	x		
AAM32	x	x			x	x		x			
AAM37	x	x	x	x	x	x		x	x	x	x
AAM42	x	x	x	x	x			x	x		

Table 5.28: Main lithic fragments and minerals constituting the aggregate of the Roman mortars.

Further observations on the lithologies used as raw material can be made based on the mineral chemistry of the mineral phases analyzed.

The geological references used in the following are shown in

Figure 5.5 and *Figure 5.6*.

Amphibole

All the analyzed amphiboles (*Figure 5.39a, b* and *c*) are classifiable as calcic or sodic-calcic amphiboles with a tremolitic to pargasitic composition, reflecting medium-low pressure and low to medium temperature metamorphic conditions. This type of amphiboles occurs in numerous units of both oceanic

and continental origin outcropping in the Aosta Valley, which have suffered pervasive retrogression to low-pressure metamorphic conditions, possibly with subsequent heating stage. Sodic amphiboles, characteristic of high-pressure conditions, are absent. This data is consistent with the geographic position of the Roman Theatre, located west of the outcropping areas of the main oceanic units characterized by eclogitic facies of the Aosta Valley.

Chlorite

The analyzed chlorite (*Figure 5.39d*) is typical of low metamorphic grade belonging to both the basic and pelitic systems. It is therefore a phase mineral typical of rocks from different oceanic and continental crustal units outcropping in the Aosta Valley.

Feldspar

The examined feldspars (*Figure 5.39e*) show compositions falling within the albitic range, which is typical of the Aosta Valley rocks of low metamorphic grade from both the basic and pelitic systems.

Orthoclase

The presence of K-feldspar can be attributed to the dismantling of orthogneisses (in most cases), which are widespread in the continental units of the Aosta Valley, or of granitoids (probably originating from the erosion of Mont Blanc granites).

Garnet

Garnet crystals only occur within the Roman samples (**Figure 5.39f** and **g**).

These garnets are moderately zoned and reflect the average compositions of basement schists belonging to the high-pressure continental units (blue and eclogitic schist facies).

White mica

The composition of the analyzed mica (*Figure 5.39i*) reflects high-pressure conditions, typical of the continental crustal units outcropping in Aosta Valley and, in particular, in the eclogitic facies units such as the Gran Paradiso Massif and the blue schist units of the Great Saint Bernard multinape system.

The presence of paragonite is also typical of high-pressure continental units.

Biotite

The analyzed biotites (*Figure 5.39h*) were possibly part of the high-temperature metamorphic lithotypes, such as the kinzigites of the Valpelline Series, dismantled and transported downstream along the Buthier River, a left tributary of the Dora Baltea, up to the town of Aosta.

Pyroxene

The analyzed pyroxenes (*Figure 5.39j* and *k*) are calcic, while the typical sodium-calcic pyroxenes of the basic rocks balanced in eclogitic conditions of the Piemontese Zone and the sodium pyroxenes of the ortho-derivatives of the Sesia Lanzo Zone are missing. This data is consistent with the geographic position of the Roman Theatre of Aosta, located west of the outcropping areas of the main eclogitic units in the Aosta Valley. The pyroxenes could then derive from the dismantling of basic rocks of high metamorphic grade from the Valpelline Series.

Epidote

The analyzed epidote (*Table 5.23*) is of low to medium grade and reflects the typical compositions of epidotes belonging to the rocks outcropping in the Aosta Valley.

On the basis of the above considerations it is possible to attribute the source of supply of the raw material to the area of Aosta, in close proximity to the Roman Theatre. In particular the low amount of biotite and the presence of K-

feldspar suggest that the Romans took the material upstream of the Buthier and the Dora rivers (*Figure 5.45*).

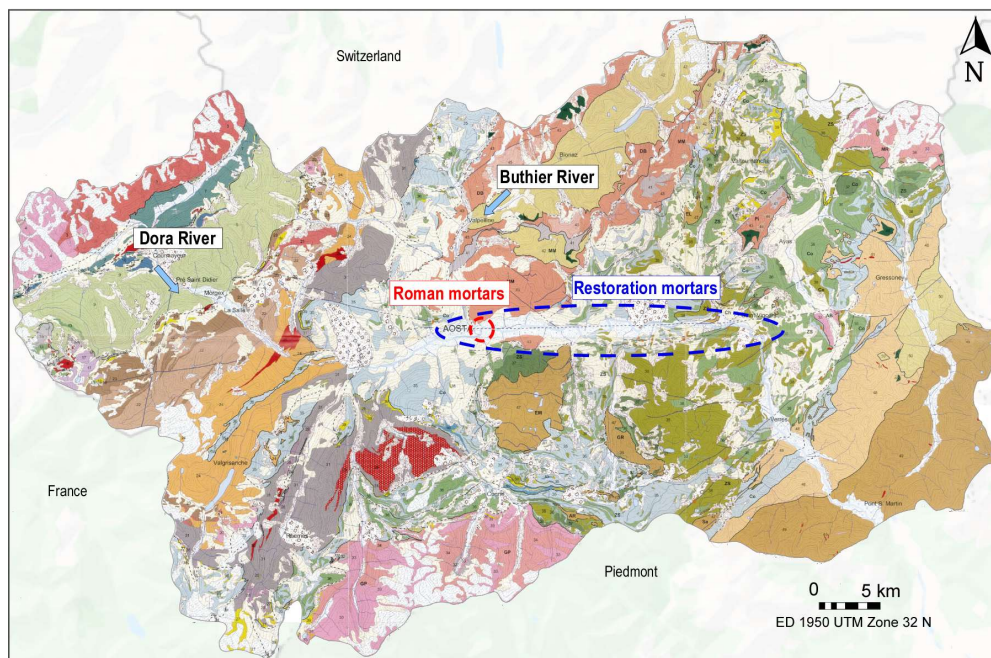


Figure 5.45: Geo-tectonic map of Aosta Valley (modified after De Giusti et al., 2004). It is indicated the source of supply of the raw material of Roman and Restoration mortars.

It represents an important information because during Roman Age the commerce was very prosperous, and the archeologists found raw materials that coming from all over the Mediterranean area. This is an example of use of raw materials from the surrounding territory.

5.8.2.2 Restoration mortars

In *Table 5.29* it is possible to review the main lithologies and minerals constituting the aggregate of the restoration mortars.

Sample	Quartz	White mica	Biotite	Quartzite	Plagioclase	K-feldspar	Gneiss	Marble	Calcschist
<i>First restoration</i>									
AAM33	x			x	x				x
AAM41	x			x	x				x
<i>Second restoration</i>									
AAM34	x	x						x	
AAM39	x	x						x	
<i>Third restoration</i>									
AAM35	x								x
AAM38	x								x
<i>Fourth restoration</i>									
AAM36	x	x				x			x
AAM40	x	x				x			x

Sample	Micaschist	Garnet	Chloritoschist	Serpentinite	Prasinite	Granitic rocks	Vein filling minerals	Slags
<i>First restoration</i>								
AAM33	x		x					
AAM41	x		x					
<i>Second restoration</i>								
AAM34	x			x		x	x	
AAM39	x			x				
<i>Third restoration</i>								
AAM35	x		x	x				x
AAM38	x		x	x				x
<i>Fourth restoration</i>								
AAM36	x					x	x	
AAM40	x					x	x	

Table 5.29: Main lithologies and minerals constituting the aggregate of the restoration mortars.

Considerations on the lithologies used as raw material can be made based on the mineral chemistry of the mineral phases analyzed.

In contrast to Roman mortars, garnet was not found in any of the restoration mortars.

For the other mineral phases, in order to avoid repetitions, only the interpretation of the plagioclase is given, as the others match those of Roman mortars. Indeed, plagioclase minerals with labradoritic and anorthitic composition can be referred to basic rocks or high temperature units. High-temperature basic rocks are present in the Valpelline Series unit (North-East of Aosta).

Except for the furnace slags of the third restoration, restoration mortars are all quite similar to each other. However, they are different from Roman mortars. In particular, they contain more basic and ultra basic rocks. These could derive from the oceanic crust units of the Aosta Valley (outcropping East of Aosta), so unlike the Roman mortars, whose source of supply was close to that of the Theatre. Then, it is possible to attribute the source of supply of the raw material of the restoration mortars along the Dora Baltea River, approximately between Aosta and Saint Vincent (*Figure 5.45*).

5.8.3 Evaluation of the methodology

The analytical protocol proposed and explained in detail in the [Paragraph 5.6.2](#) provides an innovative method for the petrographic study of mortars. Firstly, by the observation under the optical microscope, it is possible to carry out a petrographic characterization of the mortar, both from the point of view of the aggregate and the binder. Starting from this observation, the most representative area of the sample can be identified in order to proceed with SEM-EDS quantitative mapping. From the processing of the quantitative maps, at first with the Aztec software and then with the original *GeoMatMap Software*, the composition of the mineral phases, their absolute abundance expressed in percentage, as well as the percentage of binder and porosity can be identified. By re-elaborating the quantitative maps, it is also possible to obtain false colors maps and the related distribution histograms of the Hydraulicity Index. All the obtained data are useful for further analysis of the aggregate (e.g. to investigate supply areas).

In the field of the Materials Science applied to Cultural Heritage, this method is useful to provide precise information about the composition of the mortar under investigation. Its characterization allows to define several parameters that lead to a relative dating or a comparison with other samples.

It is very important to consider that ancient artifacts are exposed to very invasive environmental and/or anthropic degradation processes that do not always allow the complete legibility and interpretation of the obtained data. Despite the poor state of preservation of the samples from the Roman period, the data obtained were satisfactory and useful for the intended purposes, namely the study of production technology and the investigation of supply areas. From the point of view of the characterization of geomaterials in a

wider sense, the high level of applicability of the method is more evident for the samples of restoration mortars, which are necessarily characterized by a higher state of conservation.

This method allows to characterize the geomaterials in a way that is both expeditious and very detailed at the same time and certainly provides a complementary contribution to all those chemical and mechanical parameters that are generally used for the study of this type of material.

6. Conclusions

The main goal of this PhD project was to propose a multidisciplinary approach that allowed to collect different types of data in the field of the study of geomaterials used in the Cultural Heritage.

The main conclusions, considerations and future perspectives are summarized in the following.

6.1 Geo-lithological Map of ornamental stones of Piemonte region

The 1:250,000 Geo-lithological Map of ornamental stones of Piemonte ([Chapter 2](#) and [Appendix I](#)), besides scientific aspects, represents a source of information for all those operating in the fields of Cultural Heritage and geo-environmental sciences. It is thus a simplified lithological map, consisting of 21 lithological classes, showing the distribution of the ornamental stones exploited in Piemonte and it was obtained by modifying the Geological Map of Piemonte (GeoPiemonteMap, Piana et al., 2017a) and its Data Model. The Map represents a lithological synthesis of a very complex geological setting that comprehends a large number of lithotypes and geological units.

6.2 Petrographic geodatabase of Alpine ornamental rocks

A geodatabase referred to Geo-lithological Map was created. Each mapped quarry, labelled by a number on the Geo-lithological Map, corresponds to a specific row in the geodatabase ([Appendix II](#)). This contains the following informations: the quarry district, coordinates, quarry state—active/inactive, tectonic unit, commercial name of ornamental stone, petrographic name, rock type, a short petrographic description and finally the main uses in architecture in Piemonte region and the main references.

This is an original work that brings together geological, historical and modern knowledge, archaeometry and architecture.

Six representative historical buildings representative of Piemonte region were chosen to provide an important overview of the employments of some of the most used ornamental stones quarried in Piemonte.

6.3 The case study of Palazzo Madama façade

The aim of this study is to furnish a detailed petro-architectonic survey and a minero-petrographic characterization of the *Chianocco Marble* mainly aimed to define the causes of its degradation.

The summary of the main results is the following:

- Original and historical restoration stone materials were defined and a petro-architectonic relief realized. It can be consulted by restorers, architects and engineers who will deal with the future restoration of the façade;
- the *Chianocco Marble* is the most abundant stone material and it is affected by a strong degradation;
- the minero-petrographic study of the *Chianocco Marble* shows that some characteristics detected on the Palazzo Madama façade, such as a vacuolar structure and local reddenings, usually absent in ornamental marbles, are primary features of the rock itself and are not due to degradation in an urban context. Only gypsum crystals grown in voids and the application of mortars in natural voids, enhancing the physical degradation of the stone, are due to pollution and anthropic interventions respectively.

This research highlights the importance of defining the characteristics of stone materials in conservation issues in Cultural Heritage where ornamental stones are used in order to properly understand the the reasons of their degradation.

6.4 Petrographic studies of mortars

This chapter proposes a new approach and analytical protocol on the study of ancient and modern mortars. A new Software called *GeomatMap* has been developed consisting in a semi-automated image processing procedure based on multivariate statistical analysis of X-Ray spectrum images.

Data regarding the production technology of mortars, both Roman and restoration, the supply areas of raw materials and the Hidraulicity Index are investigated.

The study of the aggregate of Roman mortars confirm the archaeological data (Appolonia, et al. 2010) that placed the analyzed samples as bedding mortars and sited their provenance possibly from fluvial sediments.

It is also possible to attribute the source of supply of the raw material to the area of Aosta, it is therefore material found in close proximity to the Roman Theatre. The ratio B/A is around 1/2 and both the composition of the binder and its HI values suggest that it is a calcic aerial to moderately hydraulic lime (Mariani, 1976). This type of binder is entirely compliant with its function as a bedding material.

The study of the aggregate of restoration mortars highlights an increased selection of aggregate grain size, a hydraulic composition of the binder which places them in the field of cement mortars (Mariani, 1976) and a B/A ratio of around 1/1. It is also possible to attribute the source of supply of the raw material to the entire Aosta Valley, an area, although local, larger than that of Roman mortars.

6.5 Future perspectives

Concerning the study of geomaterials, the proposed new analytical protocol regarding the petrographic study of mortars is highly promising to improve their study.

Regarding mortars, the immediate next step would be to test different restoration mortars of known composition. This would serve on the one hand to further validate the method and on the other hand to improve its precision in the detection of different analyzed phases. In fact, the proposed study is a protocol which, if applied on a large scale, could speed up and unify the methods of analysis of these types of materials.

Other developments of this research must concern the study of the binder in order to verify whether the method allows to better investigate the reaction rims that can be present in different types of aggregate also when they are not clearly evident from a simple observation of a thin section. Moreover, it can be investigated how the method allows to obtain new information about the different structures that may be present and structures that often influence the durability of these materials.

In this regard, the proposed method is potentially applicable to other geomaterials such as plasters, concrete and ceramics.

The approach at the base of the Geo-lithological Map and its geodatabase may be applied also to other georesources (e.g. talc) widely occurring in Piemonte as well as in other regions and countries. Importantly, the mapping of such geomaterials allows to bridge the Geology with the Architecture, the Conservation, the Science of Materials, the Engineering of Building and Construction and Geography. Moreover, following an extensive study, in addition to informations already present in the geodatabase, it will be

fundamental adding data concerning the durability and the conservation problems of these stone materials. In parallel, current technologies would make it possible to develop a smartphone application that allows to identify these rocks by taking a picture. This could be used not only in science but also in education, dissemination and *public engagement*.

Finally, the case study of Palazzo Madama demonstrates that the development of a minero-petrographic approach applied to stone materials of Cultural Heritage is primarily a geological matter and has to be solved by a geologic approach. A proper characterization of these materials requires minero-petrographic studies to define their provenance, conservation state, and application of good preservation strategies. Once more, this methodology may be applied to every kind of lithotypes used in Architecture.

References

Agostoni, A., Barello, F., Borghi, A. & Compagnoni R. (2017). The white marble of Augustus (Susa, north-western Italy): mineralogical and petrographic analysis for the definition of its origin. *Archaeometry*, 59, 3, 395-416.

Alagna, K. E., Peccerillo, A., Martin, S. & Donati, C. (2010). Tertiary to present evolution of orogenic magmatism in Italy. *Journal of the Virtual Explorer*, 36, 1–63. doi:10.3809/jvirtex.2010.00233

Alciati, L. & Fiora, L. (2004). le pietre delle pievi nell'astigiano. *L'informatore del Marmista*, 524, 44-60.

Allemani, P. & Gomez Serito, M. (2018). La Pietra di Visone: un significativo indicatore per la lettura dell'edilizia storica del Basso Piemonte. IV ciclo di studi medioevali, Firenze, NUME, 505-509.

Amieux, P. & Jeanbourquin, P. (1989). Cathodoluminescence et origine diagénétique tardive des cargneules du massif des Aiguilles Rouges (Valais, Suisse). *Bull. Soc. Géol. France*, 1, 123–132.

Appolonia, L. & Fazari, M.C. (2005). Il Teatro romano di Aosta. Regione Autonoma della Valle d'Aosta, *Bollettino della Soprintendenza*, 86-89.

Appolonia, L., Vaudan, D. & Glarey, A. (2010). Lo studio delle malte del Teatro romano di Aosta: una ricerca in corso. Regione Autonoma della Valle d'Aosta, *Bollettino della Soprintendenza n°6*, 249-252.

Arnaldi di Balme, C. (2013). Consolidamento e manutenzione della facciata di Palazzo Madama (2010–2011). *Palazzo Madama. Studi Notizie. Riv. Annu. Mus. Civ. d'Arte Antica Torino*, 2, 144–157.

Badino, V., Bottino, I., Bottino, G., Fornaro, M., Frisa Morandini, A., Gomez Serito, M. & Marini, P. (2001). Valorizzazione delle risorse lapidee del bacino estrattivo dei marmi del Monregalese. *Geingegneria ambientale e mineraria*, 38, 97-108.

Baldelli, C., Dal Piaz, G.V. & Polino, R. (1983). Le quarziti manganesifere di Vareche-St.Bartelemy. Sequenza sopraoceanica della falda piemontese. *Ofioliti*, 8, 207-221.

Bany Yaseen I. A., Al-Amoush H., Al-Farajat M., Mayyas A. (2013). Petrography and mineralogy of Roman mortars from buildings of the ancient city of Jerash, Jordan, *Construction and Building Materials*, Volume 38, 465-471. doi:10.1016/j.conbuildmat.2012.08.022.

Barale L., Borghi A., d'Atri A., Gambino F.*, Piana F. (2020). Ornamental Stones of Piemonte (NW Italy): an updated geo-lithological map. *Journal of Maps*, 16:2, 867-878, doi: 10.1080/17445647.2020.1837685

Barisone, G., Bottino, G., Coccolo, V., Compagnoni, R., Del Greco, O., Mastrangelo, F., Sandrone, R., & Zucchetti, S. (1979). Il bacino estrattivo della «Pietra di Luserna» (Alpi Cozie). *Atti Conv. «La Pietra di Luserna»*, Luserna San Giovanni, 15 luglio 1979, 11–26 and *Not. Ass. Mineraria Subalpina*, 5, 35–50.

Belfiore, C.M., Fichera, G.V., Ortolano, G., Pezzino, A., Visalli, R. & Zappalà, L. (2016). Image processing of the pozzolanic reactions in Roman mortars via X-ray Map Analyser. *Microchem. J.* 125, 242–253. doi:10.1016/j.microc.2015.11.022

Beltrando, M., Compagnoni, R. & Lombardo, B. (2010). (Ultra-) high-pressure metamorphism and orogenesis: an alpine perspective. *Gondwana Research*, 18, 147–166.

Berti, C. (1998). Il Palazzo di marmo. In *Ricerche sui Materiali Lapidei Della Facciata di Palazzo Madama in Torino*. Associazione Georisorse e Ambiente: Turin, Italy, 95, 237–242.

Berti, C. & Gomez Serito, M. (1999). I Marmi Della Facciata di Palazzo Madama a Torino. *Associazione Georisorse e Ambiente: Turin, Italy*, 96, 13–22.

Bertok, C., Barale, L., d’Atri, A., Martire, L., Piana, F., Rossetti, P. & Gerdes, A. (2019). Unusual marbles in a non-metamorphic succession of the SW Alps (Valdieri, Italy) due to early Oligocene hydrothermal flow. *International Journal of Earth Sciences*, 108(2), 693–712. doi:10.1007/s00531-019-01676-z

Bigioggero, B., Colombo, A., Del Moro, A., Gregnanin, A., Macera, P. & Tunesi, A. (1994). The Oligocene Valle del Cervo pluton: An example of shoshonitic magmatism in the Western Italian Alps. *Mem. Sci. Geol. Padova*, 46, 409–421.

Bonetto S., Fornaro M (2005). Il verde alpi cesana: un contributo geominerario alla memoria delle sue cave in un percorso fra tecnica e natura, 7-9. *Atti del*

Convegno di medio periodo "Le pietre del Territorio. Cultura, Tradizione, Sviluppo sostenibile". Palmaria, 17-18 ottobre 2005.

Borghi, A., Cossio, R., Fiora, L., Pianea, E. & Sandrone, R. (2005). Catodoluminescenza pan e monocromatica di marmi bianchi piemontesi. In: D'Amico C. Ed. *Innovazioni tecnologiche per i beni culturali*, 351-360, Patron Editore Bologna.

Borghi, A., Fiora, L., Marcon, C. & Vaggelli, G. (2009). The Piedmont white marbles used in Antiquity: An archaeometric distinction inferred by a mineralogical and C-O stable isotope study. *Archaeometry*, 51(6), 913–931. doi:10.1111/j.1475-4754.2008.00447.x

Borghi, A., d'Atri, A., Martire, L., Castelli, D., Costa, E., Dino, G., Favero Longo, S.E., Ferrando, S., Gallo, L.M., Giardino, M., Groppo, C., Piervittori, R., Rolfo, F., Rossetti, P. & Vaggelli, G. (2014). Fragments of the western Alpine Chain as historic ornamental stones in Turin (Italy): Enhancement of Urban geological heritage through Geotourism. *Geoheritage*, 6(1), 41–55. doi:10.1007/s12371-013-0091-7

Borghi, A., Berra, V., d'Atri, A., Dino, G.A., Gallo, L.M., Giacobino, E., Martire, L., Massaro, G., Vaggelli, G., Bertok, C. et al. (2015). Stone materials employed for monumental buildings in the historical centre of Turin (NW Italy): Architectonical survey and petrographic characterization of via Roma. In *Global Heritage Stone: Towards International*; Pereira, D., Marker, B.R., Kramar, S., Cooper, B.J., Schouenborg, B.E., Eds.; Special Publications; The Geological Society of London: London, UK, 2015; Volume 407, pp. 201–218.

Borghgi, A., Cadoppi, P. & Dino, G. (2016). The Dora-Maira Unit (Italian Cottian Alps): a reservoir of ornamental stones locally and worldwide employed since Roman age. *Geoscience Canada*, 43(1), 13–30. doi:10.12789/geocanj.2016.43.084

Boriani, A., Burlini, L., Caironi, V., Giobbi Origoni, E., Sassi, A. & Sesana, E. (1988). Geological and petrological studies on the hercynian plutonism of the Serie dei Laghi-geological maps. The Verbano Cusio Ossola province: A land of quarries in northern Italy (Piedmont) of its occurrence between Valsesia and Lago Maggiore (N-Italy). *Rend. Soc. It. Mineral. Petrol.*, 43, 367–384.

Burri, M., Alliman, M., Chessex, R., Dal Piaz, G.V., Della Valle, G., Du Bois, L., Gouffon, Y., Guermani, A., Hagen, T., Krummenacher, D. & Looser, M.O. (1998). Feuille 1346 Chanrion, avec partie nord de la feuille 1366 Mont Vélan. *Atlas géol. Suisse 1:25.000*, Serv. hydrol. géol. national, Berne.

Bussy, F. & Cadoppi, P. (1996). U–Pb zircon dating of granitoids from the Dora-Maira massif (western Italian Alps): *Schweizerische Mineralogische Petrographische Mitteilungen*, v. 76, p. 217–233.

Caby, R. (1981). Le Mésozoïque de la zone du Combin en val d'Aosta (Alpes graïes): Imbrications tectoniques entre séries issues des domaines pennique, austroalpin et océanique. *Geol. Alpine*, 57, 5-13.

Cadoppi, P. (1990). *Geologia del basamento cristallino nel settore settentrionale del Massiccio Dora-Maira (Alpi Occidentali)*: Unpublished PhD thesis, University of Turin, Italy, 208 p.

- Cagnini A., Fratini F., Lorenzi P., Pasolini S., Porcinai S. (2013). *Periodico di Mineralogia*, 82, 3, 381-391. doi: 10.2451/2013PM0022.
- Campanino, F. & Ricci, B. (1991). Il Calcare di Gassino. Retrospectiva bibliografica e problemi aperti. *Boll. Museo Regionale Scienze Naturali*, Suppl, 9, 57–81.
- Cannic, S., Lardeaux, J.M., Mugnier, J.L. & Hernandez, J. (1996). Tectono-metamorphic evolution of the Roignais-Versoyen Unit (Valaisan domain, France), *Eclogae Geologicae Helvetiae*, 89, 321–43.
- Cantù M., Giacometti F., A. G. Landi, Riccardi M.P., Tarantino S. C. , Grimoldi A. (2015). Characterization of XVIIIth century earthen mortars from Cremona (Northern Italy): Insights on a manufacturing tradition, *Materials Characterization*, Volume 103, 81-89. doi:10.1016/j.matchar.2015.03.018.
- Caron, J. M. (1971). Contribution à l'étude lithostratigraphique et structurale de la région de Sestrière (Alpes Cottiennes, Italie). *Trav. Lab. Géol. Grenoble*, 21, 45–68.
- Carraro, F., Dal Piaz, G. V., Franceschetti, B., Malaroda, R., Sturani, C. & Zanella, E. (1970). Carta geologica del Massiccio dell'Argentera alla scala 1:50.000 e note illustrative. *Mem. Soc. Geol. It*, 9, 557–663.
- Catella M. (1969). Marmi Piemontesi. *Cronache economiche CCIAA*, 33(4), 51-64.
- Cavallo, A., Bigioggero, B., Colombo, A., & Tunesi, A. (2004a). The Beola: A dimension stone from the Ossola Valley (NW Italy). *Periodico di Mineralogia*, 73, 85–97.

Cavallo, A., Bigioggero, B., Colombo, A. & Tunesi, A. (2004b). The Verbano Cusio Ossola province: A land of quarries in northern Italy (Piedmont). *Periodico di Mineralogia*, 73, 197–210.

Cavallo, A., Dino, G. & Primavori, P. (2019). Gneisses (Serizzo and Beola) of the Verbano-Cusio-Ossola district (Piedmont, Northern Italy): possible candidates for the designation as a Global Heritage Stone Province. Geological Society of London, Special Publication, 486, SP486–2018-8.

Cimmino, F., Faccini, F. & Robbiano, A. (2004). Stone and coloured marbles of Liguria in historical monuments. *Periodico di mineralogia*, 73, 71-84.

Compagnoni, R., Hirajima, T., and Chopin, C. (1995). Ultra-high-pressure metamorphic rocks in the Western Alps. In R.G. Coleman and X. Wang, Eds., *Ultrahigh pressure metamorphism*, Cambridge University Press, 206–243.

Compagnoni, R., Ferrando, S., Lombardo, B., Radulesco N. & Rubatto, D. (2010). Paleo-European crust of the Italian Western Alps: Geological history of the Argentera Massif and comparison with Mont Blanc-Aiguilles Rouges and Maures-Tanneron Massifs. *Journal of the Virtual Explorer*, 36(3), 1–25. doi:10.3809/jvirtex.2010.00228

Cortesogno, L. & Haccard, D. (1984). Note illustrative alla carta geologica della zona Sestri-Voltaggio. *Mem. Soc. Geol. It*, 28, 115–150.

Cossio, R. & Borghi, A. (1998). Petromap: MS-dos software package for quantitative processing of X-ray maps of zoned minerals. *Computers and Geosciences*, 24, 805-814.

Cossio, R., Borghi, A. & Ruffini, R. (2002). Quantitative modal determination of geological samples based on X-ray multielemental map acquisition. *Microsc. Microanal.* 8, 139–149. doi:10.1017/S1431927601020062

Cottino T. (1999). *La piazzaforte di Fenestrelle*, Roberto Chiaramente Ed.

Craig, H. (1957). Isotopic standards for carbon and oxygen and correction factor for mass-spectrometric analysis of carbon dioxide. *Geochim. Cosmochim. Acta*, 12, 133–149.

Dal Piaz, G.V. (1999). The Austroalpine-Piedmont nappe stack and the puzzle of Alpine Tethys, in G. Gosso et al., eds, *Third Meeting on Alpine Geological Studies: Memorie di Scienze Geologiche*, 51, 155-176.

Dal Piaz, G. V., Bistacchi, A. & Massironi, M. (2003). Geological outline of the Alps. *Episodes*, 26(3), 175–180. doi:10.18814/epiiugs/2003/v26i3/004

Dal Piaz, G.V., Gianotti, F., Monopoli, B., Pennacchioni, G., Tartarotti, P., Schiavo, A. (2010). Foglio 091 Chatillon e note illustrative. *Carta Geologica d'Italia alla scala 1:50.000*, APAT, 152 pp.

De Giusti, F., Dal Piaz, G.V., Massironi, M. & Schiavo, A. (2004). Carta geotettonica della Valle d'Aosta. *Mem. Sci. Geol.*, 55, pp. 129-149.

Dematteis, L. (1985). *Case contadine nelle Valli dell'Ossola, Cusio e Verbano*. *Quaderni di cultura alpina*, 12, 127 pp., Priuli & Verlucca Editrice, Ivrea.

Derrick M.R., Stulik D., Landry J.M., 1999 – *Infrared Spectroscopy in Conservation Science*. The Getty Conservation Institute, Los Angeles CA.

Deville, E., Fudral, S., Lagabriele, Y., Marthaler, M. & Sartori, M. (1992). From oceanic closure to continental collision: A synthesis of the "schistes lustrés" metamorphic complex of the Western Alps. *Geological Society of America Bulletin*, 104(2), 127–139. doi:10.1130/0016-7606(1992)104<0127:FOCTCC>2.3.CO;2

Dewey, J. F., Pitman, W. C., Ryan, W. B. F. & Bonnin, J. (1973). Plate tectonics and the evolution of the Alpine system. *Geological Society of America Bulletin*, 84(10), 3137–3180. doi:10.1130/0016-7606(1973)84<3137:PTATEO>2.0.CO;2

Di Pierro, S. & Fiora, L. (1998). Caratterizzazione petrografica della oficalcite "Verde Cesana" e di potenziali rocce oficarbonatiche sostitutive. In: "Le Scienze della Terra e l'Archeometria", Bari, 19 e 20 febbraio 1998, Patron Editore, Bologna, 99-108.

Dino, G.A. (2004). La gestione degli scarti dell'industria dei lapidei. Tesi di Dottorato di ricerca in Geoingegneria Ambientale. Politecnico di Torino

Dino, G. A. & Cavallo, A. (2014). Ornamental stones of the Verbano Cusio Ossola quarry district: Characterization of materials, quarrying techniques and history and relevance to local and national heritage. *Geological Society of London, Special Publication*, 407, 407–415.

Dino, G.A., Borghi, A., Castelli, D., Canali, F., Corbetta, E. & Cooper, B. (2019). The Candoglia Marble and the "Veneranda Fabbrica del Duomo di Milano": A Renowned Georesource to Be Potentially Designed as Global Heritage Stone. *Sustainability*, 11, 4725; doi:10.3390/su11174725

Elter, G. (1971). Schistes Lustrés et ophiolites de la zone piémontaise entre Orco et Doire Baltée (Alpes Graies). Hypothèses sur l'origine des ophiolites. *Géol. Alpine*, Grenoble, 47, 147–169.

Elter, G. (1972). Contribution à la connaissance de briançonnais interne et de la bordure piémontaise dans les Alpes Graies nord-orientales. *Memorie Istituto di Geologia e Mineralogia, Università di Padova*, 28.

Elter, G. & Elter, P. (1965). Carta geologica della regione del Piccolo S. Bernardo (versante italiano): note illustrative. *Memorie Istituto Geologico Mineralogico Università di Padova*, 25, 1–53.

Ernst, W. & Dal Piaz, G. (1978). Mineral parageneses of eclogitic rocks and related mafic schists of the Piemonte ophiolite nappe, Breuil-St. Jacques area, Italian Western Alps. *American Mineralogist*, 63, 621–640.

Fantoni R. (2005). Gli studi di Pietro Calderini sulla geologia del Monte Fenera. Il contributo dei ricercatori locali nell'Ottocento valsesiano. estratto da Fantoni R., Cerri R. & Dellarole E. (2005) –D'acqua e di pietra. Il Monte Fenera e le sue collezioni museali, 44-52.

Fiora, L. (2009). Le varietà dei marmi bianchi italiani. *L'Informatore del Marmista*, 573, 80-92.

Fiora, L. & Audagnotti, S. (2001). Il Marmo di Chianocco e Foresto: caratterizzazione minero-petrografica ed utilizzi, *in* Martini, M., *ed.*, Atti 1° congresso nazionale di archeometria: Verona, 2–4 dicembre 1999, Patron Editore, p. 235–246.

Fiora L., Borghi A., Canalis T.R. & Sandrone R. (2006). I materiali lapidei del Forte di Fenestrelle (Val Chisone, Piemonte). In: G.M. Crisci, C. Gattuso (eds) "Archeometria del costruito", Edipuglia Bari, 147- 155.

Fiora, L. & Gambelli, E. (2006). Le principali pietre da costruzione e da ornamento in Valle Susa (Piemonte). *Restauro Archeologico*, 1, 18-20.

Fratini, F., Mattone, M., Rescic, S. (2018). Il restauro delle superfici di Palazzo Madama a Torino: Metodi ed esiti. In *Intervenire Sulle Superfici dell'Architettura tra Bilanci e Prospettive; Ricerche*, A., Ed.; Scienza e Beni Culturali: Bressanone, Italy, 2018; pp. 109–119.

G.A.L. Mongioie. (2005). *Marmi e pietre del Cebano Monregalese. Litotipi del territorio del G.A.L. (Gruppo di Azione Locale) Mongioie*. 256 pp.

Gambino F., Borghi A., d'Atri A., Gallo L.M., Ghiraldi L., Giardino M., Martire L., Palomba M. Perotti L. & Macadam, J. (2017). TOURinSTONES: a Free Mobile Application for Promoting Geological Heritage in the City of Torino (NW Italy). *Geoheritage*, 11, 3-17. doi:10.1007/s12371-017-0277-5

Gambino, F., Borghi, A., d'Atri, A., Martire, L., Cavallo, M., Appolonia, L. & Croveri, P. (2019). *Minero-Petrographic Characterization of Chianocco Marble Employed for Palazzo Madama Façade in Turin (Northwest Italy)*. *Sustainability*, 11(15), 4229.

Gambino M. (2004). *LA SACRA DI SAN MICHELE: Caratterizzazione petrografica e rilievo architettonico*. Master Thesis, University of Turin, Earth Sciences Department.

Gasco, I. & Gattiglio, M. (2011). Geological map of the middle Orco Valley, Western Italian Alps. *Journal of Maps*, 7, 463-477.

Gasco, I., Gattiglio, M. & Borghi, A. (2011). New insight on the lithostratigraphic setting and on tectono-metamorphic evolution of the Dora Maira vs Piedmont Zone boundary (middle Susa Valley). *Journal of Earth Sciences*, 100, 1065–1085.

Gorgoni, C.; Lazzarini, L.; Pallante, P.; Turi, B. An updated and detailed minero-petrographic and C–O stable isotopic reference database for the main Mediterranean marbles used in antiquity (2002). In *ASMOSIA 5: Interdisciplinary Studies on Ancient Stone, Proceedings of the Fifth International Conference of the Association for the Study of Marble and Other Stones in Antiquity*, Museum of Fine Arts, Boston, MA, USA, 11-15/06/ 1998; Herrmann, J.J., Herz, N., Newman, R., Eds.; Archetype: London; 115–131.

Govi, M. (1975). *Carta del Ricoprimento Gran San Bernardo tra il Paramont ed il Vallone di Vertosan (Alta Valle d’Aosta) al 1:30.000*. Litografia Artistica Cartografica, Firenze.

Guidotti, C.V. (1984). Micas in metamorphic rocks. *Micas*, pp. 357-467.

Handy, M. R., Schmid, S. M., Bousquet, R., Kissling, E., & Bernoulli, D. (2010). Reconciling plate-tectonic reconstructions of Alpine Tethys with the geological–geophysical record of spreading and subduction in the Alps. *Earth-Science Reviews*, 102(3–4), 121–158. doi:10.1016/j.earscirev.2010.06.002

Hawthorne, F. C., Oberti, R., Harlow, G. E., Maresch, W. V., Martin, R. F., Schumacher, J. C., Welch, M. D. (2012). Nomenclature of the amphibole supergroup. *American Mineralogist*, 97, 2031–2048.

Hey, M.H. (1954). A new review of chlorites. *Mineralogical Magazine*, 30, 277-292.

Hugo, R.C., Bernsen, S., Breen, K. & Ruzicka, A. (2015). Phase Analysis of Large EDS Datasets with Matlab. *Microsc. Microanal.*, 21 (Suppl 3), 2023-2024, doi:10.1017/S1431927615010892.

Ingham J. P. (2013). *Geomaterials Under the Microscope*, Academic Press. Elsevier, 137–159, Frome, UK, ISBN 9780124072305, doi:10.1016/B978-0-12-407230-5.50021-2.

Karkanias P. (2007). Identification of lime plaster in prehistory using petrographic methods: A review and reconsideration of the data on the basis of experimental and case studies, *Geoarchaeology*, Volume 22, Issue 7, 775-796. doi:10.1002/gea.20186.

Lagabrielle, Y., Polino, R., Auzende, J. M., Blanchet, R., Caby, R., Fudral, S., Lemoine, M., Mevel, C., Ohnestetter, M., Robert, D. & Tricart, P. (1984). Les témoins d'une tectonique intraocéanique dans le domaine téthysien: analyse du rapport entre les ophiolites et leur couvertures métasédimentaires dans la zone piémontaise des Alpes franco-italiennes. *Ofioliti*, 9, 67–88.

Lanari, P., Vidal, O., De Andrade, V., Dubacq, B., Lewin, E., Grosch, E. G. & Schwartz, S. (2014). XMapTools: A MATLAB©-based program for electron

microprobe X-ray image processing and geothermobarometry. *Computers & Geosciences*, 62, 227–240.

Lazzarini, L. (2004). Archaeometric aspects of white and coloured marbles used in antiquity: The state of the art. *Periodico di Mineralogia*, 73, 113–125.

Lezzerini, M., Ramacciotti, M., Cantini, F. *et al.* (2017). Archaeometric study of natural hydraulic mortars: the case of the Late Roman Villa dell'Oratorio (Florence, Italy). *Archaeol Anthropol Sci* 9, 603–615. doi:10.1007/s12520-016-0404-2

Lezzerini M., Raneri S., Pagnotta S., Columbu S., Gallelo G. (2018). Archaeometric study of mortars from the Pisa's Cathedral Square (Italy), *Measurement*, Volume 126, 322-331. doi:10.1016/j.measurement.2018.05.057.

Loprieno, A., Bousquet, R., Bucher, S., Ceriani, S., Dalla Torre, F. H., Fugenschuh, B. & SCHMID S. M. (2011). The Valais units in Savoy (France): a key area for understanding the palaeogeography and the tectonic evolution of the Western Alps. *International Journal of Earth Sciences*, 100, 963-92.

Malaroda R. (2000). Il Flysch di Demonte-Aisone e il sondaggio di Aisone. *Acc. Sci. Torino, Atti Sc. Fis.*, 24, 111-142.

Malusà, M. G., Polino, R. & Martin, S. (2005). The Gran San Bernardo nappe in the Aosta valley (western Alps): A composite stack of distinct continental crust units. *Bulletin de la Société Géologique de France*, 176(5), 417–431. doi: 10.2113/176.5.417

Marengo, A., Borghi, A., Bittarello, E. & Costa E. (2019). Touristic fruition of the disused quarry of Busca Onix: problematics and strategies. *Geoheritage*, 11, 47-54.

Mariani E. (1976). *I Leganti idraulici*, Casa E. Ambrosiana Milano.

Marthaler, M. & Stampfli G. M. (1989). Les schistes lustrées a ophiolites de la nappe du Satè: an ancien prisme d'accrétion issue de la merge active apulienne. *Schweizerische Mineralogische und Petrographische Mitteilungen*, 69, 211-16.

Martin, S., Tartarotti, P. & Dal Piaz, G. V. (1994). The Mesozoic ophiolites of the Alps: A review. *Boll. Geof. Teor. Appl*, 36, 175–216.

Matthews, K.J. (1997). The establishment of a data base of neutron activation analyses of white marble. *Archaeometry*, 39, 321–332.

Mazzucchelli, M., Quick, J. E., Sinigoi, S., Zanetti, A. & Giovanardi, T. (2014). Igneous evolutions across the Ivrea crustal section: The Permian Sesia Magmatic System and the Triassic Finero intrusion and mantle. *GFT-Geological Field Trips*, 6(2.2), 1–98. doi:10.3301/GFT.2014

McCrea, J. (1950). On the isotopic chemistry of carbonates and a paleotemperature scale. *J. Chem. Phys.*, 18, 849–857.

Miriello D., Barca D., Bloise A., Ciarallo A., Crisci G. M., De Rose T., Gattuso C., Gazineo F., La Russa M. F. (2010). Characterisation of archaeological mortars from Pompeii (Campania, Italy) and identification of construction phases by compositional data analysis, *Journal of Archaeological Science*, Volume 37, Issue 9, 2207-2223. doi:10.1016/j.jas.2010.03.019

Montanari, L. (1969). Aspetti geologici del Lias di Gozzano (Lago d'Orta). Memorie della Società Italiana di Scienze Naturali e del Museo Civico di Storia Naturale di Milano, 18, 25-92.

Morimoto, N. (1988). Nomenclature of Pyroxenes. *Mineralogy and Petrology*, 73, 1123-1133.

Moropoulou A., Theoulakis P., Chrysophakis T. (1995). Correlation between stone weathering and environmental factors in marine atmosphere. *Atmospheric Environment*, Volume 29, Issue 8, 895-903. doi:10.1016/1352-2310(94)00322-C.

Moropoulou A., Bakolas A., Bisbikou H. (2000). Investigation of the technology of historic mortars. *Journal of Cultural Heritage*, Volume 1, Issue 1, 45-58. doi:10.1016/S1296-2074(99)00118-1.

NORMA UNI EN 10924:2001, Malte per elementi costruttivi e decorativi: classificazione e terminologia, Milano, febbraio 2001. Ed. UNI (Ente Nazionale Italiano Unificazione) Milano

NORMA UNI EN 13925-1:2006, Prove non distruttive – Diffrazione a raggi X dai materiali policristallini e amorfi – Parte 1: Principi generali. Ed. UNI (Ente Nazionale Italiano Unificazione) Milano

NORMA UNI EN 13925-2:2006, Prove non distruttive – Diffrazione a raggi X dai materiali policristallini e amorfi – Parte 2: Procedure. Ed. UNI (Ente Nazionale Italiano Unificazione) Milano

NORMA UNI EN 13925-3:2006, Prove non distruttive – Diffrazione a raggi X dai materiali policristallini e amorfi – Parte 3: Strumenti. Ed. UNI (Ente Nazionale Italiano Unificazione) Milano

NORMA UNI 11176:2006, Descrizione petrografica di una malta. Ed. UNI (Ente Nazionale Italiano Unificazione) Milano

NORMA UNI EN 11305:2009 – Malte storiche. Linee guida per la caratterizzazione mineralogico petrografica, fisica e chimica delle malte. Ed. UNI (Ente Nazionale Italiano Unificazione) Milano

Ortolano, G., Zappalà, L. & Mazzoleni, P. (2014). X-Ray Map Analyser: A new ArcGIS based tool for the quantitative statistical data handling of X-ray maps (Geo- and material-science applications). *Computers and Geosciences*, 72, 49-64.

Ortolano, G., Visalli, R., Godard, G. & Cirrincione, R. (2018). Quantitative X-ray Analyser (Q-XRMA): A new GIS-based statistical approach to Mineral Image Analysis. *Computers and Geosciences*, 115, 56-65.

Parish, C.M. & Brewer, L.N. (2010). Multivariate statistics applications in phase analysis of STEM-EDS spectrum images. *Ultramicroscopy*, 110, 134-143.

Pecchioni, E., Fratini, F. & Cantisani, E. (2018). *Le malte antiche e moderne tra tradizione ed innovazione*. Pàtron Editore, Seconda Edizione, Bologna, 231 pp, ISBN: 978-88-555-3414-7.

Pedeli, C. (2009). L'Area del teatro romano di Aosta: le attuali condizioni e le prime misure conservative. Regione Autonoma Valle d'Aosta, Bollettino n. 6, 242-248.

Pereira D. and Marker B. (2016). "The Value of Original Natural Stone in the Context of Architectural Heritage" *Geosciences* 6, 1: 13. doi:10.3390/geosciences6010013

Pereira, D. and Pratt, B.R. (2016). Heritage Stones of the world. *Geosci. Can.*, 43, 3–4.

Perin, A. (2016). Cavare e lavorare la pietra in Monferrato. Lapidici e cave a Villadeati. *Monferrato Arte e Storia*, 28, 5-62.

Petrakakis, K. & Dietrich, H. (1985). MINSORT: A program for the processing and archivation of microprobe analyses of silicate and oxide minerals. *Neues Jahrb. Mineral. Monatshefte*, 8, 379–384.

Piana, F., Barale, L., Compagnoni, R., d'Atri, A., Fioraso, G., Irace, A., Mosca, P., Tallone, S., Monegato, G. & Morelli, M. (2017a). Geological map of Piemonte region at 1:250,000 scale. Explanatory Notes. *Acc. Sc. Torino, Memorie Sc. Fis.*, 41, 1–143.

Piana, F., Fioraso, G., Irace, A., Mosca, P., d'Atri, A., Barale, L., Falletti, P., Monegato, G., Morelli, M., Tallone, S. & Vigna, G. B. (2017b). Geology of Piemonte region (NW Italy, Alps-Apennines interference zone). *Journal of Maps*, 13(2), 395–405. <https://doi.org/10.1080/17445647.2017.1316218>

Pires, J. & Cruz, A.J. (2007). Techniques of thermal analysis applied to the study of cultural heritage. *J Therm Anal Calorim* 87, 411–415. <https://doi.org/10.1007/s10973-004-6775-0>

Polikreti, K. (2007). Detection of ancient marble forgery: Techniques and limitations. *Archaeometry*, 49, 603–619.

Polino, R. (1984). Les séries océaniques du haut Val de Suse (Alpes Cottiennes): analyse des couvertures sédimentaires. *Ofioliti*, 9, 547–554.

Průkryl, R. and Smith, B.J. (2007). *Building Stone Decay: From Diagnosis to Conservation*; Geological Society Special Publications: London, UK, p. 271.

Riccardi M. P., Lezzerini M., Carò F., Franzini M., Messiga B. (2007). Microtextural and microchemical studies of hydraulic ancient mortars: Two analytical approaches to understand pre-industrial technology process, *Journal of Cultural heritage*, 8, 350-360.

Rivalenti, G., Rossi, A., Siena, F. & Sinigoi, S. (1984). The layered series of the Ivrea-Verbano igneous complex, western Alps, Italy. *TMPM Tschermaks Mineralogische und Petrographische Mitteilungen*, 33(2), 77–99. <https://doi.org/10.1007/BF01083065>

Rogers P. (2014). Westminster Cathedral, *The Cathedral Magazine*, Oremus, 14-15.

Sacchi, R. (1977). Gli Scisti di Rimella tra Sesia e Toce: una re-interpretazione. *Mem. Ist. Geol. Miner. Univ. Padova*, 32, 3–20.

Sacco, F. (1907). Geologia applicata della Città di Torino. *Giornale Geol. Prat.*, 5, 121–162.

Sandrone, R., Cadoppi, P., Sacchi, R., & Vialon, P. (1993). The Dora–Maira Massif. In J. F. von Raumer & F. Neubauer (Eds.), *Pre-Mesozoic geology in the Alps* (pp. 317–325). Springer.

Sandrone, R., Alciati, L., De Rossi, A., Fiora, L., & Radicci, M.T. (2000). Estrazione, lavorazione ed impieghi della Pietra di Luserna, in Riganti, V., and Braga, G., eds., *Quarry-Laboratory–Monument International Congress Proceedings*, Pavia, 26–30 settembre 2000, v. 2, p. 41–49.

Sandrone, R., Colombo, A., Fiora, L., Fornaro, M., Lovera, E., Tunesi, A. & Cavallo, A. (2004). Contemporary natural stones from the Italian western Alps (Piedmont and Aosta Valley Regions). *Periodico di Mineralogia*, 73, 211–226.

Sartori, M. (1987). Structure de la zone du Combin entre les Diablon et Zermatt (Valais). *Eclogae Geol. Helv.*, 80, 789–814.

Sassone, P. (2005). La “Pietra da Cantoni” del Monferrato Casalese (AL): ipotesi di ripresa produttiva per la conservazione della tradizione edilizia locale. *GEAM*, 115, 67–76.

Seddio, S.M. & Carpenter, P.K. (2017). Very Large Area Phase Mapping of a Petrographic Thick Section using Multivariate Statistical Analysis of EDS Spectral Images. *Microsc. Microanal.*, 23 (Suppl 1), 1066–1067, doi:10.1017/S1431927617005992.

Schiele E. & Berens L.W. (1976). *La Calce. Calcare, calce viva, idrato di calcie*. Ed. Tecniche ET Milano.

Schulz H. W. and Denkmäler der Kunst des Mittelalters, (1860). Unteritalien, Atlas, Dresden, Wilhelm K.H. Schulz.

Studio Costruzioni Terrezza (2008). Costituenti delle murature e fasi costruttive individuate tramite osservazione diretta nei 18 casi studio nell'area della scaena e post scaenam. Relazione tecnica Studio Costruzioni Terrezza S.r.l.

Telluccini, A. (1928). Il Palazzo Madama di Torino. Lattes Editori: Turin, Italy, 1928; 168p.

Teng, C. & Gauvin, R. (2020). Multivariate Statistical Analysis on a SEM/EDS Phase Map of Rare Earth Minerals. Scanning, Article ID 2134516, 11 pages, <https://doi.org/10.1155/2020/2134516>

Timpanelli (2003). La Pietra da Cantoni del Monferrato Casalese: salvaguardia e valorizzazione di un patrimonio scientifico, storico e culturale. GEAM, 110, 17-25.

Tufani A. (1987). Le malte nel restauro. Studio, ricerche, operatività. Ed. Ediart Todi.

Von Raumer, J.F. (1987). Les massifs du Mont Blanc et des Aiguille Rouges: temoins de la deformation de croûte varisque dans les Alpes occidentales. Geologie Alpine, v. 63, pp. 7-24.

Whitney, D.L. & Evans B.W. (2010). Abbreviations for names of rock-forming minerals. American Mineralogist, 96, 185-187.

Web sites

Regione Piemonte. (2019). Cave e Miniere attive.

<https://www.regione.piemonte.it/web/temi/sviluppo/attivitaestrattive/competenze-regionali-materia-attivita-estrattive>

www.sacradisanmichele.com

<https://www.palazzomadamaTurin.it/en/node/1080>

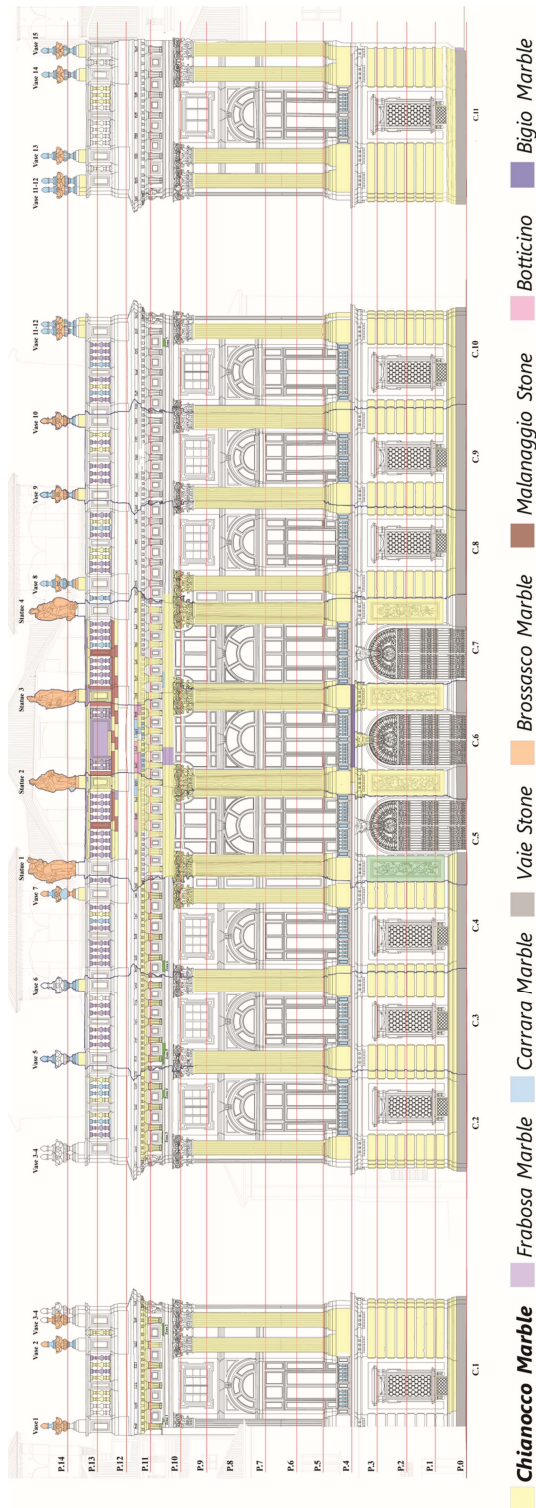
Appendix I

Geo-lithological map of ornamental stones of Piemonte region

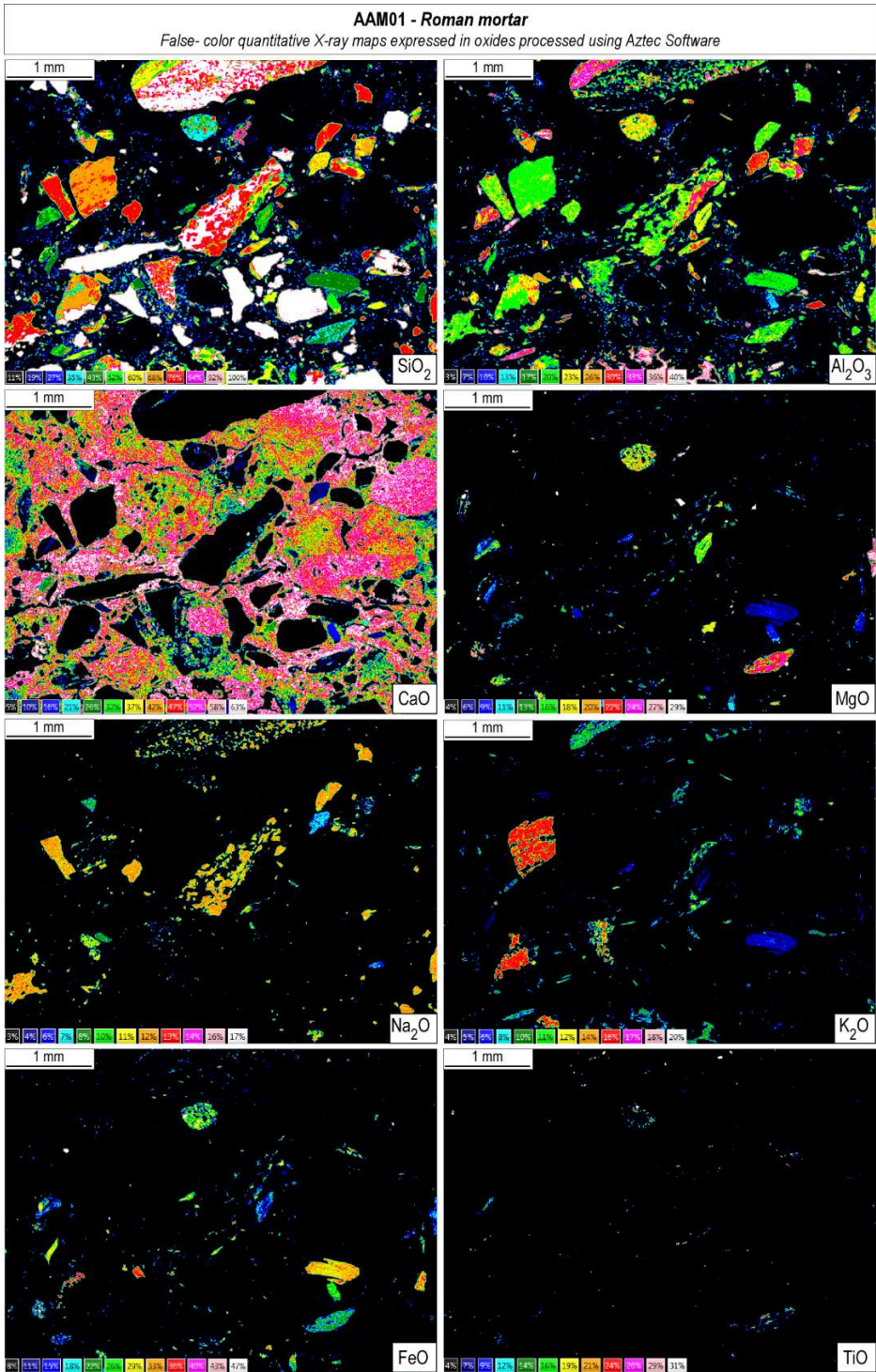
Appendix II

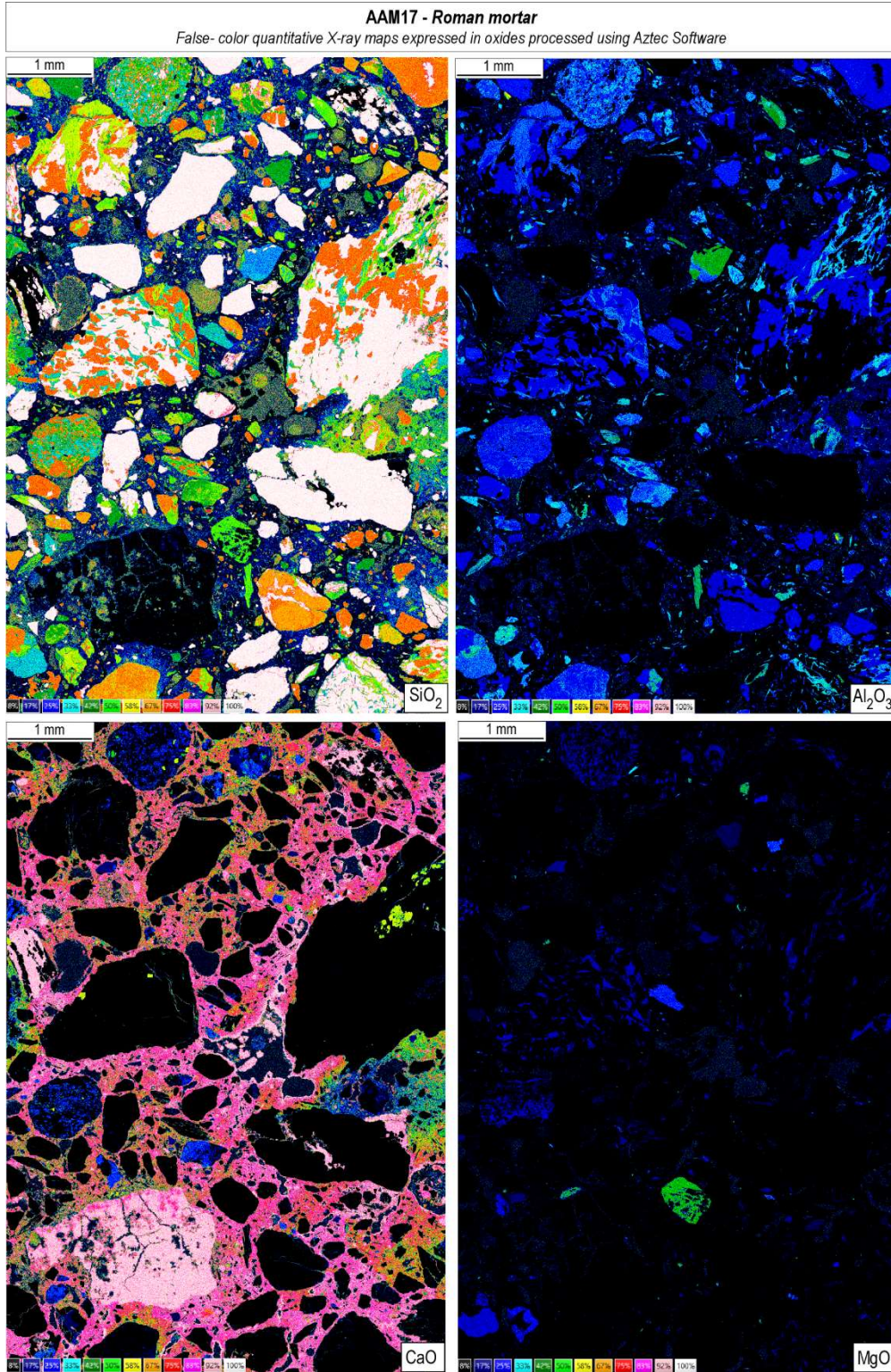
Geo-database of ornamental stones of Piemonte region

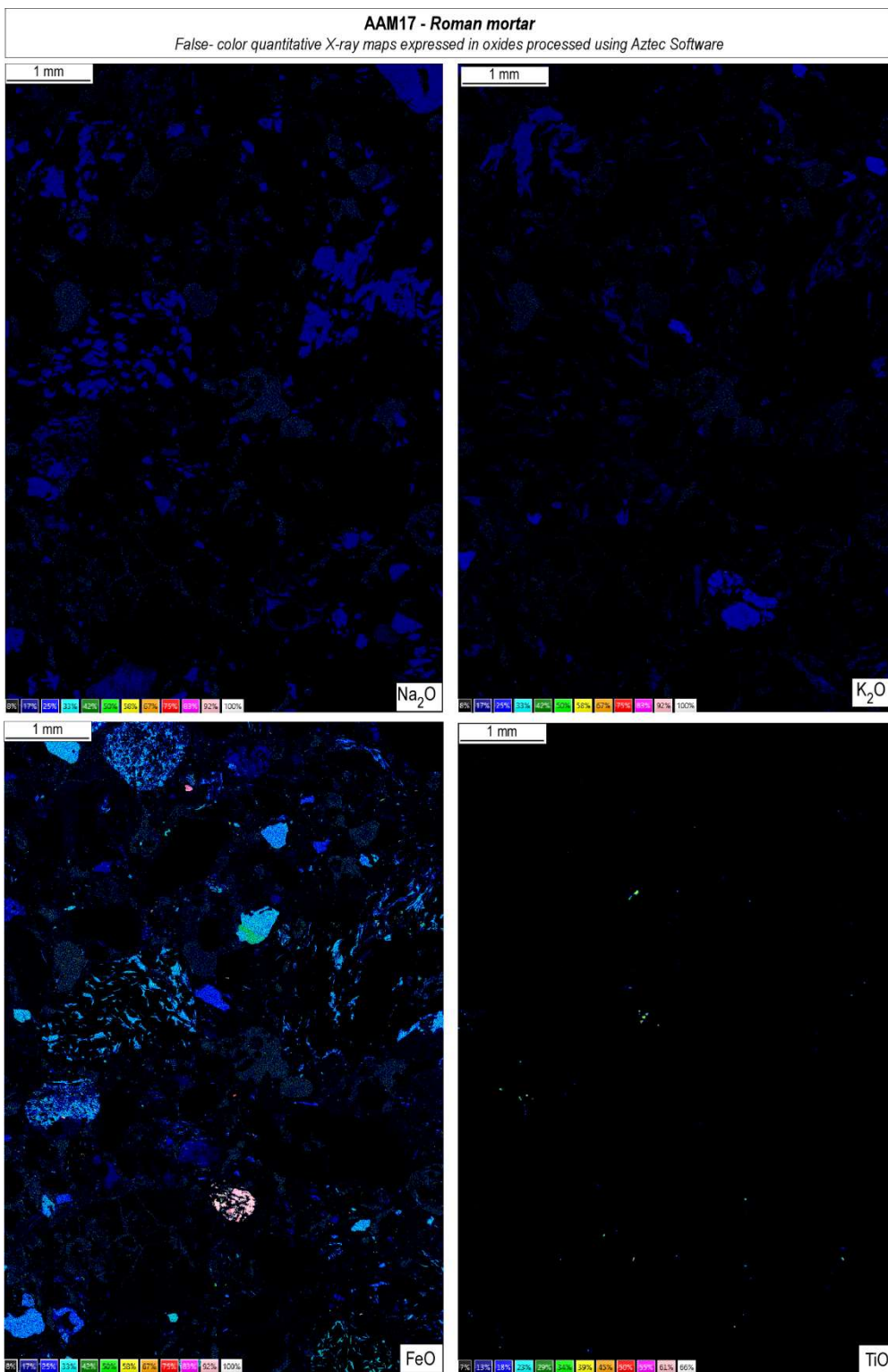
Appendix III

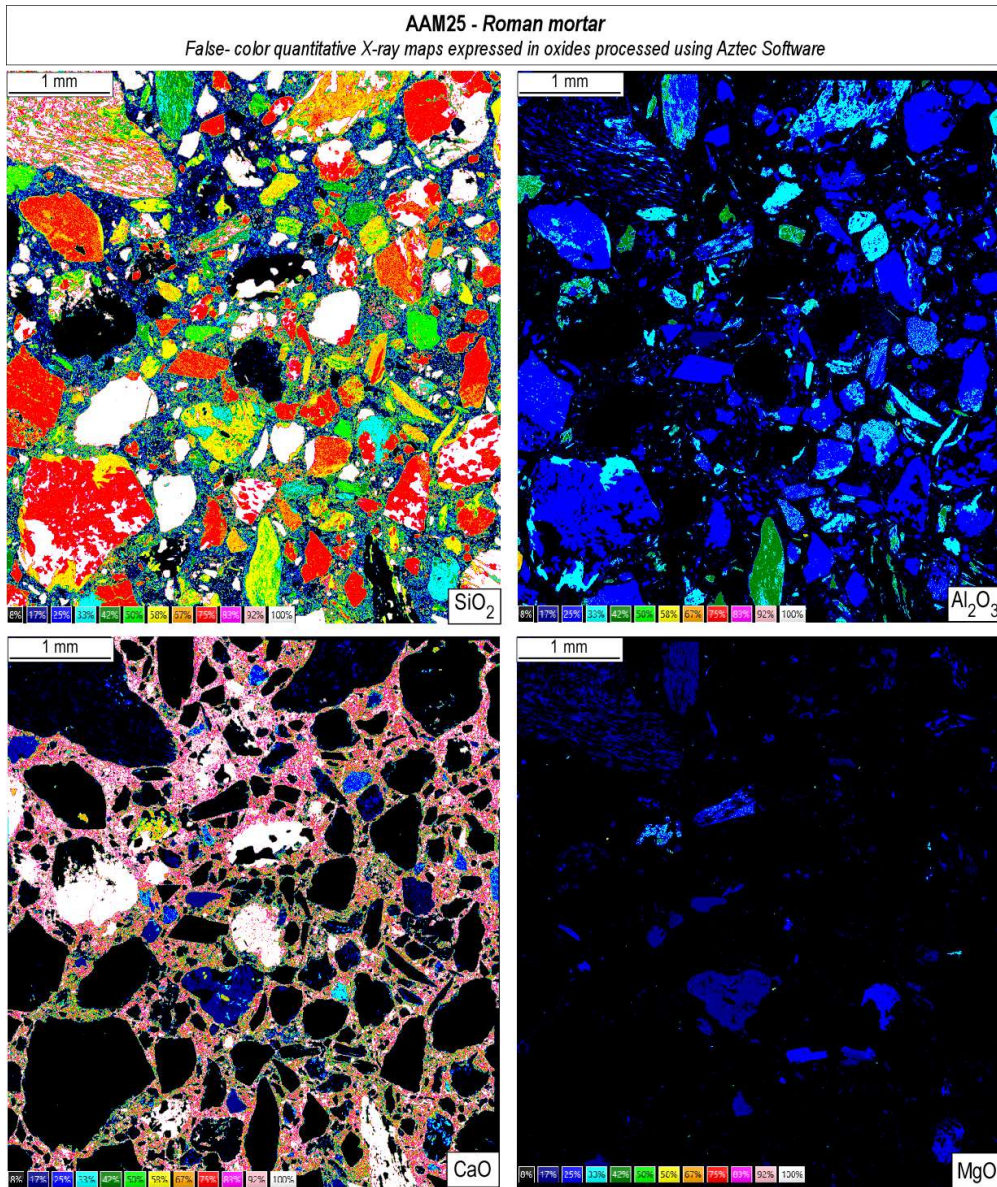


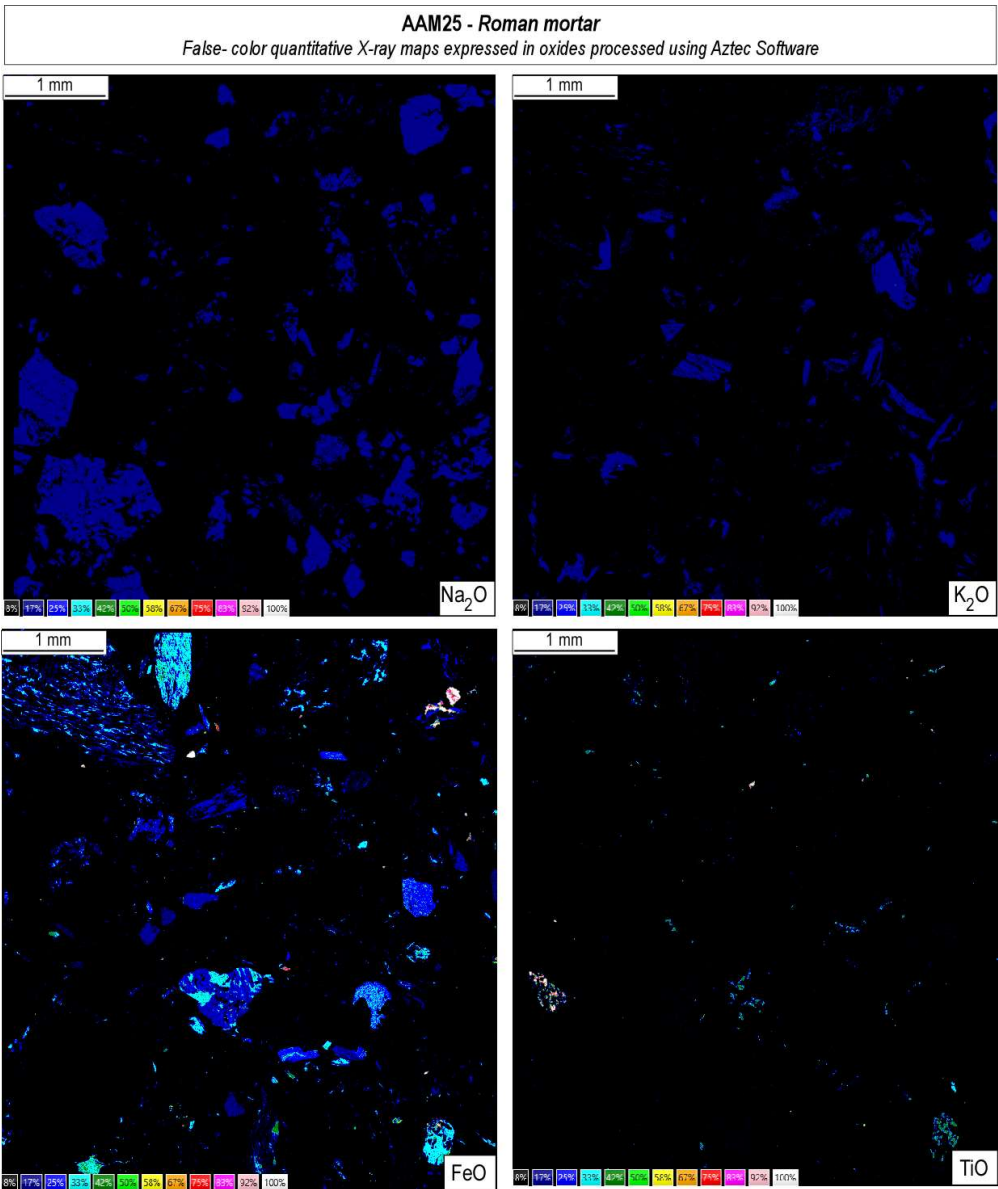
Appendix IV

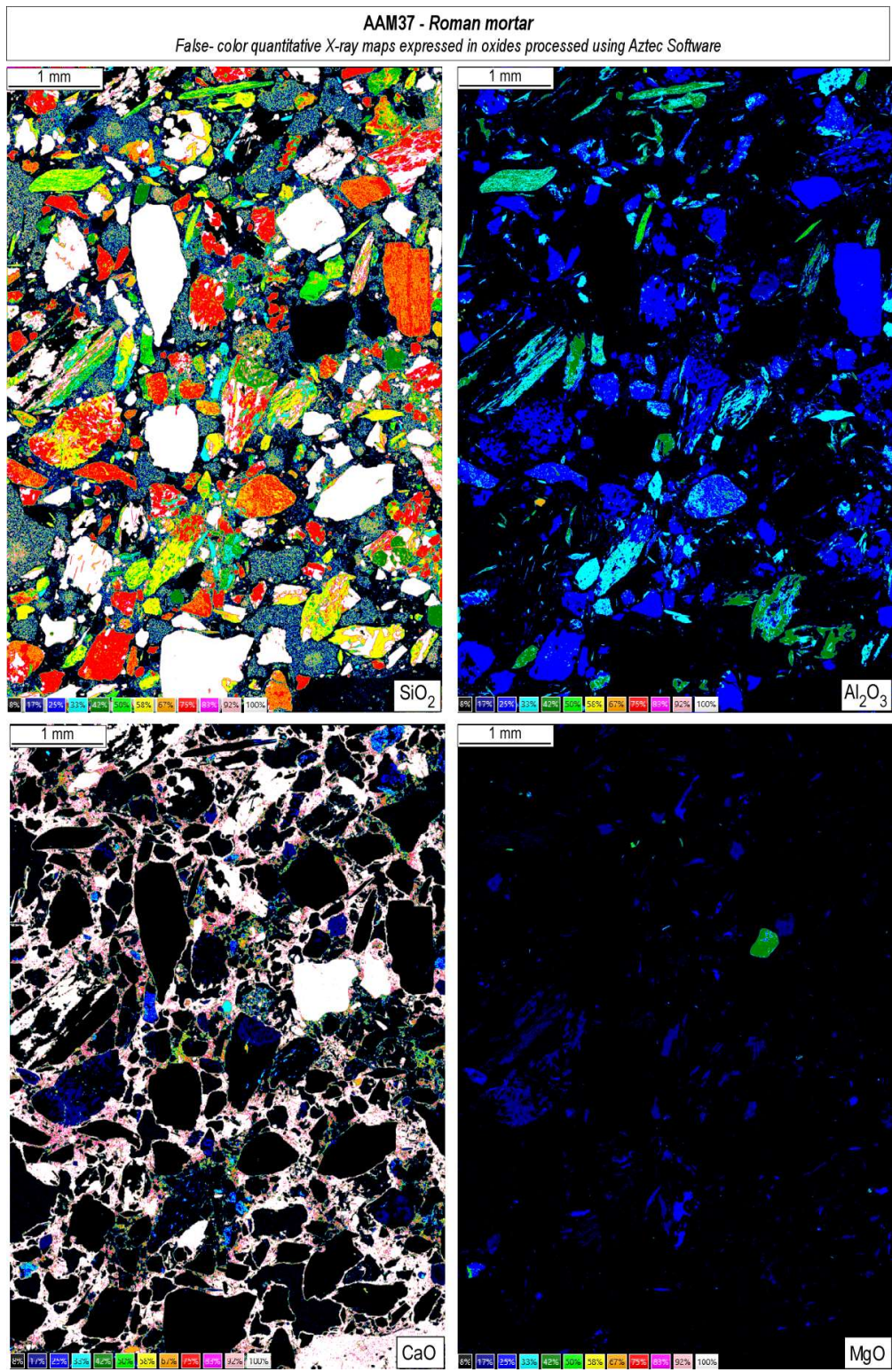


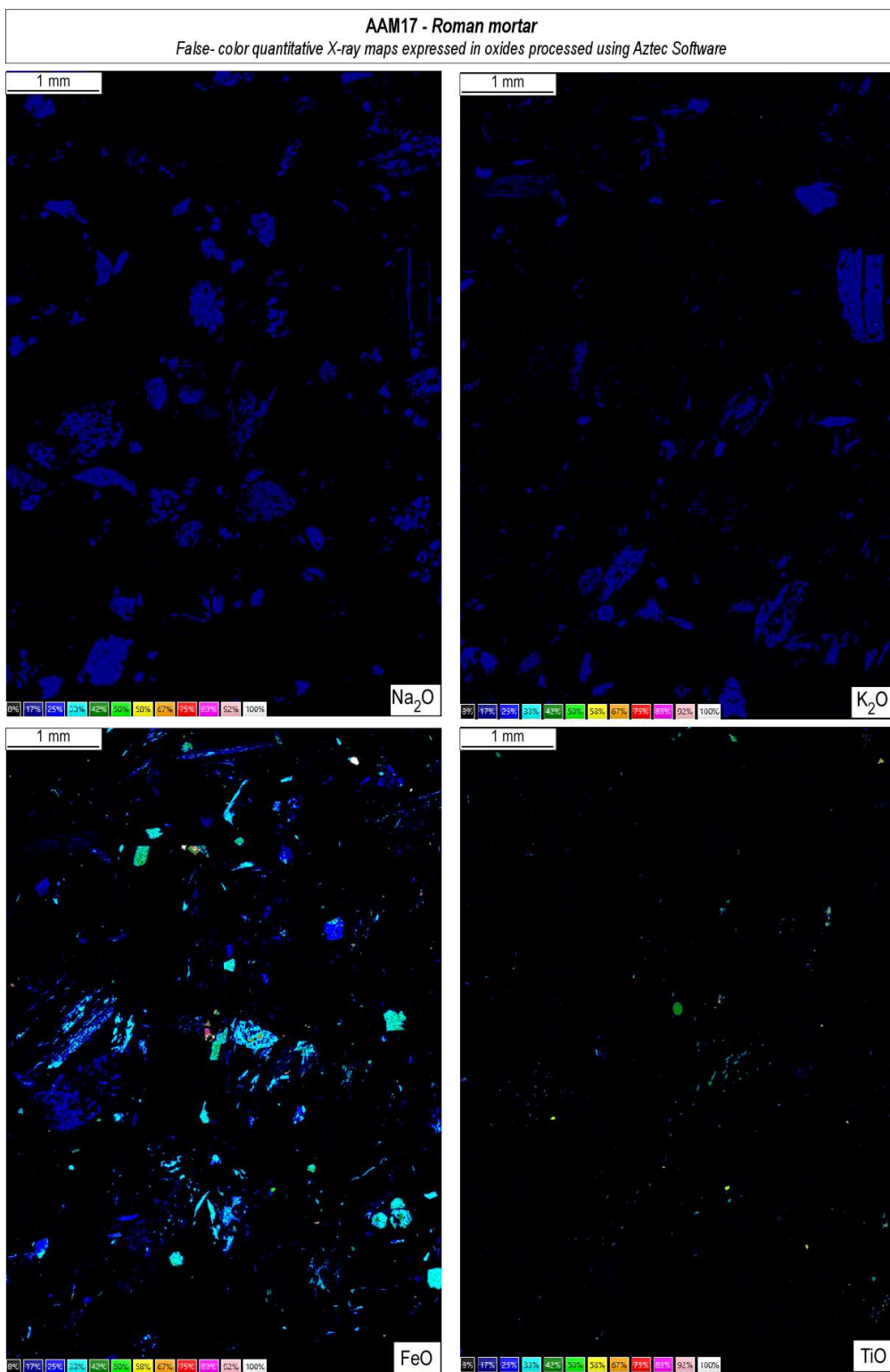


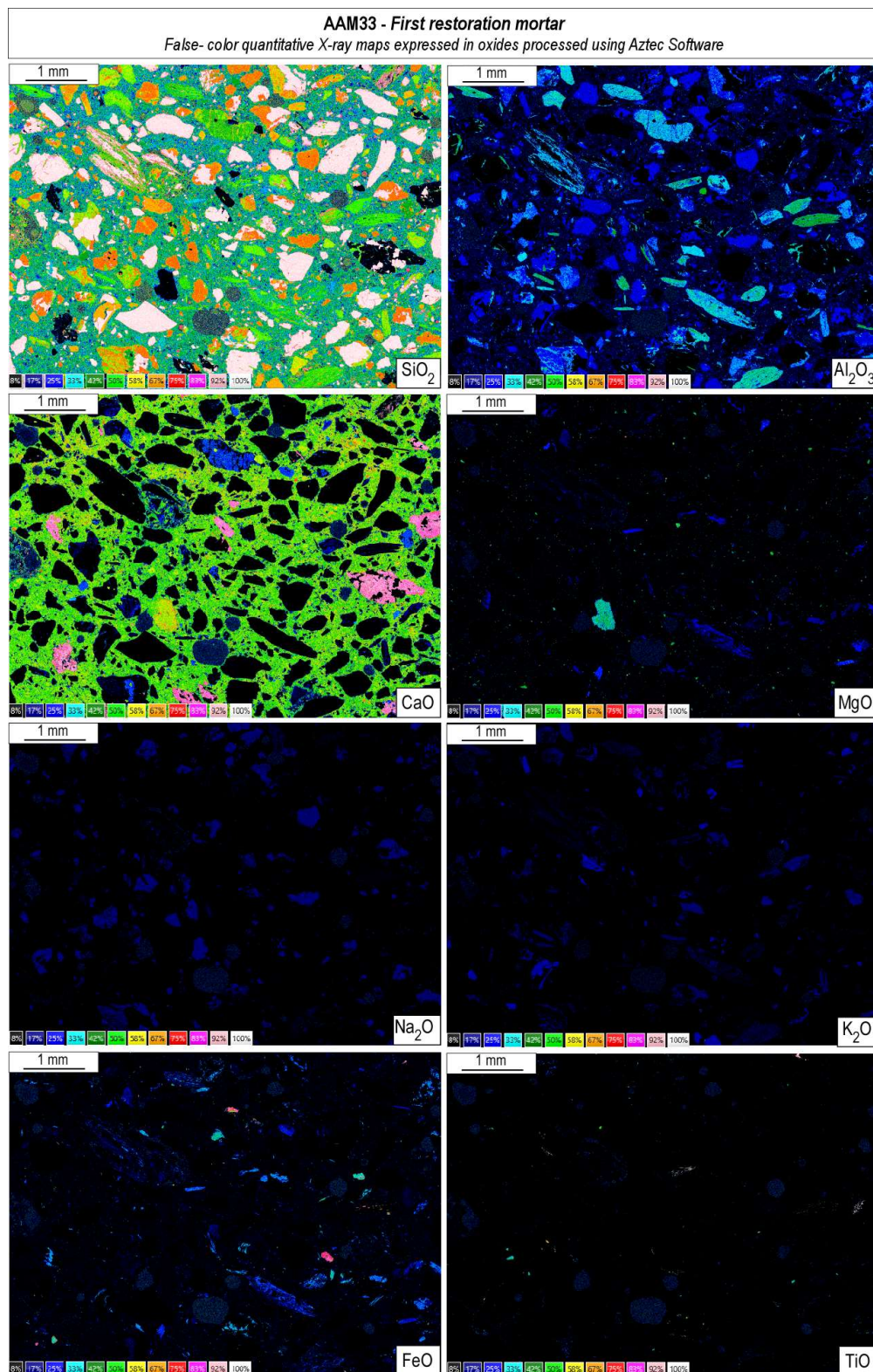


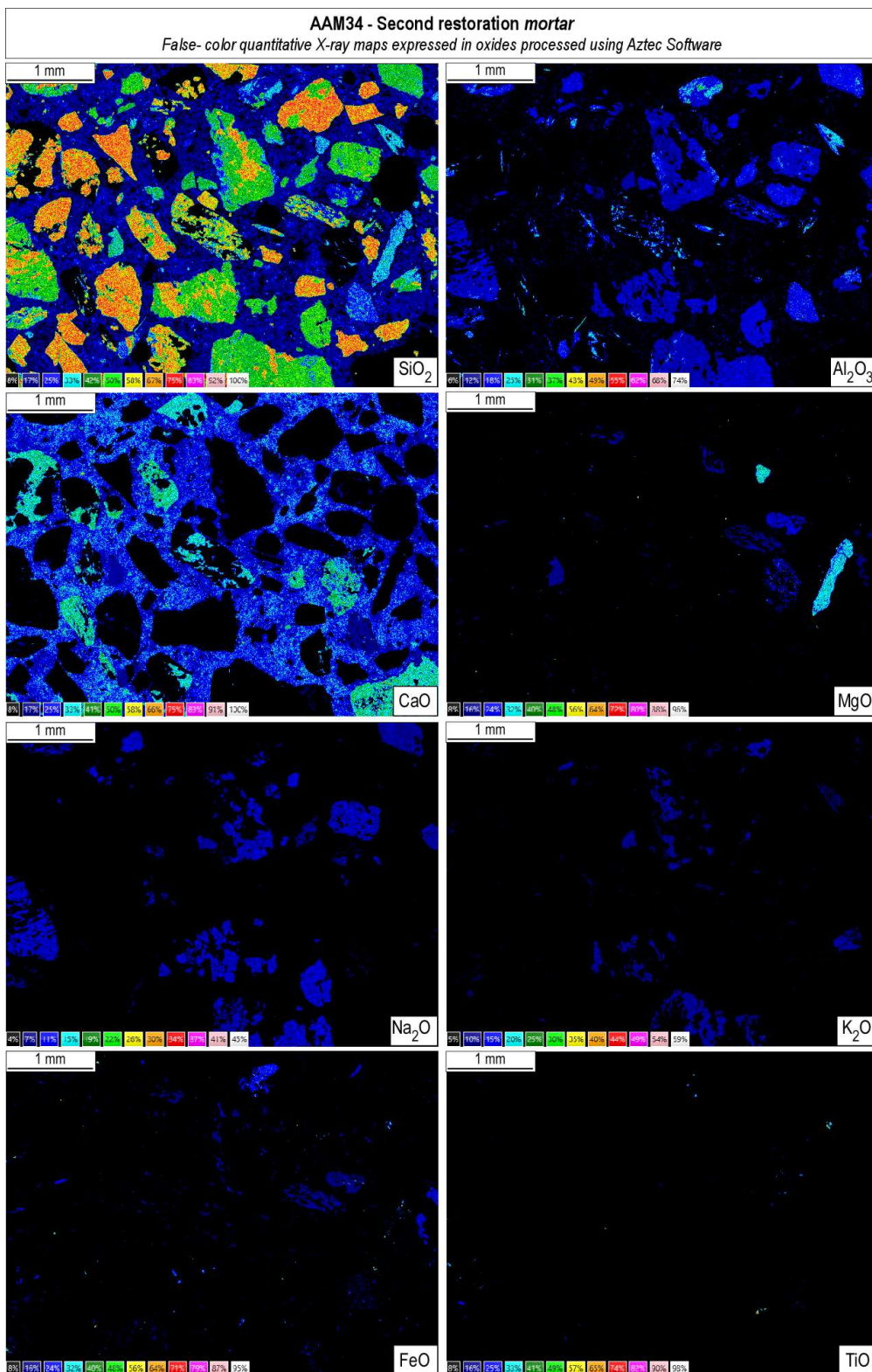


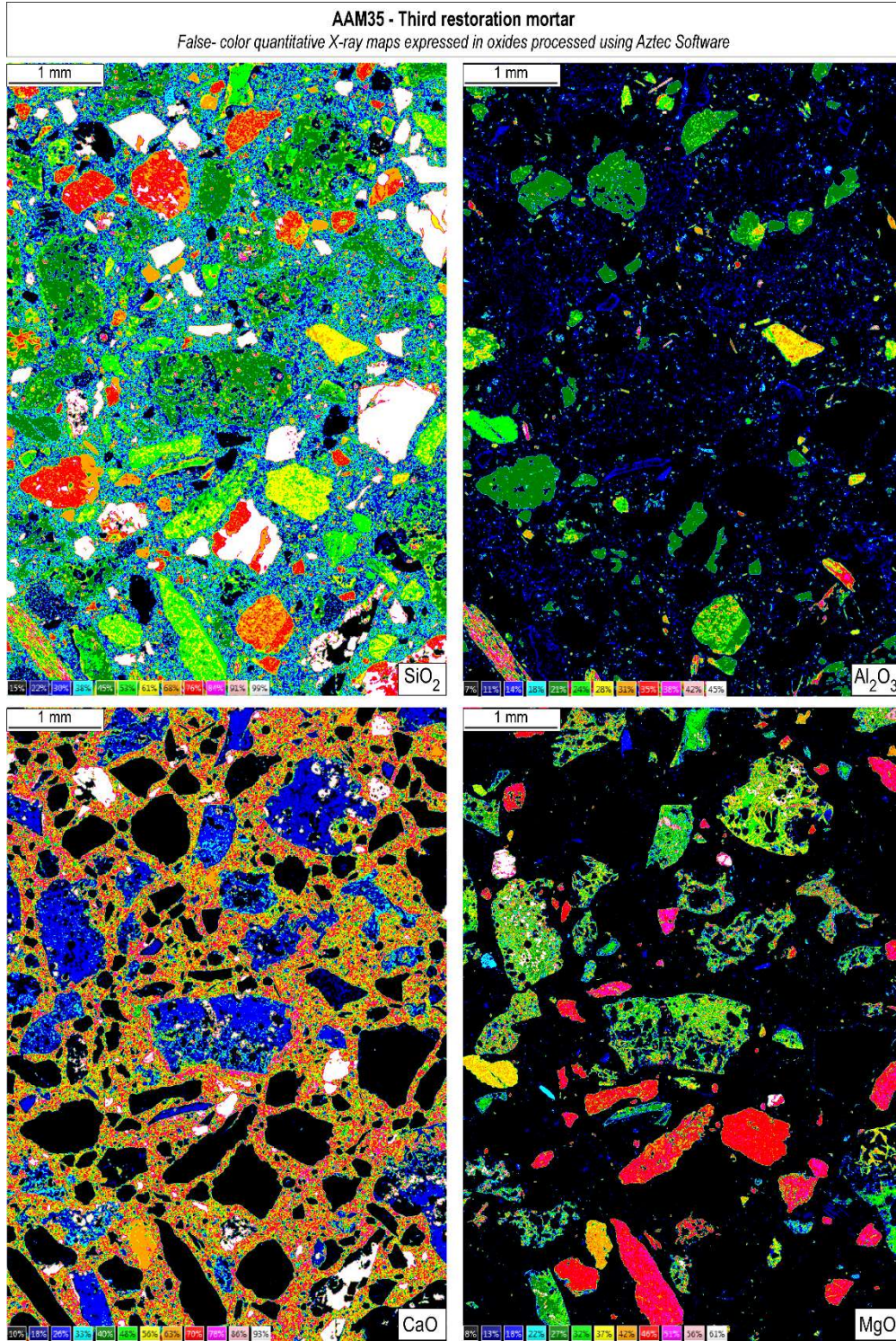


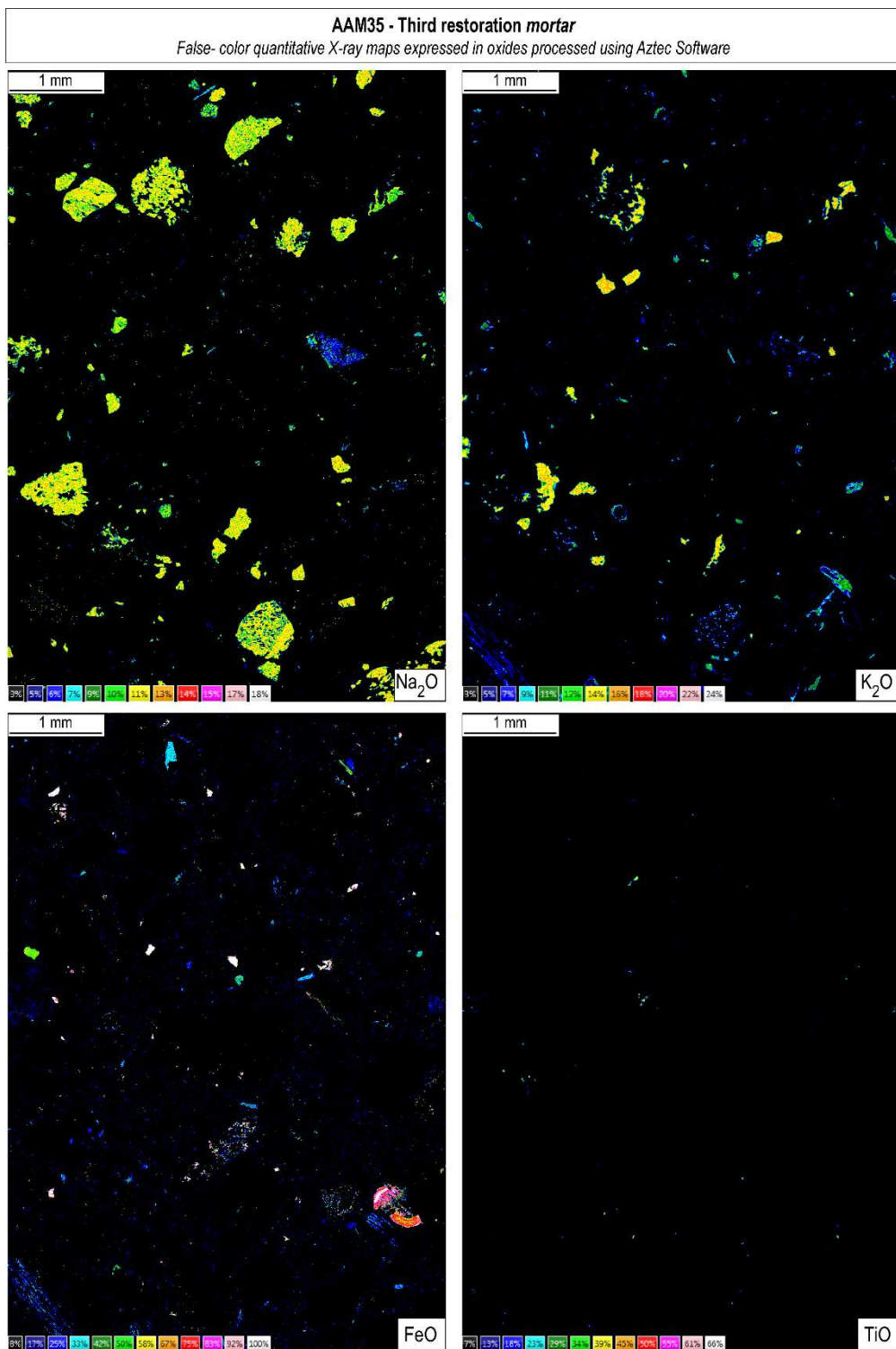












AAM36 - Fourth restoration mortar
False-color quantitative X-ray maps expressed in oxides processed using Aztec Software

